Tectonic history of the sole and roof of the Greater Himalayan Sequence: structural and metamorphic observations of garnet-staurolite schists from the Bhutan Himalaya

Laura Ritchie

Supervisor: Dr. Djordje Grujic

Submitted in partial fulfillment of the requirements of an honours degree in
Earth Sciences at Dalhousie University
April 2004

Dalhousie University

Department of Earth Sciences
Halifax, Nova Scotia
Canada B3H 3J5
(902) 494-2358
FAX (902) 494-6889

DATE April 30, 2004

AUTHOR Laura Ritchie

TITLE "Tectonic history of the sole and roof of the Greater Himalayan Sequence: structural and metamorphic observations of garnet-staurolite schists from the Bhutan Himalaya"

Degree B.Sc. (Hon.) Convocation May 25th Year 2004

TABLE OF CONTENTS

TABLE OF FIGURES

ABSTRACT

The Greater Himalayan Sequence (GHS) is the metamorphic core of the Himalaya, bounded by the Main Central Thrust (MCT) in the south and the extensional South Tibetan Detachment (STD) in the north. The GHS of the Bhutan Himalaya also contains the out-of-sequence Kakhtang Thrust and several sedimentary klippen associated with the STD. The dominant metamorphic feature of the GHS is an inverted metamorphic sequence that occurs from the MCT (amphibolite facies) with higher metamorphic grades (up to granulite facies with associated migmatites and leucogranites) occurring to the north. In Bhutan, this inverted metamorphic sequence is repeated several times within the GHS, with lower metamorphic grades (garnet-staurolite assemblages) occurring in several locations – near the MCT, at the base of the klippen, and in the footwall of Kakhtang Thrust.

A comparison of the deformational and metamorphic history of garnet-staurolite-biotite schists from the sole and roof of the GHS provides insight on the tectonic history of the GHS as a whole and in relation to the other structural units of the Bhutan Himalaya.

Geothermobarometry results from the garnet-staurolite schists show that just below the MCT peak metamorphic conditions reached 611±27 °C and 10.2±1.0 kbar, contemporaneous with dominant flattening combined with top-to-the south shearing. The Paro metasediments in the Paro region of eastern Bhutan show a peak metamorphic temperature of 702±43 °C at a pressure of 9.8±1.6 kbar. This unit, previously described as either part of the LHS or of the GHS, is reinterpreted as a window to the Lesser Himalayan Sequence because it is bounded by opposite dipping normal faults and has metamorphic conditions compatible with that structural level. Pressure conditions decrease above the STD with an increase in structural level, whereas the temperature conditions range from 715±50°C to 608±25°C. These garnet-staurolite schists of the Chekha Formation exhibit a dominant deformation of vertical shortening, overprinted by top-to-the-north to northwest normal fault kinematics as expected in the STD shear zone. A garnet-staurolite schist in the footwall of the Kakhtang Thrust is petrographically equivalent to those of the Chekha Formation and exhibits the same dominant pure shear flattening, with P-T conditions of 654±26°C and 8.2±1.2 kbar similar to those in the klippen. This unit, the Naspe Formation, is thus correlated as part of the Chekha Formation.

The metamorphic data obtained here combined with published data indicate that the peak temperature increases northwards towards higher structural levels, and then progressively decreases above the STD. At the same time, the pressure at peak temperature progressively decreases from ca. 10 kbar at the base of the GHS to approximately 8 kbar in the roof of the GHS. This relatively simple P-T pattern has been subsequently overprinted and repeated by later faulting and thrusting. The P-T pattern in the GHS obtained in this study provides an important constraint for models of Himalayan tectonics.

Acknowledgements

I would like to express my gratefulness towards my supervisor, Djordje Grujic, for his willingness to share his experience and excitement of this topic, and his patience in doing so; Becky Jamieson for her helpful input and encouragement; Joyia Chakungal for her continual support and Patricia Stoffyn for her assistance with the microprobe data.

1 INTRODUCTION

Bhutan is a small kingdom in the eastern Himalaya located between 88-92° E and 26.5-28° N. Political geography situates the Kingdom of Bhutan between the Indian states of Sikkim and Arunachal Pradesh to the west and east respectively, and between the state of Assam in the south and Tibet in north. Bhutan is the size of mainland Nova Scotia in area. In the south the mean elevation is about 200 m, marking the first foothills of the Himalaya, with a subtropical climate. In the north, on the border to Tibet, the highest peaks reach up to 7500 m. In the mountainous region, climate varies from subtropical in the low valleys to progressively more alpine above elevations of 4500 m. Geologically, Bhutan is entirely within the Himalayan ranges; it extends between the Tibetan Plateau in the north and the Precambrian basement of the Indian plate covered by the alluvial plain of Brahmaputra River in the south (Fig. 1-1).

1.1 General Statement

This study involves the structural and metamorphic analysis of schists deformed under garnet-biotite to garnet-staurolite metamorphic conditions. The primary objective of this research was to investigate and compare the tectonic histories of the upper and lower boundary zones of the Greater Himalayan Sequence (GHS) of the Bhutan Himalaya. The aim is to provide constraints on the tectonics of the Himalaya in Bhutan, and of the GHS in particular.

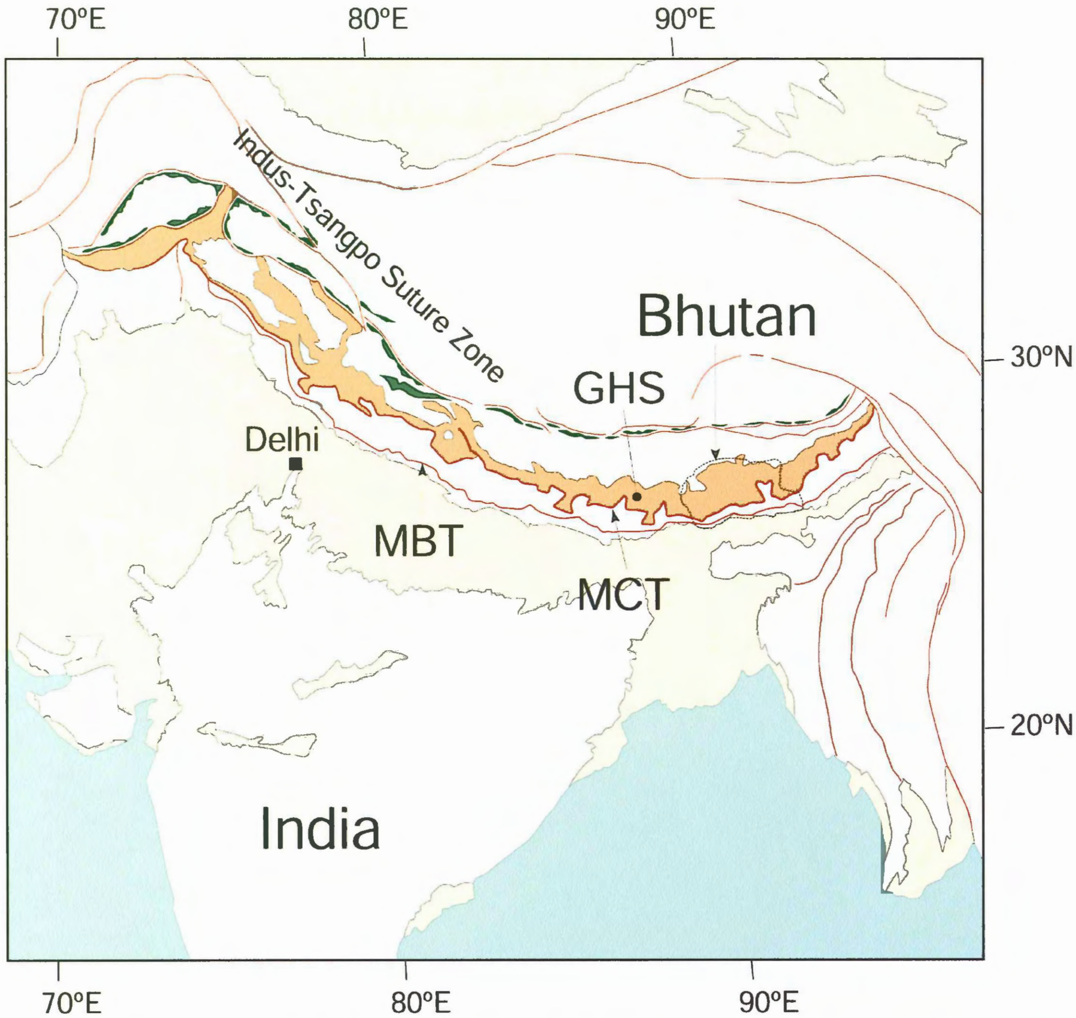

Fig. 1-1. Regional map of Central Asia and Bhutan showing the major structures of the Himalaya: GHS – Greater Himalayan Sequence (orange); MBT – Main Boundary Thrust; MCT – Main Central Thrust. Also shown is the Indus-Tsangpo Suture Zone with associated ophiolites (green). (After Gansser 1983)

1.2 Previous and Concurrent Work:

Gansser (1964; 1983) first placed the geology of Bhutan in the context of the Himalayas, defining the main tectonic units and structures and producing the first geological map of Bhutan. Members of the Geological Survey of India have also been working and mapping in Bhutan since 1960. Their work has been recently compiled by Bhargava (1995). Contemporary structural and metamorphic work in Bhutan was initiated by Prof. L. H. Hollister (Princeton University), D. Grujic and their co-workers. Work by Swapp and Hollister (1991), Grujic et al. (1996; 2002), Davidson et al. (1997) and Daniel et al. (2003) has demonstrated that the Bhutan Himalaya shares many similarities with the central Himalaya of Nepal and India, but these authors have also recognised the Kakhtang Thrust in the GHS and klippen of the Tethyan sequence as being unique to Bhutan. The major contribution of their work is the interpretation that the GHS has been exhumed as a hot and weak, ductile, penetratively creeping mass by ductile extrusion to the south over the cooler rocks of the Lesser Himalayan Sequence (LHS) and under the cooler rocks of the Tethyan sequence (Grujic et al. 1996). The primary data used to support this hypothesis were quartz microfabrics and geothermobarometric data. Through recent field and laboratory work by Grujic et al. (2002) and Daniel et al. (2003), this hypothesis has been revised in terms of the exhumation of a low-viscosity mid-crustal channel. This hypothesis has been developed in detail by concomitant finite-element thermal-mechanical modelling by Beaumont et al. (2001, 2004) and Jamieson et al. (2002; in press).

One of the major and most puzzling characteristics of the Himalaya is the inverted metamorphic sequence across the LHS and GHS. Swapp and Hollister (1991) and Davidson et al. (1997) have shown that this picture is more complicated, in that the metamorphic sequence in the GHS of the Bhutan Himalaya may have been duplicated and that the apparent distribution of the metamorphic isograds might have been caused by different and diachronous tectonic processes. Recent work by Daniel et al. (2003) has concentrated on detailed investigation of metamorphic conditions around the Main Central Thrust (MCT). Besides providing new data for the metamorphic conditions of the base of the GHS, the work supports the conclusions of the previous workers that the metamorphic assemblages in the rocks of the GHS are not in equilibrium and particular care has to be taken in any attempt to elucidate the metamorphic conditions. A combined observation of all the work is that there are several zones of garnet-staurolite schist in the Bhutan Himalaya:

(a) at the base of the GHS (Daniel et al. 2003), or at the top of the LHS where it is known as Jaishidanda Formation (Bhargava 1995);

(b) at the base of the Chekha Formation, situated at the top of the GHS as klippen (Grujic et al. 2002);

(c) at the base of the Chekha Formation, situated above the South Tibetan Detachment in the northwest of Bhutan; and

(d) within the GHS, and in the immediate footwall of the Kakhtang Thrust (Davidson et al. 1997), also known as Naspe Formation (Bhargava 1995).

Comparison of metamorphic conditions and microstructure of these garnet-staurolite schists is the subject of this thesis. Concurrent to this thesis project, geochronology is being carried out by Prof. Igor Villa at the University of Berne, Switzerland to dates the staurolite and hence determine the metamorphic ages of the samples used in this research. These ages may help to constrain the interpretations resulting from this thesis.

One of the most intriguing outcomes of the recent fieldwork in Bhutan is that possible return channel flow in the GHS may have exhumed some rocks initially associated with the Indus-Tsangpo Suture Zone, which is the suture between India and Tibet. The study of mafic and ultramafic rocks from the GHS of Bhutan is the subject of a doctoral thesis by Joyia Chakungal.

1.3 General Methodology

The rock samples used in this study were collected by D. Grujic. Optical microscopy was used for mineralogical and microstructural observations. Mineral and structural relationships were observed with respect to metamorphic and deformation events. The electron microprobe was used to obtain mineral compositional analyses and map element distribution in garnets, staurolites and plagioclase. Several representative samples were analysed with the microprobe, selected for their mineral assemblage and from each of the sampled locations across the GHS. The temperature and pressure conditions of peak metamorphism were calculated for these samples using the microprobe point data and the program THERMOCALC (Holland and Powell 2001) with an internally consistent dataset. The petrographic observations were combined with the temperature and pressure calculations from the microprobe data to interpret the metamorphic and deformational histories of each sample. These were then compared to interpret the various structural levels of the Bhutan Himalaya studied, as well as of the GHS as a whole.

2 GEOLOGICAL BACKGROUND

The Bhutan Himalaya contains all the major regional structures of the Himalaya and also contains several structures not seen elsewhere in the Himalaya.

2.1 Structures and Tectonic units of the Bhutan Himalaya

The following is a descriptive summary of the regional geology and structure of the Bhutan Himalaya in the context of the entire Himalaya. The structures and units are described in order from south to north (that is, from structurally lowest to highest).

2.1.1. Main Frontal Thrust

The Main Frontal Thrust (MFT) has discontinuous exposure along the Himalayan front, marking the front of the Himalayan thrust system (Fig. 2-1). The Main Frontal Thrust thrusts the Subhimalayan formations (e.g. the Siwalik Group) over the alluvial sediments of the Indian foreland. Activity of the MFT is thought to have initiated sometime during the Pliocene-Holocene (Hodges 2000). It is interpreted to merge with a low-angle décollement thrust at depth, known as the Himalayan Sole Thrust or Main Himalayan Thrust (MHT) (Nelson et al. 1996; Hodges 2000), along which the Indian plate is underthrust beneath the Himalaya and Tibet (Fig. 2-2).

2.1.2. The Siwaliks

The Siwalik Group is the dominant unit in the Subhimalayan zone situated between the MFT and the MBT (Hodges 2000). It consists of lower Miocene to

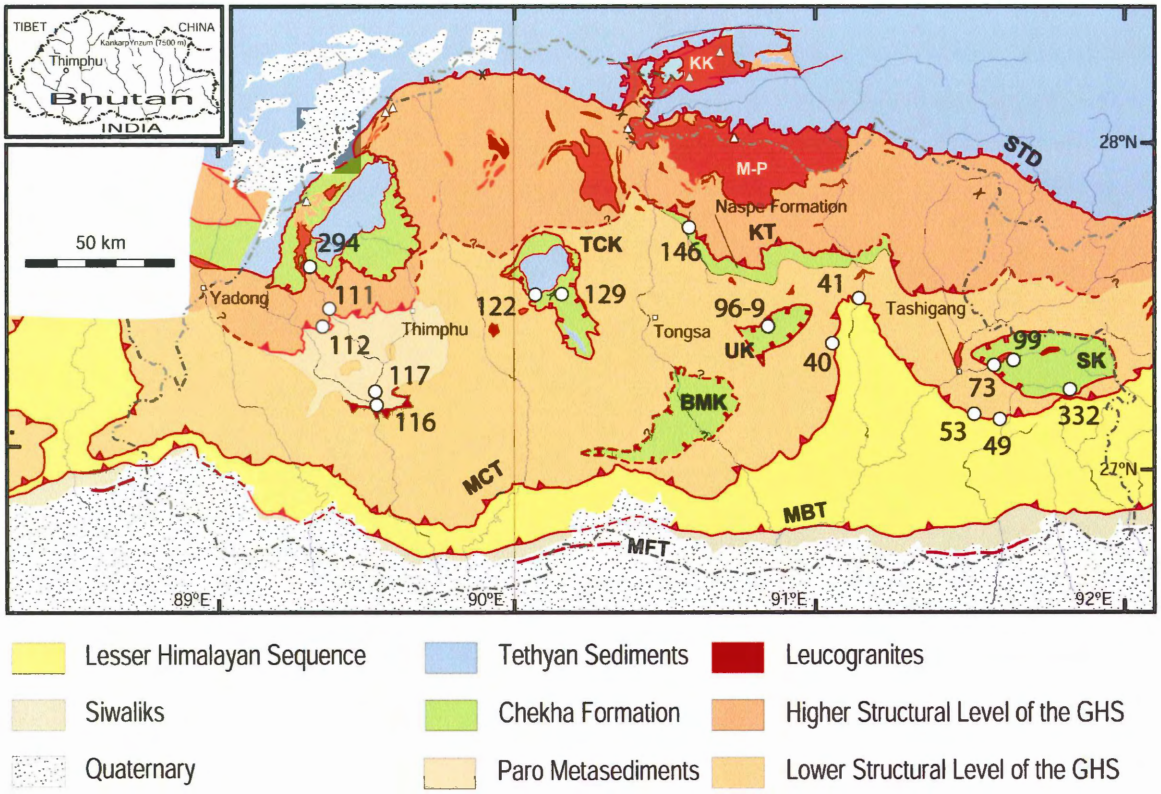

Fig. 2-1. Geological map of Bhutan showing the major structures and tectonostratigraphic units of the Bhutan Himalaya. MFT – Main Frontal Thrust; MBT – Main Boundary Thrust; MCT – Main Central Thrust; KT – Kakhtang Thrust; STD – South Tibetan Detachment; TCK, BMK, UK, SK – Klippen on the GHS. Also marked are locations of samples used in this study. (Map, also used elsewhere in this study, modified after Gansser 1983)

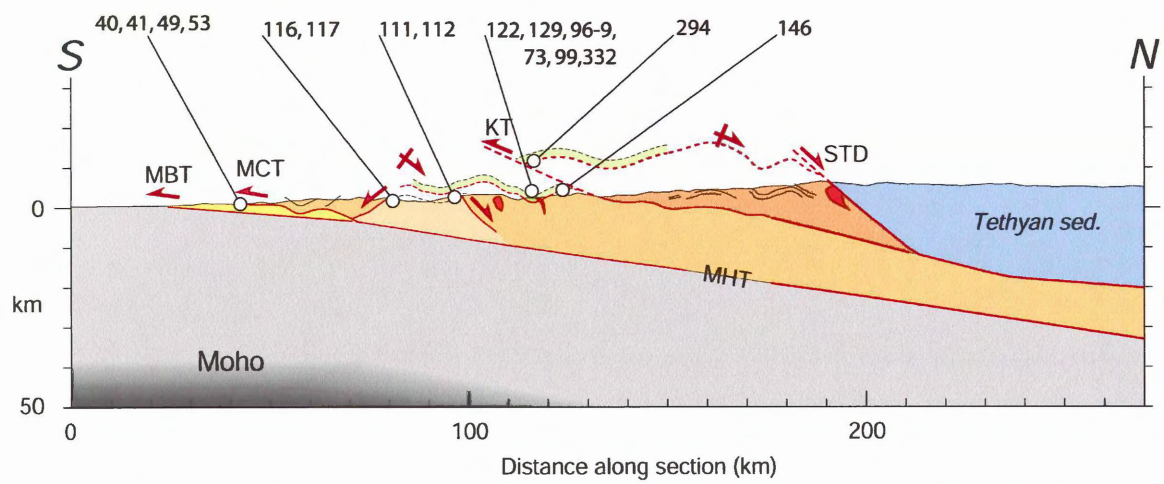

Fig. 2-2. North-south section across central Bhutan at 90°E (see Fig. 2-1) showing the structure of the Bhutan Himalaya over the underthrusting Indian Shield (grey). The MHT is the Main Himalayan Thrust. Colours represent same units as in Fig. 2-1, above. Also labelled are approximate sample locations projected onto cross-section (Modified after Grujic et al. 2002)

Pleistocene siliciclastic sediments thought to be deposited as a molasse, up to 3000 m in thickness (Gansser 1983; Najman et al. 2000; 2001). In Bhutan the Siwaliks dip steeply to the north, with a normal younging direction towards the contact with the MBT (Gansser 1983).

2.1.3. Main Boundary Thrust

The Main Boundary Thrust (MBT) places the Lesser Himalayan Sequence over the younger Siwalik Group. It is a moderate to steep north-dipping thrust zone that flattens at depth, merging with the MFT (Hodges 2000). The MBT occurs in places in southern Bhutan as a relief thrust (Gansser 1983). The MBT developed between 11 and 9 Ma and it was most recently active later than the Pliocene (Hodges 2000). The throw of the MBT is thought to be on a magnitude of tens of kilometres (Hodges 2000).

2.1.4. Lesser Himalayan Sequence

The Lesser Himalayan Sequence (LHS) is bounded by the MBT in the south and the MCT in the north. It consists of 8-10 km thick tectonized metasedimentary units in a complex fold and thrust system (Hodges 2000; DeCelles et al. 2001). The upper part of the LHS in the Bhutan Himalaya is known as the Shumar Unit (Gansser 1983; Bhargava 1995). These quartzites, slates, and generally non-fossiliferous limestones are interpreted to have been deposited on the northern passive margin of the Indian plate, with an age of Mesoproterozoic-Cambrian for the dominant units (Hodges 2000). The lower parts of the LHS, best developed in eastern Bhutan, are the Gondwanan units—continental sediments deposited in Upper Paleozoic intracontinental grabens (Gansser 1983; Bhargava 1995). This implies that there is a major thrust within the LHS, separating the older rocks in its hanging wall (Shumar) from the younger rocks in the footwall (Gondwanan).

2.1.5. Main Central Thrust

The MCT places the GHS over the LHS. It is thought to extend the full length of the Himalayan system, though its extent is not fully known and exposures are generally not good in the eastern Himalaya, including Bhutan (Hodges 2000). The MCT is actually the protolith boundary within a broad shear zone, the MCT zone (Grujic et al. 1996; Davidson et al. 1997), which separates sheared rocks of the LHS from mylonitised rocks of the GHS. The MCT zone is up to 10 km thick. The sheared rocks in the MCT zone show top-to-the-south shearing with strain decreasing with distance from the MCT (Grujic et al. 1996). Nearest to the MCT, rocks of both the hanging wall and footwall are highly deformed protomylonites to mylonites (Grujic et al. 1996; 2002). The MCT zone is also characterized by a very steep metamorphic field from greenschist facies in the LHS to amphibolite facies in the GHS (Gansser 1983; Hodges 2000, and references therein). Daniel et al. (2003) demonstrated, however, that there is an increase in temperature across the MCT and only a small increase in pressure structurally. Activity of the MCT in the Bhutan Himalaya has been constrained to between about 22.5 Ma and 7 Ma (Daniel et al. 2003).

2.1.6. Greater Himalayan Sequence

Also known as the Higher Himalayan Crystalline, the GHS is the metamorphic core of the Himalaya (Hodges 2000, and references therein). The GHS is bounded by two major coeval shear zones of opposite shear sense: in the north it is a north-directed, normal fault termed the South Tibetan Detachment (STD), and in the south, the south-directed MCT. The GHS consists of high-grade metasedimentary and meta-igneous rocks with associated Miocene leucogranites (Hodges 2000, and references therein). The protoliths of the GHS are mostly sediments of the Indian passive margin (e.g. Parrish and Hodges 1996), and to a much lesser extent, mid-Proterozoic granites (e.g. Daniel et al. 2003).

2.1.7. Kakhtang Thrust

The Kakhtang Thrust has only recently been understood as an important and unique structural feature of the Bhutan Himalaya (Grujic et al. 1996, 2002; Davidson et al. 1997; Daniel et al. 2003). It has discontinuous exposure but is inferred to exist along the whole length of Bhutan, almost doubling the exposed thickness of the GHS in Bhutan with a throw of about 10-20 km (Davidson et al. 1997; Grujic et al. 2002; Daniel et al. 2003). The Kakhtang Thrust is younger than structures associated with the MCT, cross-cutting the regional foliation and metamorphic isograds. It is thus interpreted to be an out-of-sequence thrust (Davidson et al. 1997; Grujic et al. 2002; Daniel et al. 2003). According to INDEPTH seismic data (Nelson et al. 1996; Makovsky et al. 1996; Hauck et al. 1998), the Kakhtang Thrust has been interpreted either to be a lateral ramp of the MHT (Makovsky et al. 1996) or to merge with the STD at a depth of about 25km (Grujic et al. 2002). One possible interpretation for its origin is that the Kakhtang Thrust was activated after folding occurred in the STD zone due to continuous north-south shortening (Grujic et al. 2002). The hanging wall of the Kakhtang Thrust is dominated by sillimanite-bearing gneisses, schists and migmatites, as well as leucogranites. The footwall consists of garnet-staurolite schist at the village of Naspe in central Bhutan (Davidson et al. 1997). These metasedimentary units of garnet-staurolite to garnet-kyanite grade are also known as Naspe Formation (Bhargava 1995).

2.1.8. South Tibetan Detachment

The STD is marked by a low-angle north-dipping shear zone with normal-fault kinematics (Burg et al. 1984; Burchfiel et al. 1992; Edwards et al. 1996). The STD is parallel to the MCT, separating the GHS from the Tibetan Tethyan sedimentary units, and dips moderately to steeply to the north. It is thought to have been active between about 22 and 14 Ma (simultaneous with the MCT; Grujic et al. 2002; Daniel et al. 2003). In Bhutan, rocks in the immediate footwall and hanging wall of the STD contain a primary foliation with top-to-the-south fabrics overprinted by C' shear bands with top-to-the-northwest orientation (Grujic et al. 2002), indicating several episodes of deformation with differing shear sense, including thrusting. Evidence for this also occurs in the Annapurna Range (Hodges 2000; DeCelles et al. 2001) and Mt. Everest area (Searle et al. 2003). Some authors even propose that some activity along the present STD may have been initially related to an early Paleozoic tectonic event along the north Indian Margin (e.g. Gehrels et al. 2003).

2.1.9. Tethyan Sediments

Above the STD, Tethyan sediments of Cambrian to Eocene age (Gansser 1983; Hodges 2000, and references therein) overlie the GHS. Although Gansser (1983) was the first to propose a tectonic subdivision of the Himalayas and the first to map the boundary between the GHS and the Tethyan sediments, he did not recognise the tectonic contact (STD). The tectonic character of the contact was recognised by Burg et al. (1984) and first described in detail by Burchfiel et al. (1992). The Tethyan sedimentary units, including the upper Proterozoic Chekha Formation in Bhutan, are interpreted to be sediments deposited on the northern passive margin of the Indian plate (Gansser 1983; Gehrels et al. 2003; Myrow et al. 2003). These units are generally unmetamorphosed, except along the STD zone where schists of up to garnet-staurolite grade occur in the Chekha Formation at the contact with the GHS (Daniel et al. 2003; Searle et al. 2003).

In Bhutan, several klippen of the Chekha Formation are located in synclines over the GHS. These klippen are interpreted as erosional remnants of the STD, suggesting that the STD extended much further south than at present (Grujic et al. 2002). Structures in the rocks at the base of the klippen indicate a normal north-directed shear sense overprinting earlier top-to-the south shearing event, which is consistent with deformation of the Chekha Formation further north, above the STD (Grujic et al. 2002).

2.2 Leucogranites

Several generations of leucogranite intrusions occur in the GHS as sills and dykes which increase in abundance across the GHS from the MCT, with the largest plutons located beneath the STD. Leucogranites are also observed above the Kakhtang Thrust (Grujic et al. 1996; Davidson et al. 1997), and intruded into the Chekha Formation above the STD (Grujic et al. 2002). The leucogranite intrusions were emplaced over a period of ca. 26-12 Ma, concurrent with deformation of the GHS (Daniel et al. 2003). The oldest generations of intrusions are sills deformed with the regional foliation. Younger leucogranite dykes are folded with axial planes parallel to foliation, and the most recent intrusions cross-cut the regional foliation (Daniel et al. 2003) but are affected by shearing associated with both the MCT and STD (Grujic at al. 2002).

2.3 Metamorphism

Regional metamorphism in the Himalaya occurs in the Lesser and Greater Himalayan Sequences, with metamorphic grade increasing from lower greenschist to upper greenschist facies in the LHS at the MCT (Gansser 1983; Swapp and Hollister 1991; Davidson et al. 1997; Daniel et al. 2003) (Fig. 2-3). The inversion of metamorphic isograds in relation to the MCT may be related to and best explained by ductile extrusion of the GHS as a weak mid-crustal channel (Beaumont et al. 2001; Grujic et al. 2002; Jamieson et al. in press). Above the MCT in the GHS the lowest grade (kyanite schist) rocks occur nearest the MCT and metamorphic grade increases towards the north to granulite facies associated with leucogranites (Grujic et al. 1996; Daniel et al. 2003; Chakungal et al. 2003). Nearer to the STD, metamorphic grade decreases to greenschist facies (Grujic et al. 1996; 2002). In the uppermost part of the GHS and above the STD at the base of the Chekha Formation and in the Tethyan sediments the metamorphic sequence is right way up. In Bhutan, the inverted metamorphic sequence in the GHS is repeated by the Kakhtang Thrust (Swapp and Hollister 1991; Grujic et al. 1996; Davidson et al. 1997).

2.4 Ductile Extrusion of the GHS

Simultaneous activity of the MCT and STD has been interpreted as resulting from south-directed ductile extrusion of the GHS, leading to the folding and inversion of metamorphic isograds in the GHS (Grujic et al. 1996). From finite-element thermal-mechanical modelling (Beaumont et al. 2001; in press) and field observations (Grujic et al. 2002), the GHS has been reinterpreted as the core of a low-viscosity ductile channel that flowed from the middle crust of the Tibetan Plateau, with differential pressure as the primary driving force (Fig. 2-3). Focused surface erosion at the Himalayan front aids in the ductile extrusion of this channel, leading to the exhumation of the channel

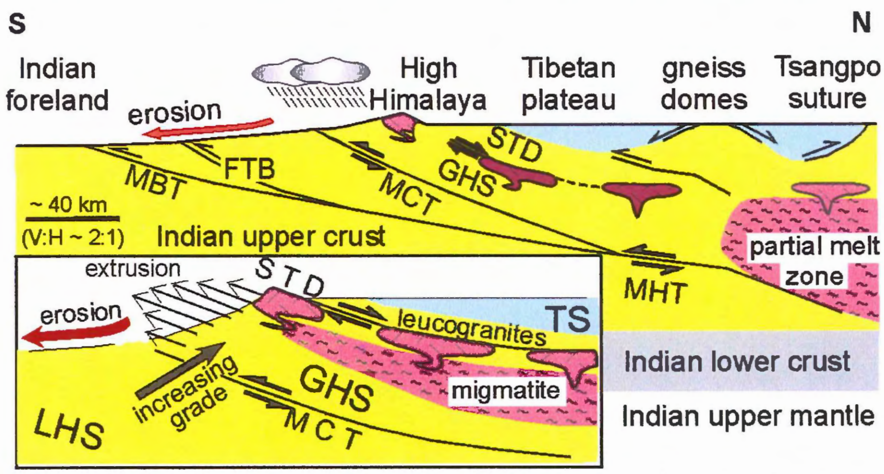

Fig. 2-3. Schematic Himalayan cross-section displaying features interpreted to be associated with the ductile extrusion of the GHS. FTB – Siwaliks fold-thrust belt; other abbreviations explained in text. (Beaumont et al. 2001)

material. In this model not only the metamorphic isograds are inverted but the thermal structure of the GHS. The channel flow model is consistent with the recent thermobarometric measurements in the GHS of central Nepal (Jamieson et al. in press).

In Bhutan, however, there are not yet sufficient data to constrain the pattern of metamorphic conditions and thermotectonic evolution along a representative north-south profile.

3 PETROGRAPHIC AND STRUCTURAL OBSERVATIONS

The petrographic and structural observations presented here are a summary of the detailed sample descriptions presented in Appendix I. Samples referred to are those highlighted in Fig. 2-1 and 2-2.

3.1 Metamorphism of the metapelites

The metasedimentary rocks involved in this study are of the staurolite zone and have typical mineral assemblages of garnet ± staurolite + biotite + muscovite ± plagioclase ± sillimanite + opaque accessory minerals. Garnet is present as porphyroblasts typically 0.5-3 mm in size. These porphyroblasts commonly contain inclusions of quartz, biotite, apatite and opaque minerals, and may be texturally zoned with inclusion-rich cores and relatively inclusion-free rims (Fig. 3-1). Staurolite is present in four samples from the Chekha Formation (96-9, 332, 129 and 128), as well as in one from the Naspe Formation (146) and in one from the Paro Metasediments (117). Staurolite forms euhedral porphyroblasts 0.5-7 mm in size. All staurolite is poikiloblastic with inclusions of quartz, biotite, ± muscovite, and opaque minerals. In most cases, staurolite appears to partially overgrow garnet grains and in one sample (332), inclusions of garnet and biotite are present in staurolite.

Biotite porphyroblasts are present in 332 as elongate books to 5 mm in size. This biotite appears to partially overgrow garnet and is in turn completely overgrown by staurolite in places, indicating that garnet and staurolite growth did not occur at the same

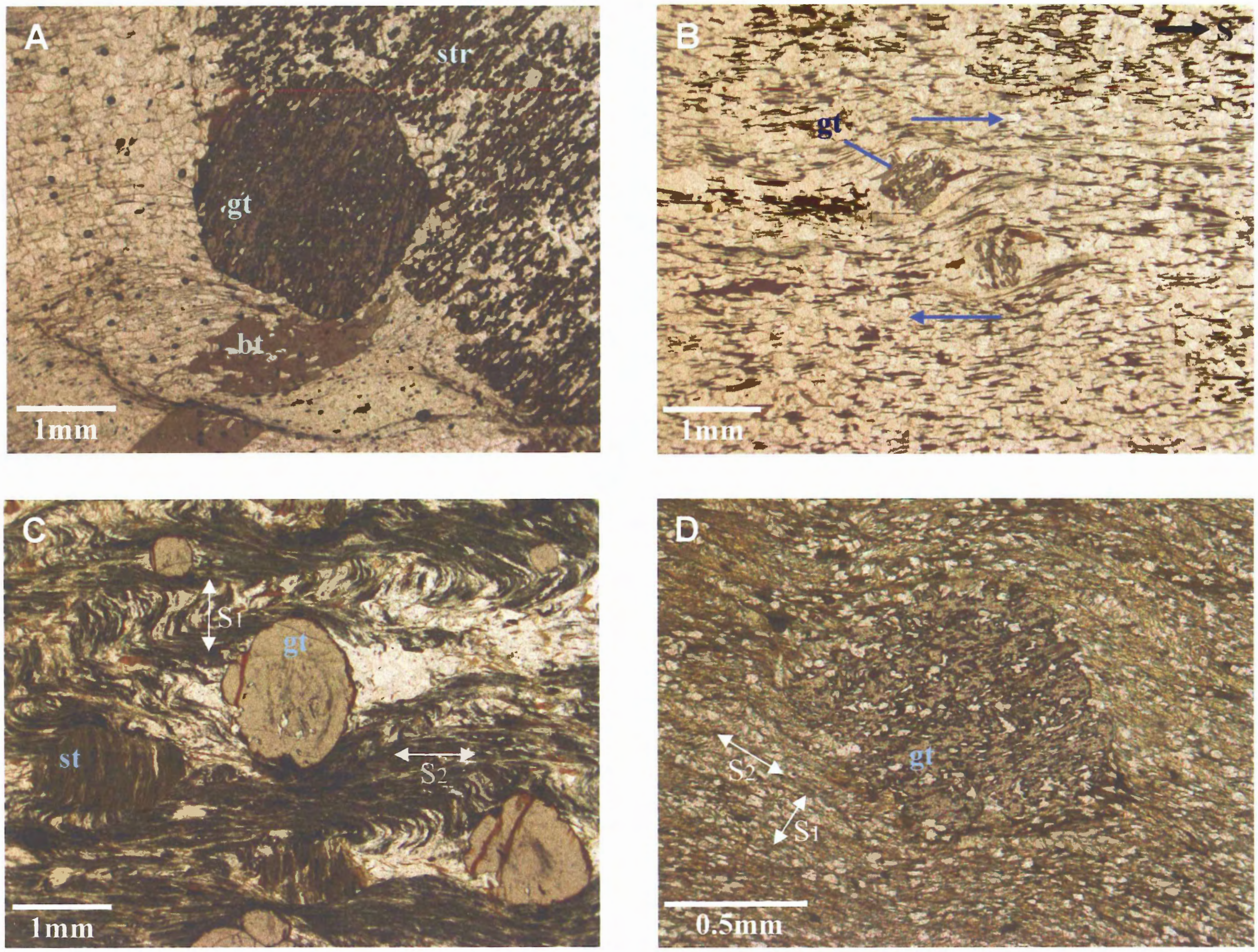

Fig. 3-1. Photomicrographs of garnet showing the variety of textures evident within the garnet schists studied: A- Staurolite partially overgrowing garnet (sample 332). B- Poikiloblastic garnets with σ-type strain shadows indicating top-to-the-south shearing (sample 116). C- ϕ-type strain shadows around garnets with few inclusions in a matrix with a late-stage crenulation cleavage. D- Syn- to post-tectonic garnet in a well-developed crenulation cleavage, preserving the crenulation cleavage in its internal foliation (sample 49b). gt – garnet; bt – biotite; str – staurolite.

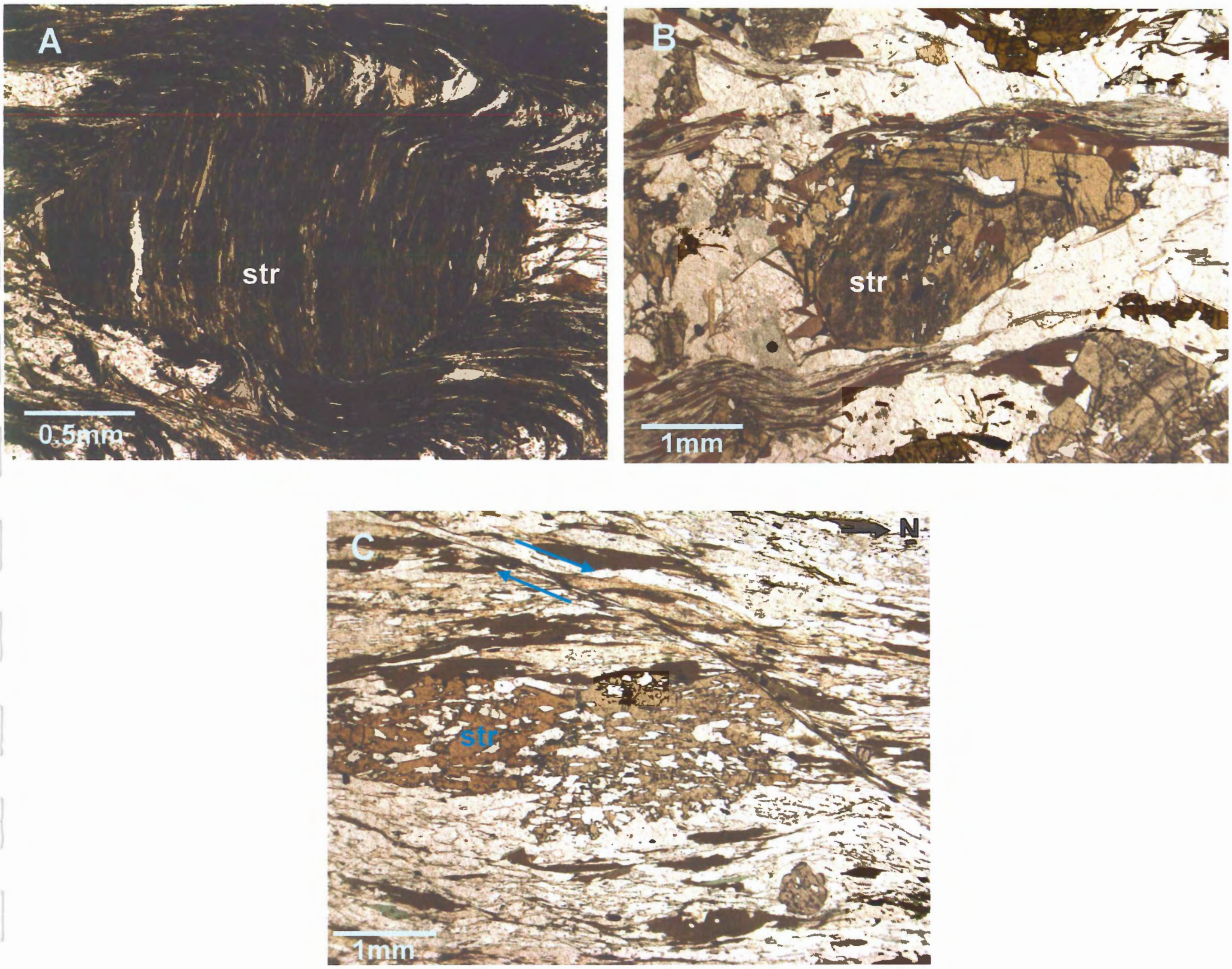

Fig. 3-2. Photomicrographs of representative staurolite grains. A – Staurolite full of graphite inclusions forming a gently curved internal foliation at a high angle to the dominant external crenulation cleavage. (sample 129). B – Staurolite porphyroblast (sample 146) that shows a rim with an inclusion trail orientation different to that of the rest of the grain, indicating syn-tectonic growth or growth over a possible mica cap. C – Poikiloblastic staurolite porphyroblast overgrowing a dominant schistosity (sample 96-9). The shear band to the left of the grain has a top-to-the-north sense of shear. str – staurolite.

time and that there may have been a hiatus between the end of garnet growth and the start of staurolite growth. This evidence is consistent with the mineral relationships and textures observed in the other Chekha Formation samples and in the Naspe Formation (sample 146).

Plagioclase porphyroblasts in sample 146 form anhedral grains up to 5 mm in size. They contain inclusions of quartz, biotite, opaque minerals and some small staurolite porphyroblasts. Staurolite grains in this sample in turn contain inclusions of fine-grained plagioclase, suggesting either that staurolite and plagioclase grew at the same time, or that there were two phases of plagioclase growth, with the later phase producing the porphyroblasts, and the earlier phase being primary/detrital or earlier metamorphic grains.

Mats of fibrolite are associated with biotite and muscovite in the matrix of samples 332, 146, 122 and 111a. In all cases the sillimanite is oriented parallel to the dominant foliation, either deformed with it or mimetically overgrowing the existing foliation. In samples 111a and 332, sillimanite is also present as pseudomorphs after a pre-existing mineral (Fig. 3-3). These pseudomorphs have an equant, subhedral hexagonal shape and are about 3 mm in size in both samples. The grain in 332 is poikiloblastic, although in both samples the pseudomorphs contain abundant inclusions of quartz as well as some muscovite and biotite, forming straight inclusion trails. The texture of the inclusion trails resembles the inclusion trails in staurolite (332), but the shape of the grains in both 332 and 111a closely resemble garnet. No replacement textures of staurolite or garnet by sillimanite were observed elsewhere in the samples, nor

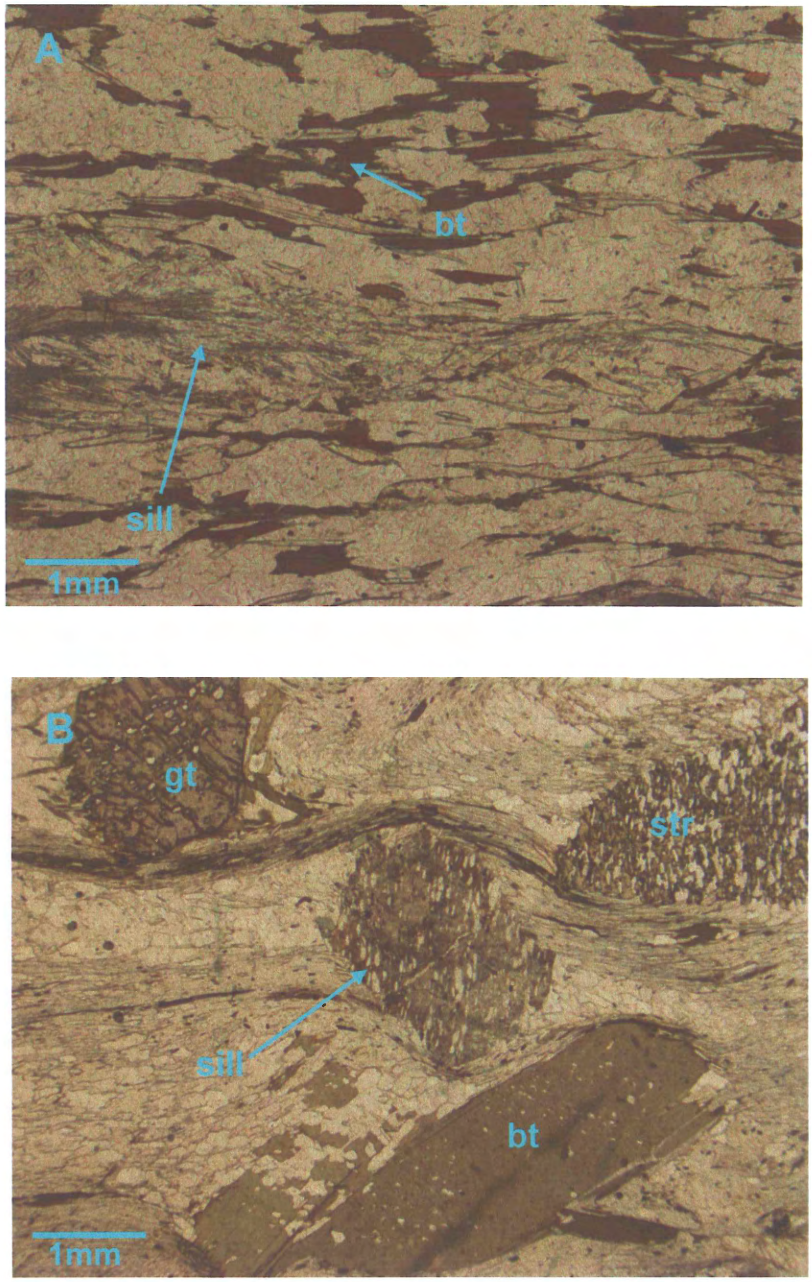

Fig. 3-3. A – Sillimanite (fibrolite) aggregates (sample 122), associated with matrix biotite and muscovite. B – Sillimanite forms pseudomorphs of an unknown mineral (sample 332). Sill – sillimanite; other labels same as in Fig. 3-1 and 3-2.

is there evidence of a pre-existing phase of kyanite or andalusite present in any of the sillimanite-bearing samples.

Graphite is present in samples 128, 129, 112 and 40 as elongate to fibrous grains in the matrix oriented parallel to the foliations, and as very fine-grained inclusions in porphyroblasts. In samples 128 and 129 there is also abundant hematite, particularly around garnet grains (Fig. 3-1c). This hematite is likely a retrograde product of the reaction graphite + magnetite = magnetite + hematite + CO_2, with some possible reaction with the Fe in the garnets (Spear 1993). This reaction, if present, may have implications for the quality of geothermobarometric estimates in these samples, due to the possible presence of H_2O + CO_2 fluids and Fe-exchange in the garnet rims. To test this uncertainty of the equilibrium conditions of the mineral assemblage in this sample, Raman spectroscopy will be performed on the carbonaceous material. This technique will provide the estimates of maximum temperature with accuracy of ca. 50 °C (Beyssac 2002).

Sample 112 contains a mineral assemblage different from that of the other rocks studied. Porphyroblasts of K-feldspar up to 4 mm in size contain inclusions of graphite and other opaque minerals. Inclusion trails in the K-feldspar grains are straight and at high angles to the dominant foliation with which the porphyroblasts have a shape-preferred orientation. This suggests that K-feldspar growth possibly involved two stages of growth. In this case, the K-feldspar cores would have first overgrown an early schistosity, and the inclusion-free rims would have developed later, syn- or post-tectonic to the development of the crenulation cleavage which is the dominant foliation in the matrix. Large grains of an elongate, rounded unknown mineral are also present. These grains contain abundant fine-grained inclusions of opaque minerals, quartz, and K-feldspar. It is possible that they may be the weathering products of pre-existing K-feldspar or grains with some relict K-feldspar included in the grains, or possibly cordierite that has been replaced by pinite.

Tourmaline is also present in most samples as compositionally zoned, euhedral grains less than 0.2 mm in size. The tourmaline may be a result of nucleation caused by magmatic fluids from nearby leucogranite intrusions. It is possible that this fluid-rock interaction occurred after peak metamorphism and deformation in some samples as the tourmaline grains clearly overprint earlier structures. In other samples, however, tourmaline occurs as inclusions in assemblage grains such as biotite and garnet, and therefore was present before peak metamorphism.

3.2 Structure and microstructure of the garnet-staurolite and garnet-biotite schists

3.2.1 Microstructure

Microstructures and deformation of the samples were studied to constrain the deformational histories and their relationships to the metamorphism. Particular attention was paid to intragranular deformation, foliations and matrix deformation, and porphyroblast-foliation relationships. Terminology used here to describe the microstructures and deformation mechanisms follows the conventions presented in Passchier and Trouw (1996).

Quartz grains in most samples show various deformational microstructures including granoblastic texture, interlobate grains, undulose extinction and subgrain rotation, pinning, window and dragging structures and left-over grains, bulging, and deformation lamellae (Fig. 3-4). These are all structures resulting from dynamic

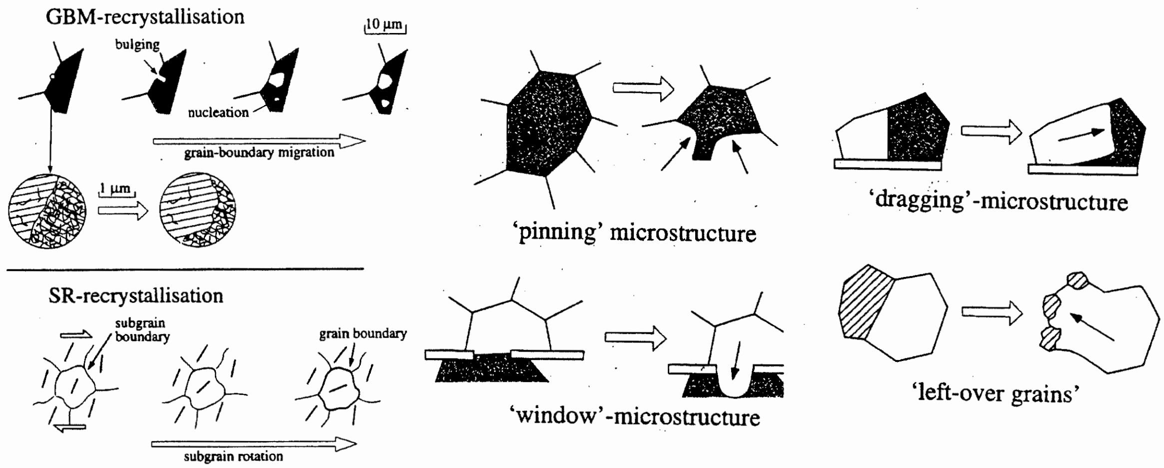

Fig. 3-4. Illustrations of several grain-scale microstructures observed in schists of the Bhutan Himalaya, labelled with the descriptive terms used in this study. White arrows represent the progression of deformation. (Passchier and Trouw 1996)

recrystallisation and recovery (undulose extinction and lamellae), providing evidence that deformation was taking place after grain growth. According to a correlation of temperature with deformational mechanisms in quartz (Stipp et al. 2002), the

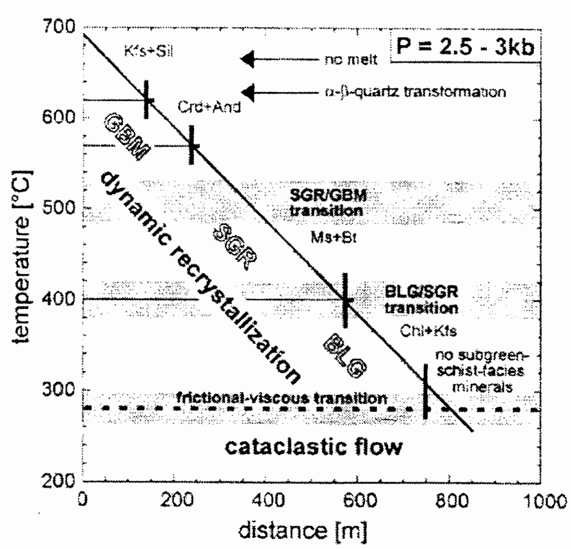

Fig. 3-5. The correlation of quartz deformation and recrystallisation with temperature. (Stipp et al. 2002)

microstructures observed in the studied samples indicate that deformation was occurring from as low as about 300 °C, indicated by quartz bulges, to at least 500 °C with some grain-boundary migration (Fig. 3-5).

Plagioclase generally exhibits intragranular deformation. Tapering albite twins, or deformation twins, are common throughout the samples, having developed as a response to high stress at the grain boundaries (Passchier and Trouw 1996). Undulose extinction is also common, although often subtle, and subgrains locally indicate subgrain rotation recrystallisation. Estimated temperature conditions of at least 400 °C to less than 800 °C for plagioclase deformation (Stünitz and Fitz Gerald, 1993) are consistent with temperatures estimated from the quartz microstructures.

Matrix biotite and/or muscovite in all samples define the dominant foliations.

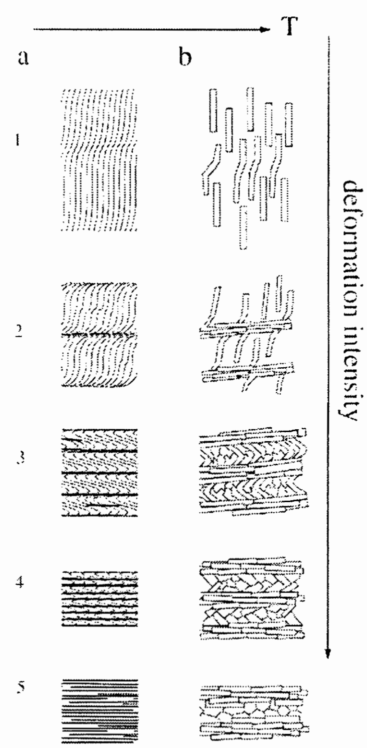

Fig. 3-6. Classification scheme of crenulation cleavages by the intensity of deformation, with a numerical scale from 1 to 6, where stage 1 involves very gentle microfolding and stage 6 represents a crenulation cleavage that is so well developed that the previous foliation is not observed. (Passchier and Trouw 1996).

Matrix biotite and muscovite typically have lattice- and shape-preferred orientations, and in some LHS samples these overprint poorly oriented relict biotites with sedimentary textures (S_0). The dominant planar foliations formed by biotite and muscovite are continuous schistosities (S_1) with homogeneous distribution of micas throughout the matrix, to spaced foliations, with biotite and muscovite forming cleavage domains separated by quartz ± feldspar-rich microlithons. Most samples contain a crenulation cleavage (S_2) that is defined by the folding of a planar schistosity into a new foliation that can be classified according to the stage of development (Fig. 3-6).

In most of the samples from Chekha Formation and in the sample from the Naspe Formation, this crenulation cleavage is developed to stage 3-4, indicating pronounced shortening normal to the crenulation cleavage plane. Sample 73 displays a stage 2-3 asymmetrical crenulation cleavage into which a sedimentary layering is folded. In 96-9 the crenulation cleavage is somewhat less well developed, at stage 1-2.

The samples of the Paro metasediments and the LHS (Jaishidanda Formation) have more poorly developed crenulation cleavages (to stage 1) if present at all. Sedimentary textures, including bedding, are still present in most of these samples. The sedimentary layering is generally parallel to the metamorphic schistosity This suggests that the sedimentary layering might have been folded into tight to isoclinal folds with strong axial planar cleavage (S_1) making the dominant foliation observed in metasediments a composite foliation (S_0+S_1) . Field observations are consistent with this hypothesis (Grujic pers. comm.). Crenulation cleavage formed normal or at high angles to the composite foliation.

Porphyroblast-foliation relationships provide further constraints on fabric development. Garnet porphyroblasts in the Chekha Formation samples and in the Naspe Formation (146) have inclusions that define internal foliations that are straight to curved with a gentle sinusoidal shape and have no continuity with the external foliations. These grains generally produce σ- to ϕ-type strain shadows parallel to the dominant foliation, which is in most cases a crenulation cleavage. This suggests that garnet grew syn- to post-tectonically with respect to S_1. Staurolite porphyroblasts contain straight to very slightly curved inclusion trails that are generally continuous with the external foliation. Sample 129 displays a very gentle anastomosing pattern of graphite inclusion trails around quartz inclusions, which could be the first stage of development of a crenulation cleavage. Textural relationships in most samples show that staurolite grew after garnet, so it is likely that staurolite growth occurred pre- to early syn-tectonically with respect to the crenulation cleavages, S_2. In sample 332, the biotite porphyroblasts have straight inclusion trails that are discontinuous with and at angles to the external foliation. Occurring around these grains parallel to S_2 are ϕ-type strain shadows. With similar structure to the garnets, it is most likely that these porphyroblasts grew inter-tectonically between S_1 and S_2.

Samples 40, 49a and 49b of the Jaishidanda formation (LHS at the MCT) contain garnet porphyroblasts with distinct internal foliations defined by inclusion trails. These garnets have gently to strongly curved internal foliations. The inclusion trails are continuous with the external foliation, and there is no deflection of the external foliation around the garnets. Sample 41 has anhedral garnets with embayed grain boundaries and an indistinct internal foliation. Biotite inclusions in these grains have the same orientation as matrix grains and are continuous with the matrix. In 49b, garnet grains clearly contain an internal foliation with a crenulation cleavage of the same curvature and orientation as the external foliation. The garnet porphyroblasts in these samples likely formed syn- to post-tectonically relative to the most recent foliation.

3.2.2 Structure

The structure and deformation of the rocks involved in this study were investigated in terms of the structural units from which they came (Fig. 3-7). The structurally lowest samples are from the LHS very near to the MCT (40, 41, 49 and 53). Sample 40 shows pure shear shortening in two directions, indicated by two symmetrical crenulation cleavages at near right angles. This is similar to the structures observed in sample 41. These samples come from the western limb of the Kuru Chu-Shumar spur (Gansser, 1983), which is a north-south trending upright antiform that deforms the GHS and the MCT. In the Himalayas, however, most of the upright folds deforming the dominant foliation trend east-west. The most likely interpretation is that the two crenulations are related to these two sets of folds. Ambiguous fold interference between the two sets of folds suggests that they might have developed simultaneously (McKinney et al. 2001).

The samples from location 49 are phyllites that display vertical shortening with a foliation parallel to sedimentary layering. Sample 53 (closer to the MCT), however, contains several microstructures consistent with top-to-the-south shear, including σ-type strain shadows around garnet grains, shear bands, and asymmetrical folding of quartz veins. Several quartz veins present in the sample have also been boudinaged as a result of

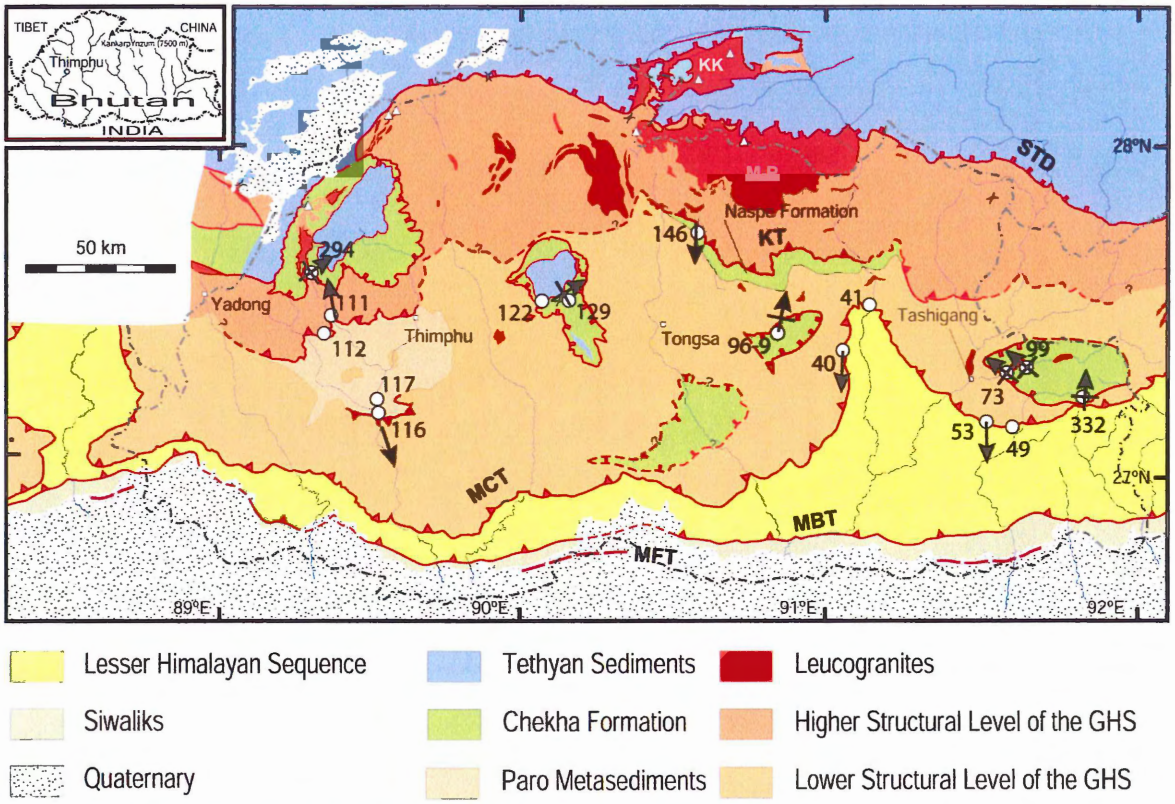

Fig. 3-7. Kinematics of structures observed in studied samples. See text for explanation. Arrows indicate top-to-the- direction of shear. Crossed arrows indicate the presence of a pure shear component of deformation.

stretching or oblique shear. A gentle stage 1 crenulation cleavage is also present in this sample, indicating a pure shortening component of deformation.

The Paro Metasediments (Gansser 1983) within the GHS are the next-to-lowest structural level from which samples were studied (111a,b, 112, 116 and 117). Observed kinematics within this unit in the Paro region are heterogeneous. Along the southern boundary, top-to-the-south shear is indicated by σ-type garnet porphyroblasts (sample 116). An adjacent sample (117) also contains a crenulation cleavage, indicating vertical shortening. Along the northern boundary of the Paro Metasediments shear bands observed in the hand sample (111a) and in outcrops (D. Grujic, field notes) indicate top-to-the north shear sense. The shear bands overprint an earlier crenulation cleavage. The weathered porphyroblast grains in sample 112 have a preferred orientation oblique to the crenulation foliation that appears to wrap around the grains, interpreted to indicate porphyroblast rotation also resulting from top-to-the-north sense of shear.

Sample 146 comes from the staurolite-bearing unit known as the Naspe Formation (Bhargava 1995) located in the footwall of the Kakhtang Thrust. This porphyroblast-rich sample (non-oriented) displays strong shortening with a well-developed late-stage crenulation cleavage.

All samples of the Chekha Formation show a component of vertical shortening with crenulation cleavages developed to various stages. Sample 73 displays top-to-the-northwest kinematics as indicated by asymmetrical folds and an asymmetrical crenulation cleavage. Field observations (Grujic et al., 2002 and Grujic pers. comm.) have determined that this asymmetry is indeed due to a shear zone rather than being asymmetrical parasitic folds on the limb of a larger fold. Shear bands present in sample 99 also indicate top-to-the-northwest shear. Sample 294 displays top-to-the-northeast shear with an asymmetrical crenulation foliation. Sample 96-9 contains two sets of discontinuous conjugate shear bands overprinting a crenulation cleavage, indicating flattening. The north-dipping set, however, is dominant to the south-dipping set and indicates top-to-the-north shear sense.

4 MINERAL CHEMISTRY AND THERMOBAROMETRY

After detailed petrography, nine samples were selected for analysis by electron microprobe. The rocks for this study were collected from the following tectonic units in an assumed tectonic order (Fig. 4-1):

(a) Shumar Formation of the LHS, sample B 53. According to Bhargava (1995) the garnet-biotite schists in the MCT zone are a separate unit, the so-called Jaishidanda Formation;

(b) Paro Metasediments (Gansser, 1983): samples BH 112 and116. This unit has also been interpreted as the Jaishidanda Formation (Bhargava, 1995);

(c) Naspe Formation (Bhargava, 1995): sample BH 146, and

(d) Chekha Formation (Gansser, 1983): samples BH 122, 129, 294, 332 and 96-9

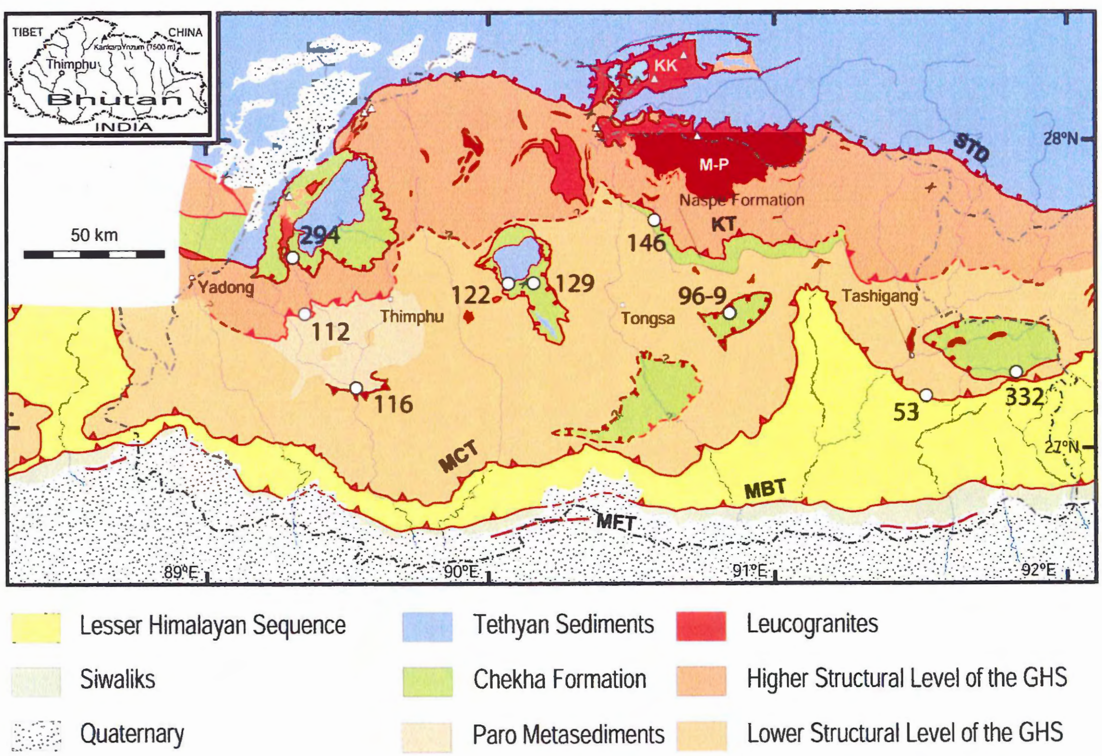

Fig. 4-1. Locations of samples used for electron microprobe analysis.

4.1 Electron Microprobe Analysis

For each sample, the mineral assemblage corresponding to the peak temperature conditions was interpreted from petrographic study (Table 4-1). During the electron microprobe work, representative point analyses were taken for each of the analysed samples, with particular focus on the identified mineral assemblages and possible reactions between these minerals. The measurements were taken both from cores and

Sample	Chlorite	Biotite	Muscovite	Garnet	Chloritoid	Staurolite	Sillimanite	Plagioclase	K-feldspar
Chekha Formation:									
BH 96-9	r	p	p	p		p		p	
BH 332	r	p	p	p		p	p		
BH 294	r	p	p	p				p	
BH 129	r	t	p	p		p			
BH 128		t	p	p		p			
BH 122		p	t	p			p	p	
Naspe Formation:									
BH 146	r	p	p	p		p	p	p	
Paro Metasediments:									
BH 117	r		p	p		p		?	?
BH 116		p	p	p				p	
BH 112		t	p						p
BH 111A		p	p				p	?	?
BH 111B		p	p					?	?
LHS (at the MCT):									
BH99		p	p					p	
BH 73		p	p	p				p	
BH 53A		p	p	p				p	
BH 49A	r	p	p	p	t			p	
BH 49B		p	p	p	t			?	
BH 41		p	t	p	t			p	
BH 40		p	p	p					

Table 4.1. The mineral assemblage of each sample as determined by optical microscopy. (p-present; t-trace; r-retrograde. All samples contain quartz)

from rims of the metamorphic index minerals. In addition, element distribution maps were made for selected grains to document the compositional zoning. Maps produced for garnet, staurolite, and plagioclase grains illustrate zoning patterns in the grains so that growth patterns and any post-growth reactions or element diffusion can be interpreted. This information is used to decrease uncertainties in the equilibrium conditions of peak metamorphism for thermobarometry.

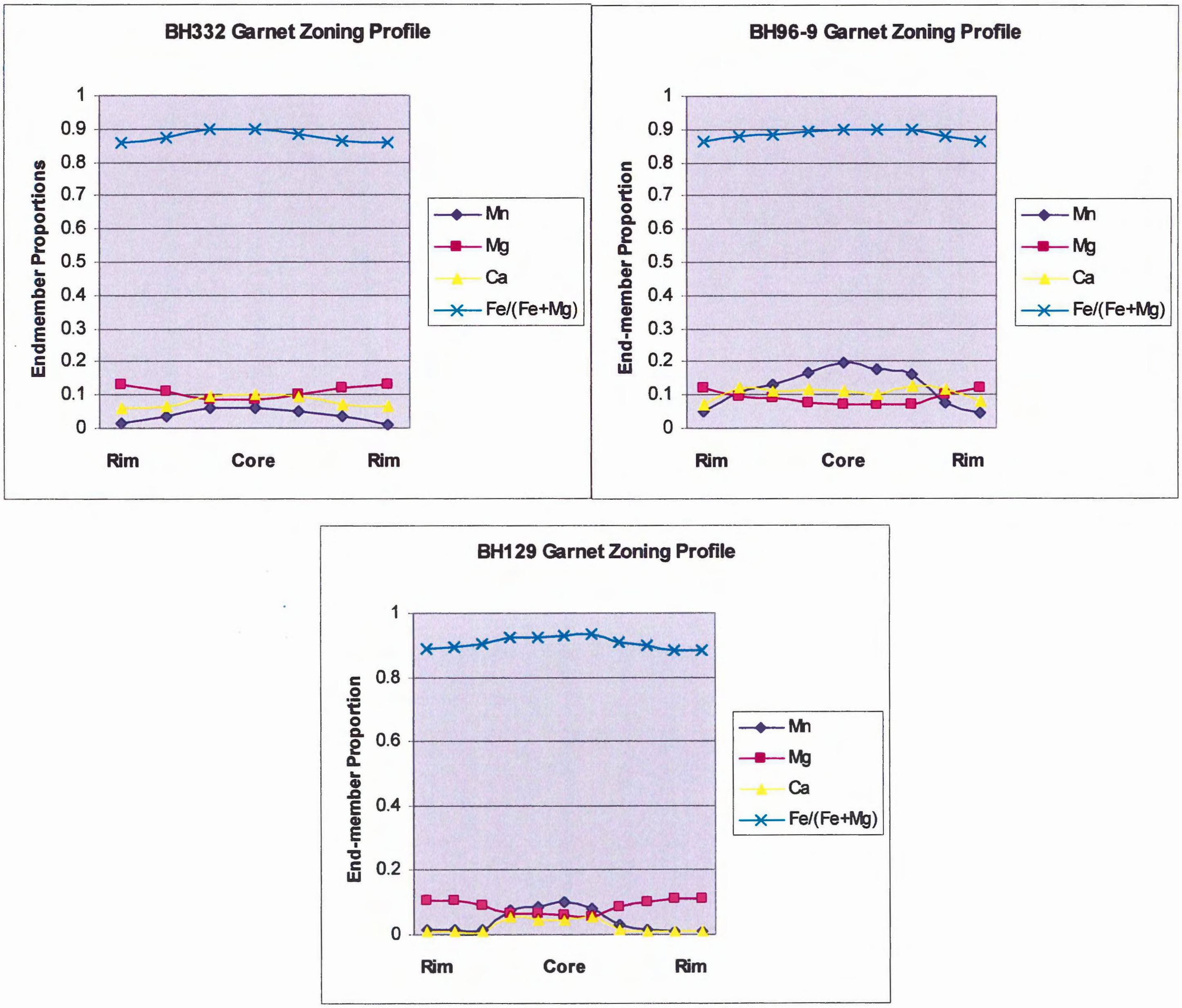

Fig. 4-2. Representative garnet zoning profiles across garnets from using point analyses. Grains profiled are the same grains used for element distribution mapping.

Garnet zoning profiles were plotted using point analyses across grains (Fig. 4-2). Grossular, pyrope and spessartine end-member proportions were plotted along with the Fe/(Fe + Mg) ratio. In general, there is a decrease in Mn and Ca from core to rim of the grains and an increase in Mg. The Fe/(Fe + Mg) ratio exhibits an increase from core to rim also. This garnet zoning pattern of Fe, Mg, and Mn is typical of garnet growth with increasing temperature and the zoning pattern of Ca suggests garnet growth with increasing pressure (Spear 1993).

4.2 Element Distribution Maps

Element distribution maps for garnet and staurolite were obtained using WDS spectrometry, in which x-ray intensities are measured for wavelengths specific to selected elements. Higher intensities, and thus higher element concentrations, are plotted as brighter colours in the maps. A current of 50 nA at 15 kV was used, with a beam diameter of 3 μm and a dwell time of 20 ms. Garnet maps included Ca, Fe, Mg, and Mn, because of their variability in garnet compositions as end-members, and Al. The staurolite grains were mapped for Ti, Fe, Mg, Al and Zn. Zoning may possibly be present in staurolite due to the exchange of Fe with Zn, Mg or Ti. Garnets in samples 96-9, 332, 129, 146 and 294 (Fig. 4-3 through 4-7) were mapped and staurolite in samples 96-9, 332, 129 and 146 was also mapped (Fig. 4-9 through 4-12). All garnet element distribution maps except 294 show distinct enrichment of calcium and manganese in the cores and relative enrichment of magnesium in the rims. The zoning pattern of iron in

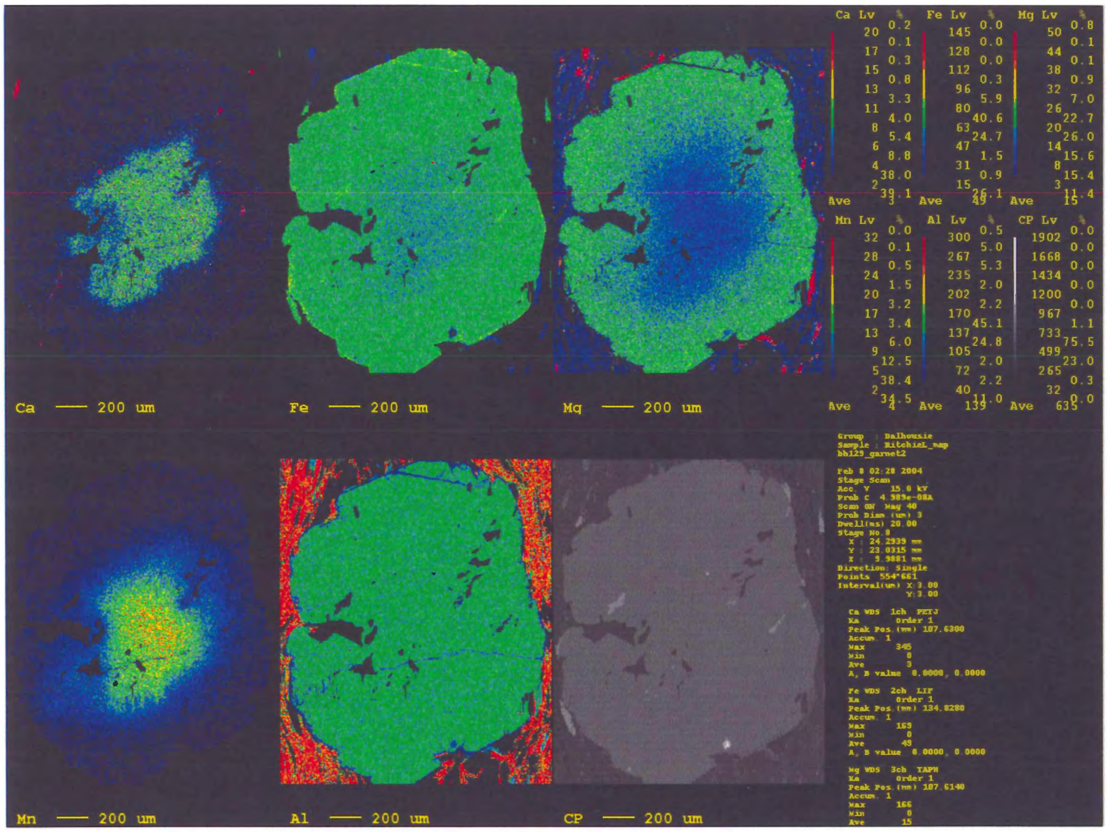

Fig. 4-3. Element distribution maps for a garnet porphyroblast from sample 129.

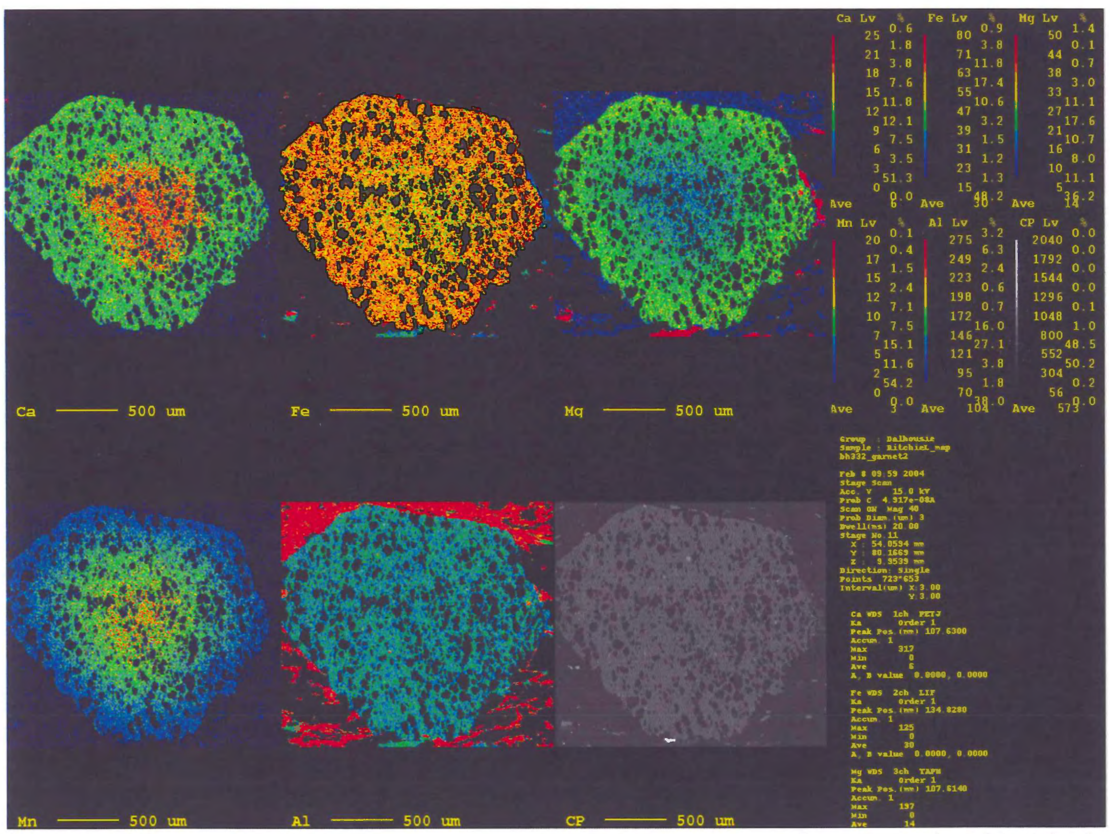

Fig. 4-4. Element distribution maps for a representative garnet from sample 332. Black 'holes' in garnet are quartz inclusions.

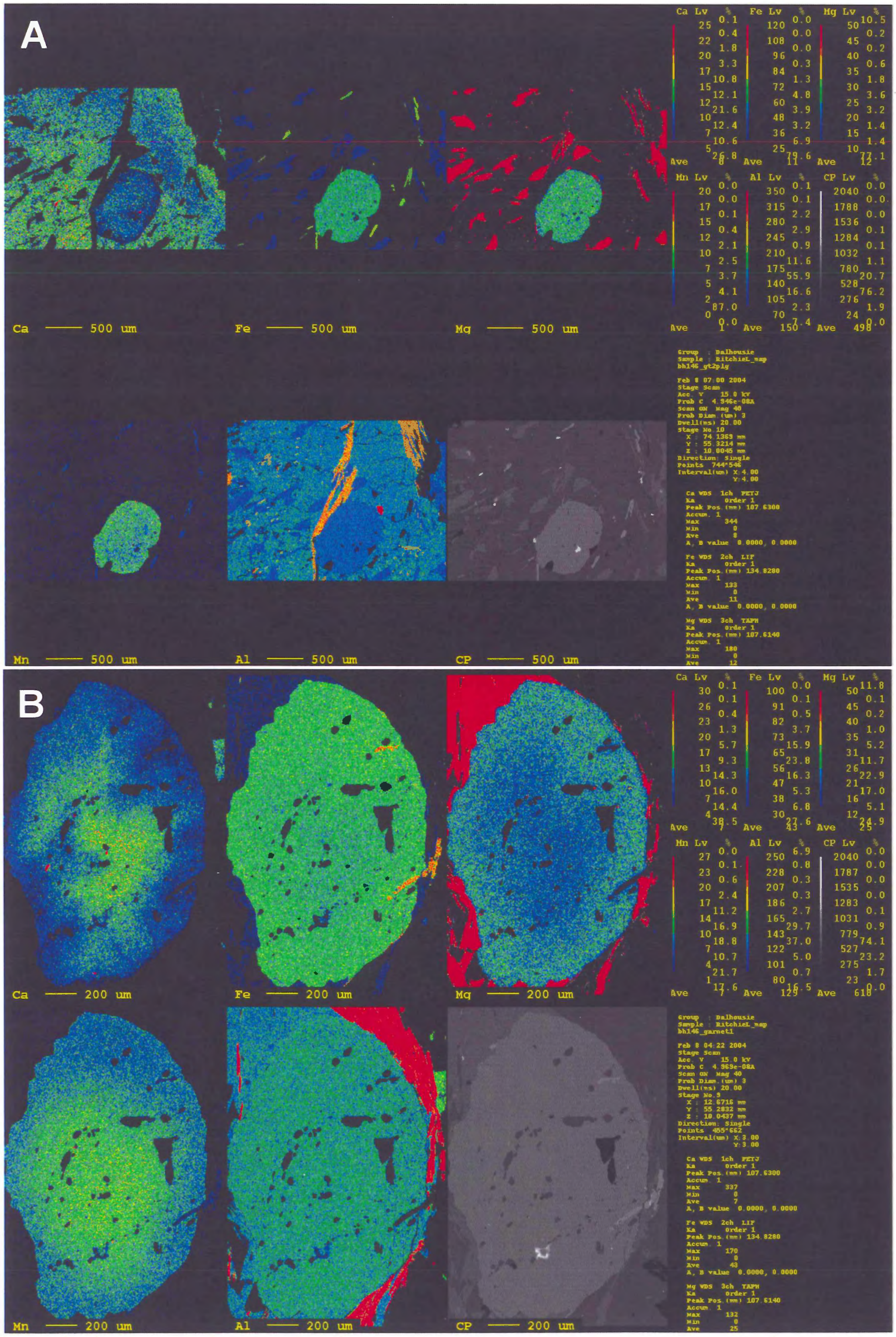

Fig. 4-5a,b. Garnet element distribution maps for sample 146. A garnet grain included in plagioclase (A) is unzoned except for a low-Ca rim. (B) shows a porphyroblast in the matrix with a distinct zoning pattern.

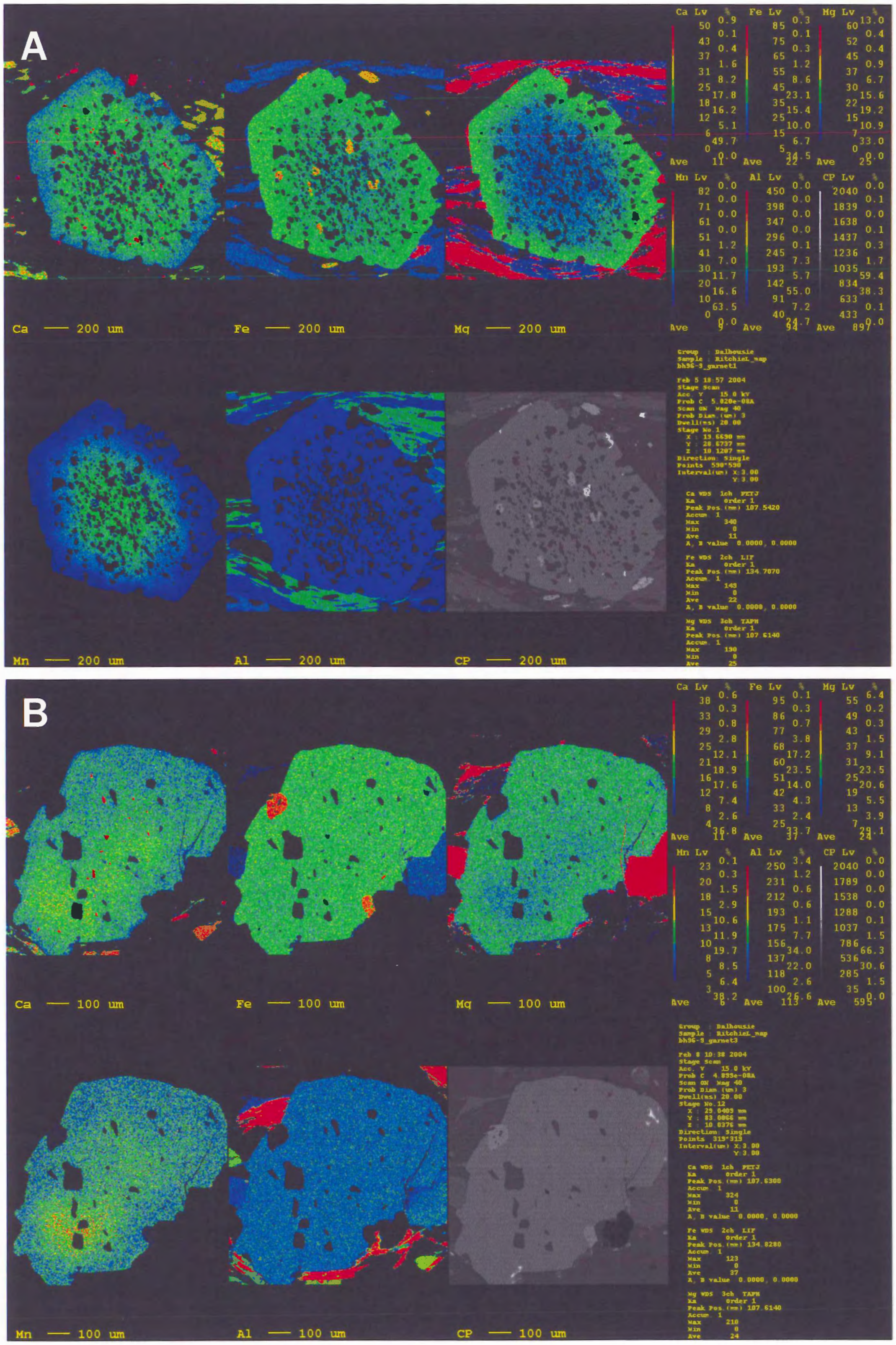

Fig 4-6a,b. Two texturally different garnets from 96-9. Although the zoning in (B) is less pronounced than in (A), it still exhibits the same zoning trends, suggesting that growth occurred simultaneously.

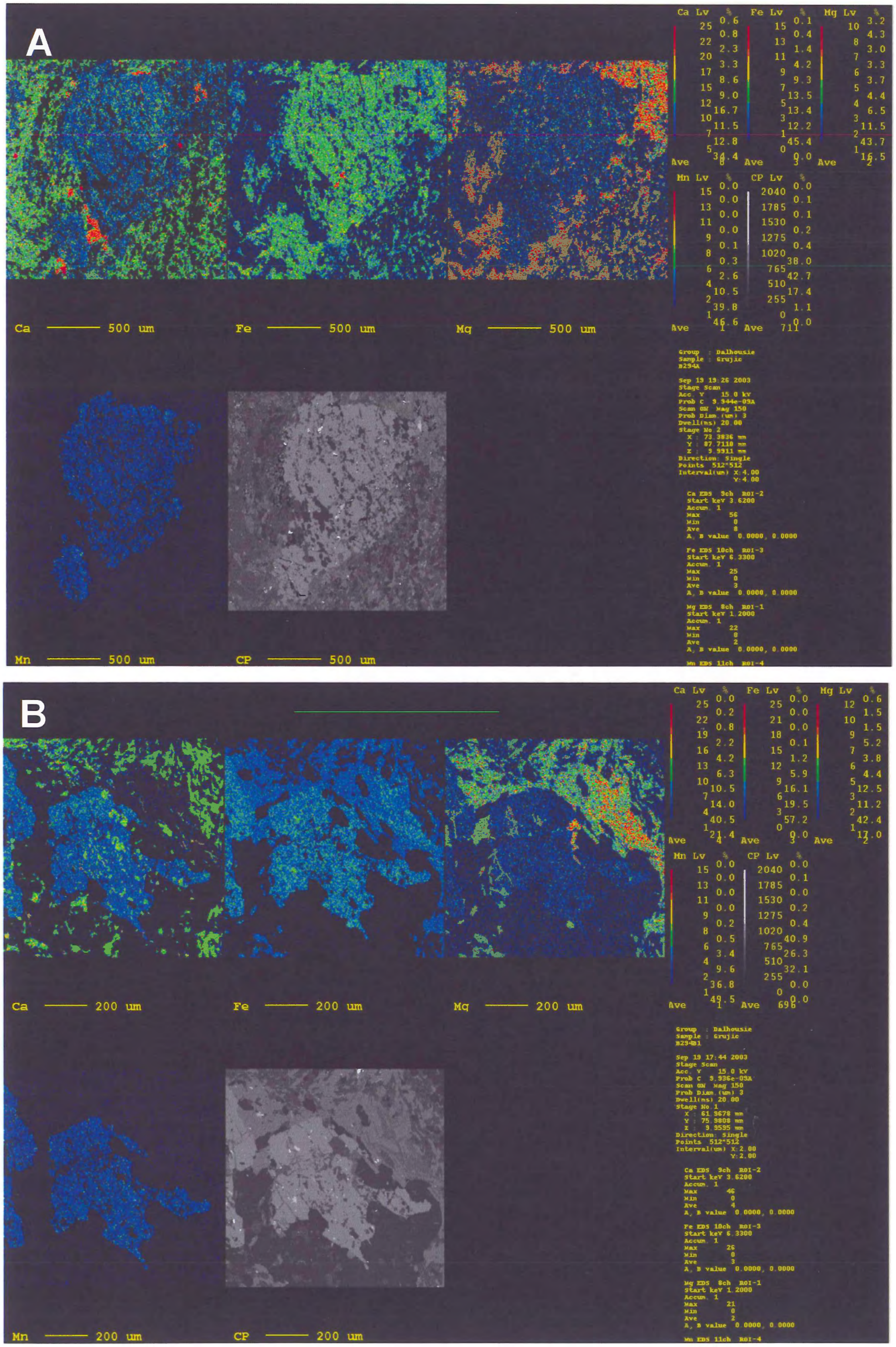

Fig. 4-7a,b. Two representative garnet grains from sample 294 with corroded grain boundaries, exhibiting a homogeneous element distribution.

these garnets is subtle and there appears to be only a small increase in Fe content from core to rim. This zoning pattern in the matrix garnets indicates prograde metamorphism with increasing temperature and pressure and suggests that the garnet rim compositions might be used in thermobarometric calculations for peak temperature.

The garnet zoning profile and element distribution maps for sample 129 show the presence of a compositionally 'flat' rim, suggesting that diffusion has occurred in the rim, homogenizing the rim composition. This observation has implications for the thermobarometry of this sample, suggesting that the rim composition is not at the composition of peak temperature.

In sample 146, a garnet inclusion in plagioclase shows an overall lack of zoning with respect to Fe, Mg and Mn. A narrow Ca-depleted rim likely results from Ca partitioning into the surrounding plagioclase during plagioclase growth or late-stage reaction (Fig. 4-5a).

One matrix garnet mapped in sample 146 with slightly corroded edges has a patchy distribution of Ca, although the relative depletion of Ca from core to rim is similar to that of the other garnets mapped (Fig. 4-5b). The patchy distribution of Ca in the garnet is possibly due to reaction with neighbouring plagioclase grains in the rock. The Ca zoning in this garnet differs from a garnet also from the footwall of the Kakhtang Thrust (Davidson et al. 1997), which showed enrichment of Ca towards the rim.

A euhedral garnet from 96-9 displays a clear zoning pattern consistent with the other zoned grains (Fig 4-6a). A second grain mapped, relatively inclusion-free and with an anhedral shape, has a much less distinct zoning pattern, although the zoning is still present and has a pattern equivalent to that of the euhedral grain (Fig. 4-6b). This

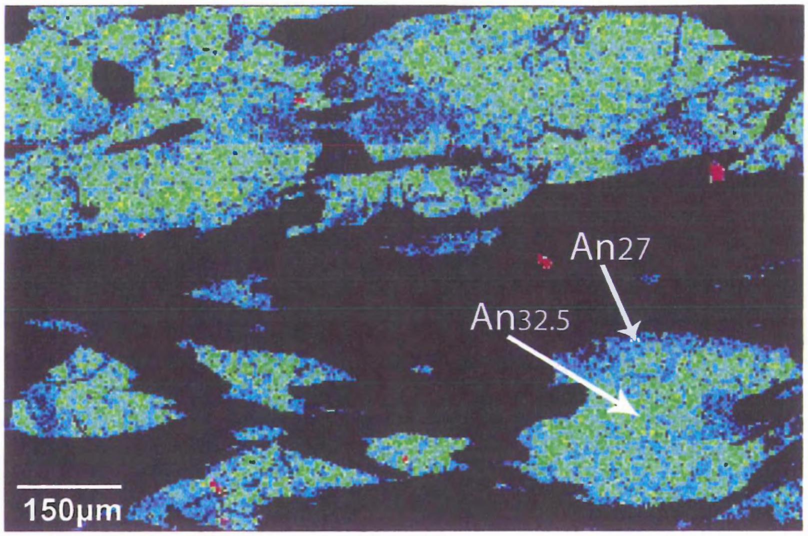

Fig. 4-8. Zoning of Ca in plagioclase matrix grains in sample 96-9. Green to yellow colours represent higher Ca content and darker blue to black indicates relatively low levels of Ca. The anorthite content from point analyses is presented for the core and rim of one grain.

suggests that the two petrographic groups of garnets are actually of the same growth phase.

Garnet grains in 294 do not show any apparent zoning of Ca, Mn, Mg or Fe (Fig. 4-7a,b). The grains in this sample are subhedral with corroded grain boundaries. It is possible then that a garnet dissolution reaction was in progress after garnet growth, as well as the diffusion of these cations towards internal homogeneity. This suggests that the rim compositions of the garnets do not represent peak metamorphic conditions, and uncertainties in P-T estimates will be greater for this sample.

The plagioclase porphyroblast mapped in sample 146 appears to be slightly zoned, with enrichment in calcium from the rim towards the core of the grain. Plagioclase matrix grains in sample 96-9 appear to be zoned with higher anorthite content towards the cores of the grains (Fig. 4-8). None of the staurolite grains in any of the samples appear to have any chemical zoning (Fig. 4-9 through 4-12).

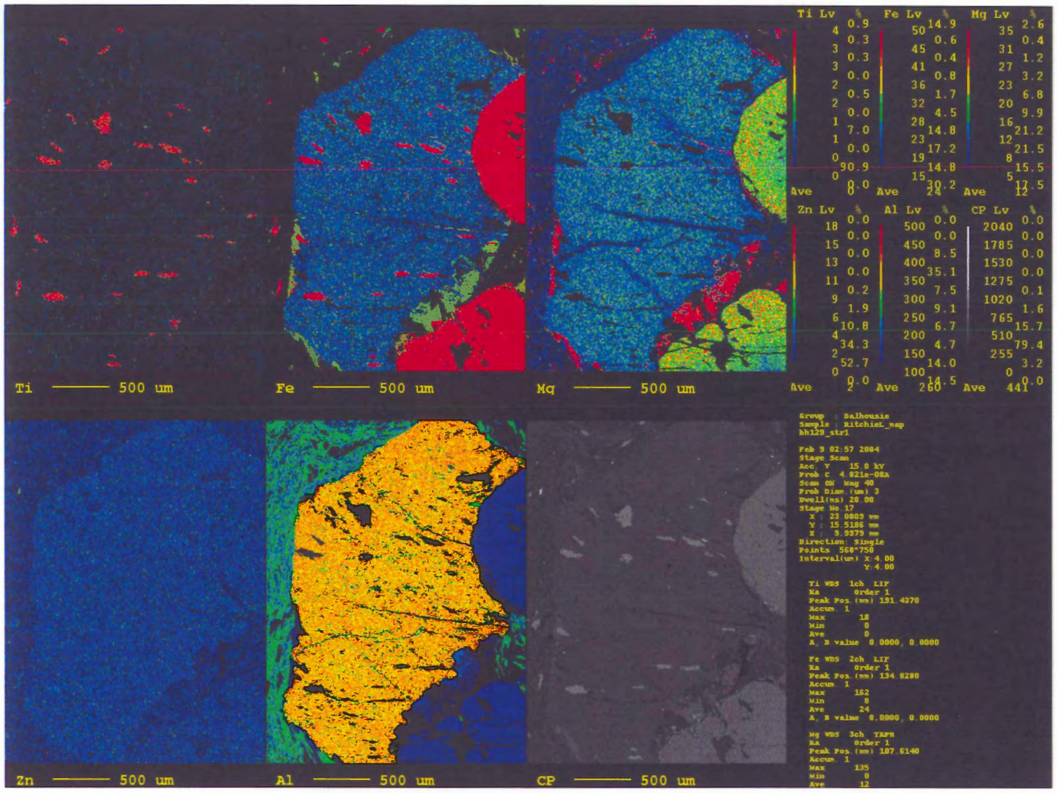

Fig. 4-9. Element distribution maps for a representative staurolite grain from sample 129.

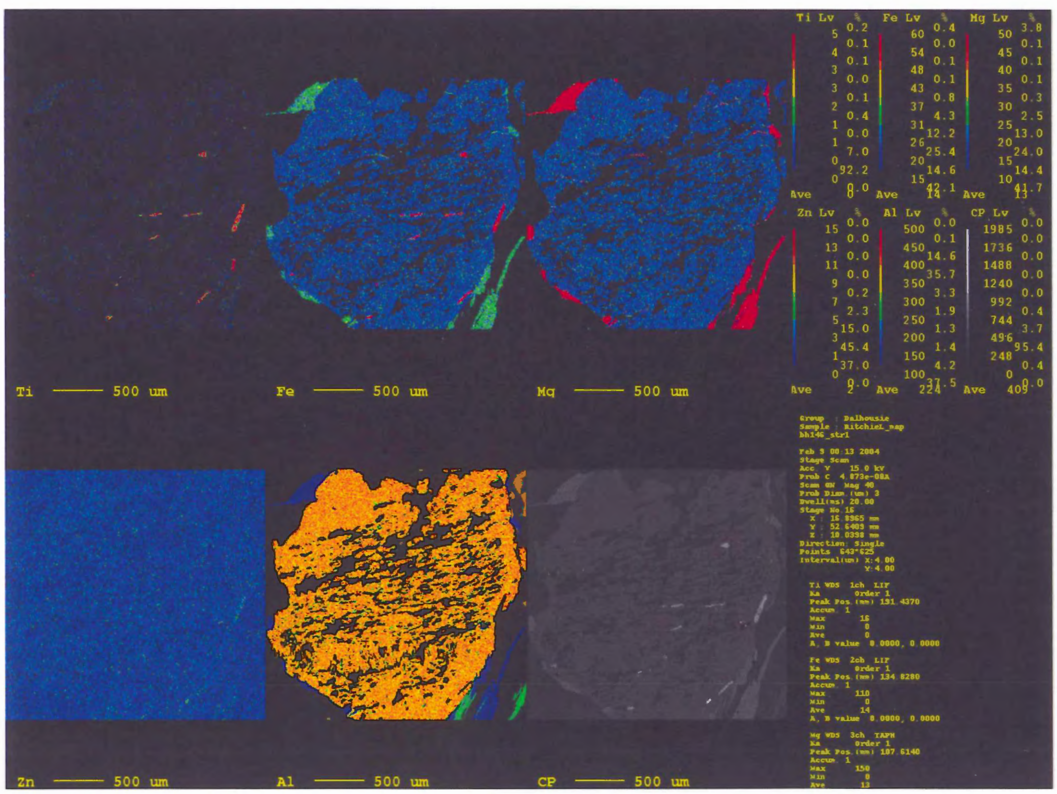

Fig. 4-10. Staurolite grain from sample 146 showing a homogeneous composition.

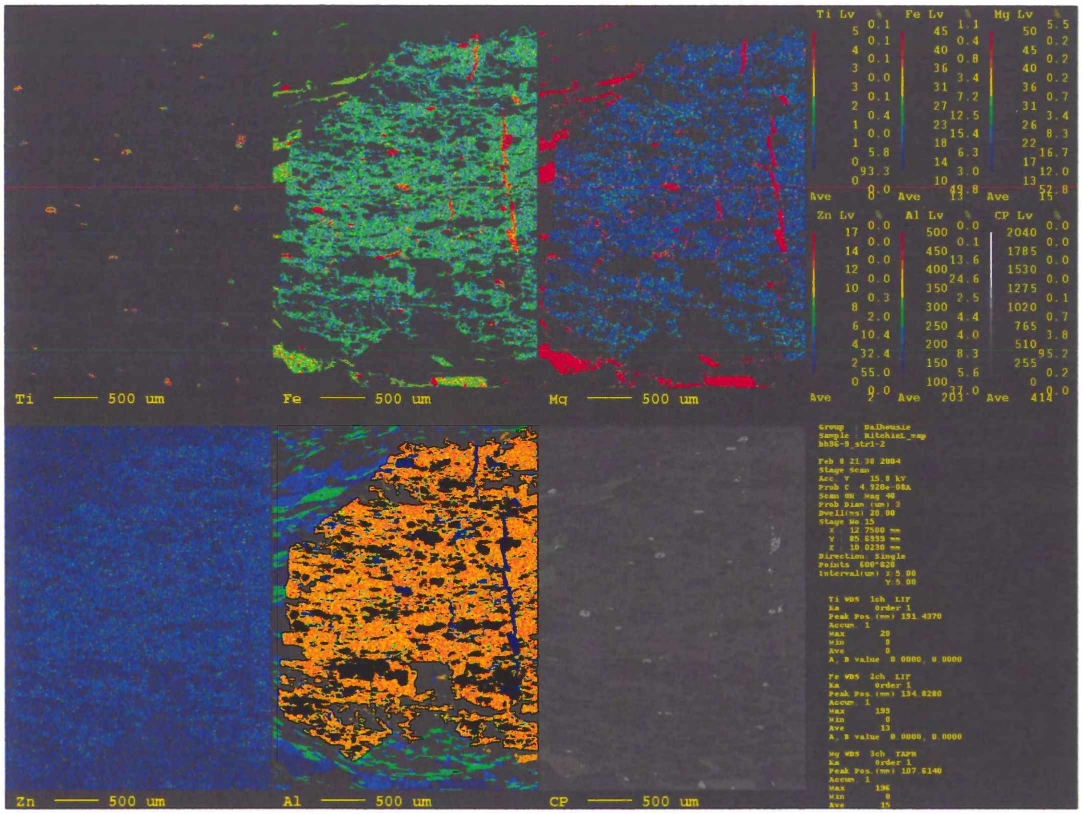

Fig. 4-11. A section of a large, unzoned staurolite grain from sample 96-9.

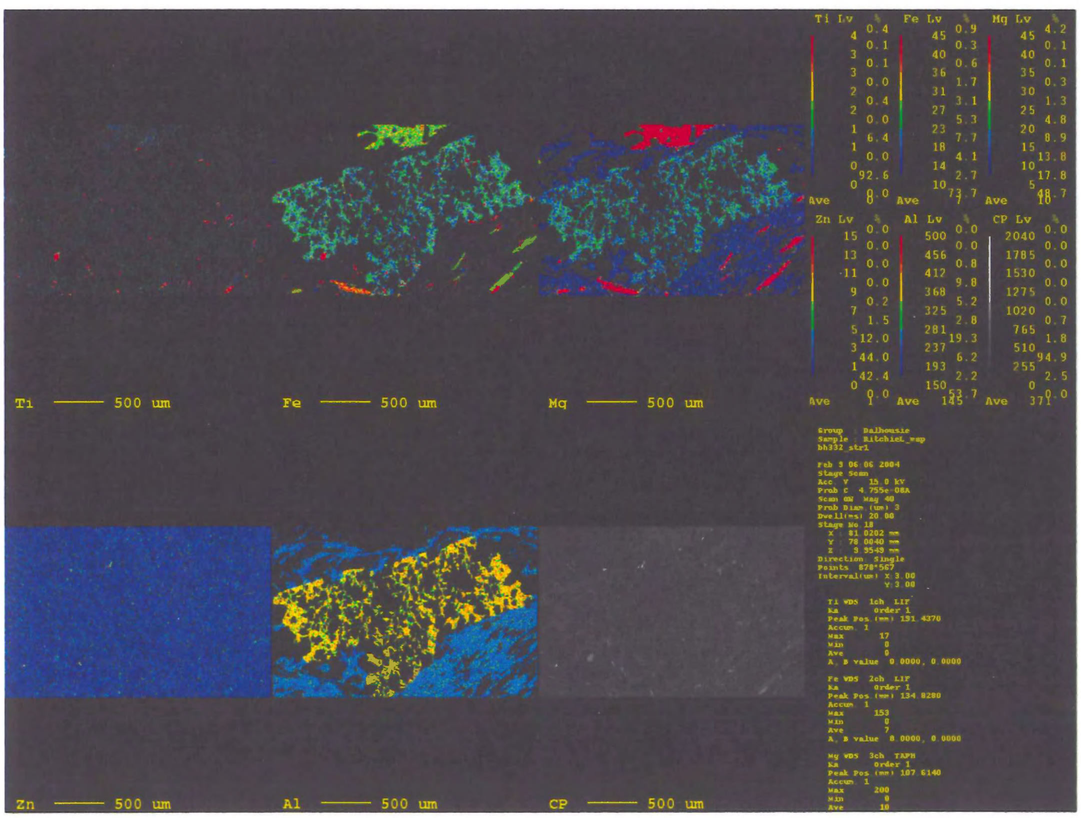

Fig. 4-12. Element distribution maps for an anhedral staurolite grain from 332.

4.3 Thermobarometry of garnet-staurolite and garnet-biotite schists

All thermobarometric estimates were calculated with the program THERMOCALC v.3.21 (Holland and Powell 2001) using the internally consistent dataset of Holland and Powell (1998). Mineral activities of end-members used in the thermobarometric calculations were calculated with the program AX (Holland 1999).

Due to the limitation of the electron microprobe in identifying oxidation states, all iron was measured as ferrous iron during microprobe work. Ferric iron, however, is present in several minerals, particularly biotite and muscovite, used in thermobarometry. To minimize the uncertainties due to the presence and amount of ferric iron in these minerals, no mineral compositions were recalculated for ferric iron. The calculation of P-T estimates without ferric iron increases the precision of the results (decreasing the uncertainty for comparison of the results) although it also adds to the overall uncertainty of the results.

Besides the uncertainty of ferric iron, other uncertainties affecting the thermobarometric calculations presented here include microprobe analytical error, uncertainty in the activity-composition relationships of the minerals used in the calculations and in the calibrations of the thermobarometers used, and petrographical error in selecting the assemblages, grains and points for analysis and use in the calculations. The latter source of uncertainty is subject to such difficulties as identification of equilibrium conditions within grains and between minerals in the samples, and avoiding grains affected by retrograde reactions and diffusional homogenisation of zoning patterns in mineral grains.

End-member activities were calculated for non-ideal solution models (with the exception of staurolite) at temperatures and pressures in agreement with the final pressure and temperature estimates. The level of uncertainty of all P and T estimates are given as $\pm 1\sigma$ of the temperatures and pressures calculated. Wherever possible, multiple independent calculations of the peak metamorphic PT conditions were carried out to ensure the consistency of the results. The output of all THERMOCALC and AX calculations is presented in Appendix III.

Mineral analyses selected for P-T calculations were taken from grains with clean appearances and as often as possible from neighbouring minerals so that compositions that might be as close to equilibrium conditions as possible could be used. Mineral analyses used for the P-T calculations are shown in Appendix III.

Final pressure and temperature estimates for all samples with the exception of 116 and 294 plot within the garnet + biotite + staurolite stability field on a petrogenetic diagram (Fig. 4-13). Calculations for 116 (Paro Metasediments) and 294 (Chekha Formation) from the Chomolhari area of western Bhutan provide higher temperatures and pressures than the staurolite stability field. Neither sample contains staurolite, however, so the P-T calculations are consistent with the petrographic observations. P-T values for sample 122 of the Tang Chu Klippe (Chekha Fm.) plot directly on the staurolite = garnet + biotite + sillimanite boundary within the sillimanite field, in accordance with its mineral assemblage.

Sillimanite is present in three samples for which thermobarometry was carried out. However, only one of these samples, 122, has P-T estimates that plot within the sillimanite stability field. In samples 332 and 146 sillimanite is present as

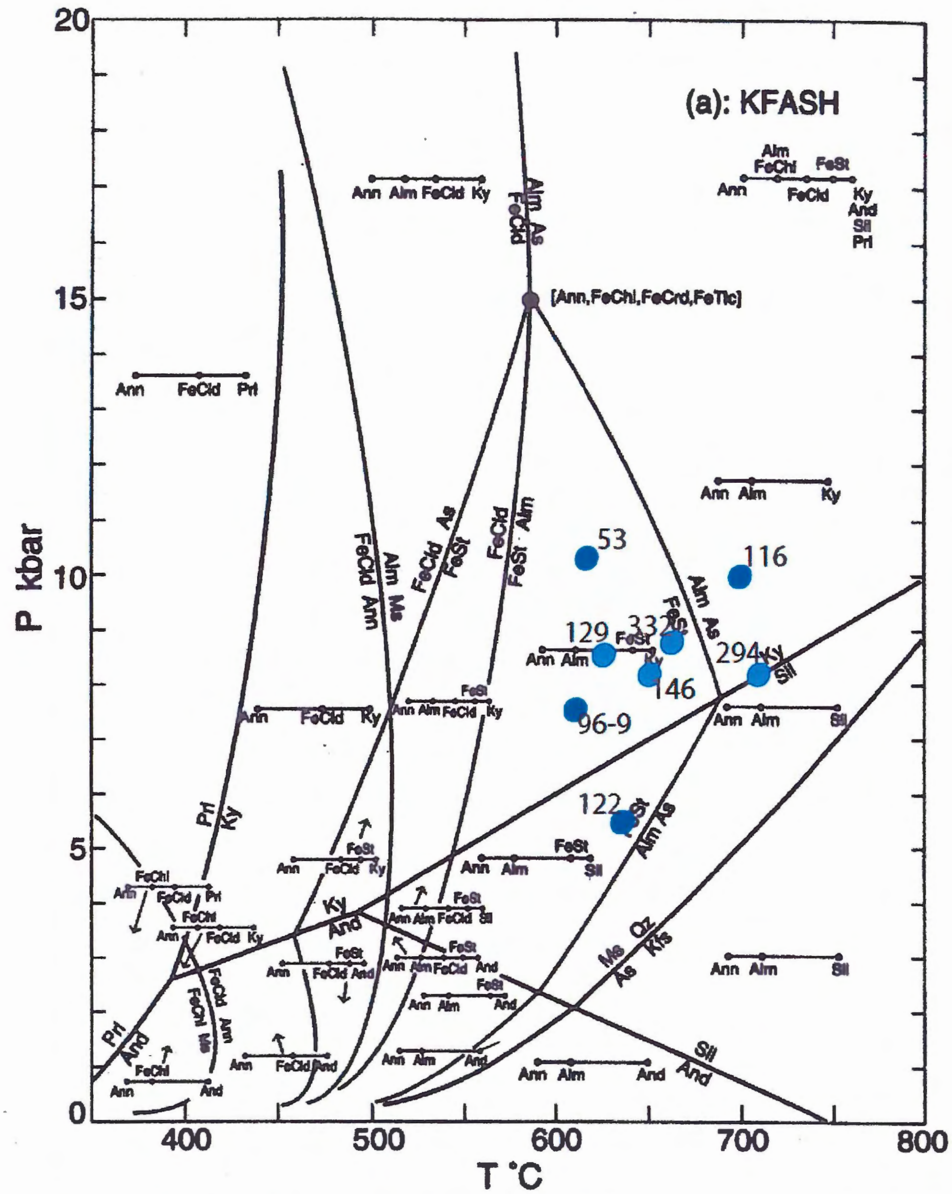

Fig. 4-13. Pressure and temperature calculations plotted on a KFASH petrogenetic grid. See text for explanation. (Spear 1993, after Spear and Cheney 1989)

pseudomorphs after unknown pre-existing minerals. Within the GHS, sillimanite commonly forms by decompression from kyanite- to sillimanite-grade after peak temperature conditions, resulting in sillimanite not being part of the peak metamorphic assemblage (Davidson et al. 1997). In addition, Daniel et al (2003) observed sillimanite replacing kyanite in a zone about 1 km structurally above the MCT. The stability field for garnet + staurolite + biotite + muscovite ± plagioclase suggests that the mineral assemblages in 146 and 332 should represent higher pressures than the sillimanite stability field (Fig. 4-14). Sillimanite therefore, is probably not part of the peak metamorphic assemblage in these samples and so was not used in P-T calculations.

Higher than desirable uncertainty values were obtained from samples 129 and 332, with 1σ values of ±1.9 kbar for pressure and greater than ± 60°C for temperature. These large errors are due to the lack of plagioclase in the assemblage, which is important for providing pressure constraints. The temperature estimate for the peak metamorphism

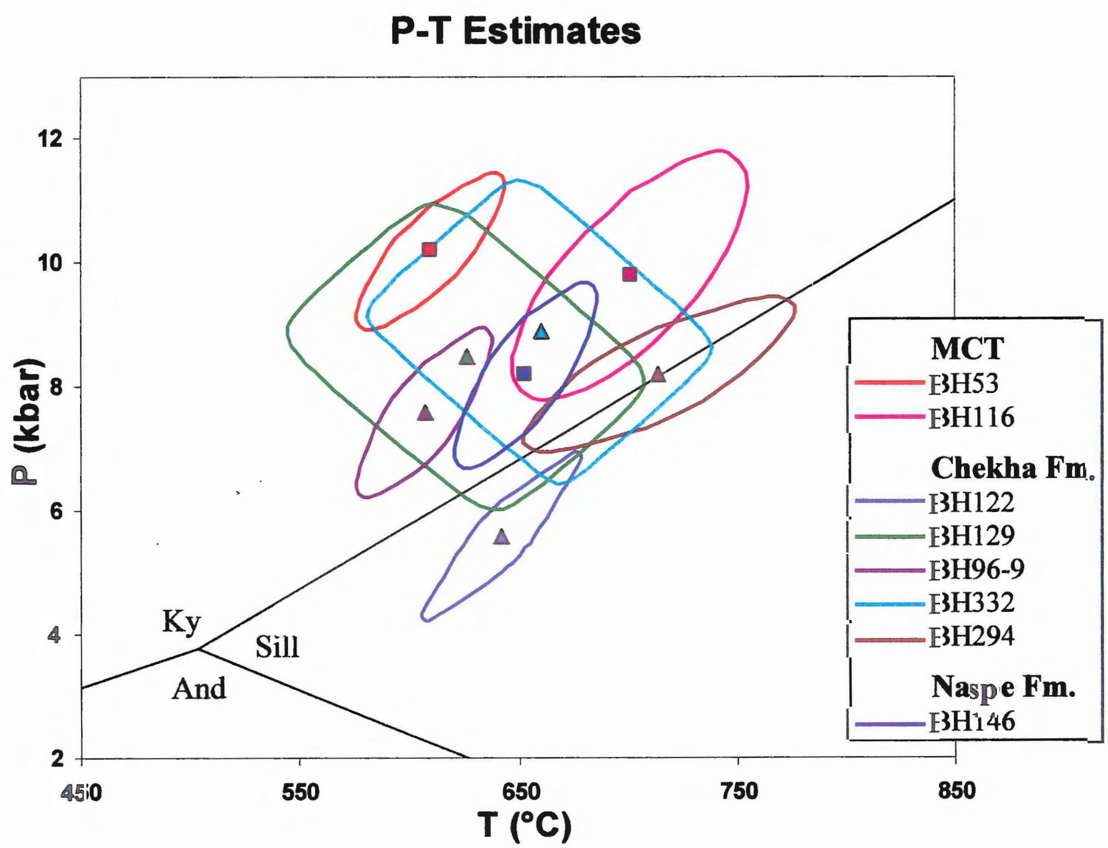

Fig. 4-14. Pressure and temperature estimates plotted with 1σ uncertainties for P and T on aluminum silicate phase diagram (Holdaway and Mukhopadhyay 1993). Adapted from Waters (unpublished).

for sample 294 also has higher uncertainty with 1σ = ±50°C. This is probably explained by the questionable quality of the unzoned, somewhat corroded garnets which suggest that equilibrium may not have been achieved in this sample and that the garnet does not preserve the conditions of peak temperature. This sample also displays the highest peak temperature of the samples studied, indicating the possibility that the high temperature allowed the internal homgenisation of the garnets as observed in the x-ray maps.

When plotted on a phase diagram with uncertainty ellipses (Fig. 4-14), the P-T estimates can be grouped according to the structural level to which they belong. The P-T estimate for the footwall of the MCT (sample 53) has a higher pressure at peak

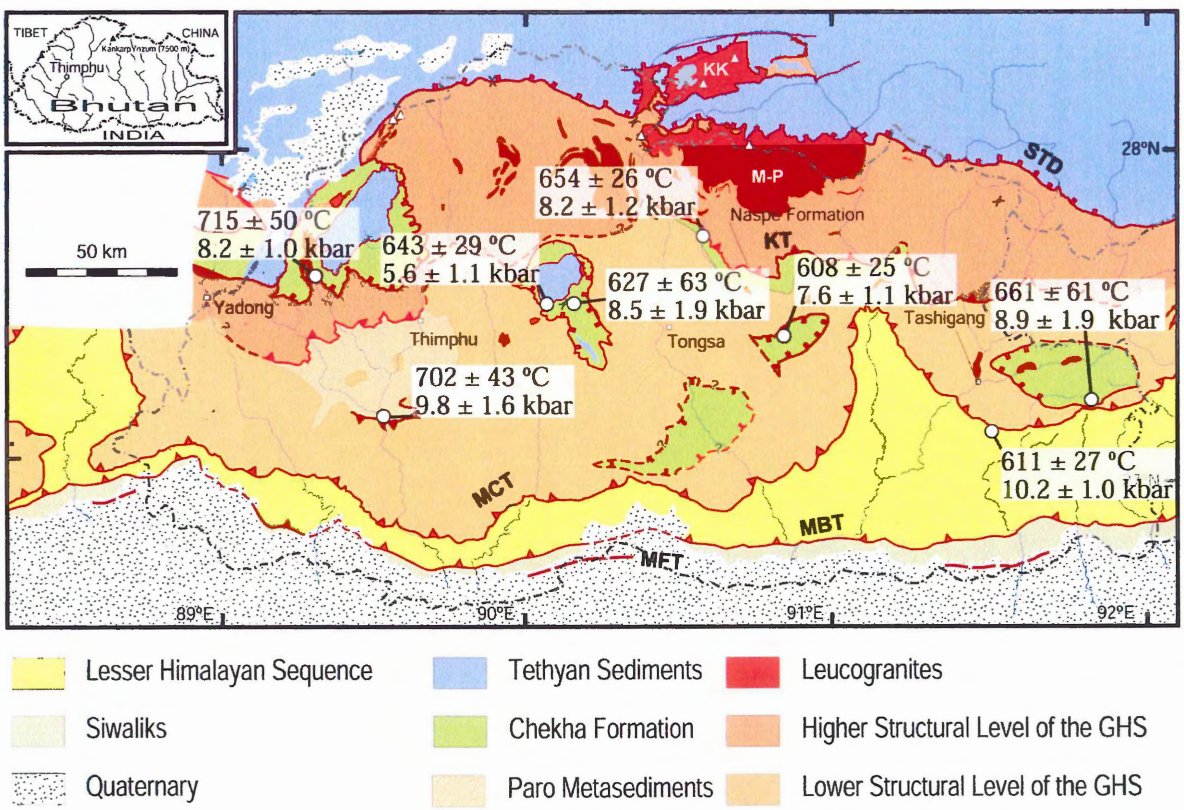

Fig. 4-15. Thermobarometry results of this study. See text for explanation.

temperature (10.2±1.0 kbar) than the other samples, as does the sample (116) from the Paro Metasediments (with a pressure of 9.8±1.6 kbar). For this reason, they are grouped together in this figure (4-14). The other P-T estimates, for the Chekha Formation and the Naspe Formation in the footwall of the Kakhtang Thrust, have lower pressures ranging from 5.6 to 8.9 kbar. Estimates for peak metamorphic temperature (Fig. 4-15) are variable, ranging from 608±25 °C to 715±50 °C.

5 DISCUSSION

5.1 Results

The following is the summary of metamorphic conditions and the inferred kinematics during a dominant deformation event.

5.1.1 Lesser Himalayan Sequence / Main Central Thrust Zone

Garnet-biotite schists within the Jaishidanda Formation (Bhargava 1995) just below the MCT (Fig. 5-1) were deformed under amphibolite-grade conditions, reaching

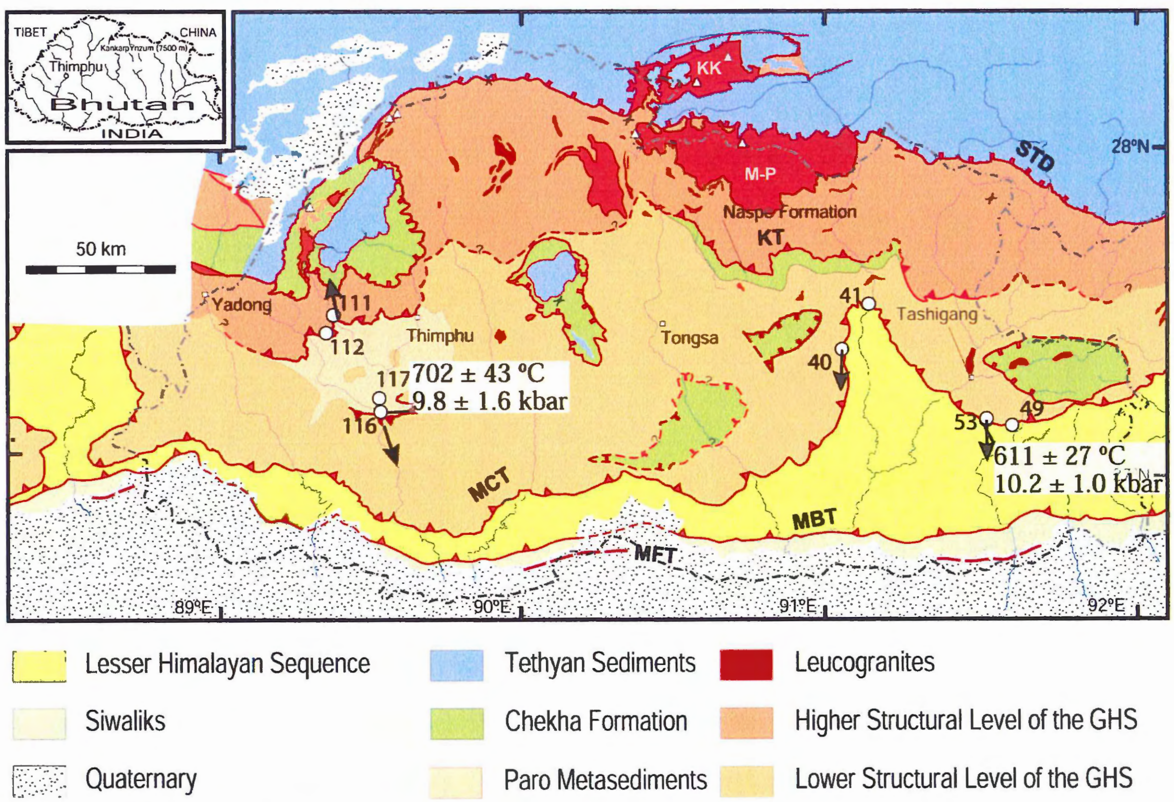

Fig. 5-1. Kinematic observations and P-T estimates for the MCT zone and the Paro Metasediments. Arrows indicate sense of shear.

peak metamorphism at temperatures and pressures of around 600°C and 10 kbar. Deformation during this metamorphic phase involved both pure shear and top-to-the-south shearing.

5.1.2 Paro Metasediments

The Paro Metasediments contain garnet-mica schists that were deformed with a component of pure shear. Two samples in the north of the Paro region unit exhibit top-to-the-north shearing (Fig. 5-1). One of these, 112, may have contained an assemblage of K-feldspar + biotite + cordierite (now possibly weathered to an aluminum-rich clay mineral? such as pyrophyllite), which would have required a peak metamorphic temperature of at least 750°C at a pressure of less than 6 kbar (Spear 1993). Top-to-the-south shear sense is present in the south of the unit in the Paro region, which according to foliation-porphyroblast relationships probably occurred at about the same time as the peak metamorphism at conditions of about 700°C and 9.8 kbar.

5.1.3 Naspe Formation / Kakhtang Thrust

The garnet-staurolite schist of the Naspe Formation in the footwall of the Kakhtang Thrust was deformed with a dominant component of vertical flattening due to pure shear (Fig. 5-2). Deformation roughly coincided with a peak metamorphic temperature of 650°C at a pressure of 8.2 kbar.

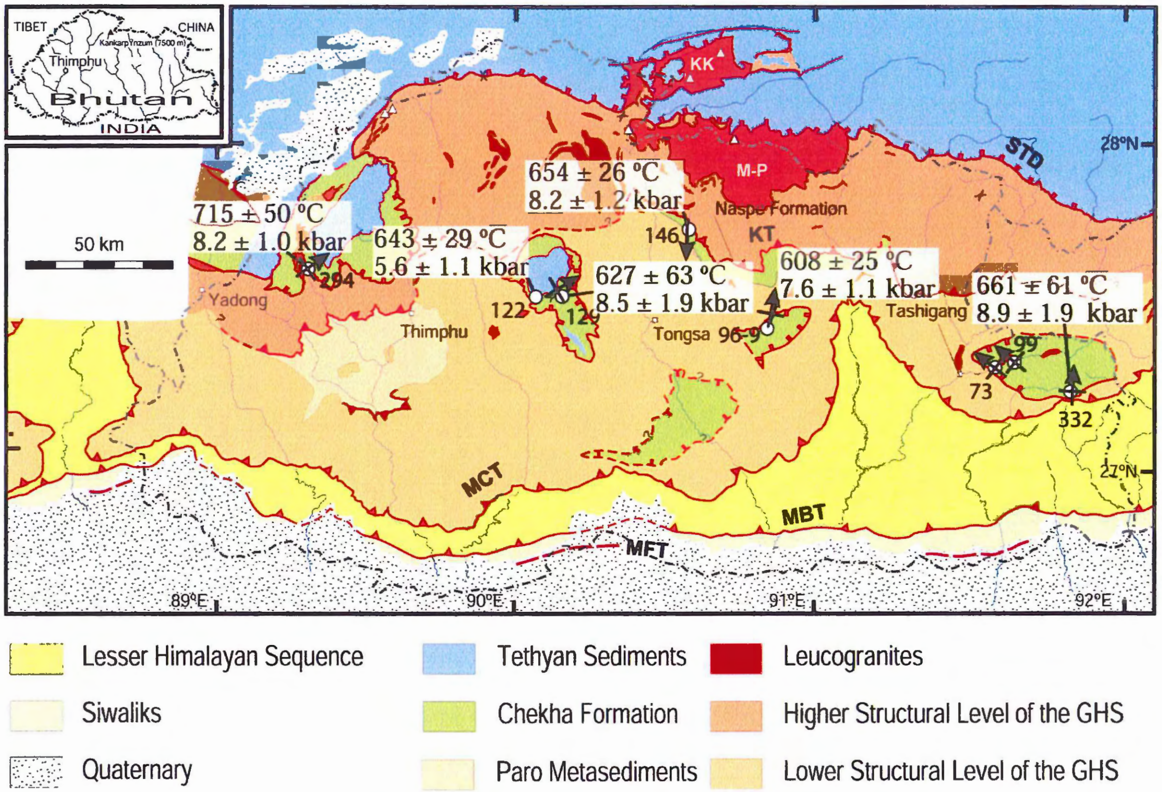

Fig. 5-2. Kinematic observations and P-T estimates for the Chekha Formation and the footwall of the Kakhtang Thrust.

5.1.4 Chekha Formation

The garnet-staurolite schists studied from various localities within the Chekha Formation exhibit similar deformational features (Fig. 5-2). A dominant component of vertical shortening is present in all the samples. Evidence for top-to-the-north and top-to-the-northwest sense of shear is also present. The degree of deformation is variable between samples and relict sedimentary layering is still present in some.

Peak metamorphic conditions are variable between samples. Thermobarometry produces P-T results from near 600°C to 715°C and from 5.6 to 8.9 kbar. Some of the variation is due to different structural position of the samples relative to the contact with the GHS.

5.2 Discussion

The garnet-staurolite schist from the footwall of the Kakhtang Thrust is petrographically and compositionally similar to the garnet-staurolite schists of the Chekha Formation. Gansser (1983) initially included this zone of metasediments with the Paro metasediments. Bhargava (1995), however, mapped this sedimentary sequence as a different unit because of somewhat lower metamorphic grade than the metasediments elsewhere in the GHS. The sample from the Naspe Formation has undergone the same deformation as the Chekha Formation rocks and peak metamorphic conditions are also comparable to those estimated for the Chekha Formation samples. The Naspe Formation can be correlated with the Chekha Formation as a klippe that, prior to erosion, was continuous with the klippen to the south of the Kakhtang Thrust (Fig. 5-3). Field observations (Grujic pers. com.) and lithological descriptions (Bhargava 1995) indicate lithological similarities to the Chekha Formation, which support this reinterpretation of the metasediments in the footwall of the Kakhtang thrust. In addition, the southward increase of metamorphism indicates a right–way up metamorphic sequence, characteristic for the base of the Chekha Formation (Grujic et al. 2002 and Grujic pers. com.).

The Paro metasedimentary unit in the Paro-Thimphu region has previously been interpreted as a window in the GHS although there has been some debate as to whether the Paro metasediments are in fact equivalent to the Lesser Himalayan Sequence to the south (Jangpanji 1978; Gansser 1983; Bhargava 1995). Geological maps of the unit interpret the crystalline rocks of the GHS to be thrusting over the Paro metasediments (i.e. Gansser 1983, Bhargava 1995). Top-to-the-north shear sense in the northern region

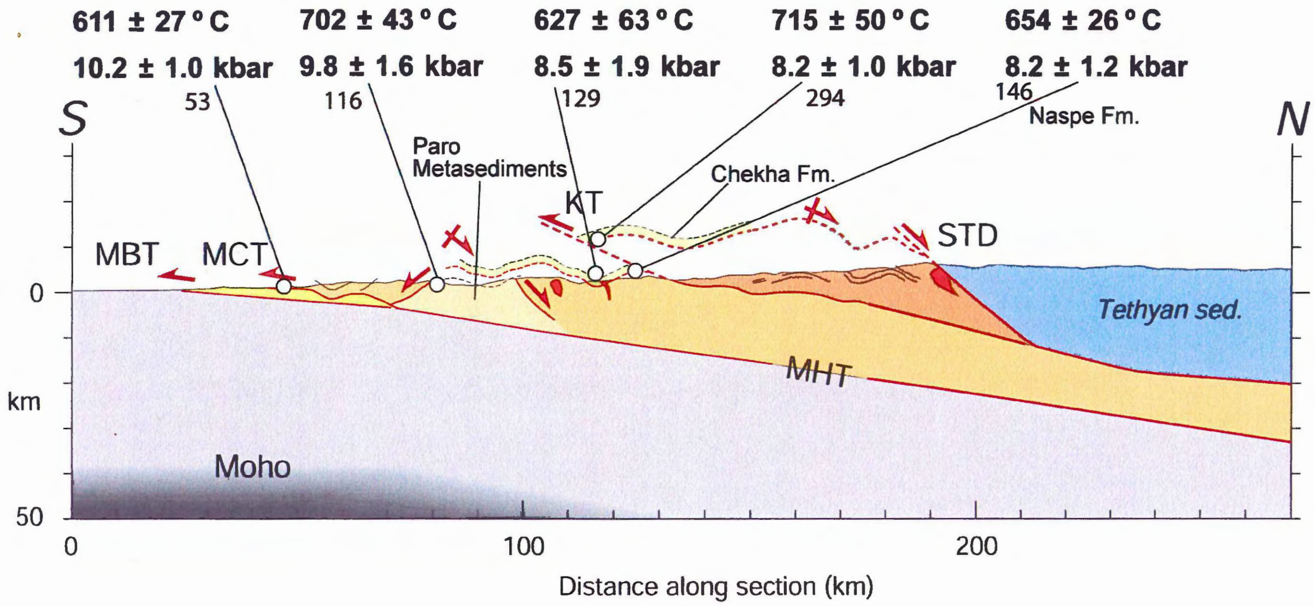

Fig. 5-3. Cross-section of the Bhutan Himalaya showing the interpretation that the Naspe Formation is part of the Tethyan sediments, continuous with the Chekha Fm. klippen. Also shown are the Paro Metasediments as a window that can be correlated to the top of the LHS or to a lower structural level of the GHS.

of this unit and top-to-the-south sense of shear in the south of the unit reinterpret the Paro Metasediments to be bounded by normal faults along which the this unit was being uplifted relative to the surrounding crystalline units of the GHS (Fig. 5-3). P-T estimates for the Paro metasediments are very similar to the estimates from the LHS in the MCT zone (Daniel et al., 2003, this work). It is thus possible that this is a complete window through to the LHS and that the Paro metasediments (i.e. Jaishidanda Formation, in that case) are in fact located below the MCT, however, the penetration or vertical displacement of this 'window' structure is not constrained. This tectonic setting is very similar to the window of the LHS through the GHS along Sutlej valley in the western Himalaya (Vannay et al., 2004).

Although all the samples come from two major shear zones, the MCT and STD respectively, none is a mylonite. Rather, these rocks show a complex deformation history dominated by flattening and production of probably two generations of crenulation cleavage. An earlier one, more developed, resulted in the foliation S_1, and a later one, S_2, developed to various stages, still preserving the S_1. In samples from the Chekha and Naspe Formations the second crenulation is associated with a simple shear component of deformation with top-to-the north sense of shear.

Measurements of quartz lattice-preferred orientation (Grujic et al. 1996; Grasemann et al. 1999; Law et al. 2003) consistently indicate pervasive ductile deformation in the top of the LHS, through the entire section of the GHS and in the Chekha Formation. The inferred sense of shear is consistent with the kinematics of the major shear zones (MCT, Kakhtang Thrust and STD zones). In addition, all the authors observe a pure shear component of the deformation. There is however no consensus on the cause and importance of the flattening. It is generally agreed that the quartz lattice fabric is a late-stage deformation feature (Stipp et al. 2003 and references therein). This study demonstrates that the pure shear deformation along the boundaries of the GHS was more important than previously thought, although some authors have proposed otherwise. The pure shear occurred at two stages, an early one, preceding the peak temperature of metamorphism and the later postdating the peak of metamorphism.

6 CONCLUSIONS

Petrography and geothermobarometry combined with field observations show that garnet-staurolite grade metamorphism occurs in a variety of localities throughout the Bhutan Himalaya, although this assemblage if found in only several structural units:

1) The Chekha Formation which includes several klippen of the STD located throughout the GHS of Bhutan, and also likely correlates with the Naspe Formation in the footwall of the Kakhtang Thrust;
2) The top of the LHS within the MCT zone; and
3) within the Paro metasedimentary unit in the Paro region.

It is possible also that the Paro metasediments are part of the uppermost unit of the LHS with the interpretation that the normal-fault bounding this unit is actually the MCT and the Paro Metasediments are a window to the LHS.

Along the boundaries of the GHS, especially in the Chekha Formation above the GHS, a flattening component dominates over the simple shear component of deformation, even though this boundary is a shear zone and, thus, the opposite would be expected.

The interpretations made here, and the questions raised concerning the true nature of the shear zones bounding the GHS, require further work to fully constrain the tectonic evolution and present geometries observed in the Bhutan Himalaya. Detailed mapping of the Paro region will be an important step in understanding the local structures observed in this area, and possibly also to understanding the boundary zones of the LHS and GHS. Continued thermobarometric work across the Bhutan Himalaya will also aid in the interpretation of the tectonic history of the Bhutan Himalaya and also of the Himalayas in its entirety .

REFERENCES

Beaumont, C., Jamieson, R.A., Nguyen, M.H., and Lee, B. 2001. Himalayan tectonics explained by extrusion of a low-viscosity crustal channel coupled to surface denudation. Nature, **414**: 738-742.

Beaumont, C., Jamieson, R.A., Nguyen, M.H., and Medvedev, S. 2004. Crustal channel flows: 1. Numerical models with applications to the tectonics of the Himalayan-Tibetan orogen. Journal of Geophysical Research, in press.

Beyssac, O., Goffé, B., Chopin, C., and Rouzaud, J.N. 2002. Raman spectra of carbonaceous material in metasediments: a new geothermometer. Journal of Metamorphic Geology, **20**: 859-871.

Bhargava, O.N. 1995. The Bhutan Himalaya: A Geological Account. Geological Survey of India, Calcutta. pp. 245

Burchfiel, B.C., Chen, Z., Hodges, K.V., Liu, Y., Royden, L.H., Deng, C., and Xu, J. 1992. The South Tibetan detachment system, Himalayan orogen: Extension contemporaneous with and parallel to shortening in a collisional mountain belt. Geological Society of America Special Paper, 41.

Burg, J.-P., Brunel, M., Gapais, D., Chen, G.M., and Liu, G.H. 1984. Deformation of leucogranites of the crystalline Main Central Sheet in southern Tibet (China). Journal of Structural Geology, **6**: 535-542.

Chakungal, J., Grujic, D., Dostal, J., and Ghalley, K.S. 2003. Towards understanding eohimalayan tectonics: Do gabbroic cumulates and ultramafics of the Bhutan Himalaya hold the clues? 18th Himalaya-Karakorum-Tibet Workshop, at Ascona, Switzerland.

Daniel, C.G., Hollister, L.S., Parrish, R.R., and Grujic, D. 2003. Exhumation of the Main Central Thrust from Lower Crustal Depths, Eastern Bhutan Himalaya. Journal of Metamorphic Petrology, **21**: 317-334.

Davidson, C., Grujic, D., Hollister, L.S., and Schmid, S.M. 1997. Metamorphic reactions related to decompression and synkinematic intrusion of leucogranite, High Himalayan Crystallines, Bhutan. Journal of Metamorphic Geology, **15**: 593-612.

DeCelles, P.G., and al., e. 2001. Stratigraphy, structure, and tectonic evolution of the Himalayan fold-thrust belt in western Nepal. Tectonics, **20**: 487-509.

Deer, W.A., Howie, R.A., and Zussman, J. 1992. An Introduction to the Rock-Forming Minerals. Longman, Hong Kong, pp.

Edwards, M.A., Kidd, W.S.F., Li, J., Yue, Y., and Clark, M. 1996. Multi-stage development of the southern Tibet detachment system near Khula Kangri: New data from Gonto La. Tectonophysics, **260**: 1-19.

Gansser, A. 1964. Geology of the Himalayas. Wiley Interscience, London, pp. 289.

Gansser, A. 1983. Geology of the Bhutan Himalaya. Birkhäuser, Basel, pp. 181.

Gehrels, G.E., DeCelles, P.G., Martin, A., Ojha, T.P., Pinhassi, G., and Upreti, B.N. 2003. Initiation of the Himalayan orogen as an early Paleozoic thin-skinned thrust belt. GSA Today, **13**: 4-9.

Grasemann, B., Fritz, H., and Vannay, J.-C. 1999. Quantitative kinematic flow analysis from the Main Central Thrust Zone (NW-Himalaya, India): implications ofr a decelerating strain path and the extrusion of orogenic wedges. Journal of Structural Geology, **21**: 837-853.

Grujic, D., Casey, M., Davidson, C., Hollister, L.S., Kündig, R., Pavlis, T., and Schmid, S. 1996. Ductile extrusion of the Higher Himalayan Crystalline in Bhutan: evidence from quartz microfabrics. Tectonophysics, **260**: 21-43.

Grujic, D., Hollister, L.S., and Parrish, R.R. 2002. Himalayan metamorphic sequence as an orogenic channel: insight from Bhutan. Earth and Planetary Science Letters, **198**: 177-191.

Hauck, M.L., Nelson, K.D., Brown, L.D., Zhao, W., and Ross, A.R. 1998. Crustal structure of the Himalayan orogen at ~90° east longitude from Project INDEPTH deep reflection profiles. Tectonics, **17**: 481-500.

Hodges, K.V. 2000. Tectonics of the Himalaya and southern Tibet from two perspectives. Geological Society of America Bulletin, **112**: 324-350.

Holdaway, and Mukhopadhyay. 1993. American Mineralogist, **78**: 298-315.

Holland, T.J.B., and Powell, R. 1998. An internally consistent thermodynamic data set for phases of petrological interest. Journal of Metamorphic Geology, **16**: 309-343.

Jamieson, R.A., Beaumont, C., Nguyen, M.H., and Lee, B. 2002. Interaction of metamorphism, deformation and exhumation in large convergent orogens. Journal of Metamorphic Petrology, **20**: 1-16.

Jamieson, R.A., Beaumont, C., Medvedev, S., and Nguyen, M.H. 2004. Crustal channel flows: 2 Numerical models with implications for metamorphism in the Himalayan-Tibetan Orogen. Journal of Geophysical Research, in press.

Jangpanji, B.S. 1978. Stratigraphy and structure of Bhutan Himalaya. Today and Tomorrow's Printers and Publ., New Delhi. pp. 221-242

Law, R.D., Searle, M.P., and Simpson, R.L. 2004. Strain, deformation temperatures and vorticity of flow at the top of the Greater Himalayan Slab, Everest Massif, Tibet. Journal of the Geological Society of London, **161**: 305-320.

Makovsky, Y., Klemperer, S.L., Liyan, H., and Deyuan, L. 1996. Structural elements of the southern Tethyan Himalaya crust from wide-angle seismic data. Tectonics, **15**: 997-1005.

McKinney, A., Klepeis, K., Grujic, D., and Hollister, L.S. 2001. Structural and kinematic evolution of eathern Bhutan: interplay between thrust faulting and normal faulting in an orogenic wedge. 36th Annual Meeting of the Northeast Section of the Geological Society of America, at Burlington, Vermont.

Myrow, P.M., Hughes, N.C., Paulsen, T.S., Williams, I.S., Parcha, S.K., Thompson, K.R., Bowring, S.A., Peng, S.C., and Ahluwalia, A.D. 2003. Integrated tectonostratigraphic analysis of the Himalaya and implications for its tectonic reconstruction. Earth and Planetary Science Letters, **212**: 433-441.

Najman, Y., and Garzanti, E. 2000. Reconstructing early Himalayan tectonic evolution and paleogeography from Tertiary foreland basin sediments, northern India. Geological Society of America Bulletin, **112**: 435-449.

Najman, Y., Pringle, M., Godin, L., and Oliver, G. 2001. Dating of the oldest continental sediments from the Himalayan foreland basin. Nature, **410**: 194-197.

Nelson, K.D., Zhao, W., Brown, L.D., Kuo, J., Che, J., Liu, X., Klemperer, S.L., Makovsky, Y., Meissner, R., Mechie, J., Kind, R., Wenzel, F., Ni, J., Nabelek, J., Chen, L., Tan, H., Wei, W., Jones, A.G., Booker, J., Unsworth, M., Kidd, W.S.F., Hauck, M.L., Alsdorf, D., Ross, A., Cogan, M., Wu, C., Sandvol, E.A., and

Edwards, M. 1996. Partially molten middle crust beneath southern Tibet: Synthesis of Project INDEPTH Results. Science, **274**: 1684-1688.

Parrish, R.R., and Hodges, K.V. 1996. Isotopic constraints on the age and provenance of the Lesser and Greater Himalayan sequences, Nepalese Himalaya. Geological Society of America Bulletin, **108**: 904-911.

Passchier, C.W., and Trouw, R.A.J. 1996. Microtectonics. Springer-Verlag, Berlin New York, pp. xiii, 289.

Powell, R. 1985. Geothermometry and geobarometry: a discussion. Journal of the Geological Society of London, **142**: 29-38.

Powell, R., and Holland, T. 1994. Optimal geothermometry and geobarometry. American Mineralogist, **79**: 120-133.

Searle, M.P., Simpson, R.L., Law, R.D., Parrish, R.R., and Waters, D.J. 2003. The structural geometry, metamorphic and magmatic evolution of the Everest massif, High Himalaya of Nepal-South Tibet. Journal of the Geological Society, London, **160**: 345-366.

Spear, F.S. 1993. Metamorphic Phase Equilibria and Pressure-Temperature-Time Paths. Mineralogical Society of America, Washington, D.C., pp.

Stipp, M., Stünitz, H., Heilbronner, R., and Schmid, S.M. 2002. The eastern Tonale fault zone: a "natural laboratory" for crystal plastic deformation of quartz over a temperature range from 250 to 700 °C. Journal of Structural Geology, **24**: 1861-1884.

Stünitz, H., and Fitz Gerald, J.D. 1993. Deformation of granitoids at low metamorphic grade. II: Granular flow in albite-rich mylonites. Tectonophysics, **221**: 299-324.

Swapp, S.M., and Hollister, L.S. 1991. Inverted metamorphism within the Tibetan slab of Bhutan: Evidence for a tectonically transported heat-source. Canadian Mineralogist, **29**: 1019-1041.

Vannay, J.-C., Grasemann, B., Rahn, M., Frank, W., Carter, A., Baudraz, V., and Cosca, M. 2004. Miocene to Holocene exhumation of metamorphic crustal wedges in the NW Himalaya: Evidence for tectonic extrusion coupled to fluvial erosion. Tectonics, **23**:

Waters, D. Average P-T Calculations: Excel Spreadsheet. website: http://www.earth.ox.ac.uk/~davewa/pt/tools/avept.xls

APPENDICES

APPENDIX I – PETROGRAPHIC DESCRIPTIONS

SAMPLE: BH96-9
LOCATION: 27° 30’ 51.9”N, 90° 58’ 40.5”E @ 3930 m; E of Sima La
STRUCTURAL SETTING: Ura Klippe – Chekha Fm.
ROCK TYPE: garnet- staurolite- biotite- schist

HAND SAMPLE: N/A

THIN SECTION DESCRIPTION:
MINERALOGY:
MATRIX:

- quartz – 50% of rock; seriate to 0.7 mm in size; anhedral, interlobate (mostly) shape; undulose extinction and subgrains present; irregular grain boundaries with bulging present; some larger grains contain smaller quartz inclusions; weak shape-preferred orientation parallel to macroscopic foliation
- biotite – 15% of rock; seriate to 1.5 mm long; elongate shape; define foliations in rock; lattice- and shape-preferred orientation; few contain small radiogenic minerals as evidenced by pleochroic haloes
- muscovite – 15% of rock; seriate to 1 mm long; elongate shape; define foliations in rock; lattice- and shape-preferred orientation
- plagioclase – 5% of rock; seriate to 0.5 mm; anhedral polygonal shape; optically has composition of An_{30}; continuous to tapering albite twinning; some undulose extinction and subgrains present; smooth grain boundaries, often embayed by micas; weak shape-preferred orientation
- ilmenite and magnetite – trace; anhedral grains <0.3 mm in size
- chlorite – <5% of rock; replacement textures with biotite; also occurs in staurolite fractures; few grains bent
- tourmaline – trace; ~0.05 mm; euhedral

PORPHYROBLASTS:

- garnet – 2 petrographic groups:
    1) 1-2 mm in size; euhedral; poikiloblastic with inclusions of quartz and few ilmenite, magnetite and apatite; rims with relatively few inclusions ~0.2 mm wide; inclusion trails generally curved/ sinusoidal, oblique to matrix foliation
    2) 0.5-1.0 mm in size; subhedral; poorly formed faces; few inclusions
- staurolite – anhedral-subhedral; some simple/penetration twinning; poikiloblastic with inclusions of quartz; inclusion trails straight; few fractures
- biotite – 1.5-3 mm long; bladed shape with tapered ends; some internal kinking/bending present; lattice- and shape-preferred orientation

STRUCTURES:

- foliation S_1 – schistosity defined by planar alignment of mica minerals
- weak crenulation foliation S_2 – defined by micas
- shear bands – most prominent set ~40° clockwise from S_1, some ~20° clockwise from S_1, a less prominent set associated with garnet and staurolite grains is ~30° counter clockwise from S_1
- straight inclusion trails in staurolites, parallel to sub-parallel with external S_1, are continuous with external foliation
- quartz-rich strain shadows around θ-type garnet porphyroblasts, in line with S_1
- quartz-rich strain shadows around biotite porphyroblasts – symmetrical, in line with S_1

Relative age diagram of minerals and structures:

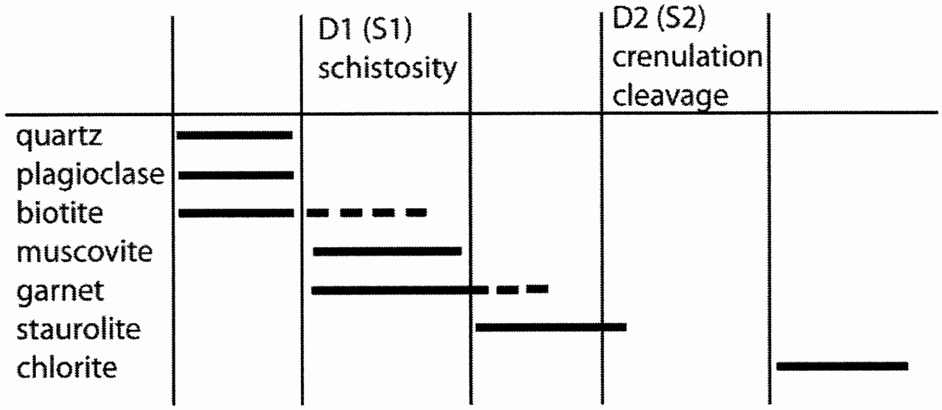

SAMPLE: BH 332
LOCATION: 27° 16.209N, 91° 55.685E; at Radi
STRUCTURAL SETTING: Sakteng Klippe – Chekha Fm.
ROCK TYPE: garnet- staurolite- biotite schist

HAND SAMPLE: fine-grained light brown-coloured schist with about 30% porphyroblasts; white mica and quartz-rich matrix; staurolite grains 2-25 mm; biotite books 2-5 mm in size; garnets 1-3 mm in size; staurolite contains inclusions of garnet and biotite

THIN SECTION DESCRIPTION:
MINERALOGY:
MATRIX:
- quartz – 40% of rock; seriate to 2 mm; anhedral; polygonal to interlobate shape; undulose extinction to subgrains present; bulging; pinning by muscovite; left-over grains present; smooth to embayed grain boundaries
- biotite – 1% of rock; seriate to 1 mm long; elongate; lattice- and shape-preferred orientation
- muscovite – 30% of rock; seriate to 3 mm long; grains folded; lattice- and shape-preferred orientation; defines foliations
- sillimanite – trace; occurs a fibrolite aggregates in matrix; shape-preferred orientation with dominant foliation
- ilmenite – 1% of rock; 0.01-0.1 mm in size; subhedral to anhedral; elongate grains have shape-preferred orientations to foliations
- tourmaline – trace; relatively abundant; 0.05 mm in size
- chlorite – trace; 0.5 mm; platy; overgrows foliations; internal microkinking

PORPHYROBLASTS:
- garnet – 2% of rock; 1-3 mm; euhedral to subhedral; grains highly fractured with parallel fractures; fine-grained inclusions of quartz, ilmenite, tourmaline; straight inclusion trails
- staurolite - 10% of rock; 1-20 mm in size; euhedral to subhedral; poikiloblastic with inclusions of quartz, ilmenite, biotite, and some garnet; straight inclusion trails
- biotite – 15% of rock; books 1-5 mm in size; inclusions of quartz, ilmenite, tourmaline; some monazite +/- other radiogenic minerals; straight inclusion trails; undulose extinction; some internal microkinking; some replacement textures by chlorite
- sillimanite – 1 grain: completely replaces another unknown mineral as a pseudomorph; hexagonal; 2.5 mm in size; inclusions of quartz, ilmenite and some muscovite; straight inclusion trails

STRUCTURES:

- foliation S_1 – planar foliation defined by muscovite; observed in microlithons of S_2
- well-developed crenulation cleavage S_2 – dominant foliation in rock; defined by muscovite; overprints S_1 at a high angle
- inclusion trails in garnet, staurolite and biotite porphyroblasts not parallel to dominant external foliation, S_2

Relative age diagram of minerals and structures:

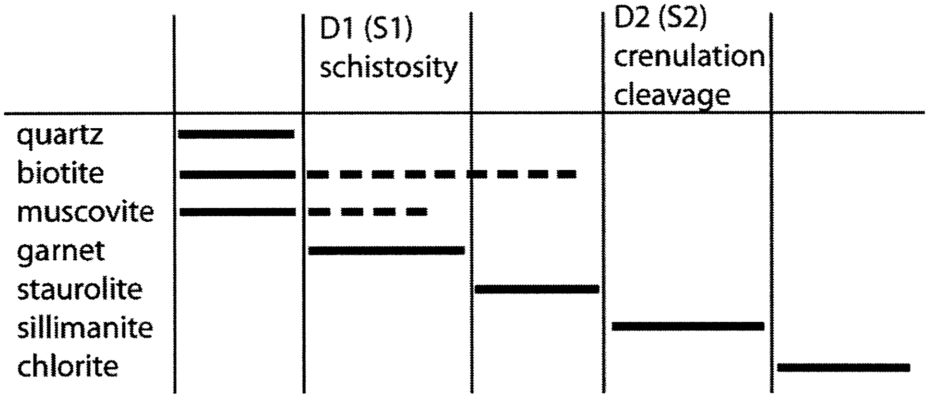

SAMPLE: BH294
LOCATION: 27° 41.933N, 89° 17.507E @ 3550 m; at Chomolhari
STRUCTURAL SETTING: Lingshi syncline, Chekha Fm.
ROCK TYPE: garnet- biotite schist

HAND SAMPLE: light-medium grey-brown coloured schist; fine-medium grained; white coloured layer parallel veins ~3-4 mm thick, associated with green-coloured mineral; quartz and biotite-rich matrix with garnet and biotite porphyroblasts

THIN SECTION DESCRIPTION:
MINERALOGY:
MATRIX:

- quartz – 50% of rock; seriate to 0.25 mm; anhedral to subhedral; polygonal with some interlobate grains; smooth grain boundaries; undulose extinction; pinning by biotite
- plagioclase – 15% of rock; seriate to 0.2 mm; anhedral, interlobate; irregular grain boundaries; albite twinning, mostly tapering; some tapering pericline twinning; undulose extinction
- biotite – 15% of rock; inequigranular <0.3mm and 0.5-1 mm long; elongate; shape and lattice-preferred orientation; defines foliations
- muscovite - <5% of rock; fine-grained, 0.1-0.2 mm long; lattice- and shape-preferred orientation
- chlorite – 10% of rock; seriate to 2 mm; replacement textures with biotite; growth in places not oriented with dominant foliation
- calcite + dolomite - <5% of rock; associated with quartz-rich layers (veins?); anhedral, polygonal; equigranular 0.1-0.25 mm
- opaque minerals – trace; <0.5 mm in size; anhedral; polygonal to irregular shape
- tourmaline – trace; euhedral grains <0.3 mm

PORPHYROBLASTS:

- garnet – anhedral grains 1-3 mm in size; embayed grain boundaries; poikiloblastic with inclusions of quartz and some biotite; inclusion trails straight to slightly curved
- biotite – 1-2.5 mm, weak shape-preferred orientation parallel to dominant matrix foliation; inclusions of quartz; poorly defined inclusion trails are straight

STRUCTURES:

- foliation S_1 – planar schistosity defined by biotite and muscovite
- crenulation foliation S_2 – symmetric crenulation foliation defined by folding of S_1; at stage 1 of development
- internal foliation of biotite porphyroblasts is discordant and at high angles to S_1
- inclusion trails of garnet porphyroblasts are discordant and at angles to S_1
- strain shadows occur around garnets, in line with S_1

- according to observations, it is possible that S_i of garnets and biotites is actually S_1, matrix schistosity is S_2 and crenulation foliation is S_3

Relative age diagram of minerals and structures:

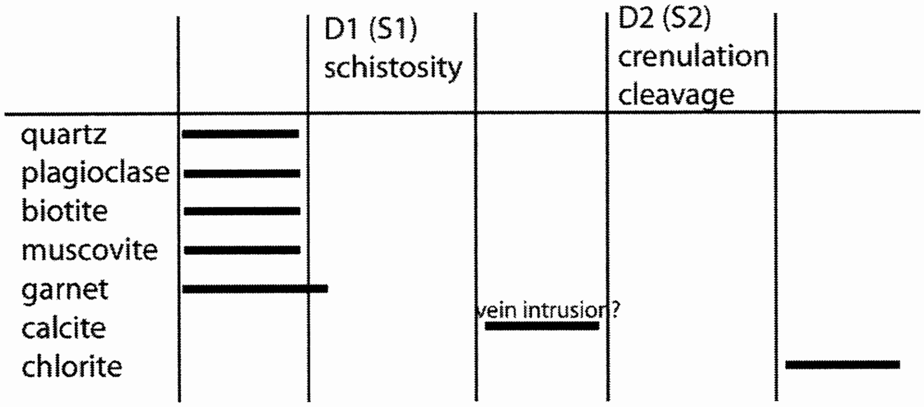

OR:

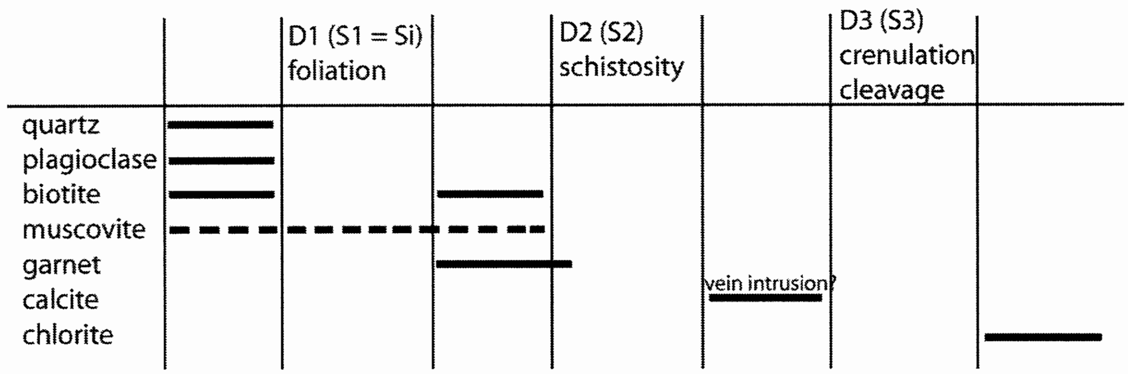

SAMPLE: BH 146
LOCATION: Near to 27° 45.837N, 90° 43.425E; at Kakhtang
STRUCTURAL SETTING: Footwall of Kakhtang Thrust; Naspe Fm.
ROCK TYPE: garnet- staurolite schist

HAND SAMPLE: medium-grained schist of grey-brown colour; crenulated foliation; matrix of quartz, biotite and white mica; garnet 1-4 mm; staurolite grains 1-7 mm in size

THIN SECTION DESCRIPTION:
MINERALOGY:
MATRIX:

- quartz – 40% of rock; inequigranular to 0.5 mm and 1-2.5 mm in size; anhedral; interlobate to near polygonal shape; undulose extinction; few subgrains present; smooth to irregular/embayed grain boundaries
- muscovite – 5% of rock; seriate to 1.5 mm long; elongate shape; defines foliations of rock; some grains are bent; lattice- and shape-preferred orientation
- biotite – 15% of rock; seriate to 3 mm; elongate, platy shape; defines foliations; lattice- and shape-preferred orientation
- plagioclase – 10% of rock; seriate to 1 mm; anhedral, rounded; smooth to irregular grain boundaries; some continuous to tapering albite and pericline twinning; some undulose extinction; optically has composition of An_{15}
- sillimanite – trace; very fine-grained fibrolite mats occur in matrix associated with biotite; crenulated
- ilmenite – 1% of rock; seriate to 0.5 mm; subhedral to anhedral
- chlorite – trace; very fine-grained; occurs in fractures through garnets

PORPHYROBLASTS:

- garnet – 2% of rock; 1-4 mm in size; euhedral to subhedral shape; fractured; few inclusions of quartz, ilmenite and very fine-grained opaque mineral (graphite?); straight inclusion trails where present
- staurolite – 10% of rock; 0.5-7 mm in size; euhedral to subhedral; straight grain boundaries; penetration twinning; fractured; inclusions of quartz, ilmenite, very fine-grained opaque mineral, and rare muscovite; inclusion trails gently curved; some grains have rims with relatively few inclusions, especially with respect to the very fine-grained opaque mineral
- plagioclase – 2-5 mm in size; anhedral interlobate; albite and pericline twinning – continuous to tapering; some microkinking; inclusions of quartz, biotite, ilmenite and some staurolite, garnet and muscovite; curved inclusion trails

STRUCTURES:

- foliation S_1 – schistosity defined by planar alignment of mica minerals – observed in microlithons of quartz and plagioclase; perpendicular to dominant matrix foliation S_2
- crenulation foliation S_2 – defined by folding of biotite and muscovite grains into dominant matrix foliation; stage 4 of development
- curved inclusion trails in staurolite and plagioclase grains, sub-parallel to dominant external foliation, S_2

Relative age diagram of minerals and structures:

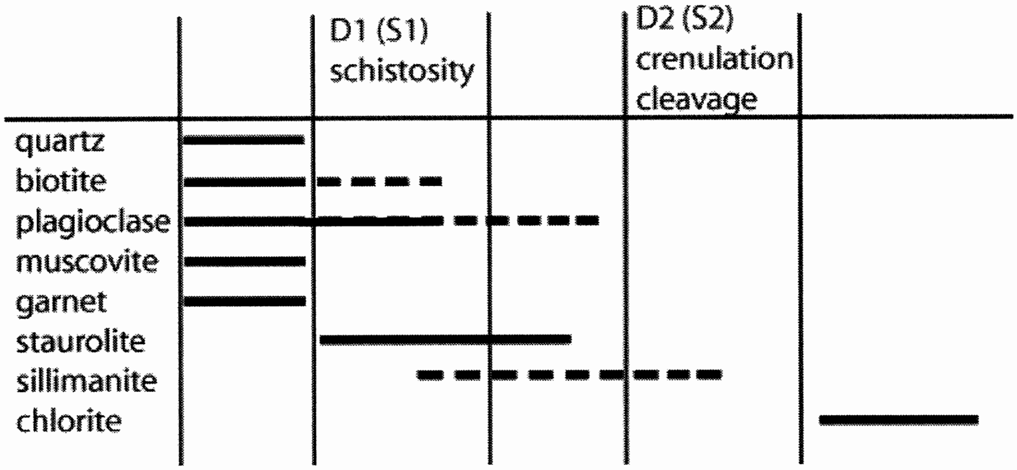

SAMPLE: BH 129
LOCATION: 27° 30.712, 90° 17.918; at Pele La
STRUCTURAL SETTING: Tang Chu Klippe – Chekha Fm.
ROCK TYPE: graphitic garnet-staurolite schist

HAND SAMPLE: fine-grained rock, very dark grey in colour; iron-oxide staining on weathered surfaces; schistosity with crenulation cleavage; white-coloured pressure shadows around garnet grains 0.5-2.5 mm in size; also staurolite grains 1-6 mm in size

THIN SECTION DESCRIPTION:
MINERALOGY:
MATRIX:

- quartz – 30% of rock; seriate to 1 mm in size; anhedral shape; strongly interlobate; undulose extinction to subgrains present; irregular, embayed grain boundaries
- biotite – 1% of rock; equigranular size of about 0.2 mm; elongate shape; shape- and lattice-preferred orientation
- muscovite – 20% of rock; seriate to 1 mm long; elongate shape; defines foliations in rock; shape- and lattice-preferred orientation
- graphite – 30% of rock; fine-grained with fibrous shape; defines foliations in rock; shape-preferred orientation
- ilmenite – trace; subhedral grains; ~0.05 mm in size
- chlorite – trace; replacement textures with biotite

PORPHYROBLASTS:

- garnet – 10% of rock; 0.5-2.5 mm in size; euhedral to subhedral shape; few inclusions of quartz and ilmenite and trace apatite; also very fine-grained opaque inclusions (graphite?) that may define indistinct inclusion trails; commonly fractured; Fe-oxide staining along fractures and on outer surfaces
- staurolite – 10% of rock; 1-5 mm in size; euhedral shape; penetrative twinning present; high concentration of graphite inclusions, with some quartz and ilmenite; inclusion trails, S_i, defined by graphite; inclusion trails are straight with some slightly curved towards the rims; some graphite inclusions form anastomosing pattern around quartz inclusions

STRUCTURES:

- foliation S_1 – schistosity defined by planar alignment of graphite and mica minerals in microlithons of crenulation cleavage; folded into S_2
- crenulation foliation S_2 – spaced foliation defined by planar alignment of graphite and mica minerals; well-developed, stage 3
- quartz-rich pressure shadows θ-type garnet porphyroblasts are parallel to S_2; S_2 is deflected around garnets
- S_i of staurolites is continuous with dominant external foliation, S_2; S_i occurs at an angle to S_2

Relative age diagram of minerals and structures:

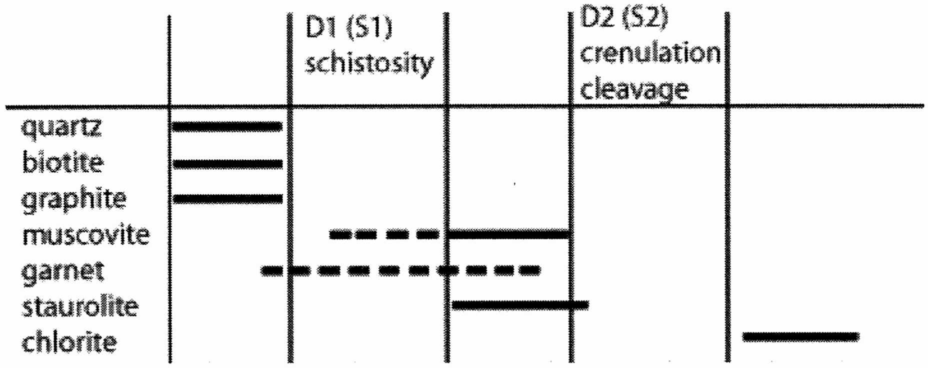

SAMPLE: BH 128
LOCATION: Pele La?
STRUCTURAL SETTING: Tang Chu Klippe – Chekha Fm.
ROCK TYPE: graphitic garnet-staurolite schist

HAND SAMPLE: fine-grained rock, dark grey in colour; weathered surfaces somewhat yellowed; schistosity with crenulation cleavage; white-coloured pressure shadows around garnet grains to 2 mm in size; also staurolite grains

THIN SECTION DESCRIPTION:
MINERALOGY:
MATRIX:

- quartz – 30% of rock; seriate to 0.5 mm; anhedral; strongly interlobate; undulose extinction to subgrains present; irregular, embayed grain boundaries; subgrain boundaries also embayed; bulging present
- graphite – 20% of rock; fine-grained; fibrous; defines foliations
- biotite – 1% of rock; equigranular about 0.3 mm in size; elongate shape
- muscovite – 20% of rock; seriate to 0.5 mm in size; elongate shape; defines foliations
- ilmenite – trace; anhedral; less than 0.1 mm in size

PORPHYROBLASTS:

- garnet – 15% of rock; euhedral to anhedral; 0.5-2.0 mm in size; fractured with Fe-oxide staining in fractures and on outer surfaces of grains; few inclusions of quartz, ilmenite and very fine-grained graphite; inclusions occur in core of grains, with inclusion-free rims
- staurolite – 10% of rock; 0.5-1.5 mm; euhedral to subhedral; penetrative twinning present; high concentration of very fine-grained graphite inclusions, with few inclusions of quartz and ilmenite; inclusion trails, S_i, defined by graphite; S_i is straight to slightly curved

STRUCTURES:

- foliation S_1 – schistosity defined by planar alignment of graphite and mica minerals in microlithons of crenulation cleavage; folded into S_2
- crenulation cleavage S_2 – spaced foliation defined by planar alignment of graphite and mica minerals; well-developed?; anastomosing around microlithons
- quartz-rich pressure shadows associated with garnet grains are parallel to S_2; S_2 is deflected around garnets
- S_i of staurolites is continuous with dominant external foliation, S_2
- S_i of staurolite occurs parallel or at angles to S_2
- some strain shadows around staurolite, in line with S_2

Relative age diagram of minerals and structures:

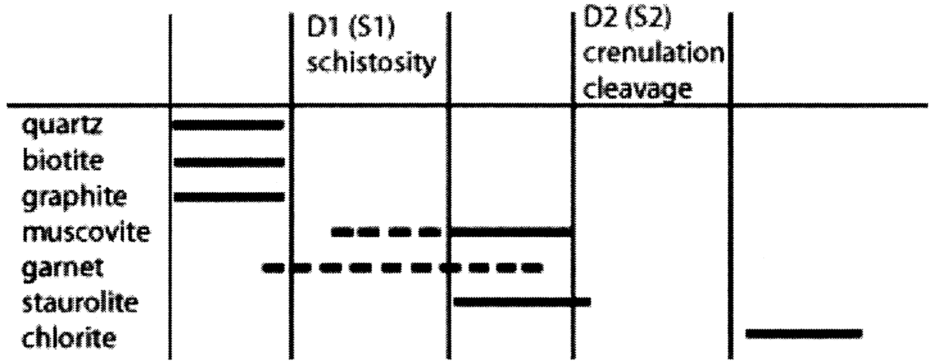

SAMPLE: BH122
LOCATION: 27° 32.883N, 90° 01.271E
STRUCTURAL SETTING: Tang Chu Klippe – Chekha Fm.
ROCK TYPE: garnet schist

HAND SAMPLE: fine-grained schist of light-medium grey colour; quartz-rich; planar foliation; euhedral garnet porphyroblasts 2-3mm in size; compositional layering of coarser biotite-rich layers and finer quartz-rich layers

THIN SECTION DESCRIPTION:
MINERALOGY:
MATRIX:

- quartz – 70-80% of rock; seriate to 1 mm; anhedral; interlobate; undulose extinction to subgrains present; irregular, embayed grain boundaries; bulging present in places; weak shape-preferred orientation parallel to main foliation
- biotite – 15% of rock; seriate to 1 mm long; elongate shape; lattice- and shape-preferred orientation; defines continuous schistosity
- muscovite – <1% of rock; elongate grains 0.3-1 mm long; grains oriented subparallel to dominant matrix foliation
- plagioclase – 5% of rock; seriate to 0.5 mm; anhedral; rounded to polygonal shape; some with albite twinning; undulose extinction; An(30)
- opaque minerals – trace; very fine-grained; rounded, equigranular shape
- sillimanite – very fine-grained fibrolite forming elongate aggregates; associated with biotite in matrix; aggregates occur parallel to foliation, although individual fibrolite needles radiate from aggregate

PORPHYROBLASTS:

- garnet – <1% of rock; 1-3 mm; subhedral to anhedral, poorly formed shape; inclusions of quartz, opaque minerals, plagioclase; no clear inclusion trails; have parallel fractures that extend through the grains

STRUCTURES:

- compositional layering S_0 – observed as changes in biotite content forming poorly defined layers in rock; layer thickness on the scale of cm's
- foliation S_1 – planar, continuous schistosity defined by orientation of biotite in matrix
- possible weak crenulation foliation S_2 – weak, stage 1 folding of biotite observed in biotite-rich layer
- much muscovite occurs discordant to main foliation S_1, overgrowing S_1 at high angles
- pressure shadows of dynamically recrystallized quartz occur around garnets, parallel to S_1

Relative age diagram of minerals and structures:

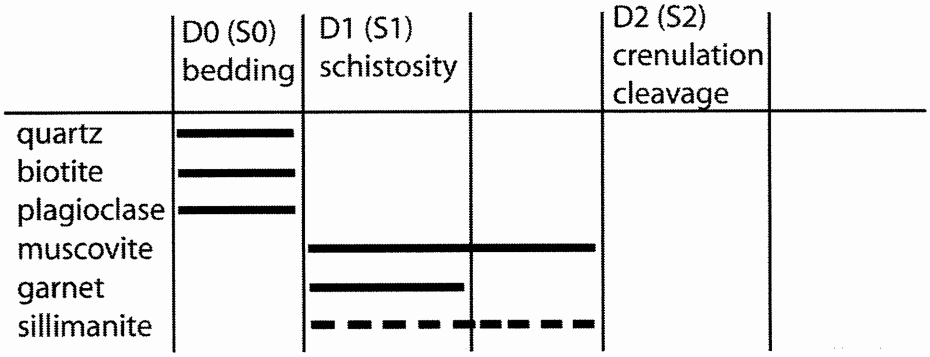

SAMPLE: BH117
LOCATION: 27° 09.669N, 89° 32.606E @ ca. 2400 m; at Bunaka
STRUCTURAL SETTING: GHS – Paro Metasediments
ROCK TYPE: garnet-quartz schist

HAND SAMPLE: medium-grained schist of yellow-white colour; compositional zoning parallel to macroscopic foliation – garnet-rich layer 1.5 cm thick of red-brown 2-7 mm grains; possible dextral shear sense (i.e. top-to-the south) observed from white mica foliation wrapping around garnet grains.

THIN SECTION DESCRIPTION:
MINERALOGY:
MATRIX:

- quartz – >50% of rock; inequigranular <0.5 mm and 0.5-1 mm; anhedral; interlobate to polygonal shape; undulose extinction; few subgrains present; generally embayed, irregular grain boundaries, some smooth boundaries; some bulging
- muscovite – 20% of rock; elongate shape to 2 mm long; lattice- and shape-preferred orientation; defines foliation
- feldspar – 5% of rock; seriate 0.3-0.5 mm, anhedral; elongate shape; embayed grain boundaries; contains some inclusions of quartz, muscovite
- opaque minerals – trace; anhedral; <0.3 mm in size
- chlorite – trace; grains <0.2 mm; associated with garnet fractures

PORPHYROBLASTS:

- garnet – 20% of rock; euhedral to subhedral, equant shape; 1-7 mm in size; poikiloblastic with inclusions of biotite, quartz, opaque minerals. K-feldspar; inclusion trails straight to curved; fractured; some have hematite on outer surfaces

STRUCTURES:

- foliation S_1 – continuous schistosity defined by preferred orientation of micas
- foliation S_1 wraps around garnets, with minor strain shadows of quartz present in line with S_1
- a weak crenulation cleavage S_2 is possible – interference of garnet porphyroblasts however makes determination of the cleavage trend difficult

Relative age diagram of minerals and structures:

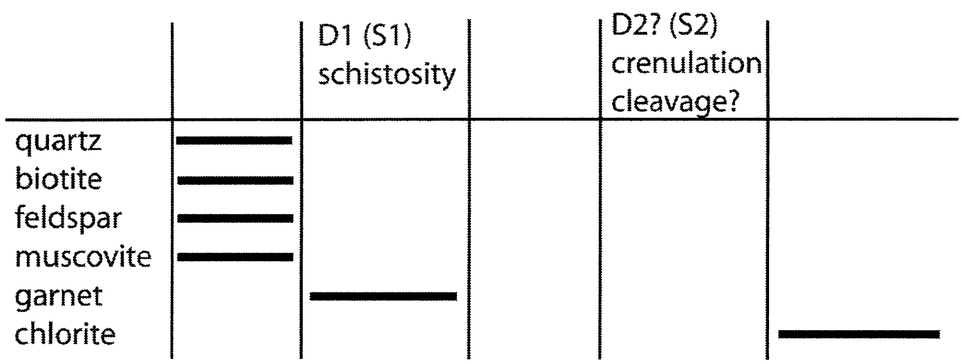

SAMPLE: BH116
LOCATION: 27° 08.698N, 89° 32.999E + 1 km south @ ca. 2300 m; at Bunaka
STRUCTURAL SETTING: GHS – Paro Metasediments
ROCK TYPE: garnet-biotite schist

HAND SAMPLE: medium-dark grey-coloured schist, fine-grained; planar schistosity; compositional layering parallel to foliation defined by lighter-coloured layer

THIN SECTION DESCRIPTION:
MINERALOGY:
MATRIX:

- quartz – 70% of rock; equigranular 0.1-0.3 mm; anhedral; strongly interlobate to polygonal; irregular, smooth to embayed grain boundaries; undulose extinction; subgrains; subgrain boundaries generally irregular; bulging; weak shape-preferred orientation parallel to main foliation
- plagioclase – 10% of rock; equigranular 0.1-0.3 mm; anhedral; polygonal; smooth to embayed grain boundaries; albite twinning; some simple twinning; some pinning with biotite
- biotite – 10% of rock; grains 0.1-0.5 mm long; lattice- and shape-preferred orientation; defines foliation
- muscovite – 5% of rock; to 0.5 mm long; elongate; lattice-and shape-preferred orientation; defines foliation
- opaque minerals – trace; <0.2 mm; anhedral; equant to elongate shape

PORPHYROBLASTS:

- garnet – rounded shape; embayed grain boundaries; poikiloblastic with inclusions of quartz and some opaques, biotite, muscovite; inclusion trails slightly curved

STRUCTURES:

- foliation S_1 – well-defined spaced schistosity defined by muscovite and biotite; microlithons of quartz and plagioclase; parallel to possible compositional layering S_0
- garnet inclusion trails S_i not continuous with external foliation; occur at high angles to S_1
- strain shadows of quartz around garnets in line with S_1 ; possible sigma-type with dextral shear sense

Relative age diagram of minerals and structures:

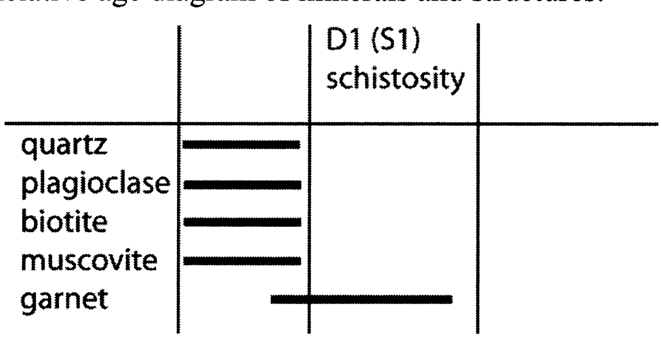

SAMPLE: BH 112
LOCATION: 27° 22.151N, 89° 20.969E @ 3988 m; at Jule La
STRUCTURAL SETTING: GHS; Paro metasediments
ROCK TYPE: graphitic feldspar schist

HAND SAMPLE: fine-grained schist of medium grey colour; quartz and graphite-rich matrix; grey-coloured, soft mineral grains to 5 mm in size

THIN SECTION DESCRIPTION:
MINERALOGY:
MATRIX:
- quartz – 30% of rock; seriate to 2 mm in size; anhedral; interlobate; undulose extinction - subtle to not present; irregular to smooth grain boundaries
- biotite – 1% of rock; seriate 0.2-0.8 mm long; bladed shape; shape- and lattice-preferred orientation
- muscovite – 25% of rock; seriate to 0.5 mm long; elongate shape; shape- and lattice-preferred orientation; defines foliations
- K-feldspar – 10% of rock; 0.5-1 mm in size; anhedral; rounded elongate shape
- opaque minerals (including graphite?) – 10% of rock; rounded blebs less than 0.1 mm in size and platy, elongate grains (graphite?) to 0.5 mm long – defines foliations

PORPHYROBLASTS:
- garnet –
- K-feldspar – 1-4 mm in size; anhedral; rounded, elongate shape; few ribbon grains; subtle undulose extinction; smooth to irregular grain boundaries; shape-preferred orientation; opaque inclusions; straight inclusion trails
- unknown mineral? – 1-5 mm in size; rounded shape; dark under crossed polarized light; poikiloblastic with inclusions of quartz, K-feldspar, opaque minerals and some muscovite; inclusion-free rims; a weathering product?
- muscovite – few grains 1-3 mm long; bladed shape with tapered ends; inclusions of very fine-grained opaque minerals; straight inclusion trails

STRUCTURES:
- foliation S_1 – planar foliation defined by muscovite and opaque minerals; observed in microlithons; folded by crenulations
- crenulation cleavage S_2 – well developed foliation defined by muscovite, biotite and opaque minerals; stage 4 of development
- dominant external foliation S_2 is deflected around clay mineral grains and K-feldspar porphyroblasts; some strain shadows of quartz and K-feldspar present around these grains

- internal foliation of K-feldspar porphyroblasts is not continuous with dominant external foliation and occurs at high angles to S_2
- K-feldspar grains have shape-preferred orientation with S_2
- muscovite porphyroblasts have internal foliation that is subparallel to but continuous with S_2

Relative age diagram of minerals and structures:

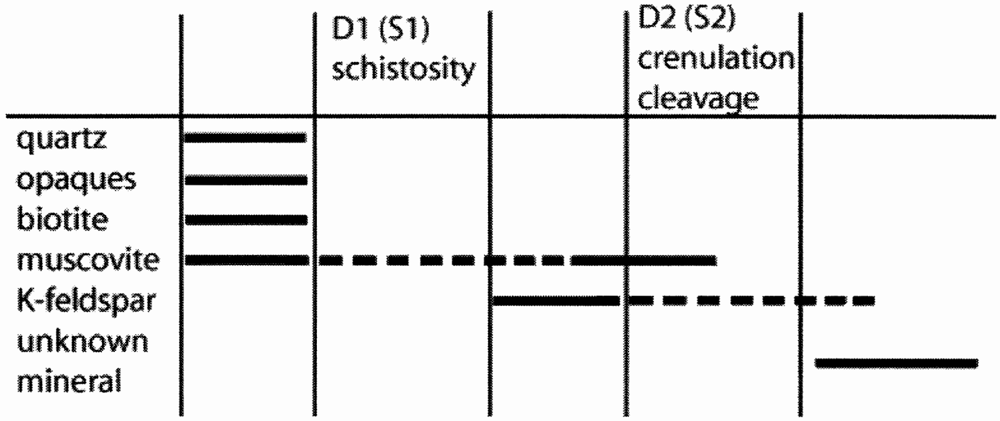

SAMPLE: BH111A
LOCATION: 27° 26.940N, 89° 25.394E @ 2260 m; at Paro
STRUCTURAL SETTING: GHS – Paro Metasediments
ROCK TYPE: sillimanite schist

HAND SAMPLE: medium-grained schist of light grey colour; crenulation foliation with fold of wavelength 1-2 cm

THIN SECTION DESCRIPTION:
MINERALOGY:
MATRIX:

- quartz – 60% of rock; seriate to 2 mm; anhedral; interlobate; undulose extinction; few subgrains present; smooth to irregular, embayed grain boundaries; some bulging; weak shape-preferred orientation parallel to main foliation
- biotite – <5% of rock; seriate to 2 mm long; elongate shape; contains inclusions of zircon +/- other radiogenic minerals; lattice- and shape-preferred orientation; defines foliations
- muscovite – 30% of rock; to 4 mm long; bladed shape; folded into crenulations; lattice- and shape-preferred orientation; defines foliations
- feldspar – 5% of rock; inequigranular <0.5 mm, 0.5-1.5mm; anhedral elongate shape; some interlobate; undulose extinction; some pinning by micas; shape-preferred orientation parallel to dominant foliation
- sillimanite –1% of rock; very fine-grained fibrolite in aggregates; replaces biotite in matrix
- opaque minerals – trace; <0.2 mm; anhedral elongate shape

PORPHYROBLASTS:

- sillimanite – occurs as pseudomorphs after porhyroclasts of other unknown mineral; equant shape; 3 mm in size; inclusions of quartz, feldspar, muscovite and biotite

STRUCTURES:

- foliation S_1 – planar spaced schistosity defined by muscovite and biotite
- crenulation foliation S_2 – defined by folding of biotite and muscovite, overprinting S_1
- strain shadows of quartz and feldspar around sillimanite pseudomorphs; in line with S_1
- elongate biotite and muscovite grains are folded at hinges of crenulations

Relative age diagram of minerals and structures:

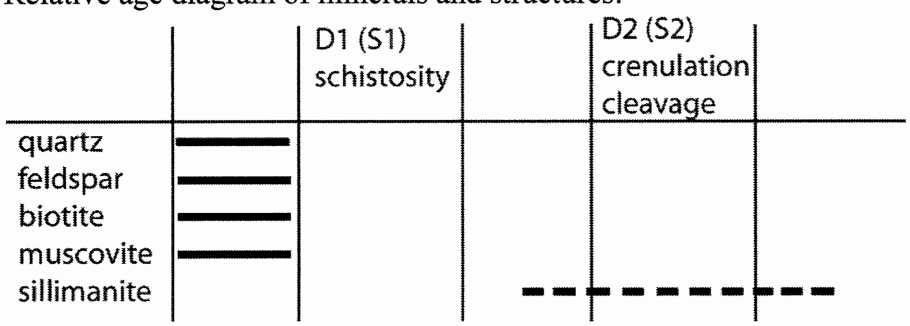

SAMPLE: BH111B
LOCATION: 27° 26.940N, 89° 25.394E @ 2260 m; at Paro
STRUCTURAL SETTING: GHS – Paro Metasediments
ROCK TYPE: mica schist

HAND SAMPLE: fine-grained schist of light grey colour; quartz and white mica-rich matrix; compositional layering – gradation of darker to lighter-coloured matrix across sample, near parallel to foliation

THIN SECTION DESCRIPTION:
MINERALOGY:
MATRIX:

- quartz – 75% of rock; seriate to 2.5 mm; anhedral, interlobate; moderate undulose extinction; subgrains present; irregular, embayed grain boundaries; some bulging; few smaller grains included in larger grains
- biotite – 10% of rock; seriate to 1.5 mm long; contains small inclusions of zircon +/- other radiogenic minerals; defines foliation; some have lattice- and shape-preferred orientation
- muscovite – 10% of rock; seriate 0.5-2 mm long; elongate shape; defines foliation; some have lattice- and shape-preferred orientation
- feldspar – 5% of rock; seriate to 1.5 mm; anhedral, interlobate; irregular, embayed grain boundaries; undulose extinction; few subgrains; no apparent twinning; weak shape-preferred orientation parallel to macroscopic foliation
- opaque minerals – trace; <0.1 mm in size
- tourmaline – trace; euhedral grains; <0.1 mm in size

PORPHYROBLASTS:

- none

STRUCTURES:

- compositional layering S_0 – observed as planar compositional variation in hand sample
- foliation S_1 – continuous schistosity defined by micas with parallel orientation
- many biotite and muscovite grains are oriented subparallel to main foliation, overprinting S_1

Relative age diagram of minerals and structures:

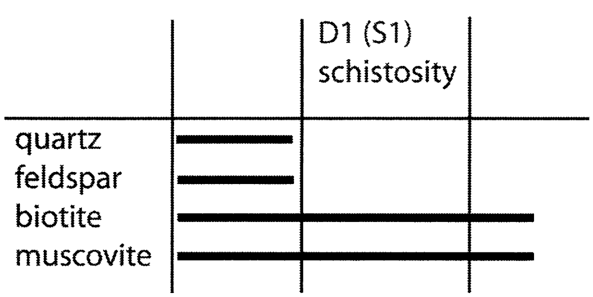

SAMPLE: BH99
LOCATION: 27° 23' 02.8"N, 91° 44' 30.8"E @ 1445m; at Radi, Phongmey
STRUCTURAL SETTING: Sakteng Klippe – Chekha Fm.
ROCK TYPE: mica schist

HAND SAMPLE: fine-grained schist of dark grey colour; compositional layering, parallel to schistosity, of lighter and darker-coloured layers ~1.5 cm thick

THIN SECTION DESCRIPTION:
MINERALOGY:
MATRIX:

- quartz – 60% of rock; inequigranular; anhedral; interlobate; embayed grain boundaries
- plagioclase – 10% of rock; seriate to 0.2 mm; anhedral, polygonal; albite twinning, some tapering; simple twinning; undulose extinction; some subgrains
- biotite – 5% of rock, to 15% in mica-rich compositional layer; elongate to 0.5 mm; generally has lattice- and shape-preferred orientation, but weakly constrained; defines foliations; 2 phases of growth – some poorly oriented with embayed grain boundaries; others with strong preferred orientation and well-formed shape
- muscovite – 5-15% of rock; elongate to 0.5 mm; generally has lattice- and shape-preferred orientation, but weakly constrained; defines foliations
- opaque minerals – 1% of rock; to 0.5 mm in size; irregular to polygonal euhedral shape; shape-preferred orientation when elongate
- tourmaline – trace; euhedral; 0.1-0.2 mm

PORPHYROBLASTS:

- none observed

STRUCTURES:

- compositional layering S_0 – defined by mica-rich and quartz-rich layers, over 1 cm thick
- foliation S_1 – continuous schistosity defined by preferred orientations of micas; not well-developed
- crenulation foliation S_2 – observed only in mica-rich layer; microfolding of muscovite and biotite schistosity to stage 1 crenulation cleavage

Relative age diagram of minerals and structures:

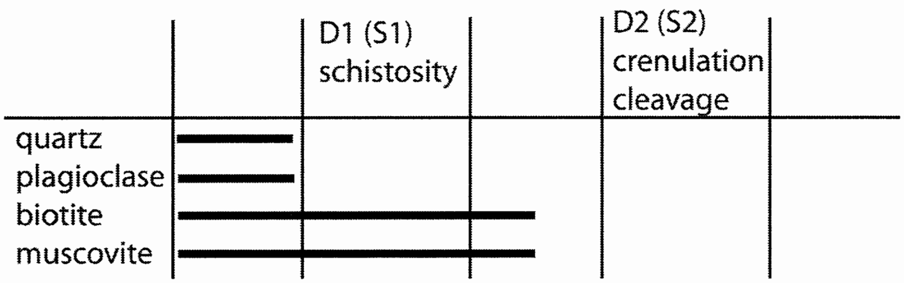

SAMPLE: BH73
LOCATION: 27° 21' 45.2"N, 91° 41' 15.2"E @ 1415 m; at Radi
STRUCTURAL SETTING: Sakteng Klippe – Chekha Fm.
ROCK TYPE: garnet schist

HAND SAMPLE: medium-grained schist of medium brown-grey colour; strong schistosity with zone of crenulation foliation at high angle to planar foliation

THIN SECTION DESCRIPTION:
MINERALOGY:

MATRIX:

- quartz – 30% of rock; seriate to 0.5 mm; anhedral; undulose extinction; smooth to embayed grain boundaries
- plagioclase – 5% of rock; seriate to 0.2 mm; anhedral, polygonal; albite twinning in some grains; simple twinning; undulose extinction; some subgrains
- biotite – 15% of rock; elongate to 1 mm; contains some monazite and zircon inclusions; lattice- and shape-preferred orientation; defines foliations
- muscovite – 30% of rock;; elongate to 1 mm; lattice- and shape-preferred orientation; some grains are folded; defines foliations
- opaque minerals – trace; 0.1-0.4 mm irregular to polygonal shape
- tourmaline – trace; euhedral grains 0.1-0.3 mm

PORPHYROBLASTS:

- garnet – 1-1.5 mm; subhedral to anhedral shape; inclusions of quartz and some opaque minerals and biotite; no apparent inclusion trails

STRUCTURES:

- foliation S_1 – schistosity defined by preferred orientation of biotite and muscovite
- crenulation foliation S_2 – stage 2 crenulation cleavage defined by angular folding of planar foliation at a high angle; slightly asymmetrical form displays anastomosing pattern of microfold limbs; not continuous throughout rock
- strain shadows of quartz and micas around garnet grains, oriented locally parallel to dominant foliation (schistosity or crenulation foliation)
- tourmaline appears to overgrow micas of schistosity and crenulation cleavage

Relative age diagram of minerals and structures:

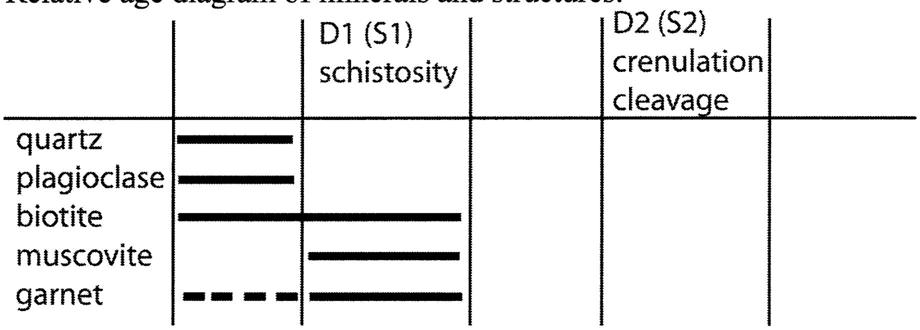

SAMPLE: BH53A
LOCATION: 27° 14' 14.5"N, 91° 32' 53.1"E @ 2405 m; at Barsong
STRUCTURAL SETTING: LHS, MCT
ROCK TYPE: garnet schist

HAND SAMPLE: fine-grained schist of medium-grey colour; discontinuous quartz veins 1-3 mm wide occur parallel to macroscopic foliation; garnet porphyroblasts to 1 mm; thinner quartz veins appear to be gently folded

THIN SECTION DESCRIPTION:
MINERALOGY:
MATRIX:

- quartz in veins – seriate to 2.5 mm; anhedral; interlobate; undulose extinction; subgrains; bulging; left-over grains
- quartz in matrix – 60% of rock; seriate to 1 mm; anhedral, polygonal to interlobate; undulose extinction; subgrains; pinning by micas; bulging
- plagioclase – 10% of rock; seriate to 1 mm; also larger grains to 2 mm associated with quartz vein; tapered albite twinning; weak undulose extinction; few subgrains; some inclusions of quartz
- biotite – 5% of rock; seriate to 2 mm long; elongate shape; some embayed grain boundaries; shape-preferred orientation; defines foliations
- muscovite – 10% of rock; to 3 mm long; elongate shape; occurs in aggregates; shape-preferred orientation; defines foliations
- opaque minerals – trace; anhedral, irregular grains; <0.2 mm in size

PORPHYROBLASTS:

- garnet – 0.3-1 mm; euhedral to subhedral; inclusions of quartz, opaque minerals and some biotite; curved inclusion trails

STRUCTURES:

- foliation S_1 – schistosity defined by preferred orientation of micas
- folding of quartz veins oriented parallel to S_1 – tight asymmetrical folds with dextral shear sense, also tight intrafolial (rootless) folds with axial planes near parallel to S_1
- crenulation foliation S_2 – stage 1 crenulation cleavage defined by the folding of S_1; symmetrical
- boudinage of quartz veins – stretching parallel to S_1
- C' type shear bands at high angle to S_1; ~60° CW from S_1; discontinuous; dextral shear sense
- strain shadows around σ-type garnet porphyroblasts show dextral sense of shear
- one garnet porphyroblast shows syn-kinematic rotation as indicated by spiral inclusion trails

Relative age diagram of minerals and structures:

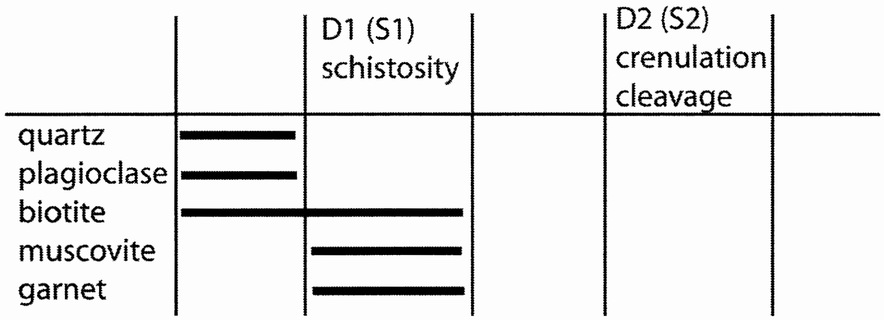

SAMPLE: BH49A
LOCATION: 27° 13’ 39.6”N, 91° 33’ 15.8”E @ 2215 m; at Barsong
STRUCTURAL SETTING: LHS/MCT
ROCK TYPE: garnet phyllite

HAND SAMPLE: fine-grained schist of dark green-grey colour; weathered surfaces brown in colour; schistosity of dark grey mineral; garnet grains 0.5-2 mm in size; angular folds ~2 cm in size on face perpendicular to thin-section cut side

THIN SECTION DESCRIPTION:
MINERALOGY:
MATRIX:

- quartz – 40% of rock; equigranular ~0.1 mm; anhedral to subhedral; polygonal to interlobate; smooth grain boundaries; undulose extinction; pinning by micas; in matrix and as veins to 2 mm wide
- plagioclase – 5% of rock; <0.1 mm; anhedral, rounded shape; albite twinning rare; some simple twinning
- biotite – 5% of rock; <0.1-0.3 mm; elongate; shape-preferred orientation; defines foliation; larger grains associated with quartz veins
- muscovite – 45% of rock; sericitic, <0.1 mm; elongate; lattice- and shape-preferred orientation; defines foliation; forms grain aggregates in places
- opaque minerals – 1% of rock; <0.1 mm; irregular shape; elongate grains have shape-preferred orientation
- chloritoid – trace; 0.2-1 mm; anhedral to subhedral; polysynthetic twinning; quartz and opaque mineral inclusions; inclusions continuous with dominant external foliation
- chlorite – trace; to 0.2 mm; associated with biotite

PORPHYROBLASTS:

- garnet – 3% of rock; 0.3-2 mm; euhedral to anhedral, many elongate parallel to foliation; poikiloblastic with inclusions of quartz, feldspar, biotite, muscovite, opaque minerals; one grain partly overgrows a chloritoid grain; slightly curved inclusion trails

STRUCTURES:

- compositional layering S_0 -
- foliation S_1 – dominant matrix foliation; strong fine-grained slaty cleavage defined by preferred orientation of mica minerals; parallel to S_0
- quartz veins have anastomosing thickness – boudinaged?
- inclusion trails of garnets, S_i, are continuous with external foliation S_1
- several anhedral garnets have strain fringes of sericite parallel to S_1

Relative age diagram of minerals and structures:

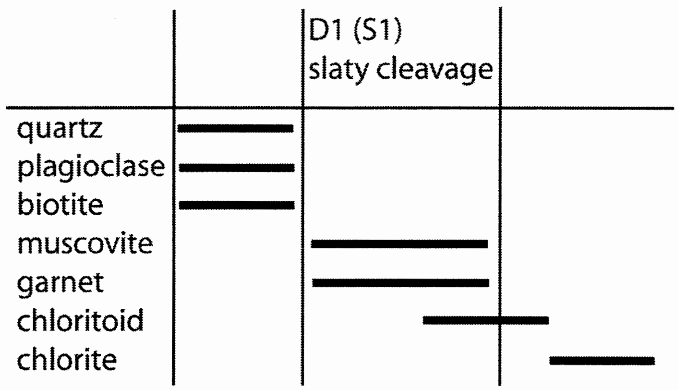

SAMPLE: BH49B
LOCATION: 27° 13’ 39.6”N, 91° 33’ 15.8”E @ 2215 m; at Barsong
STRUCTURAL SETTING: LHS, MCT
ROCK TYPE: garnet phyllite

HAND SAMPLE: fine-grained schist of dark green-grey colour; weathered surfaces brown in colour; schistosity of dark grey mineral; asymmetrical crenulation cleavage about 30° from schistosity

THIN SECTION DESCRIPTION:
MINERALOGY:
MATRIX:
- quartz – 45% of rock; equigranular ~0.1 mm; anhedral, polygonal to irregular shape; smooth to irregular grain boundaries; undulose extinction
- muscovite – 45% of rock; fine-grained, sericitic; lattice- and shape-preferred orientation; defines foliations
- biotite – 5% of rock; to 0.5 mm; elongate; shape-preferred orientation
- opaque minerals – <5% of rock; <0.1 mm; irregular shape; shape-preferred orientation where elongate
- chloritoid – 1% of rock; 0.5-1 mm; anhedral; poikiloblastic with inclusions of quartz and few opaque minerals

PORPHYROBLASTS:
- garnet – 1% of rock; to 2 mm; euhedral to subhedral; inclusion trails of quartz; inclusion trails straight to complex with spiral pattern or overprint of crenulation cleavage

STRUCTURES:
- foliation S_1 – slaty cleavage defined by preferred orientation of mica minerals
- compositional layering ~0.5-1 mm thick of white mica and quartz rich layers; oriented parallel and discordant at high angles to dominant foliation
- compositional layer 7 mm thick of 70% muscovite; parallel to dominant foliation; folded asymmetrically with axial planes near parallel to S_1; also contains a well-developed stage 3-4 crenulation cleavage of muscovite at 35° angle CW from dominant foliation
- crenulation foliation S_2 – overprints schistosity; defined by stage 1 folding of schistosity
- garnet grains appear to overprint all foliations except in places the crenulation cleavage in muscovite-rich layer

Relative age diagram of minerals and structures:

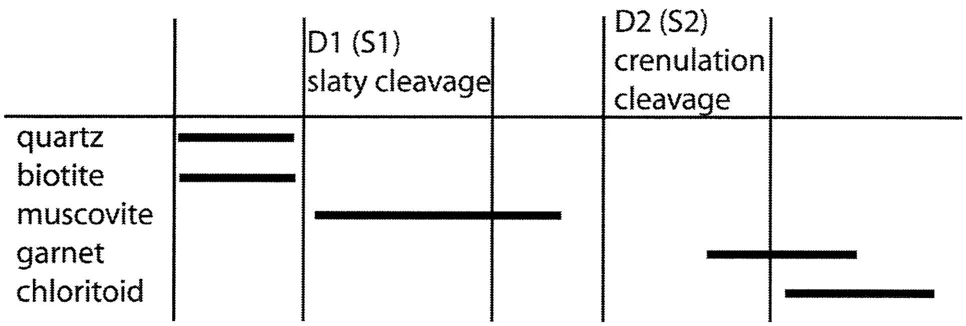

SAMPLE: BH41
LOCATION: Between 27° 36' 53.2"N, 91° 12' 46.4"E and 27° 38' 05.9"N, 91° 13' 14.3" @ 1225 m; at Kuru Chu Bridge
STRUCTURAL SETTING: LHS/MCT
ROCK TYPE: garnet-biotite schist

HAND SAMPLE: N/A

THIN SECTION DESCRIPTION:
MINERALOGY:
MATRIX:

- quartz – 40% of rock; occurs in matrix and in veins to 1 mm wide; seriate to 1 mm; anhedral; interlobate to polygonal; embayed to smooth grain boundaries; undulose extinction; subgrains; bulging; left-over grains
- plagioclase – 10% of rock; seriate to 0.3 mm; anhedral, rounded to polygonal; uneven grain boundaries; albite twinning continuous; undulose extinction
- biotite – 30% of rock; seriate to 1 mm; many grains have embayed grain boundaries; undulose extinction; inclusions of quartz, plagioclase, tourmaline and opaque minerals; general shape-preferred orientation; defines foliations
- muscovite – trace; seriate to 1 mm; elongate; lattice- and shape-preferred orientation; defines foliations
- opaque minerals – trace; irregular; <0.3 mm in size
- titanite – trace; anhedral, rounded shape; 0.5 mm in size
- tourmaline – trace; euhedral; <0.2 mm in size

PORPHYROBLASTS:

- garnet – trace; anhedral; embayed grain boundaries; inclusions of biotite with some muscovite, tourmaline, opaque minerals and quartz;

STRUCTURES:

- foliation S_1 – schistosity defined by preferred orientation of biotite and muscovite; not well-developed
- crenulation foliation S_2 – weak crenulation cleavage defined by symmetrical folding of schistosity S_1; at stage 1 of development
- quartz veins are oriented parallel to S_1 and are folded with S_2

Relative age diagram of minerals and structures:

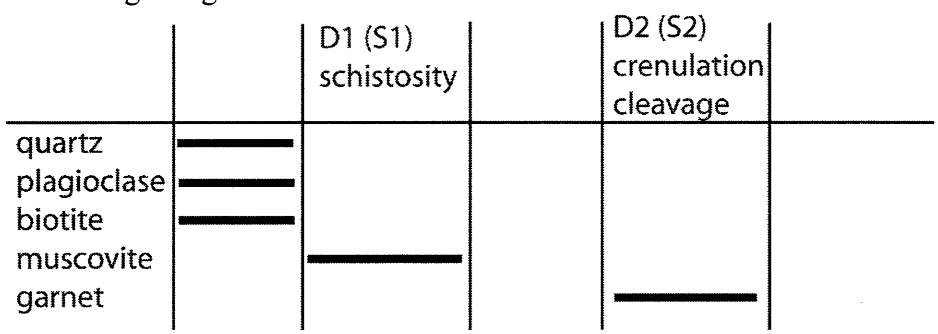

SAMPLE: BH40 A&B
LOCATION: Near 27° 34' 30.8"N, 91° 10' 28.9"E @ 1780 m
STRUCTURAL SETTING: LHS/MCT
ROCK TYPE: garnet schist

HAND SAMPLE: fine-grained schist of medium-dark grey colour; weathered surfaces light brown-grey colour; schistosity; crenulation foliation observed on both A&B (perpendicular) sections; coarse-grained quartz veins 1-5 mm wide oriented parallel to macroscopic schistosity; veins also folded in both crenulation cleavages

THIN SECTION DESCRIPTION:
MINERALOGY:
MATRIX:

- quartz in matrix – 60% of rock; seriate to 1 mm; euhedral to anhedral; polygonal; granoblastic texture; some undulose extinction and subgrains present; some pinning structures with micas
- quartz in veins – 0.5-3 mm in size; euhedral to anhedral; polygonal to interlobate; smooth to embayed grain boundaries; undulose extinction; left-over grains; bulging
- biotite – 5% of rock; seriate to 0.5 mm; elongate; lattice- and shape-preferred orientation; internal kinking
- muscovite – 20% of rock; seriate to 1 mm; elongate; lattice- and shape-preferred orientation; defines foliations
- graphite? – 5% of rock; fine-grained, opaque fibrous grains associated with muscovite
- tourmaline – trace; euhedral; <0.2 mm

PORPHYROBLASTS:

- garnet – 1 grain in 'B face'; 5 mm in size; anhedral, elongate shape; inclusions of quartz, opaque minerals and biotite; curved inclusion trails

STRUCTURES:

- foliation S_1 – schistosity defined by preferred orientation of micas and graphite(?)
- crenulation foliations S_2 and S_3 – 2 crenulation foliations approximately perpendicular to each other; defined by folding of schistosity; symmetrical; time relationship between them not apparent
- quartz veins oriented parallel to S_1 and folded with both crenulation foliations
- garnet inclusion trails, S_i, continuous with and parallel to schistosity; S_i is crenulated with schistosity

Relative age diagram of minerals and structures:

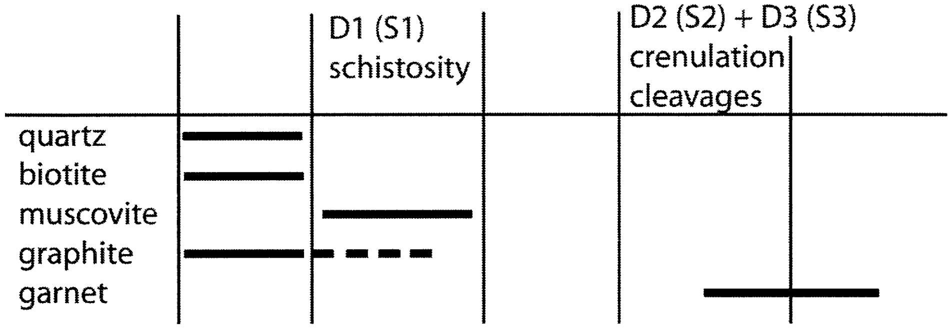

APPENDIX II – ELECTRON MICROPROBE DATA

Electron microprobe data accompanied by back-scatter electron images with point locations. Data is sorted alphabetically by mineral for each sample. Data is presented as weight % oxides and, where possible, the cations per formula unit for each analysis. The numbers of oxygen atoms upon which the cations per formula unit are based follow the conventions presented in Deer, Howie and Zussman (1992). Where corrections have been applied to the data only the corrected data is presented.

Table of numbers of oxygen atoms used to calculate cations per formula unit for mineral analyses. (Based on Deer, Howie and Zussman 1992.)

Mineral	#oxygens per formula unit
apatite	26
biotite	22
chlorite	28
garnet	24
ilmenite	6
K-feldspar	32

Mineral	#oxygens per formula unit
magnetite	32
muscovite	22
plagioclase	32
quartz	2
staurolite	48
tourmaline	31

laura969001

BH96-9 Image 1

-points 1-36

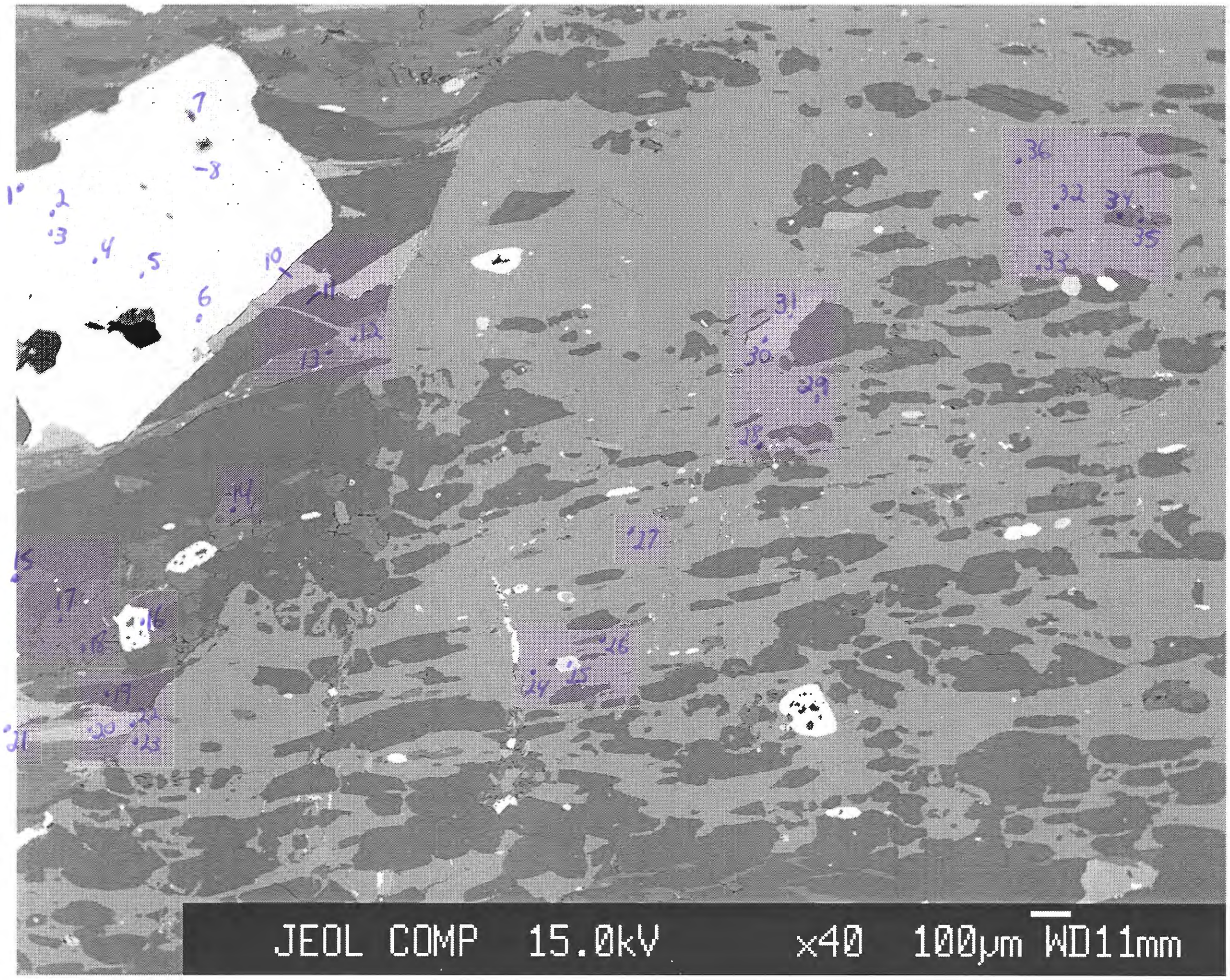

laura969002

BH96-9 Image 2

-points 37-46
-points g1-g6

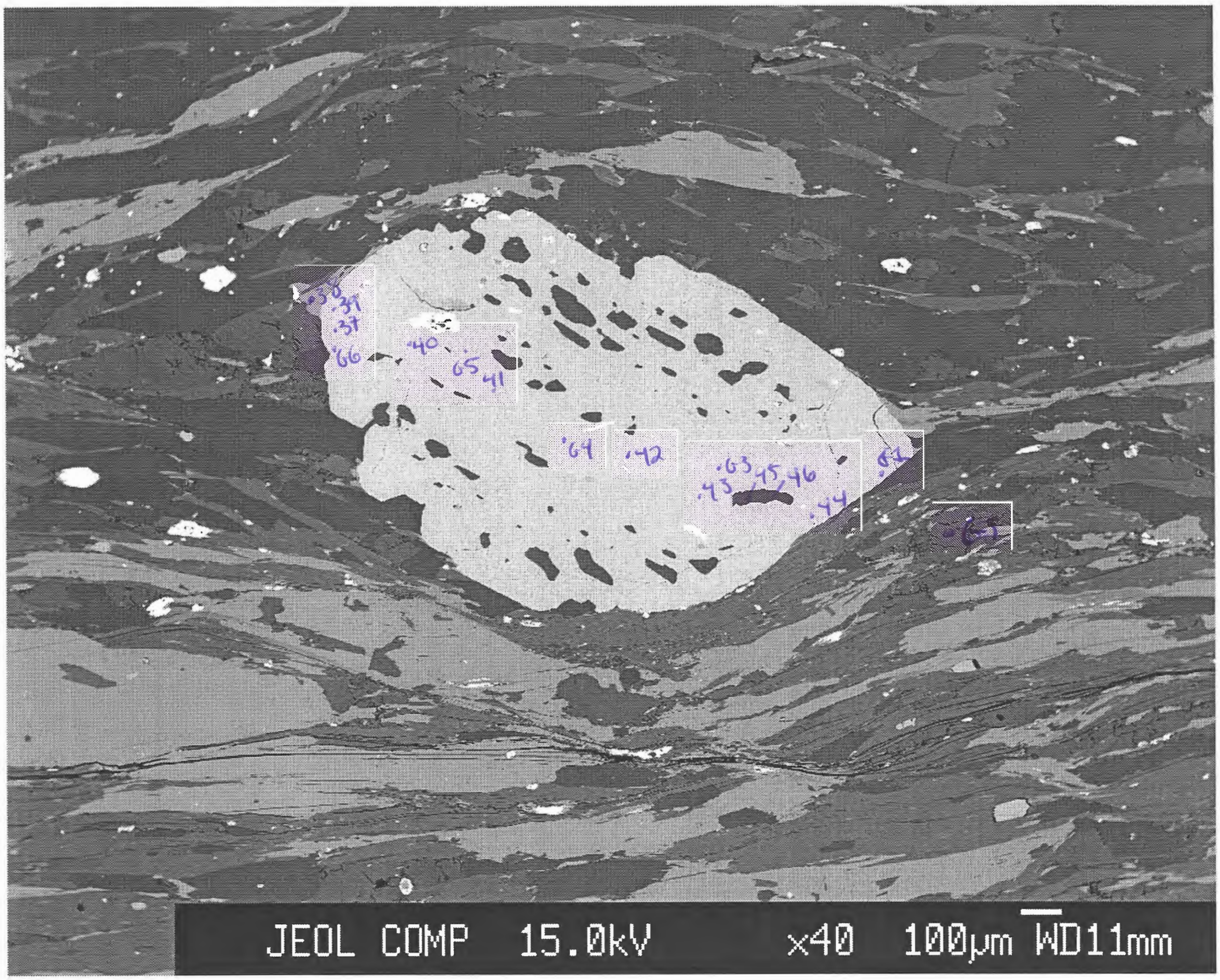

laura969003

BH96-9 Image 3

-points 47-67

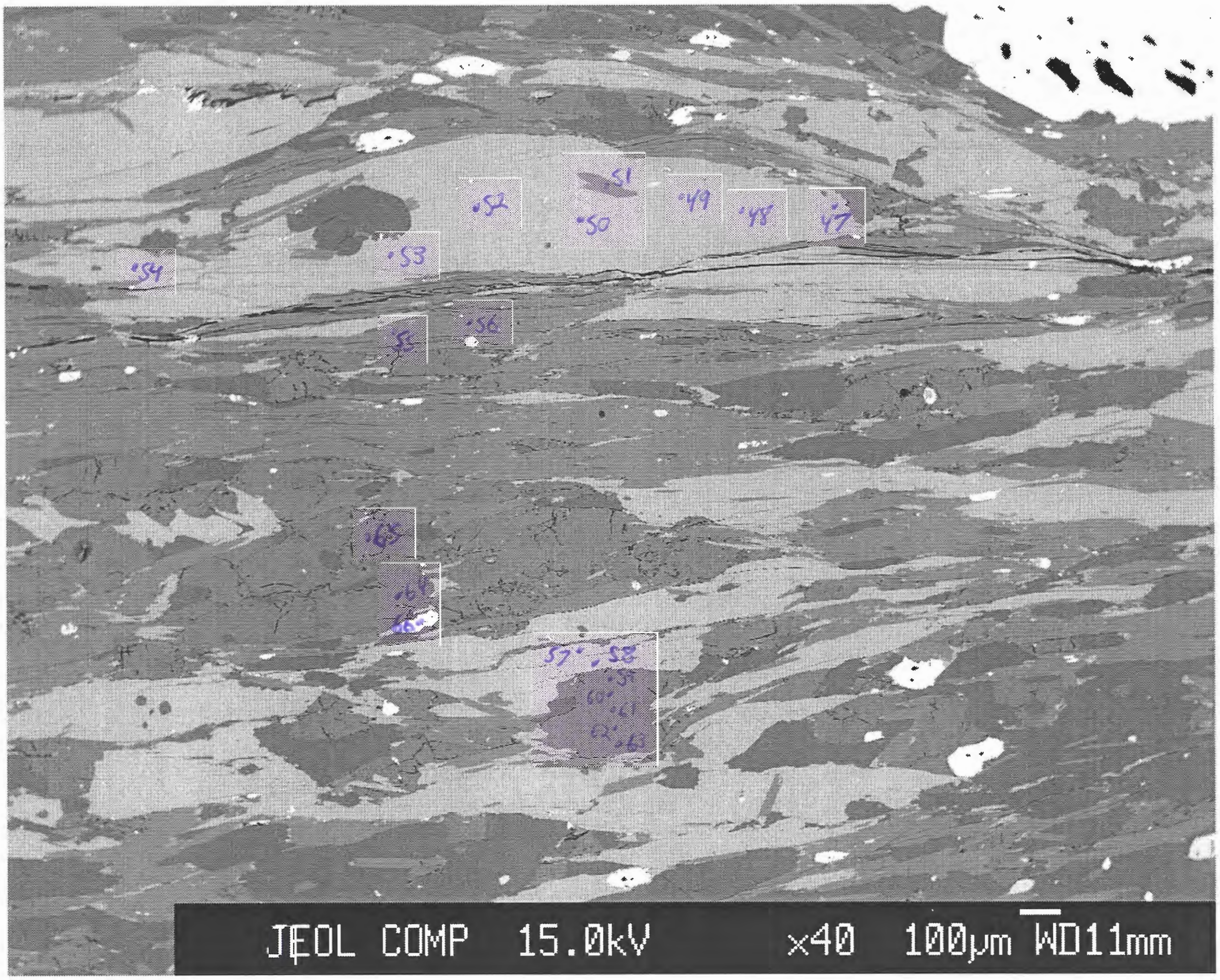

laura969004

<u>BH96-9 Image 4</u>

-points 68-75

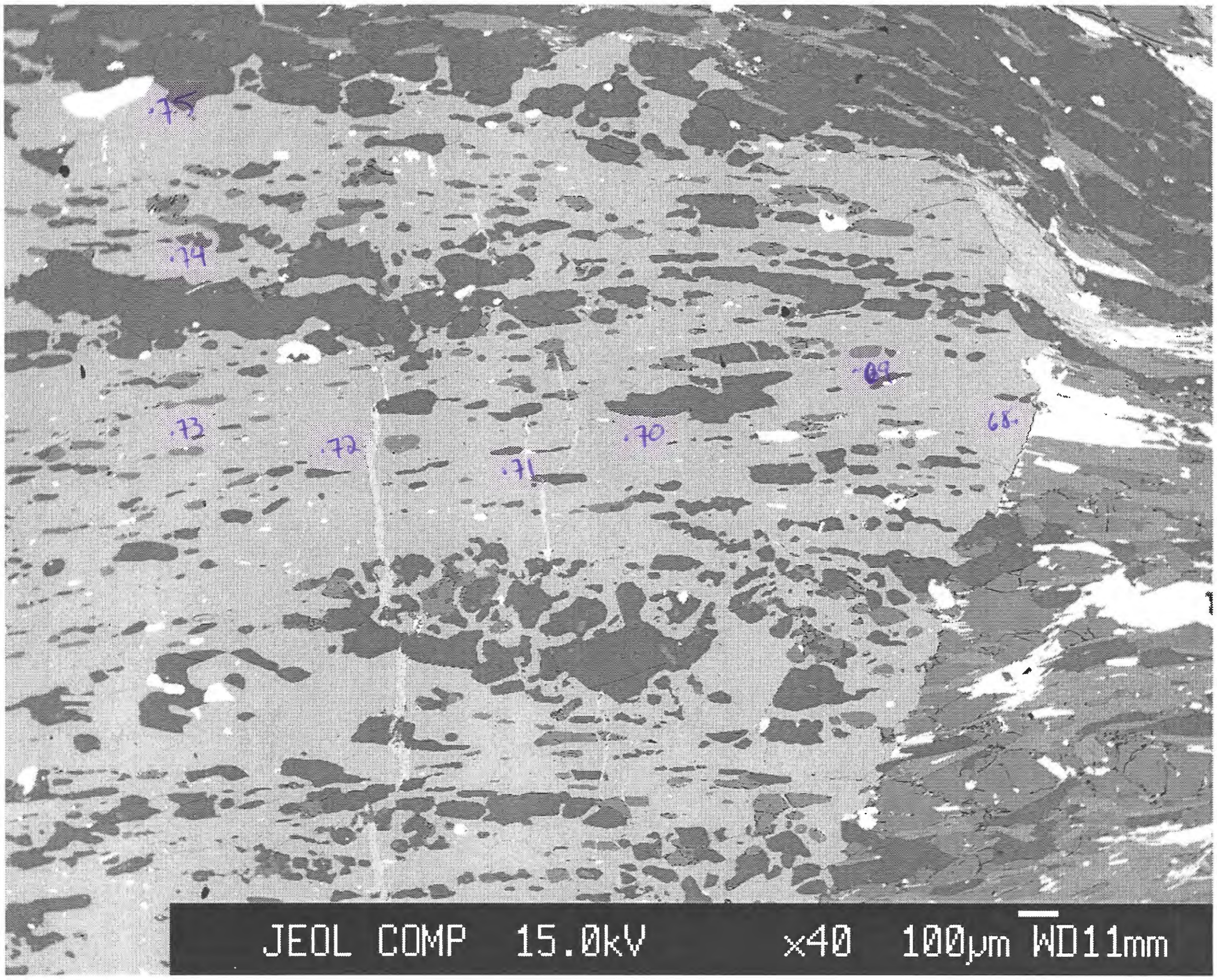

ritch969001

BH96-9 Image 5

-points g8-g12

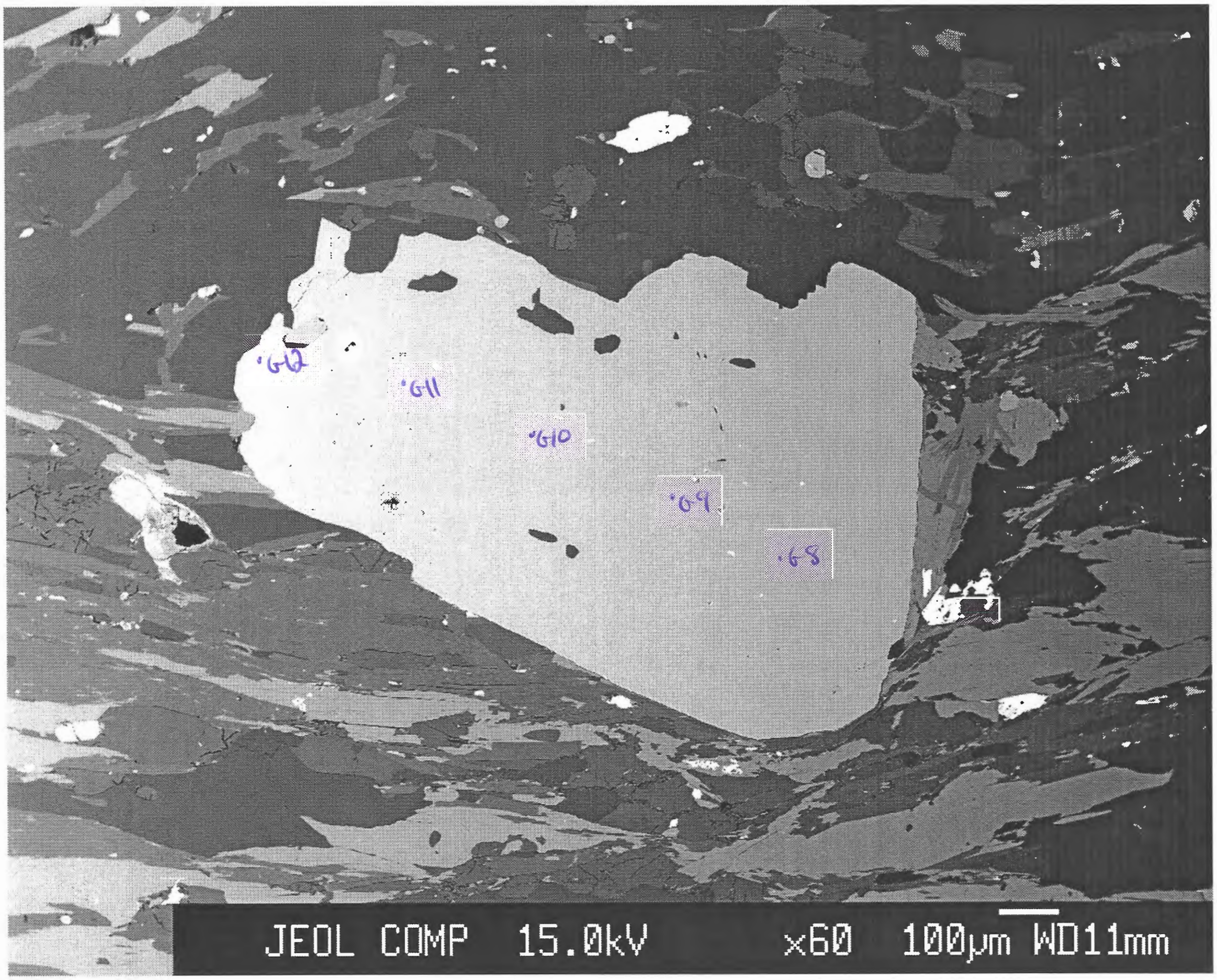

ritch969002

BH96-9 Image 6

-points g13-g21

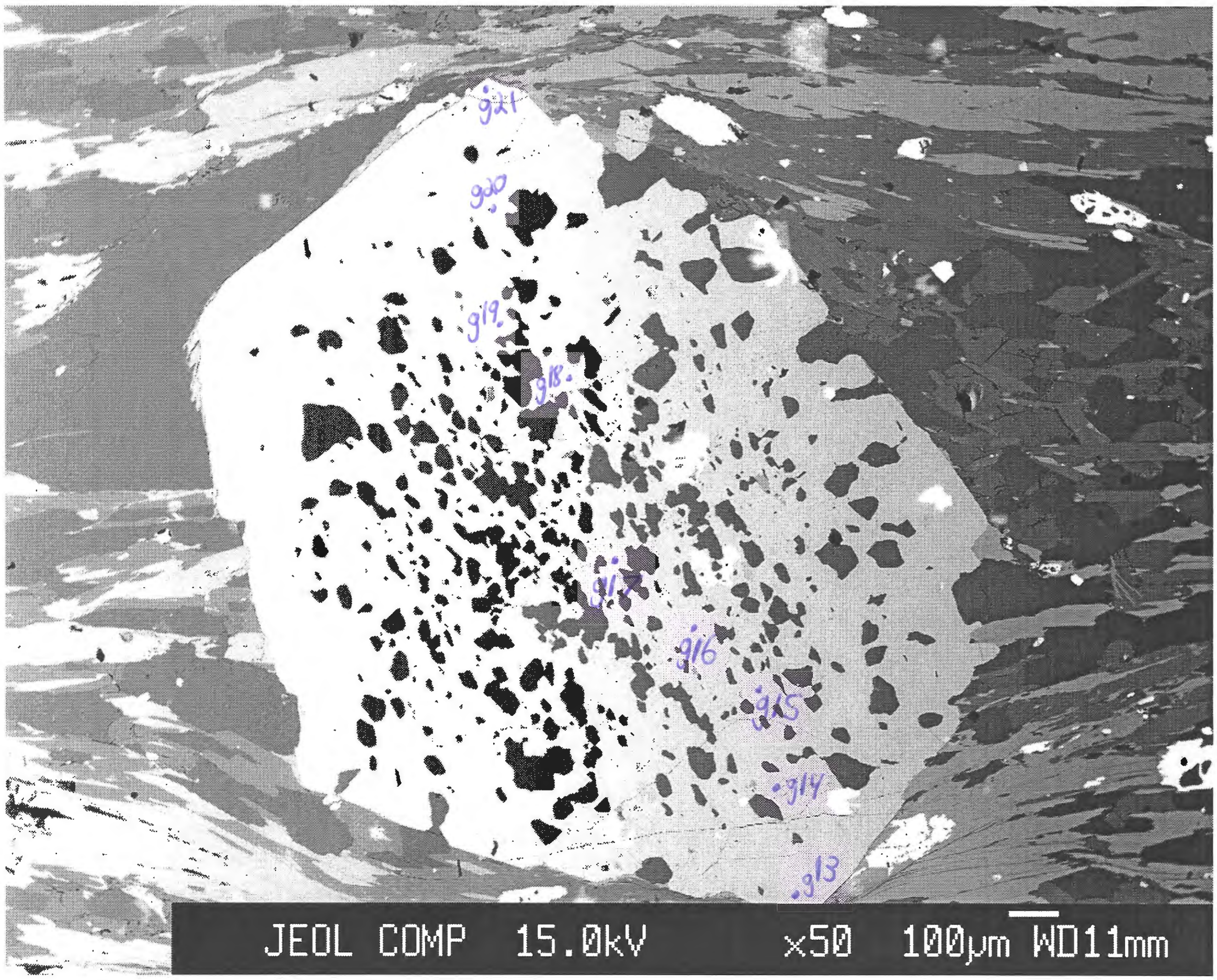

SAMPLE BH96-9

No.	5	28	36	13	23	33	34	42	53	54	55
Comment	bh96-9-3	bh96-9-25	bh96-9-33	bh96-9-10	bh96-9-20	bh96-9-30	bh96-9-31	bh96-9-38	bh96-9-47	bh96-9-48	bh96-9-49
Mineral	apatite	apatite	apatite	biotite	biotite	biotite	biotite	biotite	biotite	biotite	biotite
Weight % oxide:											
SiO2	0	0	0	35.4842	35.2752	35.4344	35.1901	35.5617	36.8398	36.1437	35.8858
TiO2	0	0.0309	0.0458	1.0361	1.8203	1.19	1.3526	1.403	0.9128	1.242	1.2726
Al2O3	0	0	0	9.3278	9.5615	9.3923	9.2979	18.4959	20.3014	19.2428	18.9234
Cr2O3	0	0.0497	0.06	0.032	0.0595	0.0543	0.0496	0.0467	0	0	0
FeO	1.516	0.4038	0.255	19.5345	19.1225	17.9146	17.9928	19.6556	19.3525	18.3808	19.1369
MnO	0.1684	0.0543	0.0434	0	0	0.0157	0	0.0157	0.0432	0.0703	0.081
MgO	0.0047	0	0.0052	11.923	11.4399	12.8905	12.6968	10.7816	11.6012	11.6448	11.5282
CaO	54.9549	55.2024	56.23	0.0394	0.0295	0.0151	0.0311	0.0516	0.0163	0	0.0093
Na2O	0.0658	0.0223	0.0656	0.2897	0.4018	0.4313	0.4575	0.3414	0.2483	0.332	0.353
K2O	0	0.0245	0.0165	8.5222	9.0439	8.7006	8.7163	8.7214	6.0017	8.5809	8.7647
ZnO	0	0.1472	0.2271	0.1016	0.085	0.0565	0.0791	0.0954	0	0.0031	0.0238
Total	56.7098	55.9352	56.9486	86.2906	86.8391	86.0954	85.8639	95.1701	95.3173	95.6404	95.9788
Number of cations per formula unit:											
Si	0	0	0	6.0522	5.9906	6.017	6.0016	5.412	5.456	5.4186	5.3944
Ti	0	0.0104	0.0156	0.132	0.2332	0.1518	0.1738	0.1606	0.1012	0.1408	0.143
Al	0	0	0	1.8744	1.914	1.8788	1.87	3.3176	3.5442	3.399	3.3528
Cr	0	0.0182	0.0208	0.0044	0.0088	0.0066	0.0066	0.0066	0	0	0
Fe	0.063	0.1456	0.091	2.7852	2.7148	2.5432	2.5674	2.5014	2.398	2.3034	2.4046
Mn	0.0072	0.0208	0.0156	0	0	0.0022	0	0.0022	0.0044	0.0088	0.011
Mg	0.0003	0	0.0026	3.0316	2.8952	3.2626	3.2274	2.4464	2.5608	2.6026	2.5828
Ca	2.9265	25.7244	25.727	0.0066	0.0044	0.0022	0.0066	0.0088	0.0022	0	0.0022
Na	0.0063	0.0182	0.0546	0.0968	0.132	0.143	0.1518	0.1012	0.0704	0.0968	0.1034
K	0	0.013	0.0078	1.8546	1.9602	1.8854	1.8964	1.694	1.133	1.6412	1.6808
Zn	0	0.0468	0.0728	0.0132	0.011	0.0066	0.011	0.011	0	0	0.0022
Total	3.0033	26	26.0078	15.851	15.8664	15.9016	15.9148	15.664	15.2702	15.6112	15.6794

56	58	59	60	63	64	15	24	3	4	6	7
bh96-9-50	bh96-9-52	bh96-9-53	bh96-9-54	bh96-9-57	bh96-9-58	bh96-9-12	bh96-9-21	bh96-9-1	bh96-9-2	bh96-9-4	bh96-9-5
biotite	biotite	biotite	biotite	biotite	biotite	chlorite	chlorite	garnet	garnet	garnet	garnet
35.9902	35.5794	35.7838	35.75	35.4811	35.7712	23.6208	23.8057	37.1238	37.4706	37.2448	37.2567
1.4014	1.5303	1.5307	1.4431	1.6931	1.5638	0.0826	0.1174	0	0.0186	0.0263	0.0306
18.9451	18.9775	18.929	18.5799	18.9325	18.8083	12.1559	12.3058	21.4395	21.3066	21.3685	21.328
0	0	0	0	0	0	0.0467	0.0543	0	0	0	0
19.0514	18.8641	18.1739	18.7996	19.2385	18.6207	22.5659	23.7491	33.8085	33.9649	33.1981	32.9106
0.0864	0.0594	0.0811	0.0378	0.1025	0.1134	0	0	2.0498	1.9588	2.2008	2.3692
11.2927	11.2662	11.329	11.3213	10.8346	11.0007	17.251	17.141	3.1287	3.0622	3.0173	2.9632
0	0.0098	0.0082	0	0.0027	0	0.05	0.0227	2.9821	3.2824	3.256	3.4462
0.3435	0.3769	0.3305	0.3412	0.3407	0.373	0.004	0	0.0336	0.042	0.0216	0.0147
8.7287	8.6561	8.5855	8.8592	8.9588	8.9667	0.0411	0.023	0	0	0	0
0.0169	0	0.0062	0.0369	0.0207	0	0.0541	0.0533	0	0	0	0.022
95.8564	95.3197	94.758	95.1691	95.6053	95.2179	75.8722	77.2724	100.5659	101.106	100.3333	100.3411
5.4098	5.379	5.4186	5.4186	5.3702	5.4164	5.8212	5.7904	5.9376	5.9616	5.9616	5.964
0.1584	0.1738	0.1738	0.165	0.1936	0.1782	0.014	0.0224	0	0.0024	0.0024	0.0048
3.3572	3.3814	3.3792	3.3198	3.377	3.3572	3.5308	3.528	4.0416	3.996	4.032	4.0248
0	0	0	0	0	0	0.0084	0.0112	0	0	0	0
2.3958	2.3848	2.3012	2.3826	2.4354	2.3584	4.6508	4.8328	4.5216	4.5192	4.4448	4.4064
0.011	0.0066	0.011	0.0044	0.0132	0.0154	0	0	0.2784	0.264	0.2976	0.3216
2.53	2.5388	2.5564	2.5586	2.4442	2.4838	6.3364	6.216	0.7464	0.7272	0.72	0.708
0	0.0022	0.0022	0	0	0	0.014	0.0056	0.5112	0.5592	0.5592	0.5904
0.1012	0.11	0.0968	0.1012	0.099	0.11	0.0028	0	0.0096	0.012	0.0072	0.0048
1.6742	1.6698	1.6588	1.7138	1.7292	1.7314	0.014	0.0084	0	0	0	0
0.0022	0	0	0.0044	0.0022	0	0.0112	0.0084	0	0	0	0.0024
15.642	15.6464	15.598	15.6684	15.6662	15.6508	20.4036	20.4232	16.0488	16.044	16.0248	16.0296

8	43	44	45	46	47	48	457	459	460	461	462
bh96-9-6	bh96-9-39	bh96-9-40	bh96-9-41	bh96-9-42	bh96-9-43	bh96-9-44	bh96-9_g1	bh96-9_g3	bh96-9_g4	bh96-9_g5	bh96-9_g6
garnet	garnet	garnet	garnet	garnet	garnet	garnet	garnet	garnet	garnet	garnet	garnet
37.5394	37.6133	37.2359	37.1596	37.0612	37.169	37.5141	36.781	36.4897	36.5683	36.3033	36.731
0	0.0543	0.1238	0.1073	0.0532	0.0489	0.0152	0.0055	0.0133	0.0575	0.0409	0.0088
21.3168	21.584	21.0657	20.9411	21.3566	21.3796	21.3266	20.9748	20.9673	20.9135	20.83	21.0155
0	0	0	0	0	0	0	0	0	0	0	0
34.5825	34.4846	31.6966	30.4294	30.8495	32.4659	34.0869	33.6689	30.3997	30.1687	29.5806	34.2239
1.942	2.3024	5.1606	6.4877	5.4888	3.6537	2.3918	1.7453	4.317	5.9172	6.2645	2.2226
3.1799	3.2183	2.2507	2.02	2.1035	2.6394	3.1445	3.0291	2.2208	1.9498	1.8652	2.9938
2.92	2.9313	4.0754	4.0422	4.4259	3.798	3.0573	2.8221	4.0463	4.0472	4.0498	2.8818
0.0435	0.0244	0.0309	0.0401	0.0147	0.0188	0.0276	0.0187	0.014	0.0122	0.0215	0.0292
0	0.0381	0.0226	0.0293	0.0297	0.0403	0.0432	0	0	0	0	0
0.0023	0.2439	0.2647	0.2501	0.2569	0.1997	0.2668	0	0	0	0	0
101.5263	102.4945	101.9268	101.5067	101.64	101.4132	101.8739	99.0455	98.4681	99.6344	98.9559	100.1065
5.9568	5.9232	5.928	5.9448	5.9088	5.9208	5.9424	5.9706	5.9652	5.9422	5.9399	5.9277
0	0.0072	0.0144	0.012	0.0072	0.0048	0.0024	0.0007	0.0016	0.007	0.005	0.0011
3.9864	4.0056	3.9528	3.948	4.0128	4.0152	3.9816	4.0132	4.0401	4.0056	4.0172	3.9976
0	0	0	0	0	0	0	0	0	0	0	0
4.5888	4.5408	4.2216	4.0704	4.1136	4.3248	4.5168	4.5709	4.1562	4.0999	4.0478	4.6191
0.2616	0.3072	0.696	0.8784	0.7416	0.492	0.3216	0.24	0.5978	0.8144	0.8682	0.3038
0.7512	0.756	0.5352	0.4824	0.4992	0.6264	0.7416	0.733	0.5412	0.4723	0.4549	0.7202
0.4968	0.4944	0.696	0.6936	0.756	0.648	0.5184	0.4909	0.7088	0.7047	0.71	0.4983
0.0144	0.0072	0.0096	0.012	0.0048	0.0048	0.0096	0.0059	0.0044	0.0038	0.0068	0.0091
0	0.0072	0.0048	0.0048	0.0072	0.0072	0.0096	0	0	0	0	0
0	0.0288	0.0312	0.0288	0.0312	0.024	0.0312	0	0	0	0	0
16.056	16.08	16.0896	16.0776	16.0824	16.068	16.0776	16.0252	16.0154	16.0499	16.0498	16.0769

534	535	536	537	538	539	540	541	542	543	544	545
bh969_g7	bh969_g8	bh969_g9	bh969_g10	bh969_g11	bh969_g12	bh969_g13	bh969_g14	bh969_g15	bh969_g16	bh969_g17	bh969_g18
garnet	garnet	garnet	garnet	garnet	garnet	garnet	garnet	garnet	garnet	garnet	garnet
36.841	36.664	36.6933	36.6648	36.6693	36.8597	36.6527	36.7946	36.6645	36.7235	36.6377	36.6122
0.0187	0	0.011	0.0077	0.0122	0.0121	0	0.0121	0.0672	0.0881	0.1142	0.0637
21.0712	20.7426	20.8702	20.9321	20.9644	20.9562	21.0758	21.161	20.9094	20.8764	20.8029	20.8386
0	0	0	0	0	0	0	0	0	0	0	0
34.4377	31.9255	31.7939	32.3655	31.575	33.9705	34.0827	30.693	30.3343	28.7679	28.4359	29.1945
1.9494	2.9069	3.6374	3.819	3.9818	1.9974	2.2451	4.7757	5.7671	7.4806	8.7101	7.9786
3.0804	2.568	2.2982	2.3245	2.3604	3.1076	3.0365	2.3766	2.2727	1.9555	1.7496	1.8097
3.037	3.7327	3.9885	3.9204	4.0732	2.9376	2.5455	4.2339	3.9302	4.1677	3.8767	3.6265
0.0281	0.0358	0.0135	0.0051	0.0089	0.0351	0.0248	0.053	0.0644	0.0452	0.0637	0.0295
0	0	0	0	0	0	0	0	0	0	0	0
0.0015	0.0322	0.033	0.0115	0.0337	0.0306	0.0352	0.0092	0	0.0015	0	0.0008
100.4649	98.6078	99.3391	100.0505	99.6789	99.9069	99.6984	100.109	100.0098	100.1063	100.3907	100.154
5.9225	5.9839	5.9619	5.9323	5.9416	5.948	5.9325	5.9317	5.933	5.9426	5.9328	5.9391
0.0023	0	0.0013	0.0009	0.0015	0.0015	0	0.0015	0.0082	0.0107	0.0139	0.0078
3.9927	3.9903	3.9969	3.992	4.0039	3.986	4.0209	4.021	3.9881	3.9819	3.9706	3.9844
0	0	0	0	0	0	0	0	0	0	0	0
4.63	4.3577	4.3203	4.3796	4.2788	4.5845	4.6136	4.1382	4.1052	3.8933	3.851	3.9607
0.2655	0.4019	0.5006	0.5234	0.5465	0.273	0.3078	0.6521	0.7905	1.0254	1.1947	1.0963
0.7382	0.6248	0.5566	0.5606	0.5701	0.7475	0.7326	0.5711	0.5482	0.4717	0.4223	0.4376
0.5231	0.6528	0.6944	0.6797	0.7072	0.5079	0.4415	0.7314	0.6815	0.7226	0.6726	0.6303
0.0088	0.0113	0.0043	0.0016	0.0028	0.011	0.0078	0.0166	0.0202	0.0142	0.02	0.0093
0	0	0	0	0	0	0	0	0	0	0	0
0.0002	0.0039	0.004	0.0014	0.004	0.0037	0.0042	0.0011	0	0.0002	0	0.0001
16.0834	16.0266	16.0403	16.0716	16.0564	16.0631	16.0609	16.0647	16.0749	16.0627	16.0779	16.0656

546	547	548	19	72	27	73	17	25	57	61	62
bh969_g19	bh969_g20	bh969_g21	bh96-9-16	bh96-9-66	bh96-9-24	bh96-9-67	bh96-9-13	bh96-9-22	bh96-9-51	bh96-9-55	bh96-9-56
garnet	garnet	garnet	ilmenite	ilmenite	magnetite	magnetite?	muscovite	muscovite	muscovite	muscovite	muscovite
36.6508	36.5587	36.8148	0	0.0245	0	0.0704	44.3086	44.4257	46.0731	46.4836	46.9756
0.0342	0.0354	0.0639	48.8867	47.9566	0.2262	0.11	0.3239	0.3594	0.3121	0.2931	0.2981
20.923	21.0388	20.9645	0.0021	0	0.0683	0.1871	18.1981	17.3136	34.899	34.5451	33.7593
0	0	0	0.1247	0	0.1158	0	0.0692	0.0431	0	0	0
28.6505	31.6796	34.1174	50.2783	48.3279	93.8838	93.4896	2.3843	2.3938	2.3621	2.4746	2.1461
7.1864	3.4514	2.1018	0.3065	0.5218	0.1727	0.3455	0	0	0	0	0.033
1.7754	2.4978	3.0758	0.2922	0.1813	0	0	0.6446	0.6324	0.6023	0.6448	0.8256
4.3795	4.1553	2.8257	0.1303	0.0774	0.1111	0.136	0.016	0.009	0	0	0
0.0289	0.0344	0.0192	0	0.0291	0	0.0482	1.4443	1.6623	1.3539	1.4971	1.2599
0	0	0	0.0645	0	0.0737	0	8.8404	8.5416	8.0365	8.4719	9.1385
0.013	0.0215	0	0.4309	0.3955	0.5903	0.484	0.0306	0.0496	0	0	0
99.6418	99.473	99.9832	100.5161	97.5142	95.2419	94.8709	76.2601	75.4306	93.6391	94.4102	94.4362
5.9526	5.928	5.9404	0	0.0012	0	0.0288	7.4184	7.513	6.1952	6.2216	6.2942
0.0042	0.0043	0.0078	1.8864	1.9032	0.0672	0.032	0.0418	0.0462	0.0308	0.0286	0.0308
4.0054	4.021	3.9873	0	0	0.032	0.0896	3.5904	3.4518	5.5308	5.4494	5.3328
0	0	0	0.0048	0	0.0352	0	0.0088	0.0066	0	0	0
3.8916	4.2961	4.6041	2.1576	2.1324	31.4592	31.4048	0.3344	0.3388	0.2662	0.2772	0.2398
0.9886	0.4741	0.2873	0.0132	0.0234	0.0576	0.1184	0	0	0	0	0.0044
0.4298	0.6038	0.7399	0.0222	0.0144	0	0	0.1606	0.1584	0.121	0.1276	0.165
0.7622	0.722	0.4886	0.0072	0.0042	0.048	0.0576	0.0022	0.0022	0	0	0
0.0091	0.0108	0.006	0	0.003	0	0.0384	0.4686	0.5456	0.352	0.3894	0.3278
0	0	0	0.0042	0	0.0384	0	1.8876	1.8436	1.3794	1.4476	1.562
0.0016	0.0026	0	0.0162	0.0156	0.176	0.144	0.0044	0.0066	0	0	0
16.0452	16.0627	16.0614	4.1118	4.098	31.9168	31.9136	13.9172	13.9128	13.8776	13.9436	13.959

16	18	20	21	29	31	38	41	65	66	67	68
bh96-9-14	bh96-9-15	bh96-9-17	bh96-9-18	bh96-9-26	bh96-9-28	bh96-9-35	bh96-9-37	bh96-9-59	bh96-9-60	bh96-9-61	bh96-9-62
plagioclase	plagioclase	plagioclase	plagioclase	plagioclase	plagioclase	plagioclase	plagioclase	plagioclase	plagioclase	plagioclase	plagioclase
56.7664	56.478	57.2304	59.2154	57.5707	57.3836	56.9308	60.4342	59.9667	59.1472	58.4925	58.6534
0.0243	0.0267	0.0243	0.0162	0.0428	0.0208	0.0174	0	0	0	0	0
12.5124	12.5557	12.4163	11.7587	11.7169	11.7857	12.4692	24.4191	23.9023	24.9181	24.9781	25.1744
0.0157	0	0.0214	0.0121	0	0.0128	0.01	0	0	0	0	0
0	0	0	0	0.303	0.4465	0.0744	0.1375	0.2041	0.0221	0	0.1103
0	0	0	0	0	0	0	0.0107	0	0	0	0
0	0	0	0	0	0	0	0	0	0	0	0
6.8539	6.9481	6.3187	5.044	5.8123	6.1434	6.6585	5.9753	5.7717	6.8061	6.8805	6.8864
8.2058	8.1686	8.5607	9.3958	8.9423	8.9358	8.4381	8.7433	8.4522	7.98	7.8845	7.8014
0.0768	0.0754	0.087	0.0696	0.1114	0.0607	0.0787	0.0625	0	0	0	0
0	0	0	0	0	0	0	0	0	0	0	0
84.4554	84.2526	84.6589	85.5119	84.4995	84.7894	84.6772	99.7827	98.2971	98.8736	98.2356	98.626
12.0256	12	12.08	12.32	12.1888	12.1344	12.0352	10.8	10.8576	10.6688	10.624	10.6144
0.0032	0.0032	0.0032	0.0032	0.0064	0.0032	0.0032	0	0	0	0	0
3.1232	3.1456	3.088	2.8832	2.9248	2.9376	3.1072	5.1424	5.1008	5.2992	5.3472	5.3696
0.0032	0	0.0032	0.0032	0	0.0032	0.0032	0	0	0	0	0
0	0	0	0	0.0544	0.08	0.0128	0.0192	0.032	0.0032	0	0.016
0	0	0	0	0	0	0	0.0032	0	0	0	0
0	0	0	0	0	0	0	0	0	0	0	0
1.5552	1.5808	1.4304	1.1232	1.3184	1.392	1.5072	1.1456	1.12	1.3152	1.3376	1.3344
3.3696	3.3664	3.504	3.7888	3.6704	3.664	3.4592	3.0304	2.9664	2.7904	2.7776	2.736
0.0192	0.0192	0.0224	0.0192	0.0288	0.016	0.0224	0.0128	0	0	0	0
0	0	0	0	0	0	0	0	0	0	0	0
20.1024	20.1184	20.1344	20.144	20.192	20.2336	20.1536	20.1568	20.0768	20.0768	20.0864	20.0736

69	70	71	10	14	22	37	49	50	26	30	32
bh96-9-63	bh96-9-64	bh96-9-65	bh96-9-7	bh96-9-11	bh96-9-19	bh96-9-34	bh96-9-45	bh96-9-46	bh96-9-23	bh96-9-27	bh96-9-29
plagioclase	plagioclase	plagioclase	quartz	quartz	quartz	quartz	quartz	quartz	staurolite	staurolite	staurolite
59.2918	58.5227	58.2921	96.0058	96.4492	96.304	96.0928	96.1249	96.2623	26.0982	25.6527	25.5593
0	0	0	0.0116	0.029	0.0151	0.0382	0	0	0.5307	0.5312	0.5556
24.8096	25.0148	24.9239	0	0	0	0	0	0	28.3081	27.9204	28.1463
0	0	0	0.01	0.0029	0.0029	0.0158	0	0	0.0694	0.0377	0.0503
0.1545	0.0552	0.0441	0.9234	0.0375	0	0.1712	0.7618	0.6027	14.7267	14.6165	14.4891
0	0	0	0	0	0	0	0.0699	0.0269	0.115	0.0576	0.1047
0	0	0	0	0	0	0	0.0253	0.016	1.9218	2.1179	2.0844
6.5993	6.9315	6.9235	0.036	0.0005	0.0011	0.0159	0.0422	0.0074	0.0173	0.0153	0.0117
7.9345	7.8143	7.9197	0	0	0	0	0	0	0.0159	0.0125	0.0221
0	0	0	0.0001	0.0138	0.0094	0.0026	0.0128	0.0109	0.025	0	0.0095
0	0	0	0	0.0248	0	0.0302	0.027	0.0619	0.3523	0.3572	0.324
98.7898	98.3386	98.1034	96.9869	96.5578	96.3326	96.3667	97.064	96.9882	72.1805	71.3191	71.3571
10.6976	10.6208	10.6112	0.9956	0.9994	0.9998	0.9986	0.9958	0.9968	10.5504	10.5024	10.4544
0	0	0	0	0.0002	0.0002	0.0002	0	0	0.1632	0.1632	0.1728
5.2768	5.3504	5.3472	0	0	0	0	0	0	13.4928	13.4736	13.5696
0	0	0	0	0	0	0.0002	0	0	0.024	0.0144	0.0144
0.0224	0.0096	0.0064	0.008	0.0004	0	0.0014	0.0066	0.0052	4.9776	5.0064	4.9536
0	0	0	0	0	0	0	0.0006	0.0002	0.0384	0.0192	0.0384
0	0	0	0	0	0	0	0.0004	0.0002	1.1568	1.2912	1.272
1.2768	1.3472	1.3504	0.0004	0	0	0.0002	0.0004	0	0.0096	0.0048	0.0048
2.7776	2.7488	2.7968	0	0	0	0	0	0	0.0144	0.0096	0.0192
0	0	0	0	0.0002	0.0002	0	0.0002	0.0002	0.0144	0	0.0048
0	0	0	0	0.0002	0	0.0002	0.0002	0.0004	0.1056	0.1056	0.096
20.0544	20.08	20.112	1.004	1.0006	1.0004	1.001	1.0044	1.003	30.552	30.5952	30.6

35	39	74	75	76	77	78	79	80	81	11	12
bh96-9-32	bh96-9-36	bh96-9-68	bh96-9-69	bh96-9-70	bh96-9-71	bh96-9-72	bh96-9-73	bh96-9-74	bh96-9-75	bh96-9-8	bh96-9-9
staurolite	staurolite	staurolite	staurolite	staurolite	staurolite	staurolite	staurolite	staurolite	staurolite	tourmaline	tourmaline
25.1639	25.6309	27.2512	26.447	27.1657	27.0576	26.5581	27.027	26.6413	27.3535	36.3349	36.3448
0.5702	0.7062	0.5106	0.5631	0.4076	0.4403	0.4836	0.4651	0.6137	0.4564	0.0441	0.06
28.6016	28.2979	53.3542	53.5955	53.6772	53.778	53.6769	52.8434	53.577	53.3985	11.8521	11.2556
0.0331	0.0471	0	0	0	0	0	0	0	0	0.0617	0.0601
14.2419	14.007	14.6558	14.1656	14.3403	14.5355	14.1451	14.7491	14.6705	14.3471	33.6095	34.6434
0.0419	0.0942	0.1134	0.0972	0.1243	0.1998	0.1783	0.162	0.1566	0.0919	2.8796	2.3023
2.0399	2.1395	1.8019	2.0053	1.9541	1.7469	1.7963	2.1283	2.1013	1.997	2.5152	2.811
0.0128	0.0316	0	0	0	0	0	0	0.0021	0	3.9738	2.6808
0.0083	0.0066	0.0523	0.022	0.0312	0.0313	0.0327	0.0277	0.0287	0.0341	0.0191	0.0066
0.001	0.0086	0	0	0	0	0	0	0	0	0.029	0.0423
0.3739	0.3715	0.2693	0.3434	0.3049	0.3148	0.2778	0.3148	0.2484	0.2871	0.1574	0.1486
71.0886	71.3411	98.0088	97.2392	98.0054	98.1043	97.1488	97.7175	98.0397	97.9657	91.4765	90.3555
10.3152	10.4496	7.9344	7.7568	7.896	7.8672	7.7904	7.9056	7.7664	7.9536	0.2743	0.2777
0.1776	0.216	0.1104	0.1248	0.0912	0.096	0.1056	0.1008	0.1344	0.1008	0.0003	0.0003
13.8192	13.5984	18.3072	18.5232	18.3936	18.432	18.5568	18.2208	18.408	18.2976	0.1055	0.1014
0.0096	0.0144	0	0	0	0	0	0	0	0	0.0004	0.0004
4.8816	4.776	3.5664	3.4752	3.4848	3.5376	3.4704	3.6096	3.576	3.4896	0.2122	0.2214
0.0144	0.0336	0.0288	0.024	0.0288	0.048	0.0432	0.0384	0.0384	0.024	0.0184	0.0149
1.248	1.3008	0.7824	0.8784	0.8448	0.7584	0.7872	0.9264	0.912	0.864	0.0283	0.032
0.0048	0.0144	0	0	0	0	0	0	0	0	0.0321	0.0219
0.0048	0.0048	0.0288	0.0144	0.0192	0.0192	0.0192	0.0144	0.0144	0.0192	0.0003	0.0001
0	0.0048	0	0	0	0	0	0	0	0	0.0003	0.0004
0.1152	0.1104	0.0576	0.072	0.0672	0.0672	0.0624	0.0672	0.0528	0.0624	0.0009	0.0008
30.5952	30.5232	30.8208	30.8736	30.8304	30.8304	30.84	30.8832	30.9024	30.8112	0.673	0.6714

ritch332001

BH332 Image 1

-points 1-20
-points g1-g8

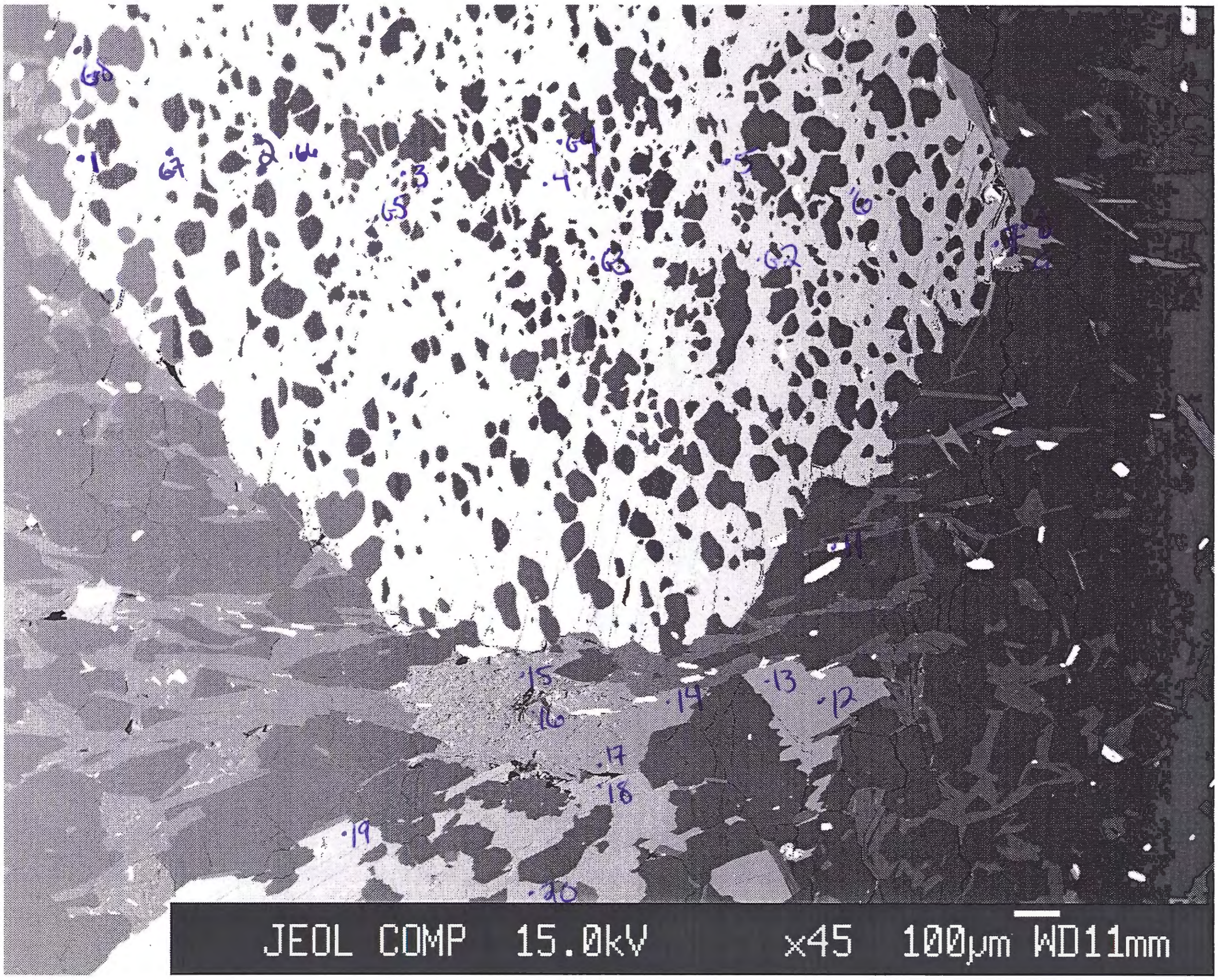

ritch332002

BH332 Image 2

-points 21-44

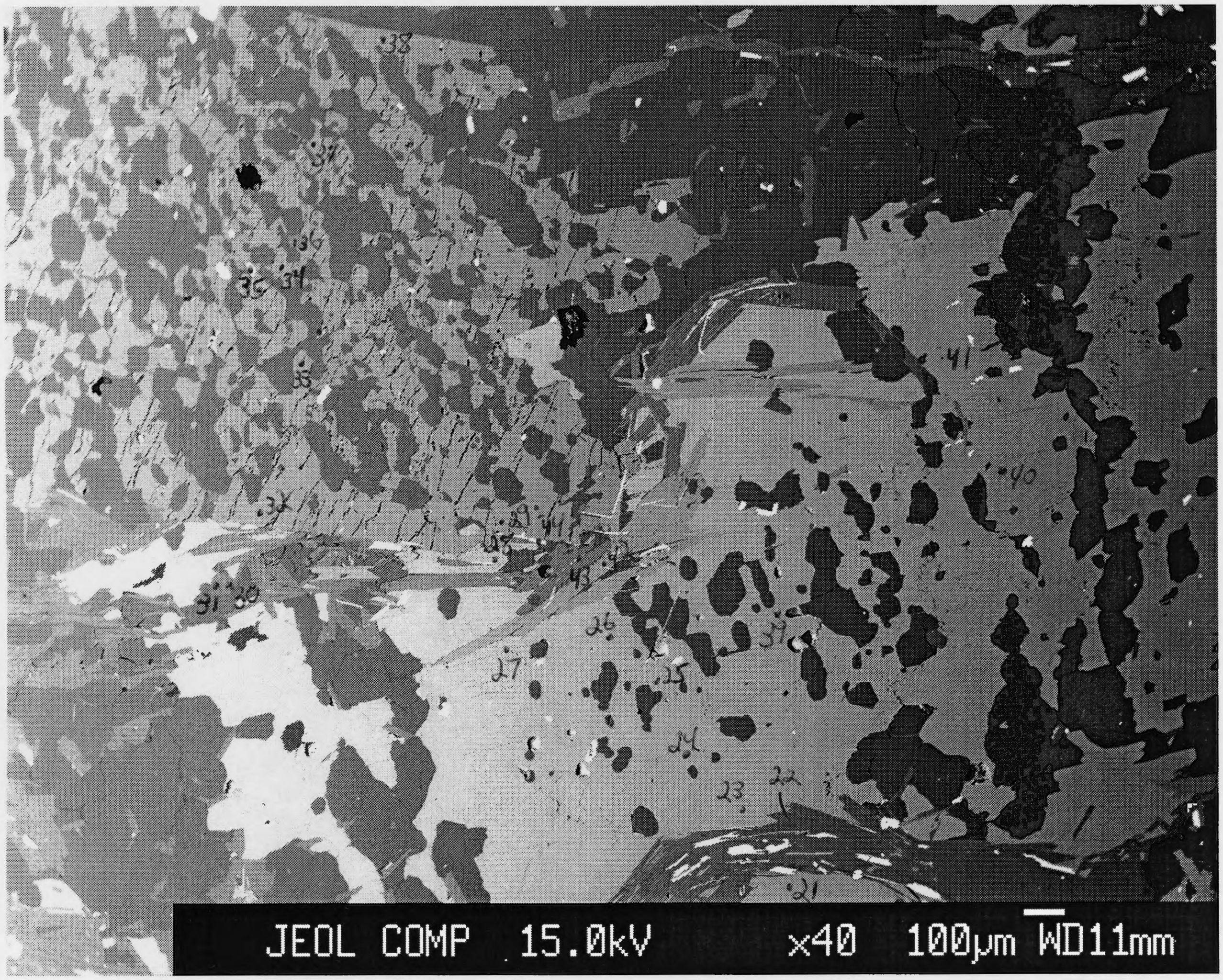

ritch332003

BH332 Image 3

-points 45-61
-points g9-g16

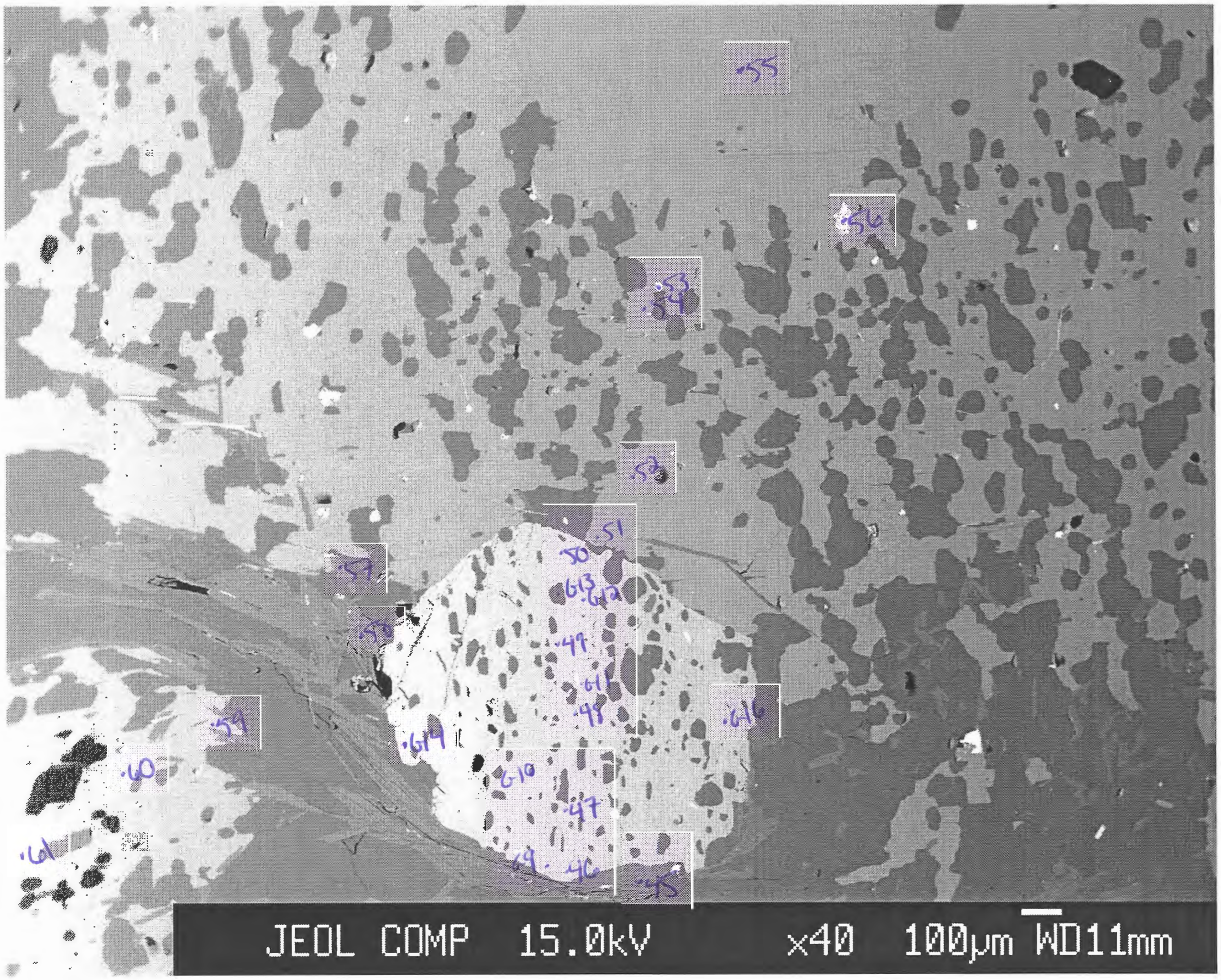

No.	382	386	387	392	393	394	395	397	398	399	400
Comment	bh332-8	bh332-12	bh332-13	bh332-18	bh332-19	bh332-20	bh332-21	bh332-23	bh332-24	bh332-25	bh332-26
Mineral	biotite	biotite	biotite	biotite	biotite	biotite	biotite	biotite	biotite	biotite	biotite
Weight % oxide:											
SiO2	36.8516	36.8066	36.4605	36.0224	36.3731	37.3312	36.7791	36.3331	36.3617	36.5173	36.1156
TiO2	1.7285	1.4919	1.3792	1.9103	1.9007	1.6124	1.5583	1.6426	1.7393	1.7737	1.5275
Al2O3	19.4205	19.6293	19.4411	18.9525	19.1259	19.8996	19.5998	19.5046	19.5823	19.6212	19.4472
Cr2O3	0	0	0	0	0	0	0	0	0	0	0
FeO	18.8776	19.7522	19.3964	20.1261	19.1433	18.669	19.6291	19.8596	19.6542	20.1784	18.504
MnO	0	0	0.0113	0	0	0	0	0	0	0	0
MgO	11.2574	10.9611	10.6578	11.3103	10.522	11.227	11.0862	10.7978	10.9533	10.7502	11.2141
CaO	0	0	0	0	0	0	0	0	0	0	0.0103
Na2O	0.331	0.2401	0.2264	0.1434	0.2438	0.2742	0.2643	0.2804	0.308	0.2579	0.2408
K2O	8.3658	8.0741	8.0671	8.0691	8.1493	8.198	8.3488	8.7283	8.5964	8.6276	8.5245
ZnO	0	0	0	0	0	0	0	0.0094	0.0026	0.0248	0.0223
Total	96.8325	96.9553	95.6399	96.5341	95.4582	97.2114	97.2657	97.1559	97.1979	97.7512	95.6064
Number of cations per formula unit:											
Si	5.445	5.4406	5.4626	5.3768	5.4604	5.4714	5.4274	5.3944	5.3856	5.39	5.412
Ti	0.1914	0.165	0.1562	0.2134	0.2156	0.1782	0.1738	0.1826	0.1936	0.1958	0.1716
Al	3.3836	3.421	3.432	3.333	3.3836	3.4386	3.41	3.4144	3.4188	3.4122	3.4342
Cr	0	0	0	0	0	0	0	0	0	0	0
Fe	2.3342	2.442	2.431	2.5124	2.4024	2.288	2.4222	2.4662	2.4354	2.4904	2.3188
Mn	0	0	0.0022	0	0	0	0	0	0	0	0
Mg	2.4794	2.4156	2.3804	2.5168	2.354	2.453	2.4398	2.3892	2.4178	2.365	2.5058
Ca	0	0	0	0	0	0	0	0	0	0	0.0022
Na	0.0946	0.0682	0.066	0.0418	0.0704	0.077	0.0748	0.0814	0.088	0.0748	0.0704
K	1.5774	1.5224	1.5422	1.5356	1.5598	1.5334	1.5708	1.6544	1.6236	1.6236	1.6302
Zn	0	0	0	0	0	0	0	0	0	0.0022	0.0022
Total	15.5078	15.477	15.4748	15.532	15.4462	15.4396	15.5188	15.5848	15.5628	15.5562	15.5496

401	402	413	414	425	426	428	429	433	434	435	436
bh332-27	bh332-28	bh332-39	bh332-40	bh332-51	bh332-52	bh332-54	bh332-55	bh332-59	bh332-60	bh332-61	bh332-62
biotite	biotite	biotite	biotite	biotite	biotite	biotite	biotite	biotite	biotite	biotite	biotite
36.1796	36.8023	36.9699	36.7621	37.1228	36.6018	36.7208	36.5886	36.7108	36.7439	37.3908	37.3968
1.6674	1.5747	1.7609	1.7926	1.872	1.7032	1.7008	1.7573	1.9228	1.6763	1.7623	1.8919
19.3382	19.4402	19.9476	19.4862	20.5127	19.979	19.8175	19.4355	19.3858	19.3061	19.8392	20.2082
0	0	0	0	0	0	0	0	0	0	0	0
19.6213	18.7279	18.9964	19.5388	19.2631	19.483	19.0136	19.4115	19.6148	19.8112	18.9138	19.2405
0	0	0.034	0	0.1021	0.0057	0.0454	0.0794	0.0737	0.0681	0.0454	0.0397
10.7063	11.1567	10.784	10.9089	10.1017	10.8523	10.8345	10.9598	10.9867	10.9333	10.9645	11.1876
0	0	0.0178	0.0183	0.0177	0.0052	0.0052	0	0	0	0	0
0.2445	0.2558	0.2949	0.2686	0.219	0.266	0.2885	0.2577	0.1569	0.2604	0.2566	0.2203
8.4543	8.1434	8.9443	8.8722	8.3752	8.747	8.8517	8.7176	9.0248	8.8929	8.4982	7.5501
0.0368	0.0103	0.1587	0.1492	0.0103	0.0326	0.0361	0.024	0.018	0	0	0
96.2484	96.1114	97.9086	97.797	97.5966	97.6758	97.3141	97.2315	97.8943	97.6923	97.6709	97.7352
5.412	5.467	5.423	5.4164	5.4384	5.3878	5.4186	5.4142	5.4076	5.4252	5.4692	5.4406
0.187	0.176	0.1936	0.198	0.2068	0.1892	0.1892	0.1958	0.2134	0.187	0.1936	0.2068
3.41	3.4034	3.4496	3.3836	3.542	3.4672	3.4474	3.3902	3.366	3.3594	3.421	3.465
0	0	0	0	0	0	0	0	0	0	0	0
2.4552	2.3276	2.3298	2.4068	2.3606	2.398	2.3474	2.4024	2.4156	2.4464	2.3144	2.3408
0	0	0.0044	0	0.0132	0	0.0066	0.011	0.0088	0.0088	0.0066	0.0044
2.387	2.4706	2.3584	2.3958	2.2066	2.3826	2.3826	2.4178	2.4134	2.4068	2.3914	2.4266
0	0	0.0022	0.0022	0.0022	0	0	0	0	0	0	0
0.0704	0.0726	0.0836	0.077	0.0616	0.077	0.0836	0.0748	0.044	0.0748	0.0726	0.0616
1.6126	1.5444	1.6742	1.6676	1.5664	1.6434	1.6654	1.6456	1.6962	1.6742	1.5862	1.4014
0.0044	0.0022	0.0176	0.0154	0.0022	0.0044	0.0044	0.0022	0.0022	0	0	0
15.5386	15.466	15.5386	15.565	15.4	15.5496	15.5452	15.5562	15.5694	15.5848	15.455	15.3494

388	389	390	391	416	375	376	377	378	379	380	381
bh332-14	bh332-15	bh332-16	bh332-17	bh332-42	bh332-1	bh332-2	bh332-3	bh332-4	bh332-5	bh332-6	bh332-7
chlorite	chlorite	chlorite	chlorite	chlorite	garnet	garnet	garnet	garnet	garnet	garnet	garnet
24.7746	25.0477	27.7758	24.9417	25.2231	36.8334	36.8347	36.5126	36.7452	36.8635	36.7092	36.7461
0.0277	0	0.0012	0.0253	0.1195	0	0.0012	0	0.0167	0.025	0	0
23.5142	23.4773	27.2254	23.5998	23.8463	21.0916	21.1458	21.0177	21.1891	21.0365	21.2379	21.1258
0	0	0	0	0	0	0	0	0	0	0	0
24.5304	24.0272	24.7481	23.9026	25.1269	34.986	34.4763	33.7704	33.4544	33.3734	33.9177	35.5252
0	0.0505	0.0112	0	0.0393	0.6638	1.528	2.7387	2.6886	2.2778	1.483	0.5094
16.4442	16.8713	18.8988	16.754	16.7531	3.2038	2.7333	2.1838	2.1591	2.4766	2.9883	3.2565
0	0	0	0	0.0034	2.1603	2.3056	3.2796	3.5386	3.3393	2.4319	2.2398
0	0	0.033	0	0.008	0.0061	0	0	0.0162	0.0035	0	0.0051
0	0	0	0	0	0	0	0	0	0	0	0
0	0	0	0	0.1671	0	0	0	0.0323	0.0058	0.0066	0
89.2912	89.4741	98.6936	89.2235	91.2868	98.9451	99.025	99.5029	99.8403	99.4015	98.7747	99.408
5.0932	5.124	5.096	5.1128	5.082	5.9784	5.9832	5.94	5.9472	5.9736	5.9664	5.9496
0.0056	0	0	0.0028	0.0168	0	0	0	0.0024	0.0024	0	0
5.698	5.6588	5.8884	5.7008	5.6644	4.0344	4.0488	4.0296	4.0416	4.02	4.068	4.032
0	0	0	0	0	0	0	0	0	0	0	0
4.2168	4.1104	3.7968	4.0964	4.2336	4.7496	4.6848	4.596	4.5288	4.524	4.6104	4.8096
0	0.0084	0.0028	0	0.0056	0.0912	0.2112	0.3768	0.3696	0.312	0.204	0.0696
5.04	5.1436	5.1688	5.1184	5.0316	0.7752	0.6624	0.5304	0.5208	0.5976	0.7248	0.7848
0	0	0	0	0	0.3768	0.4008	0.5712	0.6144	0.5808	0.4224	0.3888
0	0	0.0112	0	0.0028	0.0024	0	0	0.0048	0	0	0.0024
0	0	0	0	0	0	0	0	0	0	0	0
0	0	0	0	0.0252	0	0	0	0.0048	0	0	0
20.0536	20.0452	19.9668	20.034	20.062	16.0104	15.9912	16.044	16.0368	16.0128	15.996	16.0392

420	421	422	423	424	550	551	552	553	554	555	556
bh332-46	bh332-47	bh332-48	bh332-49	bh332-50	bh332_g1	bh332_g2	bh332_g3	bh332_g4	bh332_g5	bh332_g6	bh332_g7
garnet	garnet	garnet	garnet	garnet	garnet	garnet	garnet	garnet	garnet	garnet	garnet
36.7014	36.7469	36.7555	36.7564	36.9979	36.7765	36.9721	36.9781	36.7176	36.6618	36.861	36.7189
0.049	0.0358	0.0549	0.0716	0.0825	0.0308	0.0298	0.0805	0.0596	0.0264	0.0704	0.022
21.0824	21.1403	21.026	21.3127	21.2958	21.1897	21.2886	21.1186	21.0658	21.1435	21.2068	21.3374
0	0	0	0	0	0	0	0	0	0	0	0
34.2085	34.4471	34.2381	35.3344	34.6304	35.9117	34.5396	33.5687	33.273	34.9104	35.5167	36.6215
0.7813	1.2516	1.613	1.5146	0.8672	0.8683	1.9123	2.8284	2.8604	2.3497	2.0473	1.2898
3.0371	2.9799	2.7623	2.8503	3.1963	3.4421	2.8523	2.3259	2.1859	2.3753	2.6728	3.1153
2.3442	2.2043	2.412	2.43	2.111	2.1313	3.1573	3.6153	3.9029	3.2635	2.3721	2.0538
0.0334	0.0264	0.0417	0.0265	0.0213	0	0.0468	0.0108	0	0.0094	0.0047	0.0028
0	0	0	0	0	0	0	0	0	0	0	0
0.2053	0.2484	0.2608	0.2241	0.251	0	0.0092	0.0704	0.1049	0.0773	0.0276	0.1079
98.4427	99.0807	99.1644	100.5205	99.4535	100.3503	100.8079	100.5966	100.17	100.8173	100.7794	101.2693
5.9832	5.9664	5.9712	5.9136	5.9712	5.9139	5.9226	5.9447	5.9326	5.9038	5.925	5.8812
0.0072	0.0048	0.0072	0.0096	0.0096	0.0037	0.0036	0.0097	0.0072	0.0032	0.0085	0.0026
4.0512	4.0464	4.0272	4.0416	4.0512	4.0163	4.0196	4.0017	4.0119	4.0133	4.0179	4.0283
0	0	0	0	0	0	0	0	0	0	0	0
4.6632	4.6776	4.6536	4.7544	4.6752	4.8296	4.6273	4.5133	4.4961	4.7016	4.7745	4.9055
0.108	0.1728	0.2232	0.2064	0.1176	0.1183	0.2595	0.3851	0.3915	0.3205	0.2788	0.175
0.7368	0.7224	0.6696	0.684	0.768	0.8251	0.6811	0.5574	0.5265	0.5702	0.6404	0.7438
0.4104	0.384	0.42	0.42	0.3648	0.3672	0.5419	0.6228	0.6757	0.5631	0.4085	0.3525
0.0096	0.0072	0.012	0.0072	0.0072	0	0.0146	0.0034	0	0.0029	0.0015	0.0009
0	0	0	0	0	0	0	0	0	0	0	0
0.024	0.0288	0.0312	0.0264	0.0288	0	0.0011	0.0084	0.0125	0.0092	0.0033	0.0128
15.9936	16.0128	16.0152	16.0632	15.996	16.0742	16.0713	16.0465	16.0541	16.0878	16.0584	16.1026

557	558	559	560	561	562	563	564	565	384	385	409
bh332_g8	bh332_g9	bh332_g10	bh332_g11	bh332_g12	bh332_g13	bh332_g14	bh332_g15	bh332_g16	bh332-10	bh332-11	bh332-35
garnet	garnet	garnet	garnet	garnet	garnet	garnet	garnet	garnet	ilmenite	ilmenite	ilmenite
36.8337	36.1829	36.4333	36.5335	36.7504	36.2685	36.4814	36.3619	36.239	0	0.0618	0.4265
0.0044	0.0628	0.0242	0.0572	0.0341	0.055	0.0209	0.0561	0.0176	51.4595	51.1734	53.0253
21.3623	21.1779	21.1789	21.0438	21.3245	21.1674	21.1708	21.1668	21.2256	0	0.0379	0.0857
0	0	0	0	0	0	0	0	0	0	0	0
35.4785	35.7531	36.377	35.744	35.0734	35.634	35.7811	35.2536	35.1779	47.8603	48.136	41.2612
0.6675	0.6459	1.4429	1.3862	1.1538	0.6404	0.7779	1.6081	0.6459	0.4172	0.3575	0.2236
3.2606	3.2448	2.9605	2.909	3.1966	3.2144	3.1489	2.8466	3.1946	0.3203	0.0016	0.1089
2.395	2.2102	2.0415	2.1757	2.0572	2.157	2.2437	2.5019	2.2458	0.0699	0.0044	0.0939
0	0.0047	0.0213	0.0047	0.0103	0.0207	0.0118	0.0085	0.0103	0	0	0.0231
0	0	0	0	0	0	0	0	0	0	0	0
0.0069	0.0207	0.0314	0.0482	0.0574	0	0	0	0	0.2504	0.0323	0.4879
100.0089	99.3031	100.5109	99.9024	99.6578	99.1575	99.6366	99.8036	98.7568	100.3775	99.805	95.7362
5.9285	5.8843	5.8827	5.919	5.936	5.9008	5.9112	5.8961	5.9094	0	0.003	0.0222
0.0005	0.0077	0.0029	0.007	0.0041	0.0067	0.0025	0.0068	0.0022	1.959	1.9608	2.061
4.0527	4.0595	4.0308	4.0186	4.0599	4.0593	4.0434	4.0455	4.0797	0	0.0024	0.0054
0	0	0	0	0	0	0	0	0	0	0	0
4.7757	4.8628	4.9123	4.8432	4.7379	4.8487	4.8488	4.7808	4.7975	2.0262	2.0514	1.7832
0.091	0.089	0.1973	0.1902	0.1579	0.0883	0.1068	0.2209	0.0892	0.018	0.0156	0.0096
0.7823	0.7866	0.7126	0.7026	0.7697	0.7796	0.7606	0.6881	0.7766	0.024	0	0.0084
0.4131	0.3851	0.3532	0.3777	0.356	0.376	0.3895	0.4347	0.3924	0.0036	0	0.0054
0	0.0015	0.0067	0.0015	0.0032	0.0065	0.0037	0.0027	0.0033	0	0	0.0024
0	0	0	0	0	0	0	0	0	0	0	0
0.0008	0.0025	0.0037	0.0058	0.0069	0	0	0	0	0.0096	0.0012	0.0186
16.0446	16.0791	16.1022	16.0657	16.0317	16.066	16.0665	16.0756	16.0503	4.041	4.0344	3.9162

418	383	396	417	419	431	432	403	406	407	408	411
bh332-44	bh332-9	bh332-22	bh332-43	bh332-45	bh332-57	bh332-58	bh332-29	bh332-32	bh332-33	bh332-34	bh332-37
ilmenite	muscovite	muscovite	muscovite	muscovite	muscovite	muscovite	staurolite	staurolite	staurolite	staurolite	staurolite
0.0694	48.2642	48.1234	48.1259	47.3942	47.8859	47.62	28.3821	28.1936	28.1881	28.025	28.1226
51.3507	0.2741	0.3981	0.4774	0.5008	0.399	0.4717	0.5084	0.608	0.5441	0.5345	0.6528
0.0151	34.7791	35.0347	35.4452	34.4074	35.4738	35.2234	54.4376	54.4513	54.5788	54.3624	54.5015
0	0	0	0	0	0	0	0	0	0	0	0
47.993	1.8497	1.6852	1.9683	1.5027	1.5035	1.4855	14.4522	14.4882	14.3681	14.3457	14.363
0.4075	0	0	0.0058	0	0	0.0115	0	0	0	0	0
0.0671	0.8384	0.7535	0.6924	0.8102	0.7108	0.7533	1.5451	1.6963	1.7711	1.6766	1.9007
0.0617	0	0	0	0	0.0023	0	0	0.017	0.0023	0.0091	0.0159
0.0288	0.6935	0.7257	0.6909	0.5906	0.6471	0.6541	0.017	0.0129	0.0112	0.0203	0.0066
0.0017	8.869	9.679	9.6751	9.3962	9.4223	9.467	0	0	0	0	0
0.5062	0	0	0.0792	0.0122	0	0	0	0.1432	0.0854	0.082	0.1217
100.5011	95.5681	96.3997	97.1603	94.6144	96.0448	95.6866	99.3425	99.6106	99.5492	99.0557	99.6849
0.0036	6.336	6.2942	6.2568	6.303	6.27	6.2634	8.1024	8.04	8.0352	8.0304	8.0112
1.956	0.0264	0.0396	0.0462	0.0506	0.0396	0.0462	0.1104	0.1296	0.1152	0.1152	0.1392
0.0012	5.3834	5.401	5.4318	5.3944	5.4736	5.4604	18.312	18.2976	18.336	18.3552	18.2928
0	0	0	0	0	0	0	0	0	0	0	0
2.0328	0.2024	0.1848	0.2134	0.1672	0.165	0.1628	3.4512	3.456	3.4224	3.4368	3.4224
0.0174	0	0	0	0	0	0.0022	0	0	0	0	0
0.0048	0.165	0.1474	0.1342	0.1606	0.1386	0.1474	0.6576	0.72	0.7536	0.7152	0.8064
0.0036	0	0	0	0	0	0	0	0.0048	0	0.0048	0.0048
0.003	0.176	0.1848	0.1738	0.1518	0.165	0.1672	0.0096	0.0048	0.0048	0.0096	0.0048
0	1.485	1.6148	1.6038	1.595	1.573	1.5884	0	0	0	0	0
0.0192	0	0	0.0066	0.0022	0	0	0	0.0288	0.0192	0.0192	0.024
4.0422	13.7764	13.8666	13.8666	13.827	13.827	13.8402	30.648	30.6816	30.6864	30.6864	30.7104

412	404	405	410	415	427	430
bh332-38	bh332-30	bh332-31	bh332-36	bh332-41	bh332-53	bh332-56
staurolite	tourmaline	tourmaline	tourmaline	tourmaline	xxxxxxx	xxxxxxx
28.5079	35.9901	35.8398	36.4955	35.6005	35.2424	30.994
0.5866	0.7637	0.676	0.8609	0.8272	0.1411	0.1342
54.1748	33.0304	34.2422	30.4912	34.4121	0.0947	17.305
0	0	0	0	0	0	0
13.9976	7.0714	9.3331	9.6171	8.5862	0.9069	13.5064
0	0	0	0	0.0286	0.3301	0.4333
1.8322	6.8298	4.5682	6.3355	5.122	0.0719	0.2156
0.0108	1.4309	0.4273	0.6291	0.9949	0.0571	13.1634
0.019	1.2752	1.6742	2.102	1.6695	0.0465	0.0296
0	0	0	0	0	0	0
0.0958	0	0.0191	0.0425	0.0148	0.7347	0.4629
99.2248	86.3916	86.7799	86.5739	87.2559	37.6255	76.2444
8.136	7.4183	7.409	7.6229	7.316	0.485	0.2599
0.1248	0.1178	0.1054	0.1364	0.1271	0.0015	0.0008
18.2208	8.0259	8.3452	7.5051	8.3359	0.0015	0.1711
0	0	0	0	0	0	0
3.3408	1.2183	1.6151	1.6802	1.4756	0.0104	0.0947
0	0	0	0	0.0062	0.0038	0.0031
0.7776	2.0987	1.4074	1.9716	1.5686	0.0015	0.0027
0.0048	0.3162	0.0961	0.1395	0.2201	0.0008	0.1183
0.0096	0.5084	0.6696	0.8525	0.6665	0.0012	0.0005
0	0	0	0	0	0	0
0.0192	0	0.0031	0.0062	0.0031	0.0075	0.0029
30.6384	19.7036	19.654	19.9144	19.7222	0.5133	0.6541

ritch146001

BH146 Image 1

-points 1-36

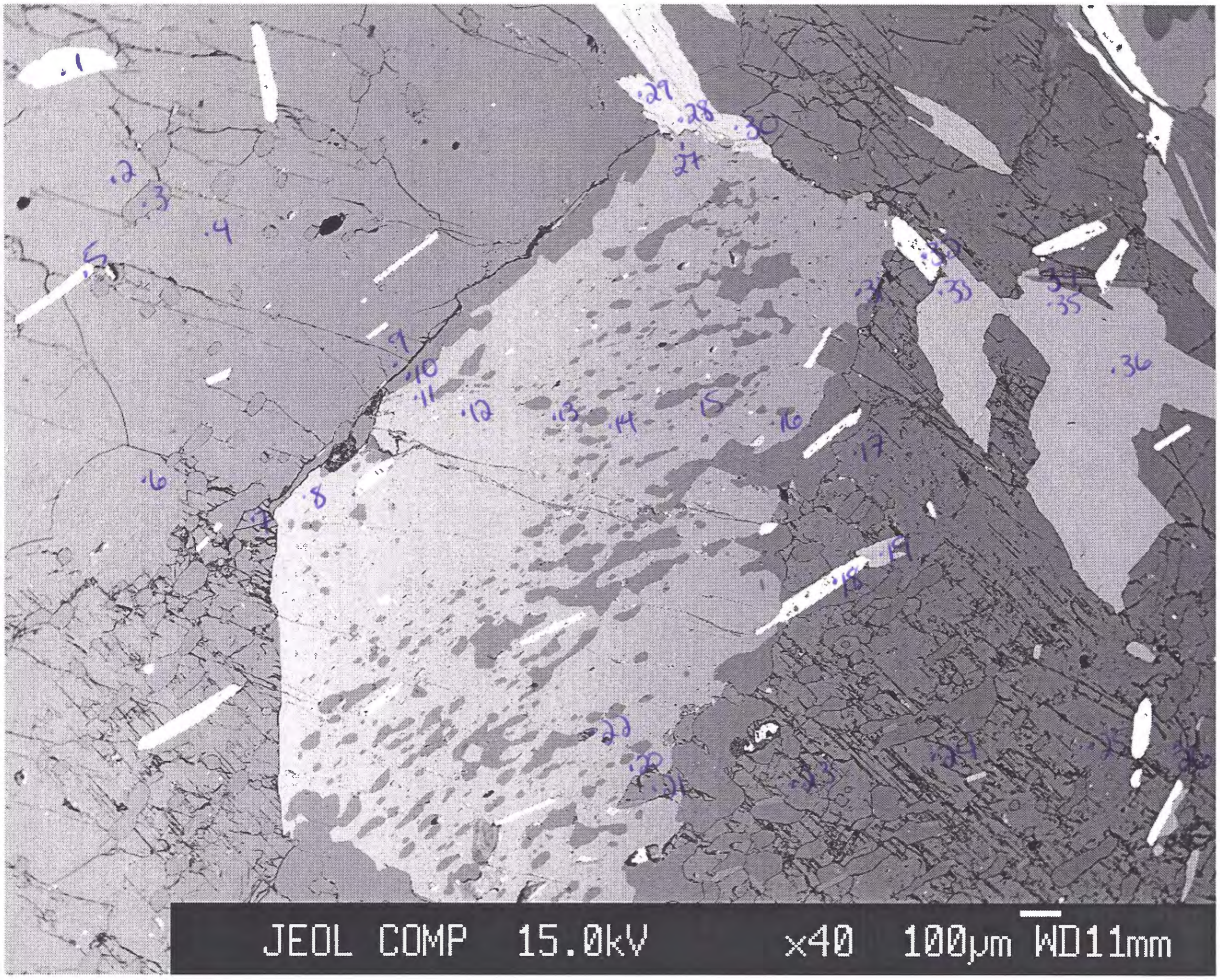

ritch146002

BH146 Image 2

-points 37-59

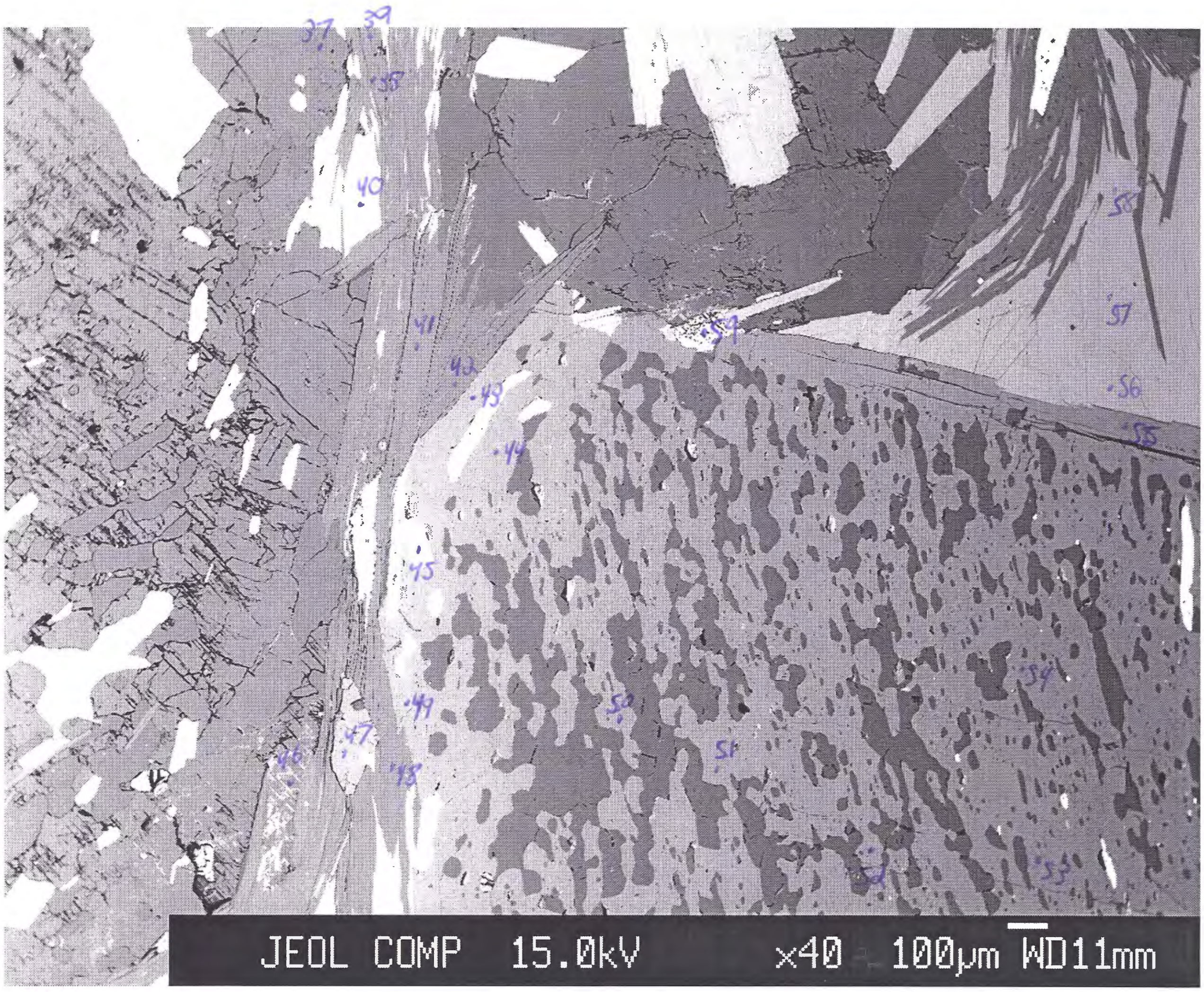

ritch146003

BH146 Image 3

-points 53, 54
-points 60-66

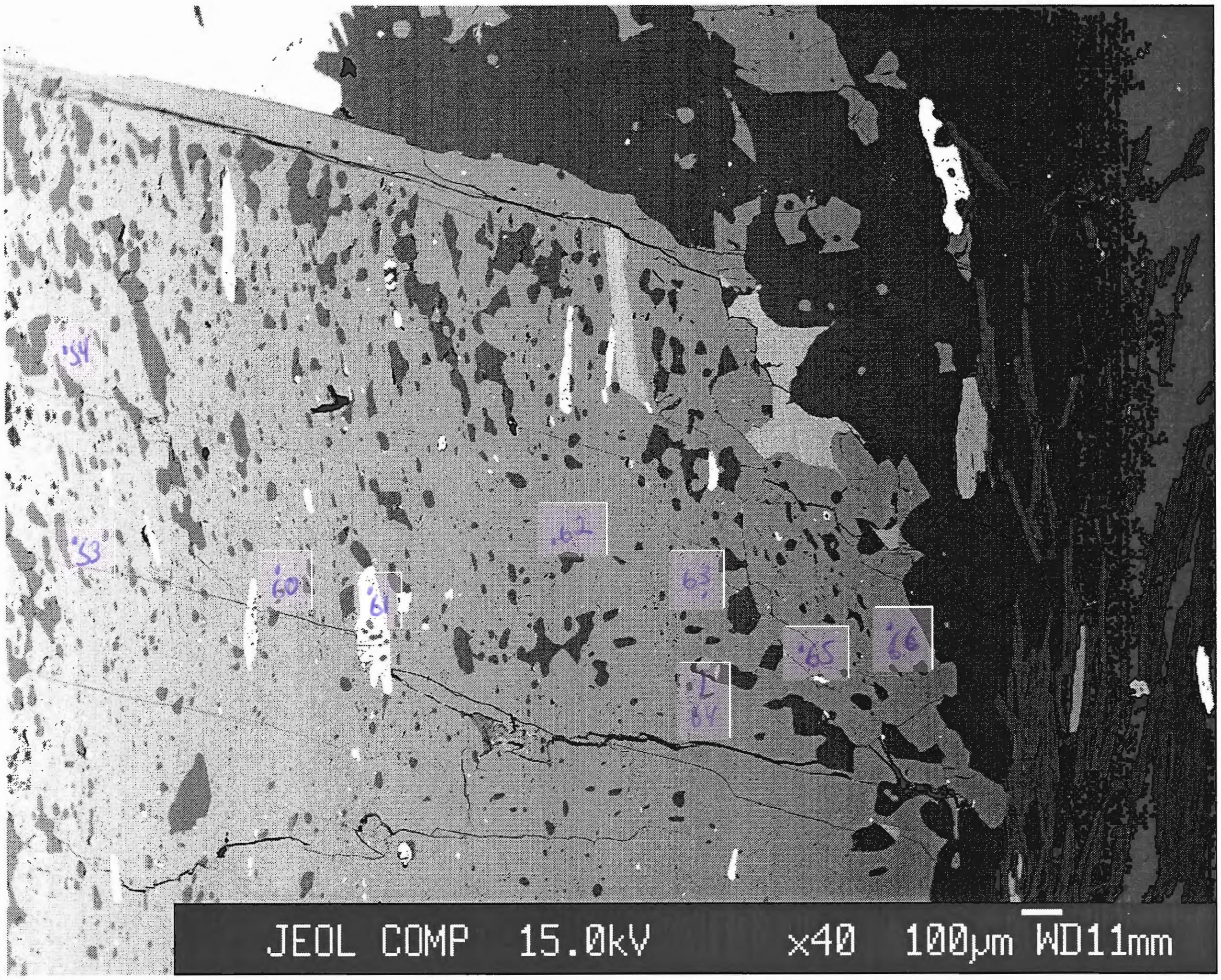

ritch146004

BH146 Image 4

-points 67-82
-points g12-15

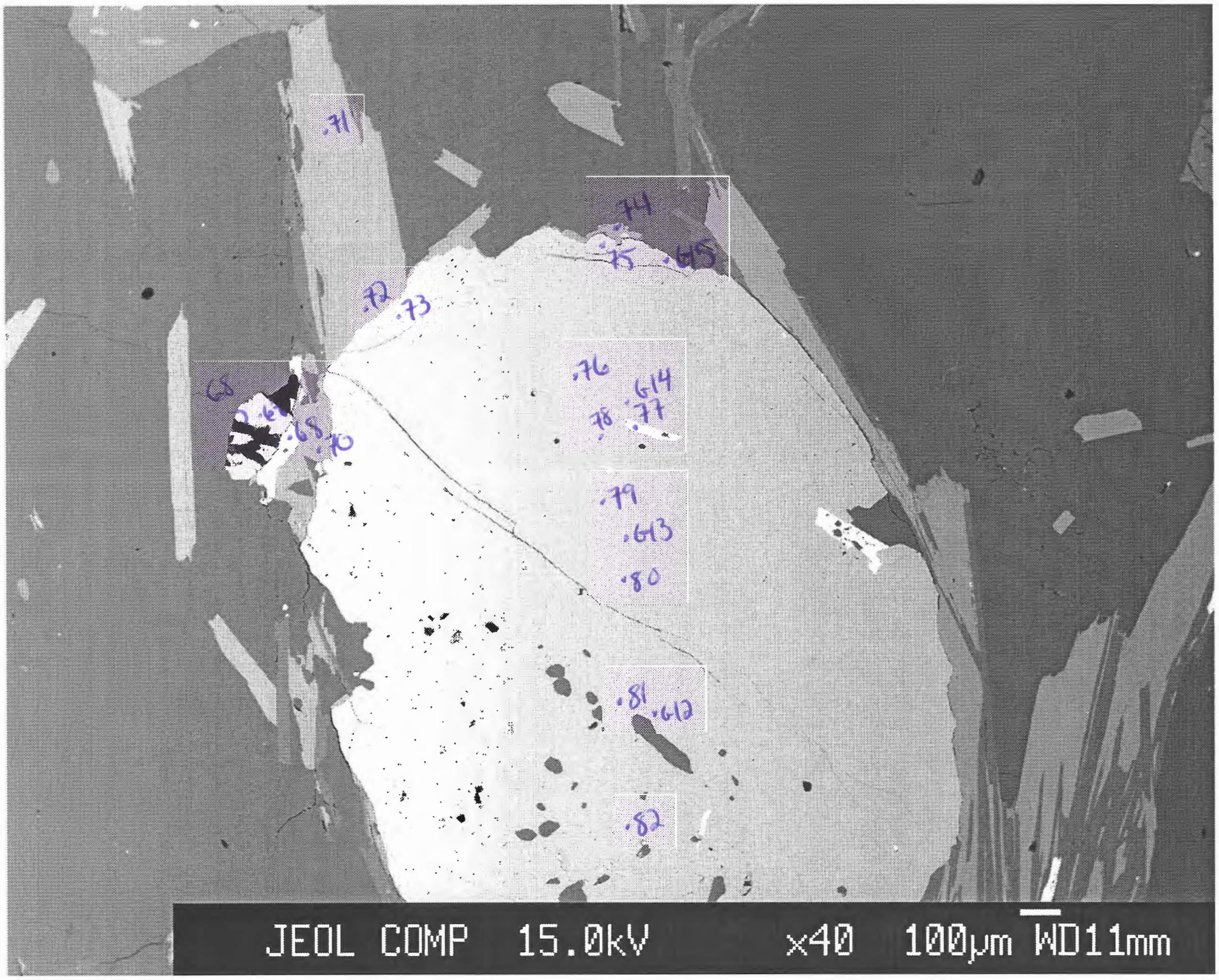

ritch146005

BH146 Image 5

-points 82-100
-points g8-g12

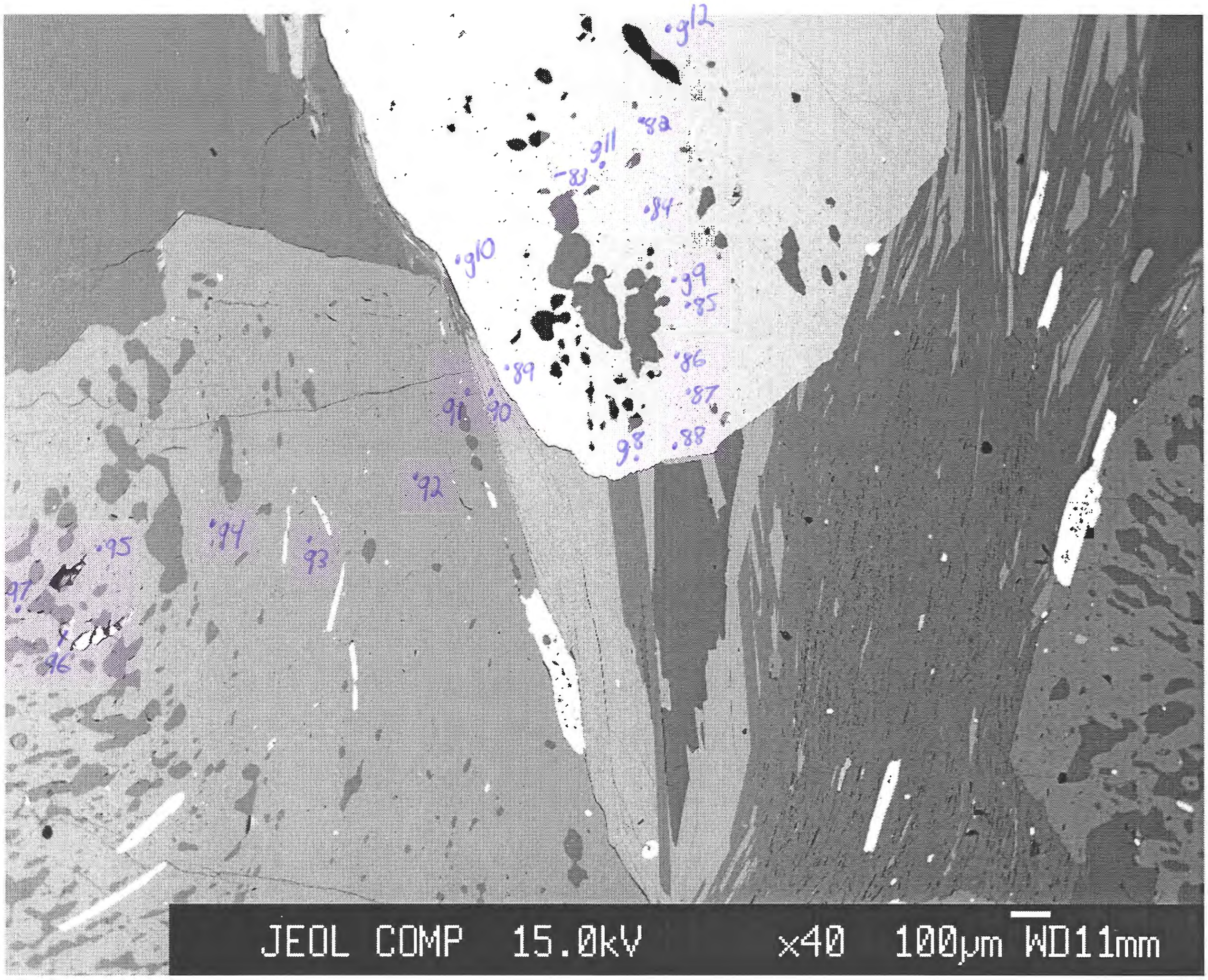

ritch146006

BH146 Image 6

-points 105-122

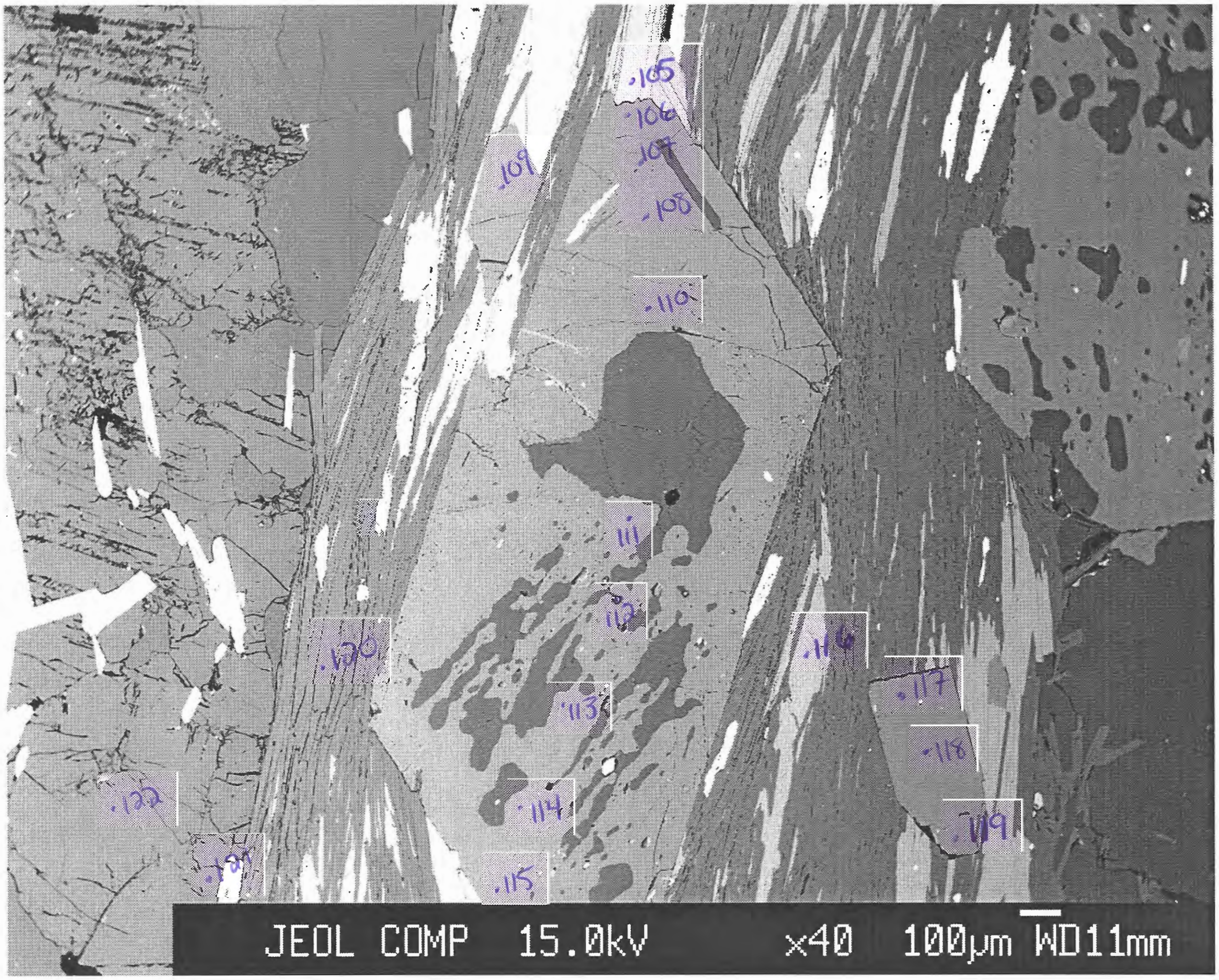

ritch146007

BH146 Image 7

-points 123-134
-points g1-g7

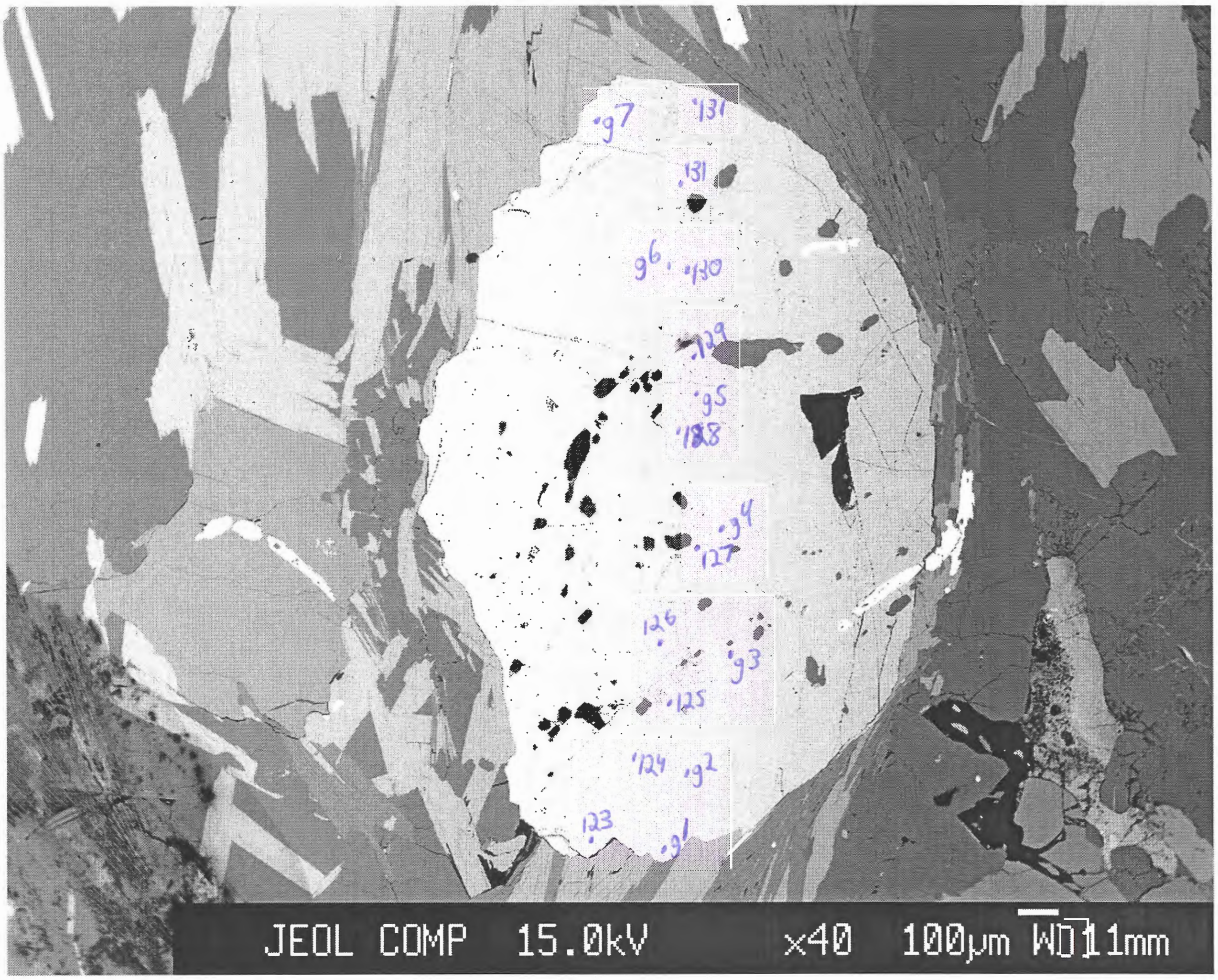

No.	226	234	250	168	186	195	196	197	200	202	203
Comment	bh146-59	bh146-67	bh146-83	bh146-1	bh146-19	bh146-28	bh146-29	bh146-30	bh146-33	bh146-35	bh146-36
Mineral	apatite	apatite	apatite	biotite	biotite	biotite	biotite	biotite	biotite	biotite	biotite
Weight % oxide:											
SiO2	0	0.0129	0.0351	34.9935	35.4173	35.4136	35.5525	35.5841	35.7581	35.4188	34.9995
TiO2	0.0131	0.0153	0.0341	1.9589	1.7852	2.1409	2.012	2.1475	1.9761	1.9632	2.1285
Al2O3	0	0	0	19.5814	20.0696	20.0165	19.9766	20.2128	20.5895	19.7196	19.7172
Cr2O3	0	0	0	0	0	0	0	0	0	0	0
FeO	0.7384	0.4339	0.9228	21.4845	19.94	20.3511	20.7679	20.3296	19.3217	21.0067	20.5446
MnO	0.1386	0.1324	0.1215	0.0619	0.0413	0.165	0.0567	0.0052	0	0.0052	0.0618
MgO	0.0526	0.0574	0.0396	9.1686	10.136	9.6583	9.2916	9.3174	9.2133	9.1838	8.925
CaO	57.3849	56.3002	56.9934	0	0	0	0	0	0	0	0
Na2O	0.1366	0.109	0.0886	0.338	0.3564	0.4121	0.3969	0.434	0.4306	0.3716	0.3997
K2O	0	0	0	7.9348	8.2692	8.1523	8.2883	8.3492	8.254	8.2192	8.3195
ZnO	0.134	0.2014	0.2004	0.0495	0.0259	0.0236	0.0044	0	0	0	0.0502
Total	58.5982	57.2626	58.4356	95.5712	96.041	96.3335	96.347	96.3799	95.5434	95.8882	95.1461
Number of cations per formula unit:											
Si	0	0.0052	0.0156	5.3218	5.3196	5.313	5.3438	5.3328	5.3702	5.3548	5.335
Ti	0.0052	0.0052	0.0104	0.2244	0.2024	0.242	0.2266	0.242	0.2222	0.2222	0.2442
Al	0	0	0	3.509	3.553	3.5398	3.5376	3.5706	3.6454	3.5134	3.542
Cr	0	0	0	0	0	0	0	0	0	0	0
Fe	0.2574	0.1534	0.3224	2.7324	2.5058	2.5542	2.6092	2.5476	2.4266	2.6554	2.618
Mn	0.0494	0.0468	0.0442	0.0088	0.0044	0.022	0.0066	0	0	0	0.0088
Mg	0.0338	0.0364	0.0234	2.079	2.2704	2.1604	2.0812	2.0812	2.0636	2.0702	2.0284
Ca	25.558	25.6334	25.4618	0	0	0	0	0	0	0	0
Na	0.1092	0.091	0.0728	0.099	0.1034	0.1188	0.1166	0.1254	0.1254	0.11	0.1188
K	0	0	0	1.54	1.584	1.5598	1.5884	1.5972	1.5818	1.5862	1.617
Zn	0.0416	0.0624	0.0624	0.0066	0.0022	0.0022	0	0	0	0	0.0066
Total	26.0546	26.0338	26.013	15.5232	15.5474	15.5144	15.51	15.499	15.4374	15.5144	15.5188

207	223	224	225	237	238	239	241	257	266	272	283
bh146-40	bh146-56	bh146-57	bh146-58	bh146-70	bh146-71	bh146-72	bh146-74	bh146-90	bh146-99	bh146-105	bh146-116
biotite	biotite	biotite	biotite	biotite	biotite	biotite	biotite	biotite	biotite	biotite	biotite
35.3772	35.4521	35.2062	35.1303	33.781	34.8165	34.1202	35.2611	35.3412	35.4017	34.8916	35.2242
1.8101	2.076	1.9384	2.2033	1.3626	2.1053	1.5019	1.655	1.8026	1.9284	1.9561	1.7302
19.736	19.5874	19.8304	19.3782	19.2205	19.5729	19.1611	19.8557	20.6424	19.7237	19.1829	19.6014
0	0	0	0	0	0	0	0	0	0	0	0
20.7224	21.8143	21.2672	20.4294	19.2015	19.6167	21.0566	20.7189	18.5726	20.1384	20.6525	20.2301
0	0.0309	0.0566	0	0.1021	0.1021	0.0816	0.1327	0	0.0969	0.0102	0.0663
9.3918	9.4051	9.1303	9.1894	9.3624	9.1697	9.3334	8.9545	9.4469	9.3131	9.1986	9.3475
0	0	0	0	0.0292	0.0128	0.0169	0.0394	0.0036	0.0036	0.0184	0.0123
0.4049	0.3531	0.4076	0.3459	0.3491	0.4128	0.4116	0.3656	0.5001	0.3846	0.3457	0.3919
8.1007	8.5544	8.4497	8.3899	8.1913	8.6565	8.2515	8.544	8.3359	8.4731	8.443	8.4649
0.028	0.0288	0.0361	0.0184	0.0564	0.1068	0.1118	0.0841	0.1171	0.111	0.122	0.1555
95.5712	97.3021	96.3226	95.0849	91.6562	94.5722	94.0467	95.611	94.7625	95.5745	94.8211	95.2244
5.357	5.3152	5.3174	5.3548	5.3328	5.335	5.2954	5.357	5.3482	5.3614	5.3504	5.3614
0.2068	0.2332	0.22	0.253	0.1628	0.242	0.176	0.1892	0.2046	0.22	0.2266	0.198
3.5222	3.4606	3.531	3.4826	3.5772	3.5354	3.5068	3.5552	3.6806	3.5222	3.4672	3.5178
0	0	0	0	0	0	0	0	0	0	0	0
2.6246	2.7346	2.6862	2.6048	2.5366	2.5146	2.7324	2.6334	2.3496	2.552	2.6488	2.5762
0	0.0044	0.0066	0	0.0132	0.0132	0.011	0.0176	0	0.0132	0.0022	0.0088
2.1208	2.101	2.0548	2.0878	2.2044	2.0944	2.1604	2.0284	2.1318	2.1032	2.1032	2.1208
0	0	0	0	0.0044	0.0022	0.0022	0.0066	0	0	0.0022	0.0022
0.1188	0.1034	0.1188	0.1012	0.1078	0.1232	0.1232	0.1078	0.1474	0.1122	0.1034	0.1166
1.5642	1.6368	1.628	1.6324	1.65	1.6918	1.6346	1.6566	1.6082	1.6368	1.6522	1.6434
0.0022	0.0022	0.0044	0.0022	0.0066	0.011	0.0132	0.0088	0.0132	0.0132	0.0132	0.0176
15.5166	15.5914	15.5672	15.5188	15.5958	15.5628	15.6574	15.5628	15.4836	15.5342	15.5694	15.565

240	242	243	245	246	247	248	249	251	252	253	254
bh146-73	bh146-75	bh146-76	bh146-78	bh146-79	bh146-80	bh146-81	bh146-82	bh146-84	bh146-85	bh146-86	bh146-87
garnet	garnet	garnet	garnet	garnet	garnet	garnet	garnet	garnet	garnet	garnet	garnet
36.3414	36.5902	36.6561	36.3104	36.4737	36.2366	36.3059	36.3431	36.6368	36.5246	36.5785	36.4368
0.0647	0.0343	0.07	0.0762	0.0699	0.0521	0.07	0.0437	0.0531	0.0281	0.0418	0.0552
21.2961	21.1979	21.2744	21.3411	21.3537	21.3064	21.2628	21.3543	21.2469	21.3133	21.4259	21.375
0	0	0	0	0	0	0	0	0	0	0	0
35.1491	36.1872	34.6322	34.7681	34.0191	34.2998	32.3804	34.6072	34.598	35.3883	35.5647	35.3205
1.9084	1.9303	1.7591	1.7333	2.4707	2.6142	3.221	2.7746	2.3189	2.2777	1.9955	1.9323
2.879	2.8108	2.6957	2.5974	2.4285	2.4066	2.4361	2.841	2.994	3.0992	3.1586	3.0797
1.7192	0.7861	2.2682	1.983	2.1855	2.369	2.6468	1.5313	1.1825	1.3604	1.151	1.4301
0.0004	0	0.0326	0.0009	0.0031	0.0121	0.0084	0.0134	0.008	0.0009	0.0104	0
0	0	0	0	0	0	0	0	0	0	0	0
0.2043	0.204	0.2	0.1796	0.2093	0.2207	0.2231	0.199	0.1897	0.2186	0.1941	0.1889
99.5627	99.7409	99.5884	98.9901	99.2135	99.5176	98.5546	99.7077	99.228	100.211	100.1204	99.8186
5.904	5.9424	5.94	5.9232	5.9352	5.8992	5.9376	5.8992	5.9544	5.9016	5.9064	5.9016
0.0072	0.0048	0.0096	0.0096	0.0096	0.0072	0.0096	0.0048	0.0072	0.0024	0.0048	0.0072
4.0776	4.0584	4.0632	4.104	4.0968	4.0896	4.0992	4.0872	4.0704	4.0584	4.0776	4.08
0	0	0	0	0	0	0	0	0	0	0	0
4.776	4.9152	4.6944	4.7424	4.6296	4.6704	4.428	4.6992	4.7016	4.7808	4.8024	4.7832
0.2616	0.2664	0.2424	0.24	0.3408	0.36	0.4464	0.3816	0.3192	0.312	0.2736	0.264
0.6984	0.6816	0.6504	0.6312	0.588	0.5832	0.5928	0.6864	0.7248	0.7464	0.7608	0.744
0.3	0.1368	0.3936	0.3456	0.3816	0.4128	0.4632	0.2664	0.2064	0.2352	0.1992	0.2472
0	0	0.0096	0	0	0.0048	0.0024	0.0048	0.0024	0	0.0024	0
0	0	0	0	0	0	0	0	0	0	0	0
0.024	0.024	0.024	0.0216	0.024	0.0264	0.0264	0.024	0.0216	0.0264	0.024	0.0216
16.0512	16.0296	16.0296	16.02	16.0056	16.0536	16.0056	16.0536	16.008	16.0656	16.0536	16.0488

255	256	290	291	292	293	294	295	296	297	298	299
bh146-88	bh146-89	bh146-123	bh146-124	bh146-125	bh146-126	bh146-127	bh146-128	bh146-129	bh146-130	bh146-131	bh146-132
garnet	garnet	garnet	garnet	garnet	garnet	garnet	garnet	garnet	garnet	garnet	garnet
36.4147	36.4449	37.0658	36.9215	36.8627	36.8662	36.7668	36.8442	37.1452	36.9612	37.0653	37.0152
0.0312	0.0374	0.0635	0.075	0.0573	0.0573	0.0573	0.0803	0.0468	0.0917	0.053	0.0528
21.3094	21.3302	21.3172	21.4243	21.6394	21.3285	21.3807	21.3097	21.4533	21.4545	21.3479	21.4547
0	0	0	0	0	0	0	0	0	0	0	0
35.5103	35.8281	35.1977	34.2121	34.647	34.082	33.4573	33.3259	35.3241	34.5922	35.7539	36.4722
1.84	2.0453	1.8842	2.3555	2.8263	3.0175	3.3919	3.0528	2.8531	2.1647	1.7519	1.9349
2.8141	2.8559	2.8757	2.7294	2.6099	2.4528	2.4653	2.4392	2.7096	2.5984	2.8802	2.77
0.8461	1.0334	1.4572	2.2951	2.4305	2.8574	2.7244	2.8857	1.8882	2.2471	1.8038	0.7708
0.0031	0.0094	0.0125	0.0013	0.0174	0.0196	0.0182	0.0098	0.0143	0.0089	0.0282	0.0031
0	0	0	0	0	0	0	0	0	0	0	0
0.2178	0.1698	0.2089	0.2306	0.1929	0.2233	0.2182	0.1907	0.2007	0.2472	0.2413	0.2049
98.9867	99.7545	100.0826	100.2447	101.2834	100.9045	100.48	100.1383	101.6352	100.3659	100.9255	100.6785
5.9424	5.916	5.9712	5.9424	5.8944	5.9184	5.9208	5.9424	5.9256	5.9448	5.94	5.9496
0.0048	0.0048	0.0072	0.0096	0.0072	0.0072	0.0072	0.0096	0.0048	0.012	0.0072	0.0072
4.0992	4.08	4.0488	4.0632	4.0776	4.0368	4.0584	4.0512	4.032	4.068	4.032	4.0656
0	0	0	0	0	0	0	0	0	0	0	0
4.8456	4.8648	4.7424	4.6032	4.6344	4.5768	4.5048	4.4952	4.7112	4.6536	4.7904	4.9032
0.2544	0.2808	0.2568	0.3216	0.3816	0.4104	0.4632	0.4176	0.3864	0.2952	0.2376	0.264
0.684	0.6912	0.6912	0.6552	0.6216	0.588	0.5928	0.5856	0.6432	0.624	0.6888	0.6648
0.1488	0.18	0.252	0.396	0.4176	0.492	0.4704	0.4992	0.3216	0.3864	0.3096	0.132
0	0.0024	0.0048	0	0.0048	0.0072	0.0048	0.0024	0.0048	0.0024	0.0096	0
0	0	0	0	0	0	0	0	0	0	0	0
0.0264	0.0192	0.024	0.0264	0.0216	0.0264	0.0264	0.0216	0.024	0.0288	0.0288	0.024
16.008	16.0416	15.9984	16.02	16.0632	16.0656	16.0488	16.0272	16.0536	16.0176	16.0464	16.0128

519	520	521	522	523	524	525	526	527	528	529	530
bh146_g1	bh146_g2	bh146_g3	bh146_g4	bh146_g5	bh146_g6	bh146_g7	bh146_g8	bh146_g9	bh146_g10	bh146_g11	bh146_g12
garnet	garnet	garnet	garnet	garnet	garnet	garnet	garnet	garnet	garnet	garnet	garnet
36.6183	36.7233	36.6784	36.6069	36.3916	36.7723	36.8622	36.5074	36.7935	36.5671	36.5617	36.6529
0.0142	0.0319	0.0374	0.0232	0.022	0.0507	0.0264	0.0131	0.012	0.0186	0	0.0176
21.0026	21.2176	21.2184	21.196	21.0873	20.9941	21.1845	21.0973	21.0561	21.2226	21.2176	21.2555
0	0	0	0	0	0	0	0	0	0	0	0
35.9893	35.2198	34.2173	33.1541	33.5776	34.4558	35.4768	36.1786	36.8302	36.1689	36.2743	34.4614
1.7288	2.5237	2.959	2.8465	2.9399	2.2256	1.7042	2.0821	2.0295	2.0031	2.6047	2.9794
2.7423	2.8812	2.5284	2.4208	2.6025	2.7015	3.0547	2.9219	3.1605	2.8814	2.9557	2.4388
0.7477	2.0032	2.6171	2.9561	2.3956	2.6026	1.5374	0.6877	1.0461	0.7047	1.0334	2.5364
0.0109	0.0208	0.0292	0.0394	0.0395	0.0334	0.0094	0.0338	0.0219	0.0309	0.0105	0.0302
0	0	0	0	0	0	0	0	0	0	0	0
0.0383	0.0482	0.0528	0.082	0.0391	0.0023	0.0452	0.0865	0.0275	0.0727	0.0895	0.0306
98.8924	100.6696	100.338	99.3251	99.0952	99.8383	99.9008	99.6085	100.9772	99.6701	100.7474	100.4027
5.9833	5.9113	5.9202	5.9468	5.934	5.9514	5.9545	5.9384	5.9174	5.9392	5.8982	5.9172
0.0018	0.0039	0.0045	0.0028	0.0027	0.0062	0.0032	0.0016	0.0015	0.0023	0	0.0021
4.045	4.0257	4.0368	4.0586	4.0529	4.0049	4.0335	4.045	3.9915	4.063	4.0345	4.0447
0	0	0	0	0	0	0	0	0	0	0	0
4.918	4.7413	4.619	4.5044	4.579	4.6637	4.7927	4.9217	4.9538	4.9131	4.8941	4.6528
0.2393	0.3441	0.4046	0.3917	0.4061	0.3051	0.2332	0.2869	0.2765	0.2756	0.3559	0.4074
0.668	0.6914	0.6083	0.5862	0.6326	0.6518	0.7356	0.7085	0.7577	0.6976	0.7108	0.5869
0.1309	0.3455	0.4526	0.5146	0.4186	0.4513	0.2661	0.1199	0.1803	0.1226	0.1786	0.4387
0.0035	0.0065	0.0091	0.0124	0.0125	0.0105	0.003	0.0106	0.0068	0.0097	0.0033	0.0095
0	0	0	0	0	0	0	0	0	0	0	0
0.0046	0.0057	0.0063	0.0098	0.0047	0.0003	0.0054	0.0104	0.0033	0.0087	0.0107	0.0037
15.9944	16.0754	16.0614	16.0273	16.0431	16.0452	16.0273	16.0431	16.0888	16.0318	16.0862	16.0631

531	532	533	172	185	212	228	236	244	265	201	205
bh146_g13	bh146_g14	bh146_g15	bh146-5	bh146-18	bh146-45	bh146-61	bh146-69	bh146-77	bh146-98	bh146-34	bh146-38
garnet	garnet	garnet	ilmenite	ilmenite	ilmenite	ilmenite	ilmenite	ilmenite	ilmenite	muscovite	muscovite
36.6848	36.7789	37.0004	0.0204	0.0122	0	0.0407	0.04	0.0501	0.0338	46.5999	45.1857
0.0494	0.0484	0	51.1127	51.327	51.0253	50.782	51.6159	50.5322	51.0323	0.4021	0.3748
21.2235	21.112	21.1813	0.0124	0.0384	0.0144	0	0	0	0	36.0552	35.5006
0	0	0	0	0	0	0	0	0	0	0	0
35.9139	35.7367	36.915	46.9164	47.1826	48.7289	46.3111	45.0876	46.6808	47.257	0.7941	2.8987
2.2741	1.6351	1.9387	0.5262	0.4118	0.5889	0.6777	0.4865	0.471	0.5489	0	0.0472
2.4364	2.6466	2.852	0.4939	0.361	0.368	0.3693	0.2018	0.3039	0.3011	0.4528	0.4691
2.1009	1.8144	1.1361	0.0644	0.0616	0.0393	0.0637	0.0887	0.0866	0.0671	0	0.0237
0.0451	0.018	0.0057	0.0252	0.0093	0.005	0	0	0	0	1.4568	1.2167
0	0	0	0	0	0	0	0	0	0	7.9207	7.1707
0.0559	0.0207	0.0199	0.3736	0.3727	0.349	0.4846	0.4318	0.426	0.3993	0	0
100.7839	99.8109	101.049	99.5452	99.7767	101.1187	98.7292	97.9524	98.5507	99.6396	93.6817	92.8873
5.913	5.958	5.9417	0.0012	0.0006	0	0.0018	0.0018	0.0024	0.0018	6.1996	6.1116
0.006	0.0059	0	1.959	1.9632	1.9368	1.9626	1.9986	1.959	1.9578	0.0396	0.0374
4.0322	4.0312	4.0092	0.0006	0.0024	0.0006	0	0	0	0	5.654	5.6606
0	0	0	0	0	0	0	0	0	0	0	0
4.8413	4.8416	4.9577	1.9998	2.0064	2.0568	1.9908	1.941	2.0124	2.016	0.088	0.3278
0.3105	0.2244	0.2637	0.0228	0.018	0.0252	0.0294	0.021	0.0204	0.024	0	0.0044
0.5854	0.6391	0.6827	0.0378	0.0276	0.0276	0.0282	0.0156	0.0234	0.0228	0.0902	0.0946
0.3628	0.3149	0.1955	0.0036	0.0036	0.0024	0.0036	0.0048	0.0048	0.0036	0	0.0044
0.0141	0.0056	0.0018	0.0024	0.0012	0.0006	0	0	0	0	0.3762	0.319
0	0	0	0	0	0	0	0	0	0	1.3442	1.2364
0.0066	0.0025	0.0024	0.0138	0.0138	0.0132	0.0186	0.0162	0.0162	0.015	0	0
16.0719	16.0233	16.0547	4.0416	4.0374	4.0632	4.0356	3.999	4.0392	4.0416	13.794	13.7962

206	208	209	215	267	287	169	171	173	174	176	184
bh146-39	bh146-41	bh146-42	bh146-48	bh146-100	bh146-120	bh146-2	bh146-4	bh146-6	bh146-7	bh146-9	bh146-17
muscovite	muscovite	muscovite	muscovite	muscovite	muscovite	plagioclase	plagioclase	plagioclase	plagioclase	plagioclase	plagioclase
47.0038	47.2316	46.6409	46.8199	47.634	46.4395	64.7297	64.9222	64.5113	64.8283	65.2663	64.9078
0.5974	0.5597	0.5549	0.5272	0.5564	0.6677	0	0	0	0	0	0
35.8679	36.1052	35.9453	36.0497	35.9395	35.2991	20.9426	20.5341	20.5326	20.7522	20.9912	21.2181
0	0	0	0	0	0	0	0	0	0	0	0
0.7841	0.7426	0.8925	0.8874	1.1136	1.1181	0	0	0	0.0104	0	0
0	0	0	0	0	0	0	0	0	0	0	0
0.5292	0.5057	0.492	0.502	0.5941	0.5548	0	0	0	0	0	0
0	0	0	0	0	0	1.9176	1.5679	1.5966	1.7907	1.7993	2.1622
1.4505	1.4702	1.5126	1.4943	1.4037	1.2592	10.3332	10.5392	10.6361	10.5477	10.3564	10.2635
8.2379	8.0775	8.1846	8.1147	8.2676	8.2873	0	0	0	0	0	0
0	0	0	0	0.0074	0.0119	0	0	0	0	0	0
94.4708	94.6926	94.2229	94.3953	95.5163	93.6376	97.9231	97.5635	97.2766	97.9294	98.4132	98.5517
6.2128	6.2194	6.1864	6.1952	6.2348	6.2084	11.6	11.6672	11.6416	11.6224	11.6288	11.5648
0.0594	0.055	0.055	0.0528	0.055	0.0682	0	0	0	0	0	0
5.588	5.6034	5.621	5.621	5.544	5.5616	4.4224	4.3488	4.368	4.384	4.4096	4.4576
0	0	0	0	0	0	0	0	0	0	0	0
0.0858	0.0814	0.099	0.099	0.121	0.1254	0	0	0	0	0	0
0	0	0	0	0	0	0	0	0	0	0	0
0.1034	0.099	0.0968	0.099	0.1166	0.11	0	0	0	0	0	0
0	0	0	0	0	0	0.368	0.3008	0.3072	0.3424	0.3424	0.4128
0.3718	0.3762	0.3894	0.3828	0.3564	0.3256	3.5904	3.6736	3.7216	3.6672	3.5776	3.5456
1.3882	1.3574	1.386	1.3706	1.3794	1.4124	0	0	0	0	0	0
0	0	0	0	0	0.0022	0	0	0	0	0	0
13.8094	13.794	13.8336	13.8226	13.8094	13.8138	19.984	19.9936	20.0384	20.016	19.9616	19.984

188	189	190	191	192	193	199	204	213	288	289	170
bh146-21	bh146-22	bh146-23	bh146-24	bh146-25	bh146-26	bh146-32	bh146-37	bh146-46	bh146-121	bh146-122	bh146-3
plagioclase	plagioclase	plagioclase	plagioclase	plagioclase	plagioclase	plagioclase	plagioclase	plagioclase	plagioclase	plagioclase	quartz
64.0506	63.9692	64.5575	63.9197	64.38	64.2346	64.8791	64.3416	65.6696	64.3243	65.3741	94.8063
0	0	0	0	0	0	0.0476	0	0	0.0613	0	0
21.5921	21.9626	21.4482	21.3402	21.7287	21.524	20.9745	21.3676	21.0869	21.2616	20.9056	0.0091
0	0	0	0	0	0	0	0	0	0	0	0
0.0052	0.3599	0	0	0	0	0.0365	0	0.0469	0.1132	0	0
0.0053	0.0053	0	0	0	0	0	0	0	0	0	0
0	0	0	0	0	0	0	0	0	0	0	0.0087
2.7774	3.1851	2.3787	2.5365	2.6541	2.7559	1.9957	2.5759	2.0919	2.4726	2.102	0
9.7375	9.4087	9.9634	9.9905	9.7462	9.8859	10.3891	9.9943	8.8169	10.0853	9.8447	0
0	0	0	0	0	0	0	0	0	0	0	0
0	0	0	0	0	0	0	0	0	0	0	0
98.1682	98.8909	98.3479	97.7869	98.509	98.4005	98.3226	98.2795	97.7123	98.3184	98.2264	94.8242
11.4688	11.3984	11.5264	11.4944	11.4784	11.4784	11.5872	11.5072	11.7088	11.5072	11.6544	0.9998
0	0	0	0	0	0	0.0064	0	0	0.0096	0	0
4.5568	4.6112	4.512	4.5216	4.5664	4.5344	4.416	4.5056	4.432	4.4832	4.3936	0.0002
0	0	0	0	0	0	0	0	0	0	0	0
0	0.0544	0	0	0	0	0.0064	0	0.0064	0.016	0	0
0	0	0	0	0	0	0	0	0	0	0	0
0	0	0	0	0	0	0	0	0	0	0	0.0002
0.5344	0.608	0.4544	0.4896	0.5056	0.528	0.3808	0.4928	0.4	0.4736	0.4	0
3.3824	3.2512	3.4496	3.4816	3.3696	3.4272	3.5968	3.4656	3.0496	3.4976	3.4016	0
0	0	0	0	0	0	0	0	0	0	0	0
0	0	0	0	0	0	0	0	0	0	0	0
19.9456	19.9264	19.9456	19.9904	19.9232	19.9712	19.9968	19.9712	19.6	19.9904	19.8528	1.0004

177	175	178	179	180	181	182	183	187	194	198	210
bh146-10	bh146-8	bh146-11	bh146-12	bh146-13	bh146-14	bh146-15	bh146-16	bh146-20	bh146-27	bh146-31	bh146-43
quartz	staurolite	staurolite	staurolite	staurolite	staurolite	staurolite	staurolite	staurolite	staurolite	staurolite	staurolite
95.7535	27.3353	27.2712	27.6472	27.3411	27.2423	27.1621	27.1113	26.8244	27.1619	27.0977	27.1793
0	0.7418	0.7717	0.5618	0.4977	0.5019	0.5166	0.6214	0.6313	0.7043	0.671	0.6178
0	53.7881	53.9392	53.4108	53.8885	53.7649	53.9905	54.1983	54.0593	53.9252	54.0383	54.6164
0	0	0	0	0	0	0	0	0	0	0	0
0	14.2562	14.0221	14.2832	14.3616	14.4058	14.7628	13.8638	14.5439	14.2918	15.0268	14.5778
0	0.1037	0.1139	0.0363	0	0.0518	0.0725	0.0518	0.0466	0.0466	0.0828	0.0259
0.008	1.646	1.6838	1.6954	1.7007	1.7263	1.7053	1.6834	1.5139	1.5156	1.5893	1.5673
0	0	0	0	0	0	0	0	0	0	0	0
0.0059	0.0077	0.0101	0.0017	0.0045	0.0038	0.0011	0.0205	0.0039	0.0042	0.0039	0.0105
0	0	0	0	0	0	0	0	0	0	0	0
0	0.0186	0.0097	0.0283	0	0.0022	0.0432	0.0216	0.0484	0.0089	0	0
95.7675	97.8975	97.8218	97.6647	97.7942	97.6991	98.2542	97.5722	97.6718	97.6586	98.5099	98.595
1	7.9344	7.9152	8.04	7.9392	7.9248	7.8768	7.8768	7.8192	7.9008	7.848	7.8384
0	0.1632	0.168	0.1248	0.1104	0.1104	0.1104	0.1344	0.1392	0.1536	0.144	0.1344
0	18.4032	18.4464	18.3024	18.4512	18.4368	18.4512	18.5664	18.5712	18.4944	18.4464	18.5664
0	0	0	0	0	0	0	0	0	0	0	0
0	3.4608	3.4032	3.4752	3.4896	3.504	3.5808	3.3696	3.5472	3.4752	3.6384	3.5184
0	0.024	0.0288	0.0096	0	0.0144	0.0192	0.0144	0.0096	0.0096	0.0192	0.0048
0.0002	0.7104	0.7296	0.7344	0.7344	0.7488	0.7392	0.7296	0.6576	0.6576	0.6864	0.672
0	0	0	0	0	0	0	0	0	0	0	0
0.0002	0.0048	0.0048	0	0.0048	0	0	0.0096	0	0	0	0.0048
0	0	0	0	0	0	0	0	0	0	0	0
0	0.0048	0	0.0048	0	0	0.0096	0.0048	0.0096	0	0	0
1.0004	30.7104	30.696	30.696	30.7344	30.744	30.792	30.7104	30.7584	30.696	30.7872	30.744

211	214	216	217	218	219	220	221	222	227	229	230
bh146-44	bh146-47	bh146-49	bh146-50	bh146-51	bh146-52	bh146-53	bh146-54	bh146-55	bh146-60	bh146-62	bh146-63
staurolite	staurolite	staurolite	staurolite	staurolite	staurolite	staurolite	staurolite	staurolite	staurolite	staurolite	staurolite
27.3358	27.2023	27.0292	27.5507	27.3647	27.5065	27.6375	27.5441	27.1354	27.3881	27.3759	27.3633
0.6504	0.6379	0.5677	0.6799	0.6669	0.7113	0.6348	0.6725	0.6335	0.6123	0.5671	0.5752
54.1413	55.1398	54.9823	54.0831	54.1031	54.0616	54.3148	53.9403	54.0976	54.4556	54.1505	54.2362
0	0	0	0	0	0	0	0	0	0	0	0
14.1984	13.6583	13.908	14.2073	14.9853	14.574	14.4052	14.2034	14.3209	13.8563	13.9905	14.355
0.0984	0.0518	0.0517	0.1034	0.124	0.0672	0.0983	0.031	0.1603	0.0565	0.0051	0.1179
1.5713	1.3199	1.4442	1.6018	1.6323	1.6905	1.7381	1.6998	1.568	1.6872	1.7212	1.6857
0	0	0	0	0	0	0	0	0	0.001	0	0.0051
0.0133	0.0087	0	0.0091	0.0098	0.0115	0	0.0132	0.007	0.0031	0.0183	0.0014
0	0	0	0	0	0	0	0	0	0	0	0
0.0476	0	0.032	0	0.0238	0.0089	0	0	0.0007	0.1447	0.0944	0.0641
98.0565	98.0188	98.0152	98.2354	98.91	98.6316	98.8288	98.1043	97.9235	98.2049	97.923	98.4039
7.9152	7.8528	7.8192	7.9632	7.8912	7.9344	7.944	7.968	7.8768	7.9104	7.9296	7.9056
0.144	0.1392	0.1248	0.1488	0.144	0.1536	0.1392	0.144	0.1392	0.1344	0.1248	0.1248
18.4848	18.7584	18.744	18.4224	18.384	18.3744	18.4032	18.3936	18.5136	18.5328	18.4896	18.4656
0	0	0	0	0	0	0	0	0	0	0	0
3.4416	3.2976	3.3648	3.432	3.6144	3.5136	3.4608	3.4368	3.4752	3.3456	3.3888	3.4704
0.024	0.0144	0.0144	0.024	0.0288	0.0144	0.024	0.0096	0.0384	0.0144	0	0.0288
0.6768	0.5664	0.624	0.6912	0.7008	0.7248	0.744	0.7344	0.6768	0.7248	0.744	0.7248
0	0	0	0	0	0	0	0	0	0	0	0
0.0096	0.0048	0	0.0048	0.0048	0.0048	0	0.0096	0.0048	0	0.0096	0
0	0	0	0	0	0	0	0	0	0	0	0
0.0096	0	0.0048	0	0.0048	0	0	0	0	0.0288	0.0192	0.0144
30.7104	30.6384	30.7008	30.6864	30.7776	30.7248	30.7152	30.7008	30.7296	30.6912	30.7104	30.7392

232	233	258	259	260	261	262	264	268	269	270	271
bh146-65	bh146-66	bh146-91	bh146-92	bh146-93	bh146-94	bh146-95	bh146-97	bh146-101	bh146-102	bh146-103	bh146-104
staurolite	staurolite	staurolite	staurolite	staurolite	staurolite	staurolite	staurolite	staurolite	staurolite	staurolite	staurolite
27.2022	27.2362	26.7867	26.8198	26.8381	26.6341	26.3256	27.2232	27.3226	27.1848	27.247	26.865
0.6827	0.6604	0.6529	0.6289	0.5623	0.675	0.6639	0.646	0.6469	0.6577	0.6598	0.8081
54.6116	54.1331	54.6388	53.9472	53.6497	53.7875	53.6053	54.1591	54.2098	54.0275	54.2309	54.0819
0	0	0	0	0	0	0	0	0	0	0	0
14.2693	14.261	14.5998	14.1988	13.8295	14.3071	13.7403	13.8895	14.783	14.5219	14.6132	14.4197
0.118	0.0667	0.1281	0.1486	0	0.1331	0.1076	0.1281	0.1382	0.1484	0.0972	0.1177
1.663	1.6472	1.4714	1.6372	1.6935	1.7144	1.6234	1.6935	1.4431	1.5957	1.555	1.445
0	0	0	0.0106	0.0142	0	0	0.0172	0.0106	0.0025	0	0.0035
0	0	0	0	0.0058	0	0.0003	0.0003	0	0	0	0.0045
0	0	0	0	0	0	0	0	0	0	0	0
0.1305	0.0819	0.0869	0.1113	0.1024	0.0891	0.1127	0.1098	0.0618	0.0942	0.0832	0.1244
98.6774	98.0866	98.3646	97.5024	96.6955	97.3404	96.1792	97.8668	98.616	98.2328	98.4864	97.8699
7.8384	7.8912	7.7568	7.824	7.8768	7.7904	7.776	7.896	7.8912	7.8816	7.8768	7.8144
0.1488	0.144	0.144	0.1392	0.1248	0.1488	0.1488	0.1392	0.1392	0.144	0.144	0.1776
18.5472	18.4848	18.6528	18.552	18.5568	18.5472	18.6624	18.5136	18.4608	18.456	18.4752	18.5472
0	0	0	0	0	0	0	0	0	0	0	0
3.4368	3.456	3.5376	3.4656	3.3936	3.4992	3.3936	3.3696	3.5712	3.5184	3.5328	3.5088
0.0288	0.0144	0.0336	0.0384	0	0.0336	0.0288	0.0336	0.0336	0.0384	0.024	0.0288
0.7152	0.7104	0.6336	0.7104	0.7392	0.7488	0.7152	0.7344	0.6192	0.6912	0.672	0.6288
0	0	0	0.0048	0.0048	0	0	0.0048	0.0048	0	0	0
0	0	0	0	0.0048	0	0	0	0	0	0	0.0048
0	0	0	0	0	0	0	0	0	0	0	0
0.0288	0.0192	0.0192	0.024	0.024	0.0192	0.024	0.024	0.0144	0.0192	0.0192	0.0288
30.744	30.7248	30.7824	30.7632	30.7296	30.7872	30.7488	30.72	30.7344	30.7536	30.7488	30.744

273	274	275	276	277	278	279	280	281	282	284	285
bh146-106	bh146-107	bh146-108	bh146-109	bh146-110	bh146-111	bh146-112	bh146-113	bh146-114	bh146-115	bh146-117	bh146-118
staurolite	staurolite	staurolite	staurolite	staurolite	staurolite	staurolite	staurolite	staurolite	staurolite	staurolite	staurolite
26.9033	26.89	26.9021	26.8398	27.5976	27.1767	27.4808	27.3278	27.4313	26.8436	27.2804	27.2648
0.6452	0.7392	0.6341	0.6367	0.7013	0.6531	0.6661	0.652	0.6811	0.6388	0.6043	0.6912
54.3052	53.7732	53.8273	54.6183	54.4583	53.8576	54.6186	54.0907	54.0504	54.2392	54.1072	53.9331
0	0	0	0	0	0	0	0	0	0	0	0
14.2567	14.1092	13.712	14.091	13.9923	14.1737	14.1218	14.4755	14.2116	13.9697	14.796	14.4204
0.1382	0.1842	0.0717	0.087	0.0512	0.2199	0.1381	0.0869	0.133	0.1586	0.0818	0.0563
1.4754	1.5018	1.4698	1.4071	1.4967	1.6158	1.6293	1.6735	1.5993	1.4057	1.5735	1.5302
0	0.0106	0	0	0	0.003	0.0035	0	0	0	0	0.0005
0.0014	0	0.0052	0	0.0076	0	0	0.0031	0	0	0	0.0066
0	0	0	0	0	0	0	0	0	0	0	0
0.081	0.0684	0.0957	0.078	0.1008	0.0662	0.0743	0.0802	0.1008	0.0795	0.0927	0.0743
97.8065	97.2766	96.718	97.758	98.4059	97.766	98.7326	98.3898	98.2075	97.3352	98.5359	97.9775
7.824	7.8576	7.8864	7.8	7.9536	7.9008	7.9008	7.9008	7.9344	7.8336	7.8864	7.9152
0.1392	0.1632	0.1392	0.1392	0.1536	0.144	0.144	0.144	0.1488	0.1392	0.1296	0.1488
18.6096	18.528	18.6	18.7056	18.4944	18.4608	18.5088	18.4368	18.432	18.6528	18.4416	18.4512
0	0	0	0	0	0	0	0	0	0	0	0
3.4656	3.4512	3.36	3.4224	3.3696	3.4464	3.3936	3.4992	3.4368	3.408	3.576	3.4992
0.0336	0.048	0.0192	0.0192	0.0144	0.0528	0.0336	0.0192	0.0336	0.0384	0.0192	0.0144
0.6384	0.6528	0.6432	0.6096	0.6432	0.7008	0.696	0.72	0.6912	0.6096	0.6768	0.6624
0	0.0048	0	0	0	0	0	0	0	0	0	0
0	0	0.0048	0	0.0048	0	0	0	0	0	0	0.0048
0	0	0	0	0	0	0	0	0	0	0	0
0.0192	0.0144	0.0192	0.0144	0.0192	0.0144	0.0144	0.0192	0.0192	0.0192	0.0192	0.0144
30.7344	30.72	30.6768	30.7152	30.6576	30.7248	30.696	30.744	30.696	30.7056	30.7536	30.7104

286	235	231	263	300	301
bh146-119	bh146-68	bh146-64	bh146-96	bh146-133	bh146-134
staurolite	xxxxx	xxxxx	xxxxx	xxxxx	xxxxx
27.1073	0	19.984	21.7609	4.2852	3.4874
0.5968	0	0.5811	0.6986	0.0583	0.0664
54.8985	0	39.9337	45.4804	11.1689	13.8455
0	0	0	0	0	0
14.6743	0	14.2769	14.2008	62.7099	55.015
0.0767	0	0.1789	0.1481	0.0906	0.0383
1.396	0	1.1865	1.6297	0	0
0	0.0014	0.0551	0	0.1363	0.3551
0.0038	0	0.0396	0.0043	0.0141	0.0758
0	0	0	0	0	0
0.0926	0	0.0647	0.1146	0.3103	0.2434
98.8461	0.0014	76.3006	84.0375	78.7737	73.127
7.8048	0	0.1593	0.156	0.0527	0.0446
0.1296	0	0.0035	0.0038	0.0005	0.0006
18.6384	0	0.3752	0.3843	0.1619	0.2086
0	0	0	0	0	0
3.5328	0	0.0952	0.0851	0.645	0.5881
0.0192	0	0.0012	0.0009	0.0009	0.0004
0.6	0	0.0141	0.0174	0	0
0	1	0.0005	0	0.0018	0.0049
0	0	0.0006	0.0001	0.0003	0.0019
0	0	0	0	0	0
0.0192	0	0.0004	0.0006	0.0028	0.0023
30.744	1	0.6501	0.6482	0.8659	0.8515

ritch1291010

BH129 Image 1

-points 1-29
-points g1-g8

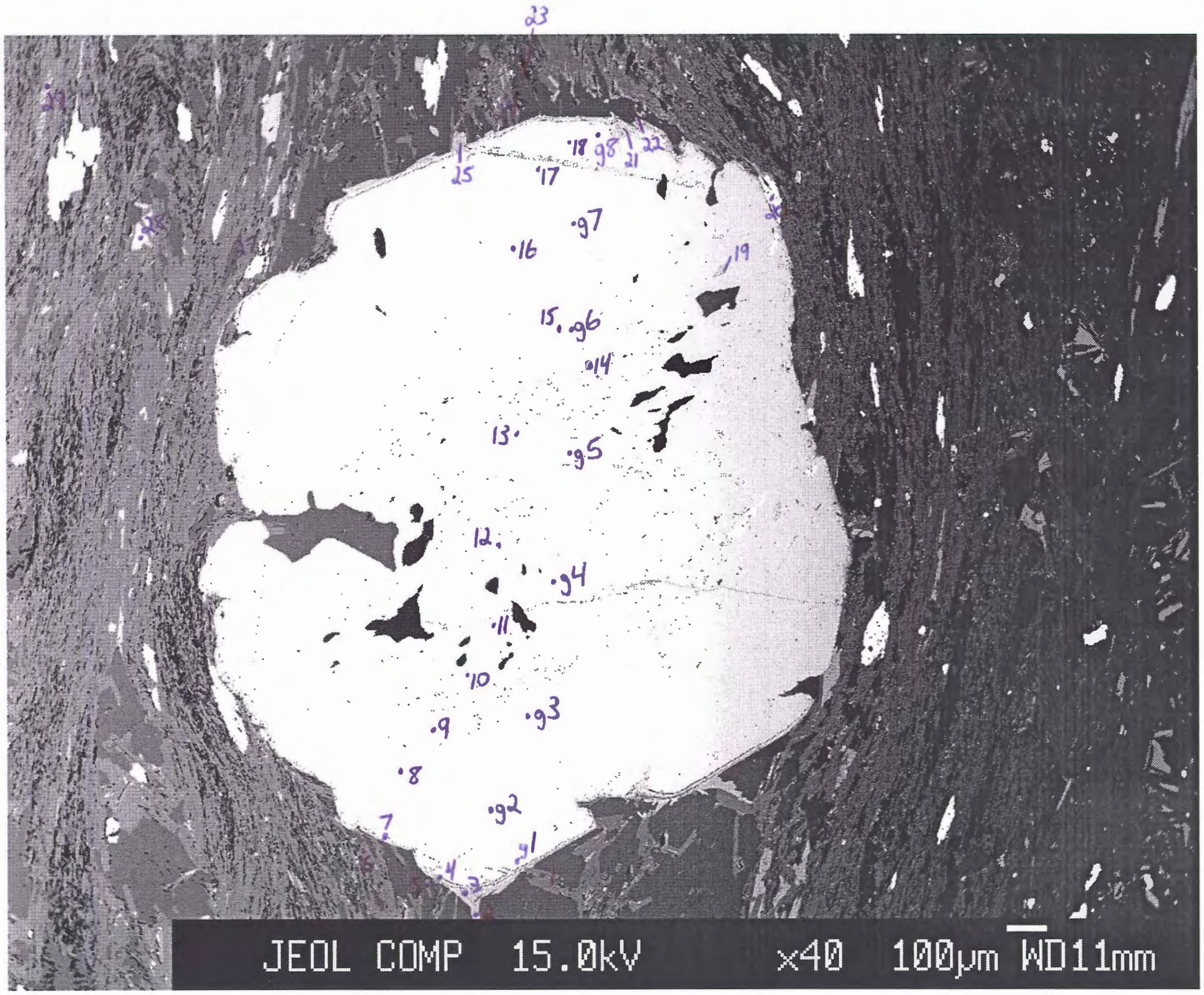

ritch1292012

BH129 Image 2

-points 30-65
-points g9-g15

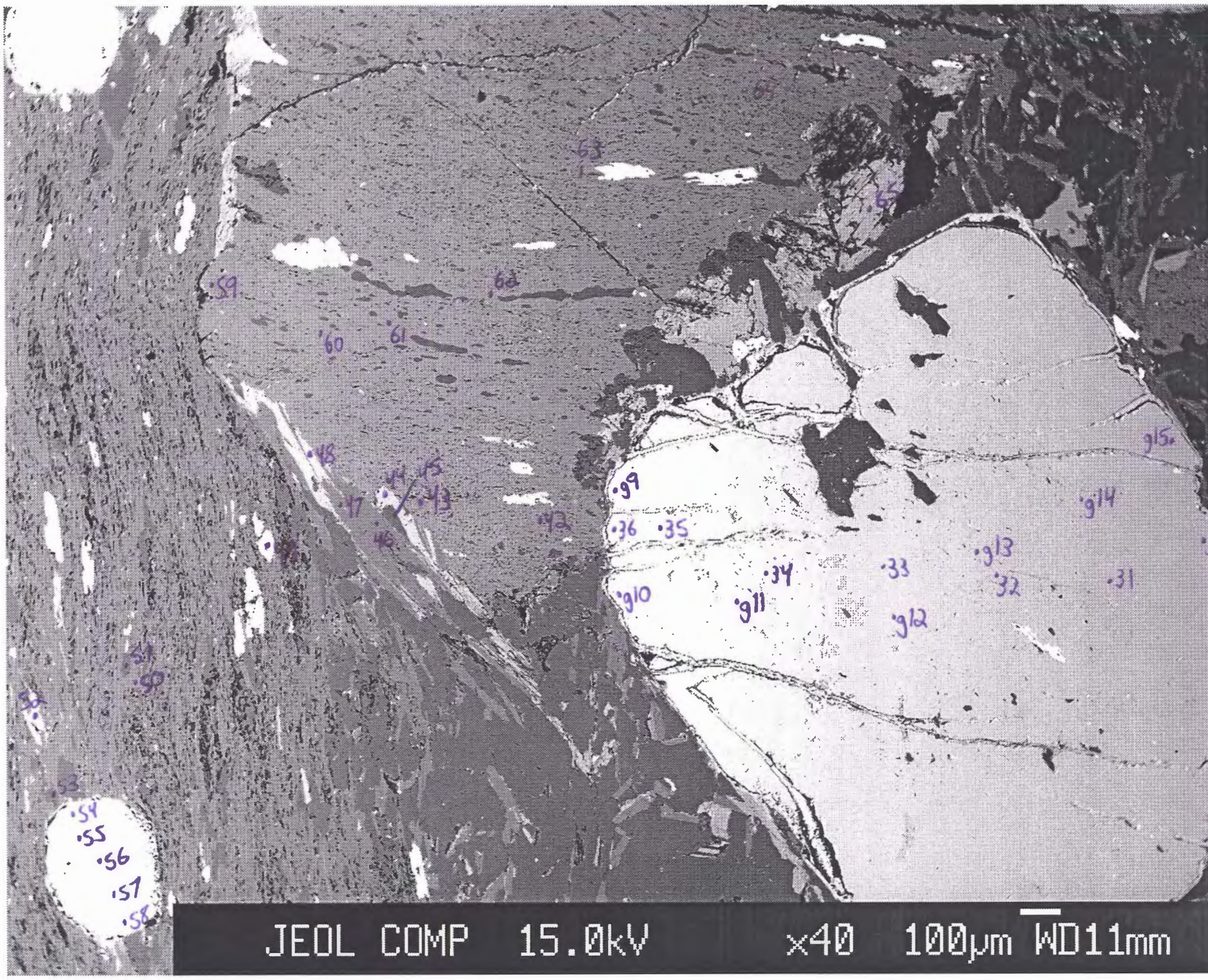

ritch1291013

BH129 Image 3

-points 36-42

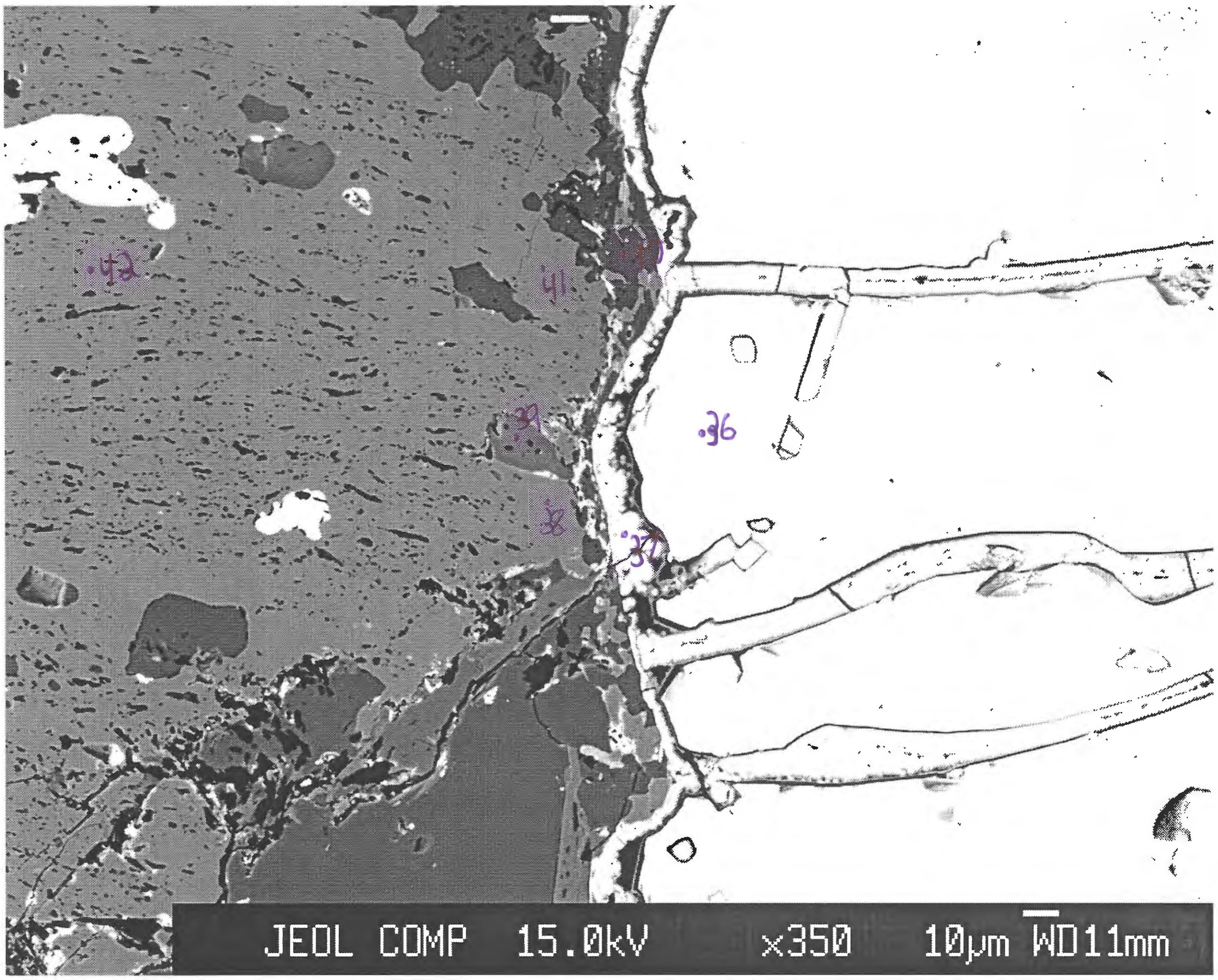

ritch1291014

BH129 Image 4

-points 66-80

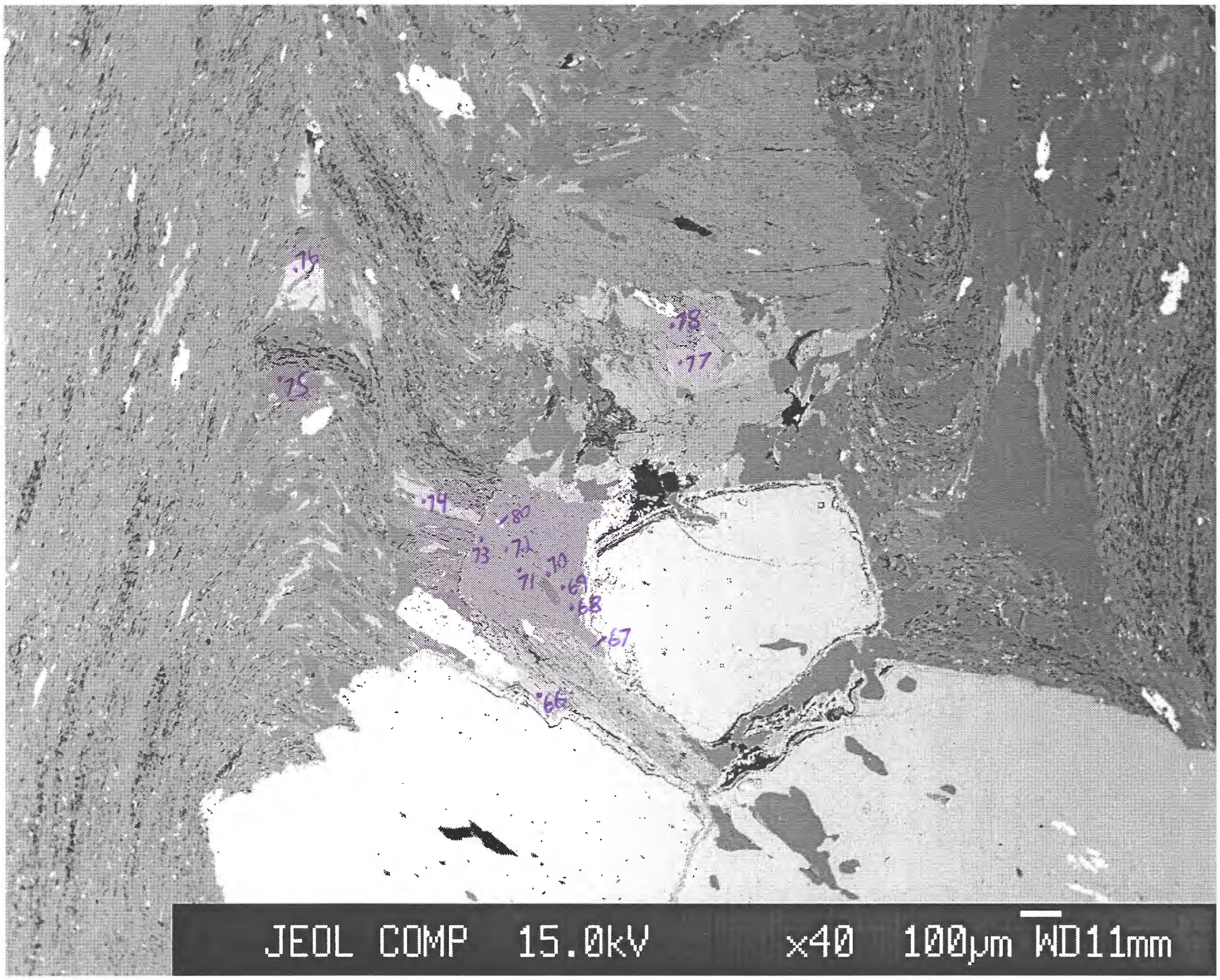

No.	102	85	86	108	109	111	112	131	135	139	152
Comment	bh129-19	bh129-2	bh129-3	bh129-25	bh129-26	bh129-28	bh129-29	bh129-44	bh129-48	bh129-52	bh129-65
Mineral	apatite	biotite	biotite	biotite	biotite	biotite	biotite	biotite	biotite	biotite	biotite
Weight % oxide:											
SiO2	0	35.4426	34.7597	34.9865	35.2699	34.8276	33.5652	34.8627	34.9476	33.6431	34.669
TiO2	0.0407	1.0888	1.0517	1.3422	1.4843	1.46	1.1431	1.2311	1.4783	1.2623	1.1529
Al2O3	0.0035	19.3317	19.2504	18.8064	18.757	18.5967	19.6489	18.8726	19.0595	19.1455	18.7006
Cr2O3	0	0	0	0	0	0	0	0	0	0	0
FeO	2.0522	20.6239	22.1724	20.8016	20.7131	20.1226	20.3215	22.5637	23.0499	22.7785	22.5449
MnO	0.1995	0.0992	0.1303	0.0261	0.0365	0.0365	0.0574	0	0	0	0
MgO	0.0709	8.283	8.2947	8.4528	8.4623	8.1661	7.6941	8.3598	8.0889	7.4648	7.5107
CaO	56.5976	0.0435	0.0335	0.0408	0.0748	0.102	0.294	0	0.0062	0.0981	0.0218
Na2O	0.0323	0.1301	0.0795	0.0991	0.1293	0.0867	0.0225	0.1974	0.1774	0.0789	0.1735
K2O	0	9.1762	9.0102	8.9125	8.7939	7.9963	3.8276	8.3783	8.5051	7.4539	7.8083
ZnO	0.1825	0.0958	0.1329	0.1413	0.1248	0.086	0.0861	0	0	0	0
Total	59.1792	94.3149	94.9153	93.6093	93.846	91.4806	86.6604	94.4657	95.313	91.9251	92.5818
Number of cations per formula unit:											
Si	0	5.4736	5.3812	5.4516	5.4714	5.5066	5.4714	5.4076	5.3856	5.357	5.4736
Ti	0.0005	0.1254	0.1232	0.1562	0.1738	0.1738	0.1408	0.143	0.1716	0.1518	0.1364
Al	0.0001	3.5178	3.5134	3.454	3.4298	3.4672	3.7752	3.4518	3.4628	3.5948	3.4804
Cr	0	0	0	0	0	0	0	0	0	0	0
Fe	0.0273	2.6642	2.871	2.7104	2.6884	2.662	2.7698	2.9282	2.97	3.0338	2.9766
Mn	0.0027	0.0132	0.0176	0.0044	0.0044	0.0044	0.0088	0	0	0	0
Mg	0.0017	1.9074	1.914	1.9624	1.958	1.925	1.87	1.9338	1.859	1.771	1.7666
Ca	0.9646	0.0066	0.0066	0.0066	0.0132	0.0176	0.0506	0	0	0.0176	0.0044
Na	0.001	0.0396	0.0242	0.0308	0.0396	0.0264	0.0066	0.0594	0.0528	0.0242	0.0528
K	0	1.8084	1.7798	1.771	1.7402	1.6126	0.7964	1.6588	1.672	1.5136	1.573
Zn	0.0021	0.011	0.0154	0.0154	0.0154	0.011	0.011	0	0	0	0
Total	1	15.5694	15.6486	15.5628	15.5342	15.4088	14.9028	15.5848	15.576	15.466	15.466

153	161	163	164	165	166	87	104	124	97	90	91
bh129-66	bh129-74	bh129-76	bh129-77	bh129-78	bh129-79	bh129-4	bh129-21	bh129-37	bh129-14	bh129-7	bh129-8
biotite	biotite	biotite	biotite	chlorite	chlorite	Fe,Al-oxide	Fe,Al-oxide	Fe,Al-oxide	Fe-oxide	garnet	garnet
32.6614	34.6649	34.0796	35.2028	23.7215	23.5473	0.4903	0.7635	0.6901	0.0029	36.7442	36.6614
1.1804	1.2805	1.311	1.7172	0.2711	0.0833	0.0737	0.0743	0.0308	0.1171	0.0447	0.0733
18.1191	19.7744	19.3102	19.0185	23.1557	22.941	9.8707	13.7761	15.0656	0	21.0593	21.2358
0	0	0	0	0	0	0	0	0	0	0	0
24.136	22.104	22.7723	23.0492	29.5912	30.7986	59.7317	56.9957	58.8213	77.4496	37.0762	37.7913
0	0	0.1707	0	0.0767	0	0.1362	0.132	0	0.44	0.6722	0.5332
8.3277	8.4141	8.7163	8.2537	12.0449	11.7597	0.0372	0.0539	0.0223	0	2.5516	2.5288
0.0382	0.0716	0.0057	0	0	0.004	0.5316	0.4907	0.2348	0.1185	0.3106	0.3038
0.095	0.1166	0.1742	0.1869	0.0084	0	0	0.0149	0.0041	0.0438	0.0171	0
7.5948	8.2749	7.9354	8.6055	0	0	0.0399	0.0352	0	0.0566	0.0086	0
0.0148	0.0393	0.0133	0.0341	0.0376	0.0044	0.3025	0.3123	0.0906	0.699	0.2022	0.1923
92.1674	94.7404	94.4887	96.068	88.9072	89.1384	71.2139	72.6487	74.9597	78.9276	98.6868	99.32
5.2558	5.3416	5.291	5.3834	5.0484	5.0288	0.0071	0.0102	0.0089	0	6.012	5.9736
0.143	0.1474	0.154	0.198	0.042	0.014	0.0008	0.0007	0.0003	0.0013	0.0048	0.0096
3.4364	3.5926	3.5332	3.4276	5.8072	5.7764	0.1674	0.2175	0.2288	0	4.0608	4.08
0	0	0	0	0	0	0	0	0	0	0	0
3.2472	2.849	2.9568	2.948	5.2668	5.502	0.7189	0.6386	0.6338	0.9807	5.0736	5.1504
0	0	0.022	0	0.014	0	0.0017	0.0015	0	0.0056	0.0936	0.0744
1.9976	1.9338	2.0174	1.881	3.8192	3.7436	0.0008	0.0011	0.0004	0	0.6216	0.6144
0.0066	0.011	0	0	0	0	0.0082	0.007	0.0032	0.0019	0.0552	0.0528
0.0286	0.0352	0.0528	0.055	0.0028	0	0	0.0004	0.0001	0.0013	0.0048	0
1.5598	1.628	1.5708	1.6786	0	0	0.0007	0.0006	0	0.0011	0.0024	0
0.0022	0.0044	0.0022	0.0044	0.0056	0	0.0032	0.0031	0.0009	0.0078	0.024	0.024
15.6794	15.543	15.6024	15.5782	20.006	20.0676	0.9089	0.8808	0.8765	0.9998	15.9528	15.9816

92	93	94	95	96	98	99	100	101	117	118	119
bh129-9	bh129-10	bh129-11	bh129-12	bh129-13	bh129-15	bh129-16	bh129-17	bh129-18	bh129-30	bh129-31	bh129-32
garnet	garnet	garnet	garnet	garnet	garnet	garnet	garnet	garnet	garnet	garnet	garnet
36.8733	36.996	36.6234	36.8312	36.6581	36.9009	36.7672	36.8408	36.9146	37.1022	36.7525	36.5502
0.0626	0.0957	0.0691	0.068	0.0957	0.0785	0.0701	0.0734	0.0681	0	0.0137	0.0159
21.1272	21.0512	20.7966	20.8555	20.8886	20.9556	21.0514	21.2308	21.3338	21.3647	21.2814	21.1235
0	0	0	0	0	0	0	0	0	0	0	0
37.9046	34.3963	34.1226	33.4824	34.3623	37.5231	37.3871	37.3061	37.1116	40.2156	39.1119	35.4474
0.6964	3.2492	3.5564	4.3219	3.369	1.2144	0.5794	0.3283	0.3901	0.4905	1.4657	4.1942
2.2328	1.5669	1.5202	1.4359	1.3777	2.0566	2.3651	2.6894	2.6978	2.6638	2.2766	1.53
0.3847	1.8117	1.4603	1.5892	1.8391	0.4193	0.2979	0.3145	0.2773	0.2709	0.3795	1.3932
0	0.035	0.0129	0	0.0055	0.0005	0	0.0208	0.0221	0.0299	0	0.02
0.0129	0.0152	0.0095	0.0095	0.0124	0.0096	0.0119	0.0006	0.0025	0	0	0
0.2285	0.2225	0.2152	0.2442	0.2412	0.2064	0.1991	0.2348	0.2023	0.0015	0	0.054
99.5231	99.4398	98.3863	98.8379	98.8497	99.365	98.7292	99.0396	99.0203	102.139	101.2812	100.3283
6.0048	6.0264	6.0336	6.0408	6.0168	6.0216	6.0192	6	6.0072	5.9232	5.9232	5.9472
0.0072	0.012	0.0096	0.0072	0.012	0.0096	0.0096	0.0096	0.0072	0	0.0024	0.0024
4.0536	4.0416	4.0392	4.032	4.0416	4.032	4.0608	4.0752	4.092	4.02	4.044	4.0512
0	0	0	0	0	0	0	0	0	0	0	0
5.1624	4.6848	4.7016	4.5936	4.7184	5.1216	5.1192	5.0808	5.0496	5.3688	5.2728	4.824
0.096	0.4488	0.4968	0.6	0.468	0.168	0.0792	0.0456	0.0528	0.0672	0.1992	0.5784
0.5424	0.3816	0.3744	0.3504	0.336	0.4992	0.576	0.6528	0.6552	0.6336	0.5472	0.372
0.0672	0.3168	0.2568	0.2784	0.324	0.0744	0.0528	0.0552	0.048	0.0456	0.0648	0.2424
0	0.012	0.0048	0	0.0024	0	0	0.0072	0.0072	0.0096	0	0.0072
0.0024	0.0024	0.0024	0.0024	0.0024	0.0024	0.0024	0	0	0	0	0
0.0264	0.0264	0.0264	0.0288	0.0288	0.024	0.024	0.0288	0.024	0	0	0.0072
15.9624	15.9552	15.9456	15.936	15.9528	15.9552	15.9456	15.9576	15.9432	16.0704	16.056	16.032

120	121	122	123	141	142	143	144	145	503	504	505
bh129-33	bh129-34	bh129-35	bh129-36	bh129-54	bh129-55	bh129-56	bh129-57	bh129-58	bh129_g1	bh129_g2	bh129_g3
garnet	garnet	garnet	garnet	garnet	garnet	garnet	garnet	garnet	garnet	garnet	garnet
36.851	36.8495	36.6088	36.8166	36.8479	36.9734	36.9211	37.0365	36.9418	36.1201	36.2394	35.9704
0	0.0116	0.0042	0	0	0.0116	0.0137	0.0095	0	0.0241	0.0262	0.012
21.2351	21.0197	21.2755	21.2606	21.3576	21.1869	21.1993	21.3268	21.4354	20.9432	20.9554	20.8857
0	0	0	0	0	0	0	0	0	0	0	0
36.346	36.2313	38.9463	40.4448	38.5931	39.8491	39.5038	39.5141	39.2417	38.5046	38.6876	38.6353
4.0812	2.934	0.5099	0.3314	0.5517	0.3931	0.2962	0.2452	0.3978	0.396	0.4382	1.5979
1.5954	1.772	2.6275	2.6854	2.6527	2.7725	2.8202	2.821	2.708	2.5987	2.5082	2.0649
1.5233	1.4698	0.2942	0.2415	0.2331	0.2493	0.4099	0.331	0.2293	0.2631	0.2702	0.4647
0.0237	0.0102	0.0273	0.0336	0.0342	0.0214	0.0181	0.0334	0.0264	0.0182	0.0308	0.0058
0	0	0	0	0	0	0	0	0	0	0	0
0.0059	0.0399	0	0.0052	0	0.0281	0.0385	0.0126	0.0059	0.0413	0.0918	0.0374
101.6615	100.338	100.2936	101.8191	100.2702	101.4853	101.2207	101.33	100.9862	98.9094	99.2478	99.6742
5.9304	5.9784	5.9328	5.9064	5.9568	5.9352	5.9352	5.94	5.94	5.9357	5.94	5.9064
0	0.0024	0	0	0	0.0024	0.0024	0	0	0.003	0.0032	0.0015
4.0272	4.02	4.0632	4.02	4.0704	4.008	4.0152	4.032	4.0632	4.0566	4.0486	4.0424
0	0	0	0	0	0	0	0	0	0	0	0
4.8912	4.9152	5.2776	5.4264	5.2176	5.3496	5.3112	5.2992	5.2776	5.2918	5.3034	5.3057
0.5568	0.4032	0.0696	0.0456	0.0744	0.0528	0.0408	0.0336	0.0552	0.0551	0.0608	0.2223
0.3816	0.4296	0.6336	0.6432	0.6384	0.6624	0.6768	0.6744	0.648	0.6366	0.6128	0.5054
0.2616	0.2544	0.0504	0.0408	0.0408	0.0432	0.0696	0.0576	0.0384	0.0463	0.0475	0.0818
0.0072	0.0024	0.0096	0.0096	0.0096	0.0072	0.0048	0.0096	0.0072	0.0058	0.0098	0.0018
0	0	0	0	0	0	0	0	0	0	0	0
0	0.0048	0	0	0	0.0024	0.0048	0.0024	0	0.005	0.0111	0.0045
16.0584	16.0104	16.0368	16.092	16.0104	16.0656	16.0608	16.0488	16.032	16.0359	16.0373	16.0718

506	507	508	509	510	511	512	513	514	515	516	517
bh129_g4	bh129_g5	bh129_g6	bh129_g7	bh129_g8	bh129_g9	bh129_g10	bh129_g11	bh129_g12	bh129_g13	bh129_g14	bh129_g15
garnet	garnet	garnet	garnet	garnet	garnet	garnet	garnet	garnet	garnet	garnet	garnet
36.1145	36.2677	36.2919	36.3091	36.5134	36.5467	36.4603	36.6585	36.1412	36.2912	36.442	36.534
0.0404	0.0382	0.0491	0.0569	0.0186	0.0251	0.0153	0.0175	0.0415	0.0175	0.0393	0.0273
20.8054	20.8889	21.0629	20.9066	21.0096	21.022	21.0305	21.0441	20.8653	20.8581	21.0579	21.0907
0	0	0	0	0	0	0	0	0	0	0	0
35.0915	35.7399	39.692	39.0589	39.1671	39.0944	38.1043	37.0057	34.5057	35.5878	38.6921	38.8101
4.2901	4.0732	1.0025	0.3222	0.3856	0.4856	0.3909	2.0607	4.4253	4.1226	1.2354	0.5072
1.3071	1.3536	2.1656	2.4732	2.6865	2.5597	2.7327	2.0859	1.5041	1.6269	2.3007	2.6858
1.6002	1.621	0.3315	0.278	0.2657	0.2553	0.2113	0.934	1.4273	1.1879	0.4016	0.1917
0.0355	0.0322	0.017	0.0241	0.0231	0.0669	0.012	0.0091	0.0307	0.0279	0.0169	0.0197
0	0	0	0	0	0	0	0	0	0	0	0
0.0558	0.0542	0.068	0.0803	0.0176	0.1063	0.0865	0.0658	0.0902	0.0321	0.0757	0.0291
99.3405	100.0688	100.6805	99.5094	100.0872	100.1619	99.0439	99.8814	99.0313	99.7521	100.2616	99.8957
5.945	5.9337	5.9014	5.9412	5.9368	5.941	5.9648	5.9683	5.9528	5.9457	5.9291	5.9431
0.005	0.0047	0.006	0.007	0.0023	0.0031	0.0019	0.0021	0.0051	0.0022	0.0048	0.0033
4.0369	4.0283	4.0371	4.0322	4.0264	4.028	4.0554	4.0384	4.0509	4.0279	4.0383	4.044
0	0	0	0	0	0	0	0	0	0	0	0
4.8311	4.8903	5.3979	5.3451	5.3259	5.315	5.2135	5.0387	4.7532	4.8762	5.2648	5.28
0.5982	0.5645	0.1381	0.0447	0.0531	0.0669	0.0542	0.2842	0.6174	0.5721	0.1703	0.0699
0.3207	0.3301	0.5249	0.6033	0.6512	0.6203	0.6664	0.5063	0.3693	0.3973	0.558	0.6513
0.2822	0.2842	0.0578	0.0487	0.0463	0.0445	0.037	0.1629	0.2519	0.2085	0.07	0.0334
0.0113	0.0102	0.0053	0.0076	0.0073	0.0211	0.0038	0.0029	0.0098	0.0089	0.0053	0.0062
0	0	0	0	0	0	0	0	0	0	0	0
0.0068	0.0066	0.0082	0.0097	0.0021	0.0128	0.0104	0.0079	0.011	0.0039	0.0091	0.0035
16.0372	16.0526	16.0767	16.0396	16.0515	16.0527	16.0075	16.0118	16.0214	16.0427	16.0498	16.0347

106	103	136	84	88	89	107	133	134	137	105	110
bh129-23	bh129-20	bh129-49	bh129-01	bh129-5	bh129-6	bh129-24	bh129-46	bh129-47	bh129-50	bh129-22	bh129-27
graphite?	ilmenite	ilmenite	muscovite	muscovite	muscovite	muscovite	muscovite	muscovite	muscovite	quartz	quartz
6.4526	0	0.1583	49.815	47.9298	48.4464	46.3619	46.8122	47.0157	47.2931	97.7507	97.6017
0	54.1732	51.1457	0.4986	0.4791	0.3964	0.5217	0.4601	0.4377	0.406	0.0079	0.026
3.6259	0	0.0048	36.3584	35.173	35.3245	34.5772	34.9332	34.7147	35.1802	0	0
0	0	0	0	0	0	0	0	0	0	0	0
0	40.3408	46.678	1.3768	1.3771	1.1303	1.1034	1.2606	1.2973	1.0736	0.2705	0.202
0	0.2571	0.235	0.0479	0	0.016	0.0213	0	0	0	0.0967	0.0592
0.0307	0	0.03	0.529	0.544	0.5598	0.5165	0.5953	0.6001	0.5807	0	0
0	0.0894	0.0256	0.0011	0.0285	0.0129	0.0252	0	0	0	0	0.0086
0.0639	0	0.0282	0.8949	0.7791	0.8798	0.8087	0.8325	0.8121	0.9071	0	0
0.9643	0.0605	0	7.3539	8.5733	9.2301	8.5157	8.448	8.4049	8.7176	0	0
0	0.4009	0.2741	0.0236	0	0.0015	0	0	0	0	0.0054	0.0116
11.1374	95.322	98.5798	96.8992	94.884	95.9978	92.4517	93.3419	93.2826	94.1583	98.1313	97.9091
0.322	0	0.0084	6.3646	6.314	6.325	6.2722	6.2722	6.2986	6.2832	0.9984	0.9986
0	2.1096	1.9758	0.0484	0.0484	0.0396	0.0528	0.0462	0.044	0.0396	0	0.0002
0.2133	0	0	5.4736	5.4626	5.4362	5.5154	5.5154	5.4824	5.5088	0	0
0	0	0	0	0	0	0	0	0	0	0	0
0	1.7472	2.0052	0.1474	0.1518	0.1232	0.1254	0.1408	0.1452	0.1188	0.0024	0.0018
0	0.0114	0.0102	0.0044	0	0.0022	0.0022	0	0	0	0.0008	0.0006
0.0023	0	0.0024	0.1012	0.1078	0.11	0.1034	0.1188	0.1188	0.1144	0	0
0	0.0048	0.0012	0	0.0044	0.0022	0.0044	0	0	0	0	0
0.0062	0	0.003	0.2222	0.198	0.2222	0.2112	0.2156	0.2112	0.2332	0	0
0.0614	0.0042	0	1.199	1.441	1.5378	1.4696	1.4432	1.4366	1.4784	0	0
0	0.0156	0.0102	0.0022	0	0	0	0	0	0	0	0
0.6053	3.8934	4.0164	13.5652	13.7302	13.7984	13.7566	13.7544	13.739	13.7786	1.0018	1.0014

127	132	138	140	162	125	128	129	130	146	147	148
bh129-40	bh129-45	bh129-51	bh129-53	bh129-75	bh129-38	bh129-41	bh129-42	bh129-43	bh129-59	bh129-60	bh129-61
quartz	quartz	quartz	quartz	quartz	staurolite	staurolite	staurolite	staurolite	staurolite	staurolite	staurolite
95.5529	95.9193	95.7439	95.4744	95.9187	27.9607	27.9453	27.8409	27.7265	27.7082	27.435	27.6867
0	0	0	0	0	0.5519	0.6199	0.5651	0.4194	0.5119	0.5084	0.4104
0.0159	0.0068	0	0	0.0191	54.6649	55.2682	54.146	54.9078	54.8297	54.1021	53.4634
0	0	0	0	0	0	0	0	0	0	0	0
0.5031	0.1112	0.0106	0.1906	0.0053	12.3879	11.9244	13.6991	12.9632	12.6498	14.6285	14.5159
0	0	0	0	0.0267	0	0	0	0	0	0	0
0.0212	0.0083	0.0177	0.0109	0	0.7963	0.6598	1.1407	0.8467	1	1.2358	1.2658
0	0	0	0	0	0	0	0	0	0	0	0
0.0047	0	0.0034	0.0044	0.0012	0.02	0.0258	0.027	0.0337	0.0225	0.0215	0.0173
0	0	0	0	0	0	0	0	0	0	0	0
0	0	0	0	0	0.0932	0.0549	0.1548	0.1827	0.1141	0.0405	0.1366
96.0979	96.0456	95.7757	95.6804	95.9711	96.475	96.4984	97.5737	97.0801	96.8363	97.9718	97.4961
0.9974	0.9994	0.9998	0.999	0.9996	8.1312	8.1024	8.0736	8.0448	8.0448	7.9632	8.0688
0	0	0	0	0	0.12	0.1344	0.1248	0.0912	0.1104	0.1104	0.0912
0.0002	0	0	0	0.0002	18.7392	18.888	18.504	18.7776	18.768	18.504	18.3696
0	0	0	0	0	0	0	0	0	0	0	0
0.0044	0.001	0	0.0016	0	3.0144	2.8896	3.3216	3.144	3.072	3.552	3.5376
0	0	0	0	0.0002	0	0	0	0	0	0	0
0.0004	0.0002	0.0002	0.0002	0	0.3456	0.2832	0.4944	0.3648	0.432	0.5328	0.552
0	0	0	0	0	0	0	0	0	0	0	0
0	0	0	0	0	0.0096	0.0144	0.0144	0.0192	0.0144	0.0144	0.0096
0	0	0	0	0	0	0	0	0	0	0	0
0	0	0	0	0	0.0192	0.0096	0.0336	0.0384	0.024	0.0096	0.0288
1.0026	1.0006	1.0002	1.001	1.0002	30.384	30.3216	30.5712	30.4848	30.4704	30.6864	30.6624

149	150	151	154	155	156	157	158	159	160	167	126
bh129-62	bh129-63	bh129-64	bh129-67	bh129-68	bh129-69	bh129-70	bh129-71	bh129-72	bh129-73	bh129-80	bh129-39
staurolite	staurolite	staurolite	staurolite	staurolite	staurolite	staurolite	staurolite	staurolite	staurolite	xxxxxxx	???
27.6703	27.3667	27.5428	27.8467	27.6429	27.7206	27.7362	27.6815	27.82	27.5112	0.4549	35.8216
0.5095	0.498	0.4163	0.6134	0.5133	0.4607	0.4873	0.5424	0.5748	0.5097	0.1667	0.655
54.0572	54.1887	54.0933	54.776	54.253	53.4436	53.6257	53.5505	53.3222	53.4573	0.175	32.7991
0	0	0	0	0	0	0	0	0	0	0	0
13.9301	14.7625	14.1768	12.1218	12.9548	13.0667	13.6388	13.8266	13.7664	12.5147	1.4741	9.336
0	0	0	0	0	0.0573	0.0573	0	0.0365	0.0729	0.4656	0
1.239	1.2333	1.2409	0.6105	0.8741	1.0445	1.1452	1.1699	1.163	1.1161	0.1011	5.0784
0	0	0	0	0	0	0	0	0	0	1.0012	0.1785
0.0179	0.0159	0.0197	0.0258	0.0326	0.0177	0.0154	0.0284	0.035	0.0187	0.1056	2.0722
0	0	0	0	0	0	0	0	0	0	0	0
0.0428	0.1051	0.1299	0.2201	0.2342	0.2838	0.2006	0.2718	0.2374	0.1693	1.3327	0
97.4669	98.1703	97.6197	96.2144	96.505	96.095	96.9066	97.0711	96.9554	95.3699	5.277	85.9408
8.04	7.9344	8.0064	8.1168	8.0736	8.1456	8.1024	8.0832	8.1312	8.1216	0.0841	0.2417
0.1104	0.1104	0.0912	0.1344	0.1104	0.1008	0.1056	0.12	0.1248	0.1152	0.0232	0.0033
18.5088	18.5184	18.528	18.816	18.6816	18.5088	18.4608	18.432	18.3648	18.5952	0.0381	0.2609
0	0	0	0	0	0	0	0	0	0	0	0
3.384	3.5808	3.4464	2.9568	3.1632	3.2112	3.3312	3.3744	3.3648	3.0912	0.228	0.0527
0	0	0	0	0	0.0144	0.0144	0	0.0096	0.0192	0.0729	0
0.5376	0.5328	0.5376	0.264	0.3792	0.456	0.4992	0.5088	0.5088	0.4896	0.0279	0.0511
0	0	0	0	0	0	0	0	0	0	0.1984	0.0013
0.0096	0.0096	0.0096	0.0144	0.0192	0.0096	0.0096	0.0144	0.0192	0.0096	0.0379	0.0271
0	0	0	0	0	0	0	0	0	0	0	0
0.0096	0.024	0.0288	0.048	0.0528	0.0624	0.0432	0.0576	0.0528	0.0384	0.182	0
30.6048	30.7152	30.6528	30.3504	30.4848	30.5088	30.5664	30.5952	30.5808	30.4848	0.8925	0.6382

ritch122001

BH122 Image 1

-points g1-g7

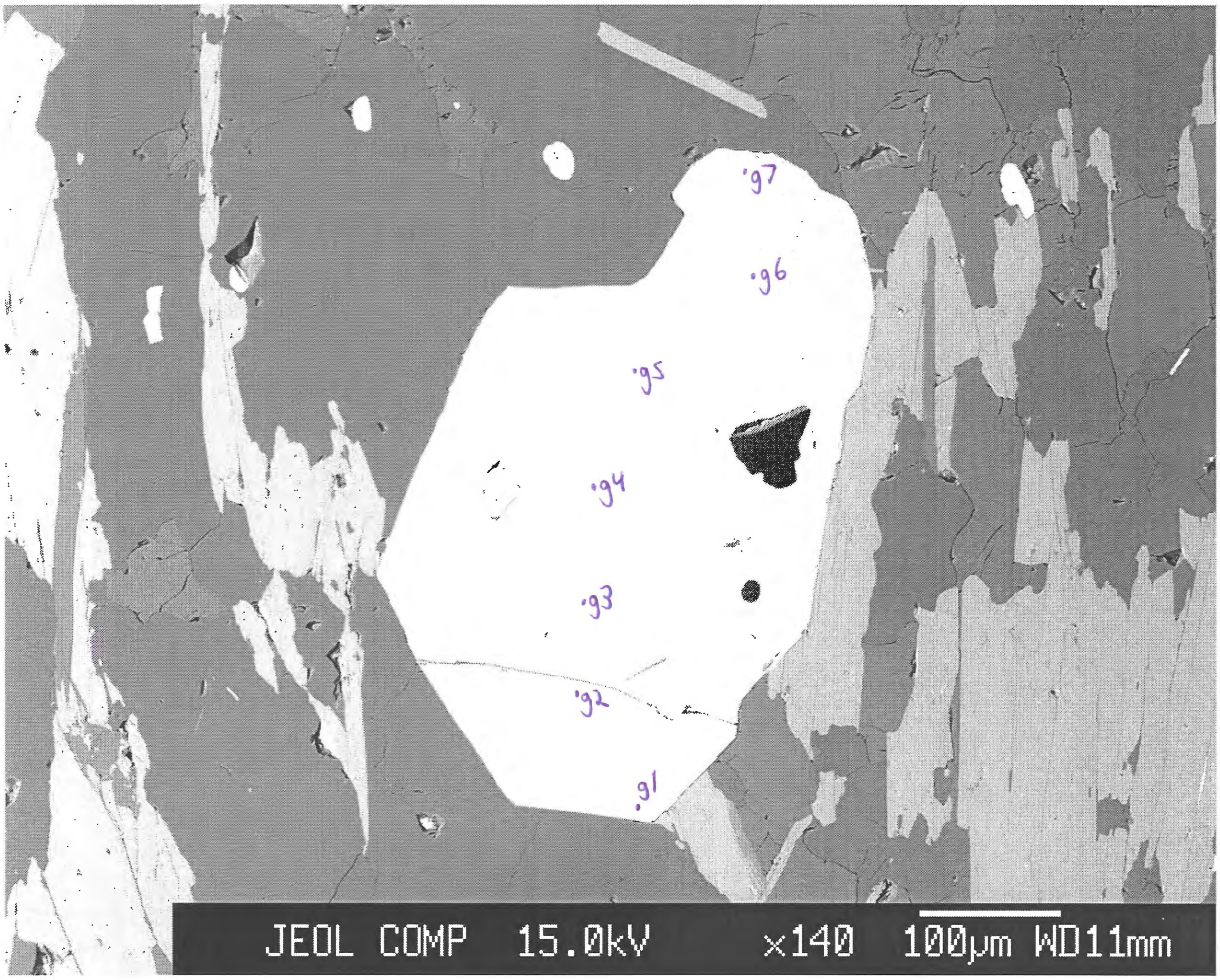

ritch122002

BH122 Image 2

-points g8-g17
-points 16-23

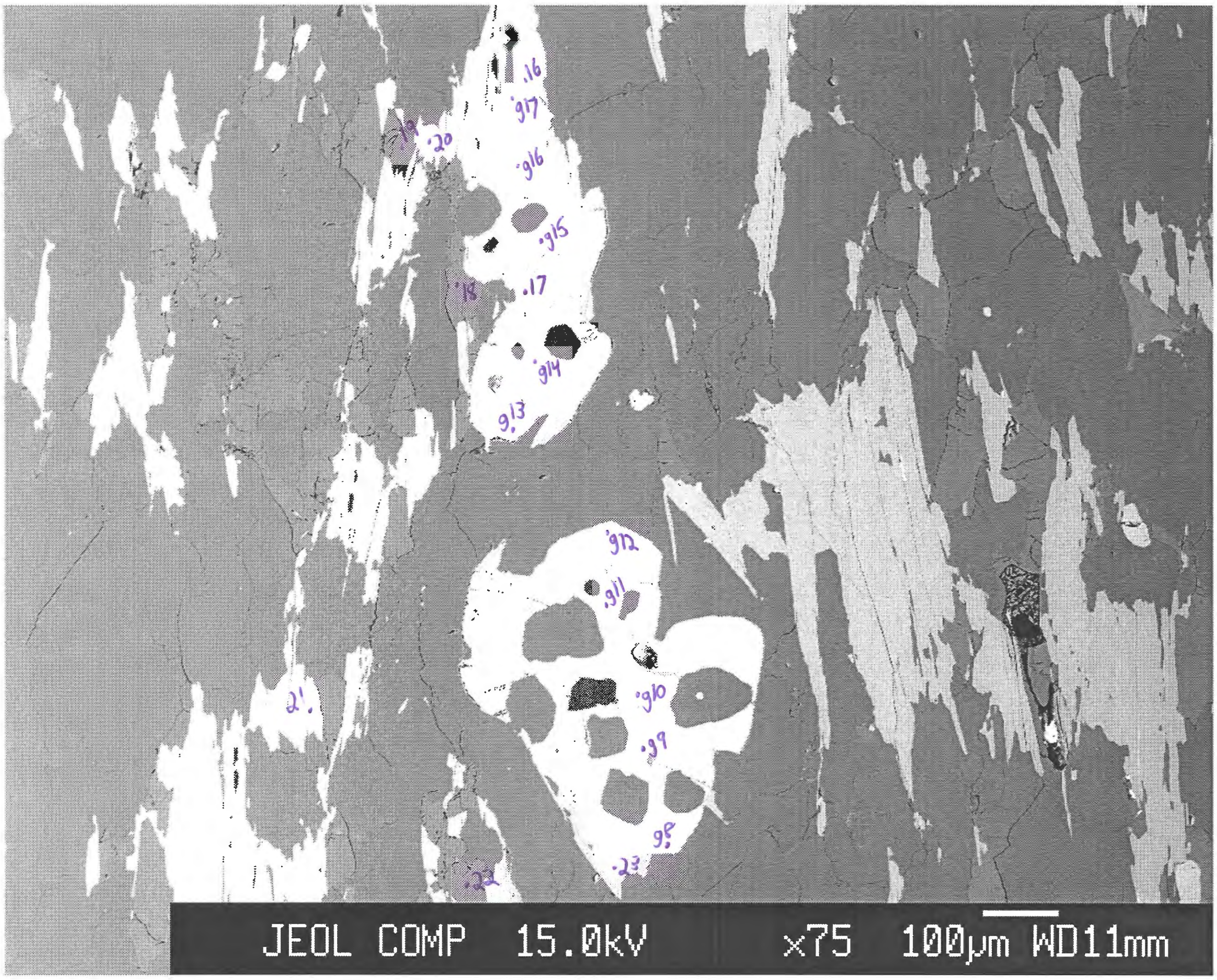

ritch122003

BH122 Image 3

-points 1-15

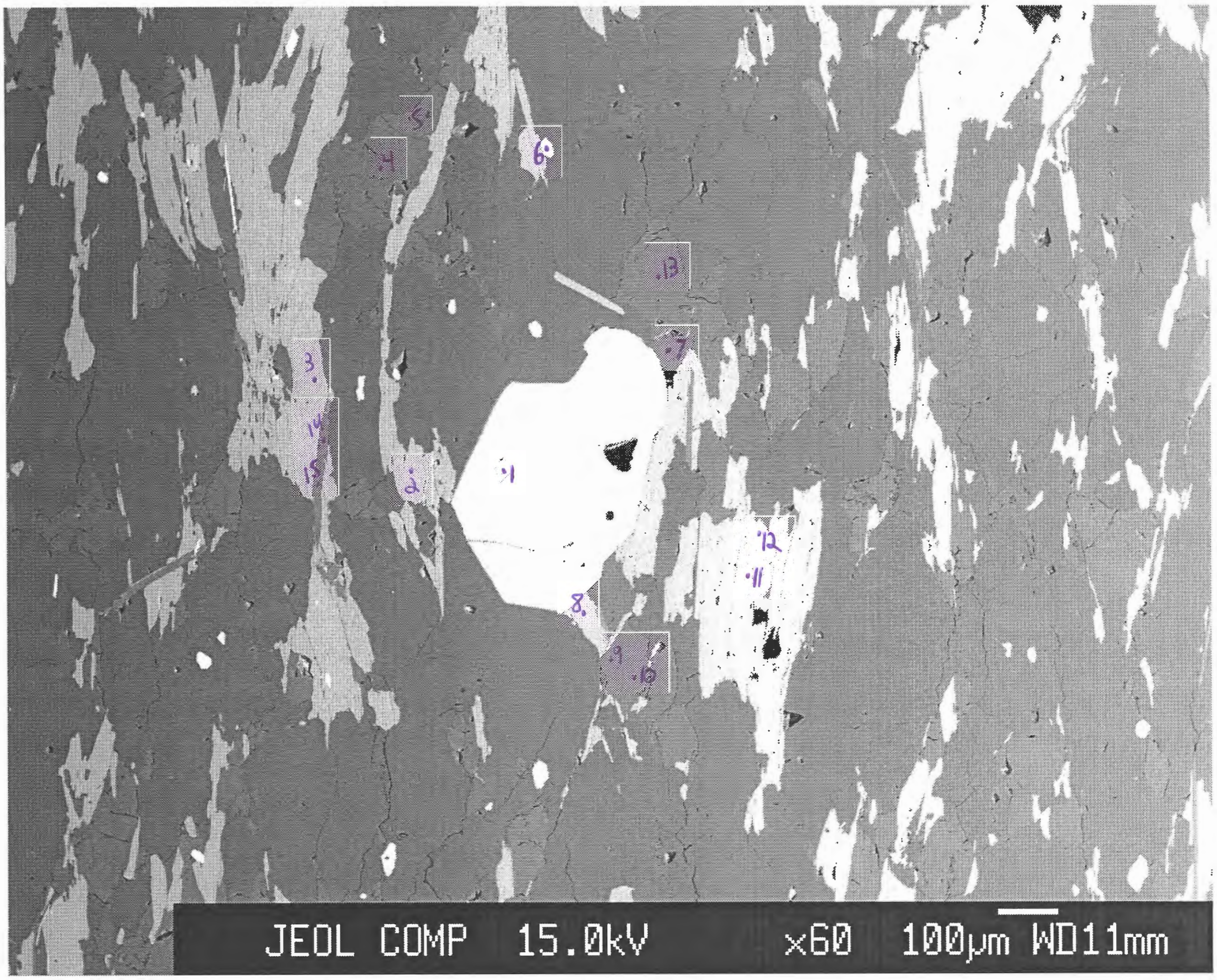

No.	678	679	684	687	688	692	693	696	697	699	585
Comment	bh122-2	bh122-3	bh122-8	bh122-11	bh122-12	bh122-16	bh122-17	bh122-20	bh122-21	bh122-23	bh122_g1
Mineral	biotite	biotite	biotite	biotite	biotite	biotite	biotite	biotite	biotite	biotite	garnet
Weight % oxide:											
SiO2	34.7901	34.5333	35.0825	35.5842	35.2296	35.2126	35.2612	35.5567	35.5688	35.4415	36.3372
TiO2	2.3376	2.3956	2.2374	2.2697	2.331	2.2977	1.215	2.5767	2.7651	2.0887	0.0338
Al2O3	18.8772	19.2791	19.1726	19.5773	19.0763	19.97	19.2478	19.1178	19.7724	20.122	20.6607
Cr2O3	0	0	0	0	0	0	0	0	0	0	0
FeO	22.5944	22.1407	22.6879	22.4488	23.2402	22.4513	24.9804	21.4875	22.0752	22.0384	33.5839
MnO	0.0211	0.0685	0.0053	0.0158	0.058	0.0844	0.3472	0.0844	0.0791	0.1951	4.4734
MgO	7.1969	7.3956	7.486	7.5967	7.8968	7.7744	7.8	7.8674	7.758	7.7773	2.1605
CaO	0	0	0	0	0	0	0	0	0	0	1.1208
Na2O	0.2272	0.2224	0.2353	0.2213	0.2071	0.2202	0.1327	0.1997	0.2015	0.195	0.0223
K2O	8.031	8.2377	8.1038	9.1299	9.2603	9.2603	9.1128	9.1102	9.2981	9.1968	0
ZnO	0	0	0	0.0473	0.0373	0.0473	0.0685	0.0373	0.0358	0.0396	0.0481
Total	94.0756	94.2729	95.0109	96.8911	97.3367	97.3183	98.1656	96.0377	97.5541	97.0944	98.4408
Number of cations per formula unit:											
Si	5.4098	5.357	5.3988	5.3856	5.3416	5.313	5.3438	5.4098	5.3416	5.346	5.9893
Ti	0.2728	0.2794	0.2596	0.2574	0.2662	0.2618	0.1386	0.2948	0.3124	0.2376	0.0042
Al	3.4606	3.5244	3.4782	3.4914	3.41	3.553	3.4386	3.4276	3.5002	3.5772	4.0139
Cr	0	0	0	0	0	0	0	0	0	0	0
Fe	2.9392	2.8732	2.9194	2.8402	2.948	2.8336	3.1658	2.7346	2.772	2.7786	4.6294
Mn	0.0022	0.0088	0	0.0022	0.0066	0.011	0.044	0.011	0.011	0.0242	0.6245
Mg	1.6676	1.7094	1.7182	1.7138	1.7842	1.749	1.7622	1.7842	1.7358	1.749	0.5308
Ca	0	0	0	0	0	0	0	0	0	0	0.1979
Na	0.0682	0.066	0.0704	0.066	0.0616	0.0638	0.0396	0.0594	0.0594	0.0572	0.0071
K	1.5928	1.6302	1.5906	1.7622	1.7908	1.782	1.7622	1.7688	1.782	1.7688	0
Zn	0	0	0	0.0044	0.0044	0.0044	0.0066	0.0044	0.0044	0.0044	0.0058
Total	15.4154	15.4506	15.4374	15.5232	15.6134	15.5716	15.7014	15.4946	15.5188	15.5452	16.0029

586	587	588	589	590	591	592	593	594	595	596	597
bh122_g2	bh122_g3	bh122_g4	bh122_g5	bh122_g6	bh122_g7	bh122_g8	bh122_g9	bh122_g10	bh122_g11	bh122_g12	bh122_g13
garnet	garnet	garnet	garnet	garnet	garnet	garnet	garnet	garnet	garnet	garnet	garnet
36.3467	36.3909	36.4561	36.3725	36.4894	36.3515	36.3179	36.4484	36.2745	36.0523	36.6078	36.6093
0.0218	0.0426	0.0044	0.0218	0.0229	0.0316	0.0338	0.048	0.0796	0.0404	0.0186	0
20.9767	20.8537	21.0183	20.9094	21.0157	20.8912	20.9583	20.9362	20.6289	20.9049	21.0185	21.0235
0	0	0	0	0	0	0	0	0	0	0	0
34.2106	34.5196	34.2261	34.196	34.5439	34.2028	33.7631	32.809	33.8635	33.0801	32.2329	32.1139
3.9581	3.8111	3.6911	3.7168	3.911	4.3774	5.3983	5.6268	4.8785	5.2793	5.2251	4.9844
2.5127	2.5434	2.6072	2.6003	2.5925	2.2705	2.2787	2.2037	2.4588	2.3724	2.3036	2.3453
1.0521	1.4591	1.3676	1.201	1.3623	1.0105	1.5202	1.3209	1.5381	1.4385	1.1323	1.2618
0.0005	0	0.0019	0.0203	0.0009	0.0062	0.0157	0	0	0.0028	0.0151	0.0009
0	0	0	0	0	0	0	0	0	0	0	0
0	0	0	0	0	0.0229	0	0	0.0076	0	0	0
99.0793	99.6205	99.3728	99.0381	99.9387	99.1647	100.2859	99.3931	99.7296	99.1707	98.554	98.3391
5.9483	5.9346	5.9445	5.9515	5.9293	5.9556	5.9057	5.9552	5.9258	5.9125	5.9992	6.0049
0.0027	0.0052	0.0005	0.0027	0.0028	0.0039	0.0041	0.0059	0.0098	0.005	0.0023	0
4.0464	4.0085	4.0397	4.0327	4.0252	4.0343	4.017	4.032	3.9722	4.041	4.06	4.0646
0	0	0	0	0	0	0	0	0	0	0	0
4.6823	4.708	4.6675	4.6795	4.6944	4.6864	4.5916	4.4832	4.6265	4.5371	4.4177	4.4054
0.5487	0.5264	0.5098	0.5152	0.5383	0.6075	0.7436	0.7787	0.6751	0.7334	0.7253	0.6925
0.613	0.6183	0.6337	0.6342	0.628	0.5545	0.5524	0.5367	0.5988	0.58	0.5627	0.5735
0.1845	0.255	0.239	0.2106	0.2372	0.1774	0.2649	0.2312	0.2692	0.2528	0.1988	0.2218
0.0002	0	0.0006	0.0065	0.0003	0.002	0.0049	0	0	0.0009	0.0048	0.0003
0	0	0	0	0	0	0	0	0	0	0	0
0	0	0	0	0	0.0028	0	0	0.0009	0	0	0
16.0261	16.056	16.0354	16.033	16.0555	16.0245	16.0842	16.0229	16.0784	16.0627	15.9708	15.963

598	599	600	601	677	682	690	691	680	681	683	685
bh122_g14	bh122_g15	bh122_g16	bh122_g17	bh122-1	bh122-6	bh122-14	bh122-15	bh122-4	bh122-5	bh122-7	bh122-9
garnet	garnet	garnet	garnet	ilmenite	ilmenite	muscovite	muscovite	plagioclase	plagioclase	plagioclase	plagioclase
36.6208	36.3782	36.4951	36.4157	0.0152	0.0375	47.5112	47.6201	62.354	61.6187	61.471	62.7755
0	0.0646	0.0263	0.0404	50.711	51.5516	0.562	0.6926	0	0	0	0
20.818	20.7343	20.8797	20.8916	0.0258	0.0454	35.2991	35.4798	22.0095	22.3509	22.2814	21.6749
0	0	0	0	0	0	0	0	0	0	0	0
33.1075	31.2139	31.9748	31.8361	47.989	46.9984	1.4159	1.4316	0	0.064	0.1494	0.1119
4.8197	5.1725	4.4927	5.1943	1.035	1.2859	0	0	0	0	0	0
2.5566	2.3578	2.5188	2.3046	0.0034	0.1538	0.5377	0.5379	0	0	0	0
1.7394	1.9903	2.0597	1.2093	0	0	0	0	3.4809	3.3679	3.5246	3.3557
0.0066	0.0239	0.015	0.0108	0	0	0.7921	0.8576	8.9386	9.2265	9.0209	9.1321
0	0	0	0	0	0	9.5727	9.8777	0	0	0	0
0.0007	0.0099	0.0031	0.0359	0	0.0065	0	0	0	0	0	0
99.6693	97.9454	98.4652	97.9387	99.7795	100.079	95.6908	96.4974	96.7831	96.6281	96.4473	97.0502
5.9586	5.9932	5.9799	6.0016	0.0006	0.0018	6.2546	6.2304	11.3344	11.2448	11.2416	11.3856
0	0.008	0.0032	0.005	1.9494	1.9662	0.055	0.0682	0	0	0	0
3.9926	4.0263	4.0326	4.0584	0.0018	0.003	5.4758	5.4714	4.7168	4.8064	4.8032	4.6336
0	0	0	0	0	0	0	0	0	0	0	0
4.5052	4.3007	4.3817	4.3881	2.052	1.9932	0.1562	0.1562	0	0.0096	0.0224	0.016
0.6643	0.7218	0.6236	0.7251	0.045	0.0552	0	0	0	0	0	0
0.6201	0.5791	0.6152	0.5662	0	0.0114	0.1056	0.1056	0	0	0	0
0.3033	0.3513	0.3616	0.2136	0	0	0	0	0.6784	0.6592	0.6912	0.6528
0.0021	0.0076	0.0048	0.0035	0	0	0.2024	0.2178	3.152	3.264	3.2	3.2128
0	0	0	0	0	0	1.6082	1.6478	0	0	0	0
0.0001	0.0012	0.0004	0.0044	0	0	0	0	0	0	0	0
16.0463	15.9892	16.003	15.966	4.0488	4.0308	13.8578	13.8974	19.8848	19.984	19.9616	19.9008

686	689	694	695	698
bh122-10	bh122-13	bh122-18	bh122-19	bh122-22
plagioclase	plagioclase	plagioclase	plagioclase	plagioclase
62.6424	63.6901	63.7524	63.6245	63.9409
0	0	0	0	0
21.7134	22.5653	22.5814	22.7764	23.1501
0	0	0	0	0
0	0.032	0.1119	0.2504	0.2397
0	0	0	0	0
0	0	0	0	0
3.4728	3.5164	3.6692	3.655	3.7392
9.1801	9.0656	9.0704	9.2059	9.0486
0	0	0	0	0
0	0	0	0	0
97.0088	98.8695	99.1854	99.5123	100.1184
11.3696	11.3312	11.3184	11.2768	11.2544
0	0	0	0	0
4.6464	4.7328	4.7264	4.7584	4.8032
0	0	0	0	0
0	0.0032	0.016	0.0384	0.0352
0	0	0	0	0
0	0	0	0	0
0.6752	0.6688	0.6976	0.6944	0.704
3.232	3.1264	3.1232	3.1648	3.088
0	0	0	0	0
0	0	0	0	0
19.9264	19.8656	19.8816	19.936	19.888

ritch116001

BH116 Image 1

-points g1-g16
-points x26-x45

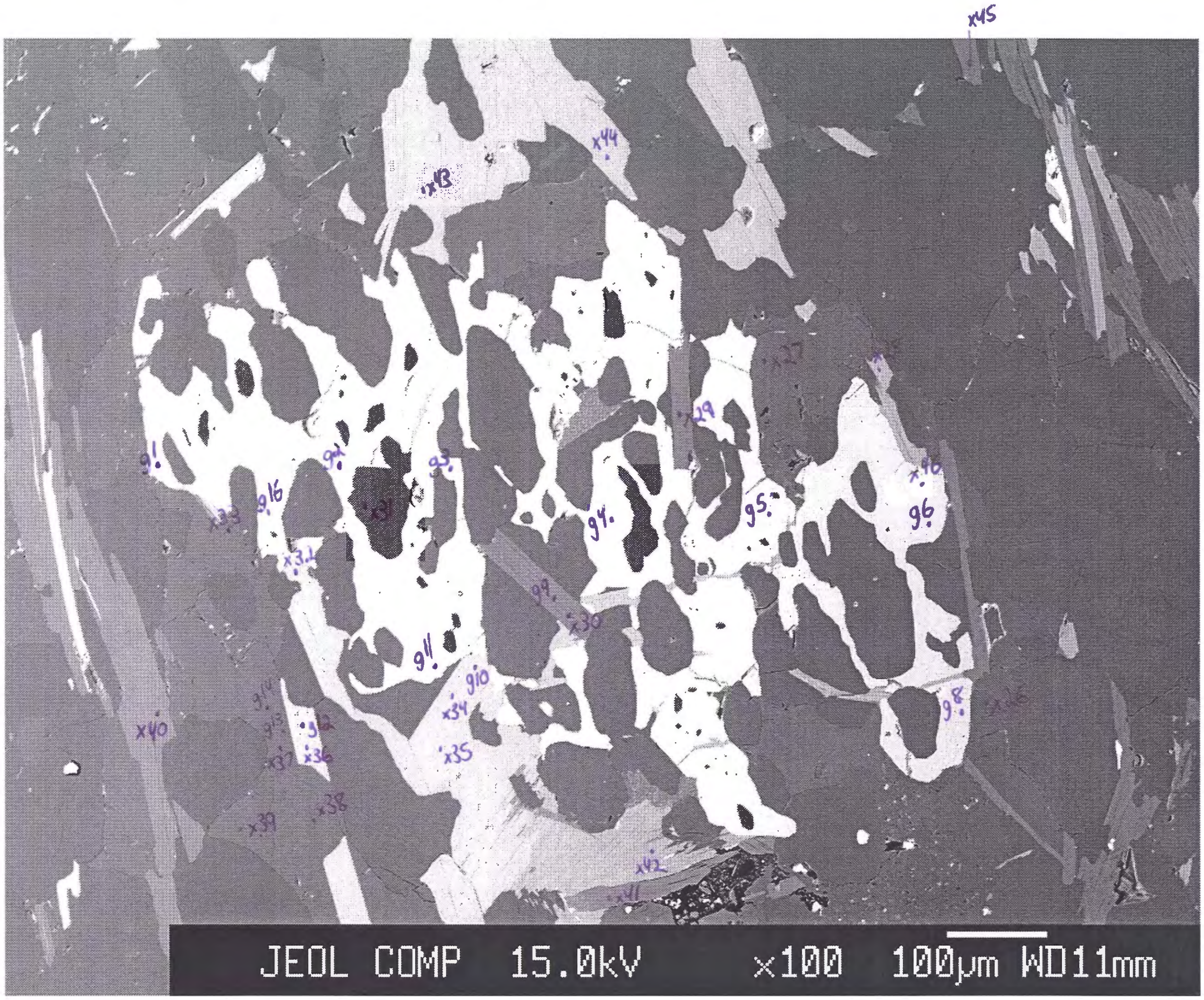

ritch122002

BH122 Image 2

-points g17-g44
-points x1-x25

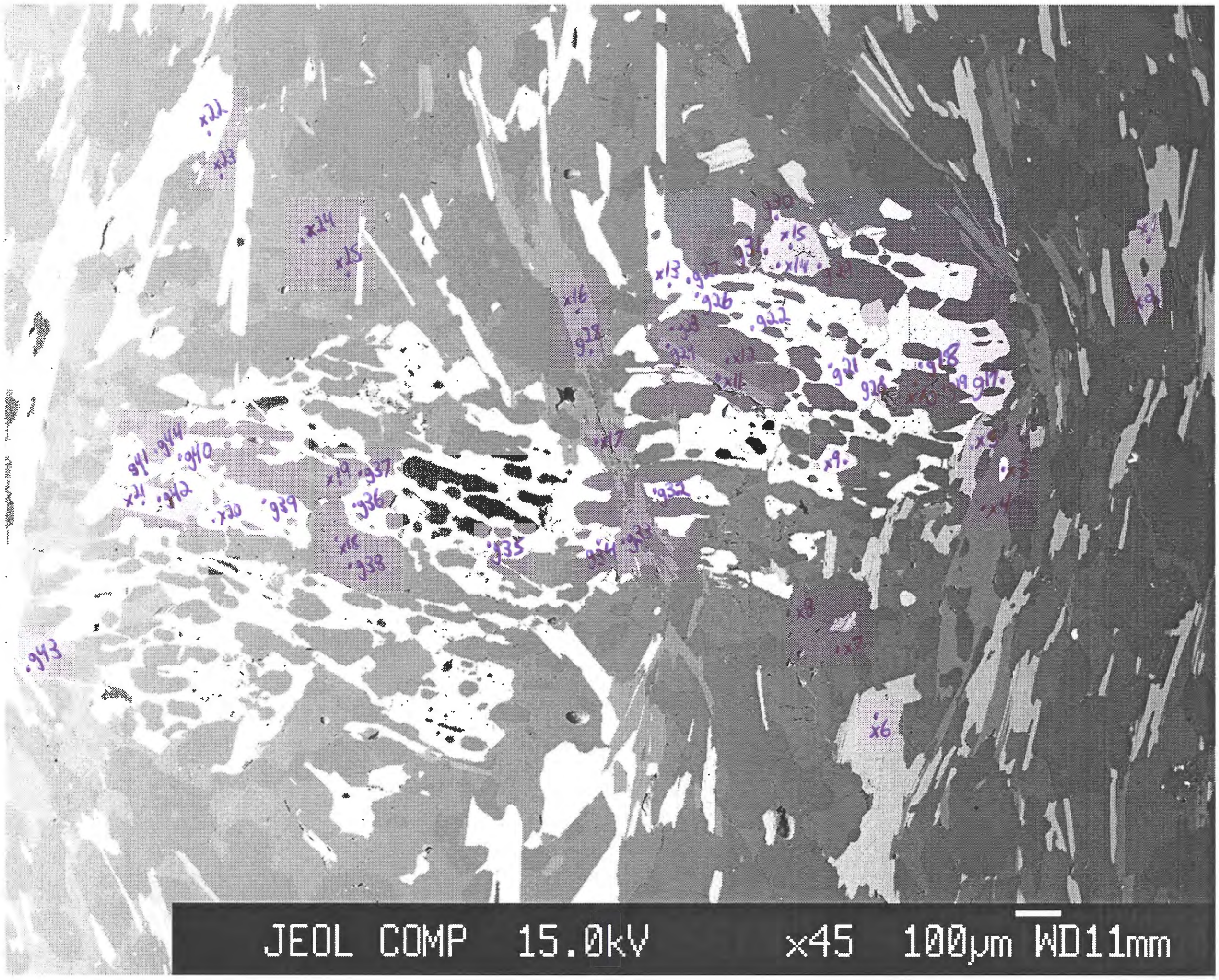

No.	659	651	655	656	663	664	665	670	672	702	706
Comment	bh116-x9	bh116-x1	bh116-x5	bh116-x6	bh116-x13	bh116-x14	bh116-x15	bh116-x20	bh116-x22	bh116-x28	bh116-x32
Mineral	apatite	biotite	biotite	biotite	biotite	biotite	biotite	biotite	biotite	biotite	biotite
Weight % oxide:											
SiO2	0.0265	35.5331	36.0328	35.8856	35.7287	35.7078	35.8978	35.5613	35.768	35.2961	35.0338
TiO2	0	3.6602	2.7618	3.255	2.3345	2.0797	2.1874	2.783	3.6645	1.8048	2.4181
Al2O3	0	17.5966	18.7673	18.3799	19.1499	18.6458	18.6907	18.75	18.2281	19.3299	19.3328
Cr2O3	0	0	0	0	0	0	0	0	0	0	0
FeO	0.2988	21.9233	20.8967	20.5612	21.3832	20.6407	22.0256	21.7601	21.8551	22.9446	23.0618
MnO	0.1699	0.2849	0.2536	0.2431	0.3274	0.2694	0.3482	0.3376	0.306	0.4209	0.5317
MgO	0	7.2024	7.2662	7.2498	7.1045	7.1057	7.1789	7.4757	7.16	7.2254	6.9571
CaO	56.5113	0.0253	0	0	0	0	0.0274	0	0.0068	0	0
Na2O	0.0657	0.0951	0.0921	0.1048	0.0768	0.0852	0.1912	0.0951	0.0967	0.0768	0.0763
K2O	0	10.1117	9.8082	9.8747	10.007	9.8417	9.1378	9.7531	9.8572	9.8345	9.9667
ZnO	0.0721	0.2863	0.0305	0.0519	0.0435	0.0893	0.0442	0.0229	0.0137	0.0646	0.0692
Total	57.1444	96.7189	95.9092	95.6061	96.1556	94.4654	95.7292	96.5389	96.9562	96.9977	97.4475
Number of cations per formula unit:											
Si	0.0104	5.4362	5.4934	5.489	5.456	5.5308	5.4978	5.4164	5.4318	5.3856	5.335
Ti	0	0.4202	0.3168	0.374	0.2684	0.242	0.253	0.319	0.418	0.2068	0.2772
Al	0	3.1746	3.3726	3.3132	3.4474	3.4056	3.3748	3.366	3.2626	3.476	3.4694
Cr	0	0	0	0	0	0	0	0	0	0	0
Fe	0.1066	2.805	2.6642	2.6312	2.7302	2.673	2.8226	2.772	2.7764	2.9282	2.937
Mn	0.0624	0.0374	0.033	0.0308	0.0418	0.0352	0.0462	0.044	0.0396	0.055	0.0682
Mg	0	1.6434	1.6522	1.6522	1.617	1.6412	1.639	1.6984	1.6214	1.6434	1.5796
Ca	25.7608	0.0044	0	0	0	0	0.0044	0	0.0022	0	0
Na	0.0546	0.0286	0.0264	0.0308	0.022	0.0264	0.0572	0.0286	0.0286	0.022	0.022
K	0	1.9734	1.9074	1.9272	1.9492	1.9448	1.7864	1.8964	1.9096	1.914	1.936
Zn	0.0234	0.033	0.0044	0.0066	0.0044	0.011	0.0044	0.0022	0.0022	0.0066	0.0088
Total	26.0182	15.5562	15.4726	15.455	15.5364	15.5122	15.4858	15.543	15.4946	15.6398	15.6332

708	709	710	717	718	720	716	444	447	452	463	464
bh116-x34	bh116-x35	bh116-x36	bh116-x43	bh116-x44	bh116-x46	bh116-x42	bh116-g8	bh116-g11	bh116-g16	bh116-g17	bh116-g18
biotite	biotite	biotite	biotite	biotite	biotite	chlorite	garnet	garnet	garnet	garnet	garnet
35.6356	35.9269	35.798	36.0739	35.7302	35.0844	23.5789	36.8643	36.4084	36.5375	36.4471	36.7009
2.4825	2.6821	3.1752	3.1917	3.2716	0.1403	0.1603	0.0088	0.0219	0	0	0
19.3649	18.9395	18.7809	18.6812	18.7451	0.0675	21.1207	20.9574	20.9254	20.693	20.8084	20.9358
0	0	0	0	0	0	0	0	0	0	0	0
23.3896	22.821	22.7738	22.079	21.7576	1.1195	31.6957	28.6955	28.9586	29.0455	30.8071	31.6296
0.3732	0.3212	0.2948	0.2108	0.2637	0.345	0.7206	9.6408	10.7052	9.5088	9.2422	8.2333
7.1447	7.1218	6.9692	7.2296	6.9154	0.076	9.2708	1.6478	1.5146	1.8124	1.8958	1.9844
0.0368	0.02	0.0273	0	0	0.0305	0.0326	2.0148	1.6521	1.7566	1.8797	1.6918
0.0734	0.0946	0.0757	0.1105	0.0972	0.0561	0.0147	0.0165	0.0153	0.0218	0.0201	0.0344
10.2163	10.1248	10.3587	9.9981	10.1277	0	0.0384	0	0	0	0	0
0.303	0.2532	0.2342	0.0388	0.0533	0.6685	0.2764	0	0.0084	0	0	0.0176
99.0201	98.3051	98.4879	97.6137	96.9619	37.5878	86.9091	99.8459	100.2098	99.3756	101.1003	101.2278
5.346	5.4098	5.3878	5.4384	5.4274	10.6568	5.2416	5.9945	5.9369	5.9811	5.9049	5.925
0.2794	0.3036	0.3586	0.363	0.374	0.033	0.028	0.0011	0.0027	0	0	0
3.4254	3.3616	3.333	3.3198	3.355	0.0242	5.5328	4.0169	4.0219	3.9927	3.9736	3.9839
0	0	0	0	0	0	0	0	0	0	0	0
2.9348	2.8732	2.8666	2.7852	2.7632	0.2838	5.894	3.9025	3.9492	3.9764	4.1742	4.2705
0.0484	0.0418	0.0374	0.0264	0.033	0.088	0.1344	1.3279	1.4786	1.3185	1.2683	1.1259
1.5972	1.5994	1.5642	1.6258	1.5664	0.0352	3.0716	0.3994	0.3682	0.4423	0.4578	0.4776
0.0066	0.0022	0.0044	0	0	0.011	0.0084	0.3511	0.2887	0.3081	0.3263	0.2927
0.022	0.0286	0.022	0.033	0.0286	0.033	0.0056	0.0052	0.0048	0.0069	0.0063	0.0108
1.9558	1.9448	1.9888	1.9228	1.9624	0	0.0112	0	0	0	0	0
0.033	0.0286	0.0264	0.0044	0.0066	0.1496	0.0448	0	0.001	0	0	0.0021
15.6508	15.5958	15.5892	15.521	15.5188	11.3168	19.9752	15.9986	16.0521	16.0261	16.1114	16.0885

466	467	468	471	472	478	480	481	482	485	486	494
bh116-g20	bh116-g21	bh116-g22	bh116-g25	bh116-g26	bh116-g32	bh116-g34	bh116-g35	bh116-g36	bh116-g39	bh116-g40	bh116-g1a
garnet	garnet	garnet	garnet	garnet	garnet	garnet	garnet	garnet	garnet	garnet	garnet
36.5895	36.5261	36.6166	36.6286	36.6689	36.2176	35.9477	36.1355	36.2841	36.3873	36.6022	36.8254
0.011	0.0252	0	0	0.0153	0.0207	0.0175	0.046	0.1772	0.0677	0.0459	0
20.9854	21.0109	20.8718	20.8528	20.8206	20.883	20.8141	20.7826	20.7562	20.24	20.2335	20.8701
0	0	0	0	0	0	0	0	0	0	0	0
31.5258	32.0569	31.1209	30.6967	29.19	30.887	30.9865	31.5341	31.2727	31.9019	30.7983	28.9953
8.0604	8.0783	7.8518	9.3825	9.3866	9.793	8.7989	7.8885	8.3463	8.9971	9.4279	10.3106
2.064	2.1222	2.0672	1.7903	1.6223	1.8186	1.8434	2.0248	1.8725	1.7307	1.9025	1.6399
1.7174	1.672	1.7126	1.5449	1.7207	1.5666	1.6172	1.7585	1.462	1.55	1.9139	1.9401
0.0305	0.0316	0.0409	0.0373	0.0403	0	0	0.0057	0.0086	0	0	0.0285
0	0	0	0	0	0.0076	0.0344	0.0067	0.0125	0.0399	0.0311	0
0.01	0.0268	0	0.0261	0.0445	0.1654	0.1494	0.1418	0.1418	0.2656	0.2503	0.0107
100.9939	101.5499	100.2817	100.9591	99.5093	101.3594	100.209	100.3241	100.3339	101.1802	101.2055	100.6205
5.9156	5.8875	5.9471	5.9347	5.9921	5.8719	5.8809	5.8934	5.9145	5.9236	5.9402	5.968
0.0013	0.0031	0	0	0.0019	0.0025	0.0022	0.0056	0.0217	0.0083	0.0056	0
3.9991	3.9918	3.9957	3.9824	4.0103	3.9907	4.0136	3.9952	3.9879	3.8837	3.8705	3.9866
0	0	0	0	0	0	0	0	0	0	0	0
4.2627	4.3214	4.2272	4.1596	3.9892	4.188	4.2396	4.3012	4.2632	4.3434	4.1802	3.9299
1.1038	1.103	1.0802	1.2877	1.2993	1.3449	1.2193	1.0898	1.1524	1.2407	1.296	1.4154
0.4974	0.5099	0.5005	0.4324	0.3952	0.4395	0.4496	0.4923	0.455	0.42	0.4603	0.3962
0.2975	0.2888	0.298	0.2682	0.3013	0.2722	0.2835	0.3073	0.2553	0.2704	0.3328	0.3369
0.0096	0.0099	0.0129	0.0117	0.0128	0	0	0.0018	0.0027	0	0	0.0089
0	0	0	0	0	0.0016	0.0072	0.0014	0.0026	0.0083	0.0064	0
0.0012	0.0032	0	0.0031	0.0054	0.0198	0.018	0.0171	0.0171	0.0319	0.03	0.0013
16.0883	16.1187	16.0616	16.0798	16.0075	16.1311	16.1139	16.1051	16.0724	16.1304	16.122	16.0433

495	496	497	498	499	500	501	654	661	666	667	671
bh116-g2a	bh116-g3a	bh116-g3a	bh116-g4a	bh116-g5a	bh116-g5a	bh116-g6a	bh116-x4	bh116-x11	bh116-x16	bh116-x17	bh116-x21
garnet	garnet	garnet	garnet	garnet	garnet	garnet	muscovite	muscovite	muscovite	muscovite	muscovite
36.0516	36.498	36.483	36.5103	36.5329	36.7478	36.4033	46.9971	47.4516	48.1271	48.2582	46.9778
0	0	0	0.0033	0.0044	0	0.0087	1.1999	0.8565	1.1536	0.3354	1.1245
20.3348	20.8282	20.9946	20.8733	20.9782	20.9385	20.951	32.2987	33.8293	33.2728	34.7074	33.1601
0	0	0	0	0	0	0	0	0	0	0	0
30.5498	30.7802	30.6441	30.3404	31.4826	31.112	30.8082	1.7771	1.6612	1.5867	1.3218	1.9572
9.2772	9.0171	8.9867	9.3192	8.8408	8.9854	9.8618	0.0108	0	0.0108	0.0539	0.0701
1.9083	2.0339	2.0541	1.857	2.0562	2.0095	1.6271	1.0279	0.8493	1.0358	0.7532	1.0911
1.6492	1.5656	1.5613	1.7363	1.6478	1.6425	1.8811	0.0114	0.007	0	0	0
0.0335	0.0119	0.0129	0.0157	0.0315	0.011	0.022	0.3906	0.4284	0.3658	0.4421	0.3886
0	0	0	0	0	0	0	10.8094	9.6682	10.8407	10.894	10.5955
0.0092	0.0092	0.0199	0	0.0145	0.0115	0	0.0318	0	0	0	0
99.8137	100.744	100.7565	100.6554	101.5889	101.4581	101.5631	94.5548	94.7515	96.3933	96.7661	95.365
5.9216	5.9214	5.9126	5.9269	5.8903	5.9222	5.8856	6.3338	6.3184	6.3404	6.3184	6.2744
0	0	0	0.0004	0.0005	0	0.0011	0.121	0.0858	0.1144	0.033	0.1122
3.9369	3.983	4.0105	3.994	3.9868	3.9774	3.9926	5.1304	5.3086	5.1678	5.357	5.2206
0	0	0	0	0	0	0	0	0	0	0	0
4.1966	4.1764	4.1535	4.1191	4.2452	4.1933	4.1657	0.2002	0.1848	0.1738	0.1452	0.2178
1.2908	1.2392	1.2337	1.2815	1.2074	1.2266	1.3506	0.0022	0	0.0022	0.0066	0.0088
0.4673	0.4919	0.4963	0.4494	0.4942	0.4828	0.3922	0.2068	0.1694	0.2024	0.1474	0.2178
0.2903	0.2722	0.2711	0.302	0.2847	0.2836	0.3259	0.0022	0	0	0	0
0.0107	0.0037	0.004	0.0049	0.0099	0.0034	0.0069	0.1012	0.11	0.0924	0.1122	0.1012
0	0	0	0	0	0	0	1.859	1.6412	1.8216	1.8194	1.8062
0.0011	0.0011	0.0024	0	0.0017	0.0014	0	0.0022	0	0	0	0
16.1154	16.0889	16.0841	16.0783	16.1207	16.0907	16.1206	13.9612	13.8204	13.915	13.9414	13.959

703	704	714	715	719	652	657	658	660	662	668	669
bh116-x29	bh116-x30	bh116-x40	bh116-x41	bh116-x45	bh116-x2	bh116-x7	bh116-x8	bh116-x10	bh116-x12	bh116-x18	bh116-x19
muscovite	muscovite	muscovite	muscovite	muscovite	plagioclase	plagioclase	plagioclase	plagioclase	plagioclase	plagioclase	plagioclase
47.6818	47.4009	48.255	46.8189	49.4462	65.1025	66.0486	66.0327	65.9145	65.7785	65.8735	65.6474
1.2291	1.2445	1.5248	0.217	1.3044	0	0	0	0	0	0.0047	0
32.8263	33.4131	33.1138	33.2107	32.1091	20.8513	21.5082	21.7694	21.8091	21.6079	21.7858	21.8339
0	0	0	0	0	0	0	0	0	0	0	0
2.1669	1.8391	1.88	4.2122	1.9542	0.032	0	0.032	0.2558	0.16	0.0053	0.1333
0.0754	0.0323	0.0108	0.0805	0	0.0054	0	0	0	0	0	0
1.1594	1.0888	1.076	1.4658	1.4572	0	0	0	0	0	0	0
0	0	0.0087	0.0195	0	2.608	2.5583	2.6027	2.8353	2.7173	2.7146	2.8241
0.4149	0.3717	0.4091	0.2936	0.3535	9.885	9.9384	9.8448	9.7095	9.9231	9.8069	9.7895
10.7276	10.1234	10.869	10.9813	10.7769	0.2043	0	0	0	0	0	0
0	0	0.0844	0.1036	0	0	0	0	0	0	0	0
96.2815	95.5139	97.2317	97.4032	97.4016	98.6886	100.0534	100.2815	100.5241	100.1868	100.1908	100.2281
6.3162	6.292	6.3206	6.2106	6.4504	11.6	11.5808	11.552	11.5232	11.5392	11.5392	11.5104
0.1232	0.1232	0.1496	0.022	0.1276	0	0	0	0	0	0	0
5.1238	5.2272	5.1128	5.192	4.9368	4.3776	4.4448	4.4896	4.4928	4.4672	4.4992	4.512
0	0	0	0	0	0	0	0	0	0	0	0
0.2398	0.2046	0.2068	0.4664	0.2134	0.0032	0	0.0032	0.0384	0.0224	0	0.0192
0.0088	0.0044	0.0022	0.0088	0	0	0	0	0	0	0	0
0.2288	0.2156	0.2112	0.2904	0.2838	0	0	0	0	0	0	0
0	0	0.0022	0.0022	0	0.4992	0.48	0.4864	0.5312	0.512	0.5088	0.5312
0.1056	0.0946	0.1034	0.0748	0.0902	3.4144	3.3792	3.3408	3.2896	3.376	3.3312	3.328
1.8128	1.7138	1.8172	1.859	1.793	0.048	0	0	0	0	0	0
0	0	0.0088	0.011	0	0	0	0	0	0	0	0
13.9612	13.8776	13.937	14.1394	13.8974	19.9456	19.888	19.8752	19.8784	19.9168	19.8784	19.9008

673	674	675	700	701	705	707	711	712	713
bh116-x23	bh116-x24	bh116-x25	bh116-x26	bh116-x27	bh116-x31	bh116-x33	bh116-x37	bh116-x38	bh116-x39
plagioclase	plagioclase	plagioclase	plagioclase	plagioclase	plagioclase	plagioclase	plagioclase	plagioclase	plagioclase
66.6003	65.8644	67.1913	64.9056	64.895	65.3237	68.1532	66.0409	66.0873	65.9376
0.0082	0	0	0	0	0	0	0.0082	0.0105	0.0221
21.5942	21.7968	21.7483	21.7955	21.6674	21.79	22.1148	21.7871	21.9744	21.6578
0	0	0	0	0	0	0	0	0	0
0.128	0	0.1546	0.0799	0.2502	0.3355	0.2504	0.1704	0.0479	0
0	0	0.0649	0	0.0054	0.0108	0.0108	0.0595	0	0
0	0	0	0	0	0	0	0	0.0038	0
2.3716	2.5868	2.6996	2.3855	2.2868	2.3047	2.8341	2.6973	2.773	2.7869
9.9624	9.8858	9.5355	9.9093	9.9567	10.0648	9.6437	10.0462	9.9092	9.8559
0	0	0.2349	0	0	0	0.144	0.1929	0.1501	0.2235
0	0	0	0	0	0	0.0297	0.0641	0.0766	0.0305
100.6646	100.1338	101.6291	99.0759	99.0615	99.8296	103.1806	101.0666	101.0328	100.5143
11.6032	11.5424	11.6032	11.5008	11.5104	11.504	11.5936	11.5104	11.504	11.536
0	0	0	0	0	0	0	0	0	0.0032
4.4352	4.5024	4.4256	4.5536	4.5312	4.5248	4.4352	4.4768	4.5088	4.4672
0	0	0	0	0	0	0	0	0	0
0.0192	0	0.0224	0.0128	0.0384	0.048	0.0352	0.0256	0.0064	0
0	0	0.0096	0	0	0.0032	0	0.0096	0	0
0	0	0	0	0	0	0	0	0	0
0.4416	0.4864	0.4992	0.4544	0.4352	0.4352	0.5152	0.5024	0.5184	0.5216
3.3664	3.36	3.1936	3.4048	3.424	3.4368	3.1808	3.3952	3.344	3.344
0	0	0.0512	0	0	0	0.032	0.0416	0.032	0.0512
0	0	0	0	0	0	0.0032	0.0096	0.0096	0.0032
19.8688	19.8944	19.808	19.9264	19.9392	19.952	19.7984	19.9712	19.9232	19.9296

ritch112001

BH112 Image 1

-points 1-32

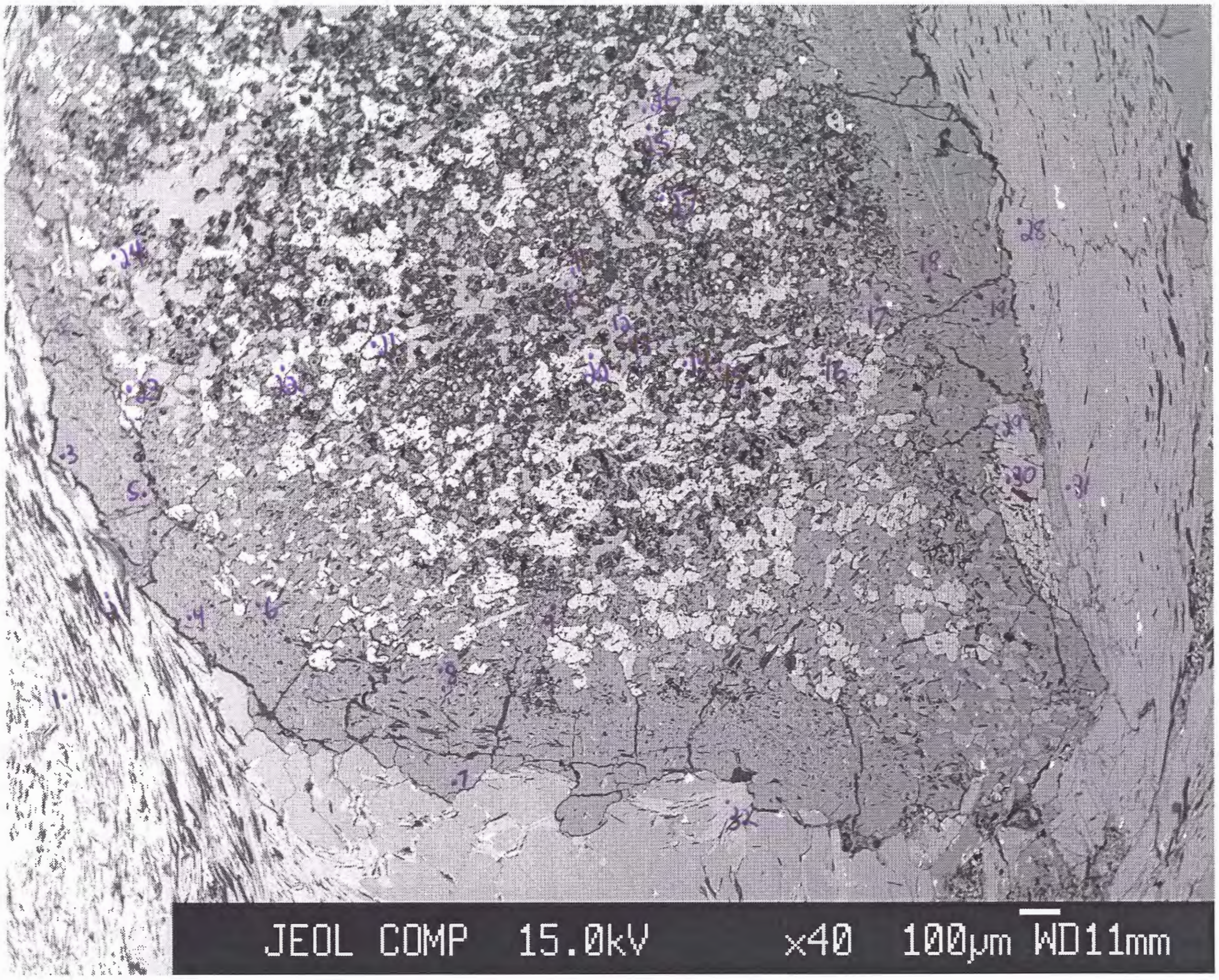

ritch112002

BH112 Image 2

-points 33-59

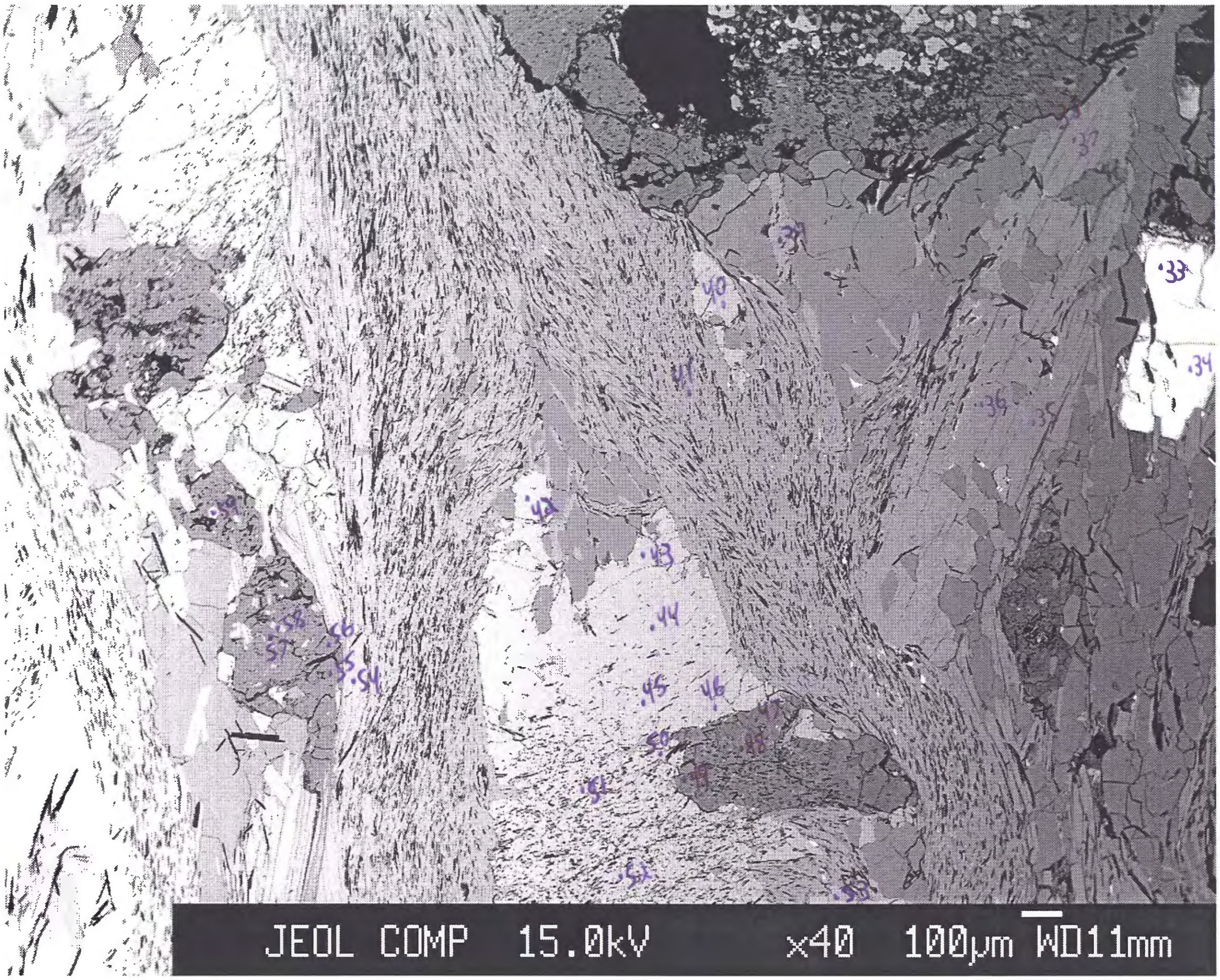

ritch112003

BH112 Image 3

-points 60-71

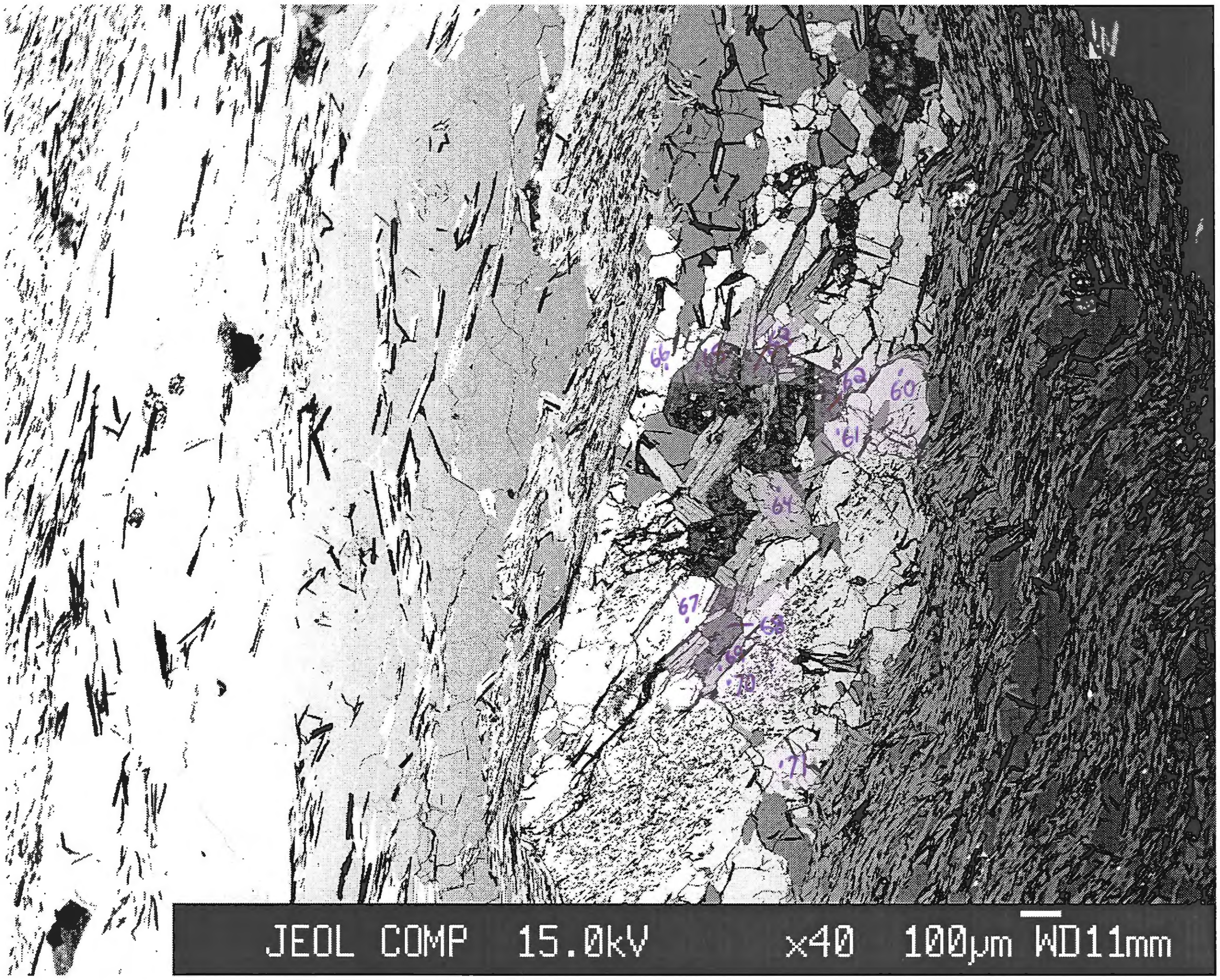

ritch112004

BH112 Image 4

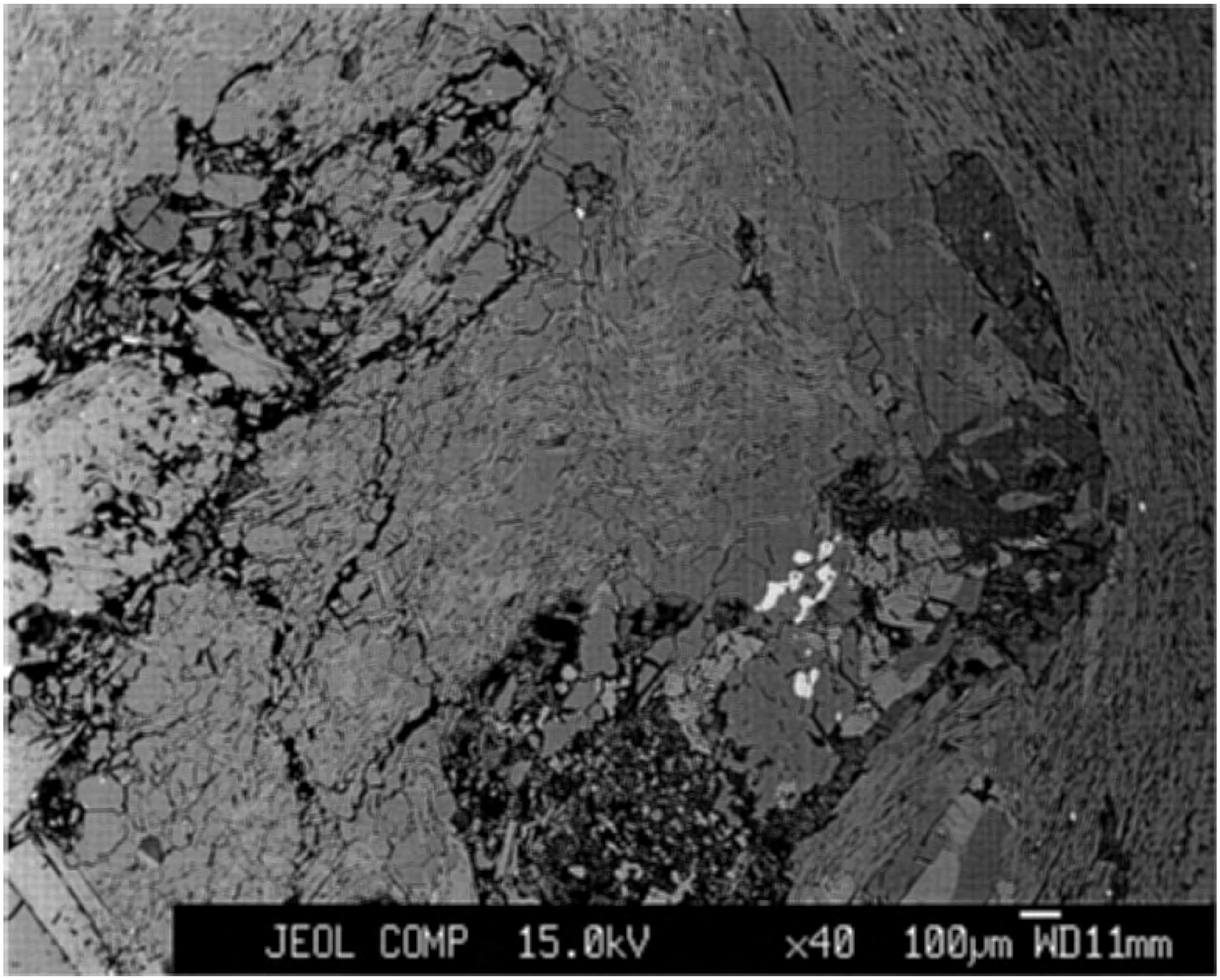

SAMPLE BH112

No.	306	307	308	309	310	312	320	321	322	341	350
Comment	lrbh112-3	lrbh112-4	lrbh112-5	lrbh112-6	lrbh112-7	lrbh112-9	lrbh112-17	lrbh112-18	lrbh112-19	lrbh112-38	lrbh112-47
Mineral	Al-silicate	Al-silicate	Al-silicate	Al-silicate	Al-silicate	Al-silicate	Al-silicate	Al-silicate	Al-silicate	Al-silicate	Al-silicate
Weight % oxide:											
SiO2	44.3035	43.9755	46.9021	40.3585	44.0288	39.1547	45.1417	46.2409	43.1551	41.0283	44.2763
TiO2	0.0405	0.0286	0.0488	0.0357	0.0262	0.0393	0.037	0.0537	0.025	0	0
Al2O3	41.5037	39.6184	42.3314	37.4074	40.3228	38.6789	41.4645	41.7829	40.5791	39.9801	40.3128
Cr2O3	0	0	0	0	0	0	0	0	0	0	0
FeO	0.2252	0.1183	0.0732	0.0788	0.1239	0.3549	0.0677	0.0734	0.0395	0.1414	0.0623
MnO	0	0	0	0.0163	0	0.0651	0	0	0.0815	0.0109	0.0382
MgO	0.0178	0.0106	0	0	0.0353	0.0371	0.0408	0.0147	0.0284	0.0207	0.0202
CaO	0.0793	0.0592	0.0533	0.0685	0.1337	0.2896	0.2047	0.0604	0.1094	0.0977	0.0967
Na2O	0.1	0.0966	0.1065	0.1392	0.08	0.0317	0.0582	0.1302	0.0894	0.0772	0.023
K2O	0.1224	0.0951	0.1406	0.1432	0.1621	0.1152	0.1277	0.1442	0.1161	0.1466	0.0776
ZnO	0.0394	0.037	0.0592	0.0008	0.0288	0	0.0264	0	0.0329	0	0
Total	86.4318	84.0394	89.7151	78.2485	84.9417	78.7666	87.1688	88.5005	84.2565	81.503	84.9072
Number of cations per formula unit:											
Si	0.2725	0.2776	0.2774	0.274	0.2754	0.2653	0.275	0.2772	0.2722	0.2679	0.2765
Ti	0.0002	0.0001	0.0002	0.0002	0.0001	0.0002	0.0002	0.0002	0.0001	0	0
Al	0.301	0.2948	0.2951	0.2994	0.2973	0.3089	0.2978	0.2953	0.3017	0.3077	0.2968
Cr	0	0	0	0	0	0	0	0	0	0	0
Fe	0.0012	0.0006	0.0004	0.0004	0.0006	0.002	0.0003	0.0004	0.0002	0.0008	0.0003
Mn	0	0	0	0.0001	0	0.0004	0	0	0.0004	0.0001	0.0002
Mg	0.0002	0.0001	0	0	0.0003	0.0004	0.0004	0.0001	0.0003	0.0002	0.0002
Ca	0.0005	0.0004	0.0003	0.0005	0.0009	0.0021	0.0013	0.0004	0.0007	0.0007	0.0006
Na	0.0012	0.0012	0.0012	0.0018	0.001	0.0004	0.0007	0.0015	0.0011	0.001	0.0003
K	0.001	0.0008	0.0011	0.0012	0.0013	0.001	0.001	0.0011	0.0009	0.0012	0.0006
Zn	0.0002	0.0002	0.0003	0	0.0001	0	0.0001	0	0.0002	0	0
Total	0.578	0.5759	0.576	0.5776	0.5771	0.5807	0.5769	0.5763	0.5778	0.5796	0.5756

351	352	358	359	360	365	367	368	371	317	319	323
lrbh112-48	lrbh112-49	lrbh112-55	lrbh112-56	lrbh112-57	lrbh112-62	lrbh112-64	lrbh112-65	lrbh112-68	lrbh112-14	lrbh112-16	lrbh112-20
Al-silicate	Al-silicate	Al-silicate	Al-silicate	Al-silicate	Al-silicate	Al-silicate	Al-silicate	Al-silicate	K-feldspar	K-feldspar	K-feldspar
39.3036	40.1181	42.0026	32.8238	41.5273	44.3165	41.7554	42.1055	43.3887	64.3089	63.1278	63.4031
0.0262	0	0.0359	0.0024	0.0096	0.0048	0.0084	0	0.024	0	0.0121	0
36.7355	39.2932	38.5627	35.3533	39.6212	40.4102	40.4776	39.6582	39.9464	18.4724	18.378	18.5503
0	0	0	0	0	0	0	0	0	0	0	0
1.8305	1.1314	0.1304	0.0963	0.0397	0.0965	0.6407	0.2496	0.5558	0	0	0
0.0218	0.0109	0	0	0	0	0	0	0	0	0	0.158
0.0754	0	0	0	0	0.0094	0.0153	0	0.0012	0.0023	0	0
0.2093	0.1305	0.134	0.0738	0.1105	0.2492	0.2839	0.1303	0.1817	0.0106	0.0067	0.0414
0.1359	0.0708	0.0221	0.0376	0.038	0.0161	0.0869	0.0151	0.0801	1.087	1.1343	1.2275
0.284	0.2046	0.1077	0.1195	0.0962	0.1222	0.1625	0.1119	0.1367	14.0013	13.7239	13.688
0	0	0	0	0	0	0	0	0	0	0	0
78.6223	80.9596	80.9955	68.5068	81.4426	85.225	83.4308	82.2707	84.3147	97.8826	96.3829	97.0684
0.2696	0.2657	0.2753	0.2556	0.2708	0.276	0.2674	0.2721	0.2741	12.016	11.9808	11.9552
0.0001	0	0.0002	0	0	0	0	0	0.0001	0	0.0032	0
0.297	0.3067	0.2979	0.3245	0.3045	0.2967	0.3056	0.302	0.2975	4.0672	4.112	4.1216
0	0	0	0	0	0	0	0	0	0	0	0
0.0105	0.0063	0.0007	0.0006	0.0002	0.0005	0.0034	0.0013	0.0029	0	0	0
0.0001	0.0001	0	0	0	0	0	0	0	0	0	0.0256
0.0008	0	0	0	0	0.0001	0.0001	0	0	0	0	0
0.0015	0.0009	0.0009	0.0006	0.0008	0.0017	0.0019	0.0009	0.0012	0.0032	0	0.0096
0.0018	0.0009	0.0003	0.0006	0.0005	0.0002	0.0011	0.0002	0.001	0.3936	0.416	0.448
0.0025	0.0017	0.0009	0.0012	0.0008	0.001	0.0013	0.0009	0.0011	3.3376	3.3216	3.2928
0	0	0	0	0	0	0	0	0	0	0	0
0.584	0.5824	0.5762	0.5832	0.5777	0.5763	0.5808	0.5774	0.578	19.8208	19.8336	19.856

324	325	326	328	333	343	345	346	347	348	349	353
Irbh112-21	Irbh112-22	Irbh112-23	Irbh112-25	Irbh112-30	Irbh112-40	Irbh112-42	Irbh112-43	Irbh112-44	Irbh112-45	Irbh112-46	Irbh112-50
K-feldspar	K-feldspar	K-feldspar	K-feldspar	K-feldspar	K-feldspar	K-feldspar	K-feldspar	K-feldspar	K-feldspar	K-feldspar	K-feldspar
64.6816	63.5614	63.4497	64.294	63.7161	63.6417	64.1011	65.4864	63.5106	63.6139	63.6428	63.4799
0.0133	0.0206	0.0085	0.052	0.0133	0.0182	0.0303	0	0	0.0012	0	0
18.6646	18.7017	18.7951	18.8095	18.6322	18.6181	18.6291	18.9104	18.8701	18.9179	18.6342	18.8993
0	0	0	0	0	0	0	0	0	0	0	0
0.0339	0.0339	0	0.0565	0.0679	0	0	0.0396	0	0	0	0.0227
0	0.0273	0	0.0327	0	0	0	0.0601	0.0055	0.0874	0.1257	0.0328
0.0005	0.002	0	0	0	0.0116	0	0.0076	0	0.0091	0	0.0119
0	0	0.0028	0.0252	0	0.0107	0.0331	0.0185	0.0331	0.0325	0.0376	0.0185
1.2276	1.2314	1.2427	1.3507	1.176	1.2057	1.3626	1.2906	1.3598	1.3884	1.3188	1.3228
14.4093	14.4809	14.3509	13.9838	14.2187	14.2773	14.1318	13.9411	14.2112	14.1467	14.1682	14.1056
0.0057	0	0.0066	0	0.0345	0	0	0.0453	0.0321	0.0132	0	0.0181
99.0366	98.0593	97.8564	98.6045	97.8587	97.7834	98.288	99.7997	98.0225	98.2104	97.9274	97.9117
11.9776	11.9136	11.9072	11.9456	11.9456	11.9424	11.9552	11.9968	11.8976	11.8912	11.9296	11.8976
0.0032	0.0032	0	0.0064	0.0032	0.0032	0.0032	0	0	0	0	0
4.0736	4.1312	4.1568	4.1184	4.1184	4.1184	4.096	4.0832	4.1664	4.1696	4.1184	4.176
0	0	0	0	0	0	0	0	0	0	0	0
0.0064	0.0064	0	0.0096	0.0096	0	0	0.0064	0	0	0	0.0032
0	0.0032	0	0.0064	0	0	0	0.0096	0	0.0128	0.0192	0.0064
0	0	0	0	0	0.0032	0	0.0032	0	0.0032	0	0.0032
0	0	0	0.0064	0	0.0032	0.0064	0.0032	0.0064	0.0064	0.0064	0.0032
0.4416	0.448	0.4512	0.4864	0.4288	0.4384	0.4928	0.4576	0.4928	0.5024	0.48	0.48
3.4048	3.4624	3.4368	3.3152	3.4016	3.4176	3.3632	3.2576	3.3952	3.3728	3.3888	3.3728
0	0	0	0	0.0032	0	0	0.0064	0.0032	0.0032	0	0.0032
19.9104	19.9712	19.952	19.8944	19.9136	19.9296	19.92	19.824	19.9648	19.9648	19.9456	19.9456

354	355	356	363	364	369	370	373	374	336	337	304
lrbh112-51	lrbh112-52	lrbh112-53	lrbh112-60	lrbh112-61	lrbh112-66	lrbh112-67	lrbh112-70	lrbh112-71	lrbh112-33	lrbh112-34	lrbh112-1
K-feldspar	K-feldspar	K-feldspar	K-feldspar	K-feldspar	K-feldspar	K-feldspar	K-feldspar	K-feldspar	magnetite	magnetite	muscovite
63.5984	63.6376	65.3348	63.4211	63.2061	63.5837	63.392	63.7423	63.6079	2.5365	2.1366	49.9441
0	0	0.0206	0.0316	0.0146	0.0097	0.0219	0.0231	0.0243	0	0	1.7394
18.8701	18.903	18.8387	18.8062	18.8005	18.8803	18.9591	18.7784	18.8908	0	0	34.2387
0	0	0	0	0	0	0	0	0	0	0	0
0.068	0	0.0283	0	0	0	0.0454	0.0057	0.0284	73.9205	73.9223	0.0675
0.0437	0.0766	0	0	0	0	0.0986	0	0	0.0637	0	0
0.0058	0.005	0	0	0.0099	0	0.0028	0	0	0	0	1.5419
0.0213	0.032	0.0421	0.023	0.0348	0.0118	0.0129	0.0326	0.0309	0	0.0039	0.0126
1.3715	1.1862	1.2589	1.1808	1.2729	1.3832	1.3655	1.227	1.2472	0.0283	0.0262	0.317
14.2294	14.1731	14.2582	14.3533	14.2312	13.9785	14.077	14.574	14.0977	0	0	8.0642
0.0346	0	0.0486	0.0231	0.0445	0.0602	0.0684	0.0445	0.0668	0.0392	0	0
98.2429	98.0136	99.8303	97.8392	97.6146	97.9074	98.0436	98.4277	97.9941	76.5883	76.0891	95.9255
11.8944	11.9104	11.9872	11.904	11.8912	11.9072	11.8752	11.9104	11.9072	1.2128	1.0336	6.4306
0	0	0.0032	0.0032	0.0032	0	0.0032	0.0032	0.0032	0	0	0.1694
4.16	4.1696	4.0736	4.16	4.1696	4.1664	4.1856	4.1344	4.1664	0	0	5.1964
0	0	0	0	0	0	0	0	0	0	0	0
0.0096	0	0.0032	0	0	0	0.0064	0	0.0032	29.5232	29.9168	0.0066
0.0064	0.0128	0	0	0	0	0.016	0	0	0.0256	0	0
0.0032	0	0	0	0.0032	0	0	0	0	0	0	0.297
0.0032	0.0064	0.0096	0.0032	0.0064	0.0032	0.0032	0.0064	0.0064	0	0.0032	0.0022
0.496	0.432	0.448	0.4288	0.464	0.5024	0.496	0.4448	0.4512	0.0256	0.0256	0.0792
3.3952	3.3824	3.3376	3.4368	3.4176	3.3408	3.3632	3.4752	3.3664	0	0	1.3244
0.0032	0	0.0064	0.0032	0.0064	0.0096	0.0096	0.0064	0.0096	0.0128	0	0
19.9712	19.9168	19.8688	19.9424	19.9616	19.9296	19.9584	19.9808	19.9168	30.8032	30.9824	13.508

305	311	314	315	327	329	331	332	334	335	344	357
lrbh112-2	lrbh112-8	lrbh112-11	lrbh112-12	lrbh112-24	lrbh112-26	lrbh112-28	lrbh112-29	lrbh112-31	lrbh112-32	lrbh112-41	lrbh112-54
muscovite	muscovite	muscovite	muscovite	muscovite	muscovite	muscovite	muscovite	muscovite	muscovite	muscovite	muscovite
50.6384	48.4164	51.6179	48.5998	50.7598	49.6072	48.5099	47.1992	48.1258	49.455	50.8571	49.0184
1.6512	0.0262	1.6193	1.8333	0.9961	1.7336	1.7448	1.5607	1.7248	1.7038	1.7891	1.7289
34.5115	43.0157	33.9256	32.5187	30.8325	32.0662	33.3966	34.2697	33.3599	33.9826	35.2979	32.7296
0	0	0	0	0	0	0	0	0	0	0	0
0.2588	0.0958	0.1916	0.169	0.175	0.0903	0.1072	0.1355	0.113	0.0395	0.2262	0.1414
0.0054	0.038	0.0326	0.0977	0.0653	0	0	0	0.0218	0.0054	0	0
1.6291	0.0149	1.7879	1.8746	2.5575	1.9481	1.5951	1.3259	1.5459	1.5816	1.6073	1.9671
0.011	0.0761	0.0252	0	0.0183	0.005	0.0122	0	0.011	0	0.011	0.0128
0.2651	0.1237	0.2314	0.2757	0.2697	0.2417	0.3065	0.245	0.2831	0.2919	0.2972	0.2952
7.9558	0.1371	6.2363	9.098	9.2489	9.0906	9.9588	8.964	7.3215	10.0477	7.9109	10.0783
0	0.097	0.0115	0	0	0.0123	0	0.0296	0	0	0	0.0263
96.9264	92.041	95.6794	94.4669	94.9232	94.7951	95.6311	93.7297	92.5069	97.1076	97.9968	95.998
6.4482	6.1424	6.5736	6.4196	6.6572	6.5142	6.3602	6.2788	6.4086	6.3756	6.402	6.4064
0.1584	0.0022	0.154	0.1826	0.099	0.1716	0.1716	0.1562	0.1738	0.165	0.1694	0.1694
5.1788	6.4328	5.093	5.0644	4.7674	4.9632	5.1612	5.3724	5.236	5.1634	5.2382	5.0424
0	0	0	0	0	0	0	0	0	0	0	0
0.0286	0.011	0.0198	0.0176	0.0198	0.011	0.011	0.0154	0.0132	0.0044	0.0242	0.0154
0	0.0044	0.0044	0.011	0.0066	0	0	0	0.0022	0	0	0
0.3102	0.0022	0.3388	0.3696	0.4994	0.3806	0.3124	0.2618	0.3058	0.3036	0.3014	0.3828
0.0022	0.011	0.0044	0	0.0022	0	0.0022	0	0.0022	0	0.0022	0.0022
0.066	0.0308	0.0572	0.0704	0.0682	0.0616	0.077	0.0638	0.0726	0.0726	0.0726	0.0748
1.2914	0.022	1.0142	1.5334	1.5488	1.5224	1.6654	1.5202	1.243	1.6522	1.2716	1.6808
0	0.0088	0	0	0	0.0022	0	0.0022	0	0	0	0.0022
13.486	12.6698	13.2616	13.6708	13.6686	13.629	13.761	13.673	13.4596	13.7368	13.4838	13.7786

361	362	338	339	340	342	366	372	313	316	318	330
lrbh112-58	lrbh112-59	lrbh112-35	lrbh112-36	lrbh112-37	lrbh112-39	lrbh112-63	lrbh112-69	lrbh112-10	lrbh112-13	lrbh112-15	lrbh112-27
muscovite	muscovite	phlogopite	phlogopite	phlogopite	phlogopite	phlogopite	phlogopite	quartz	quartz	quartz	xxxxxxx
48.0968	47.8776	40.4223	40.5711	40.0508	40.5444	41.254	40.5452	97.8243	97.2247	97.5075	1.0289
1.6015	1.2463	1.3909	1.2806	1.2793	1.2573	1.3212	1.31	0.0337	0.0024	0.0012	0.0204
32.4347	32.5545	18.9112	18.1096	19.0982	18.8822	19.5118	19.0949	0.0025	0	0	0.2745
0	0	0	0	0	0	0	0	0	0	0	0
0.1642	0.1529	1.8291	2.2012	2.0877	2.1225	2.1678	2.1056	0.0284	0.0797	0	0
0	0	0.0272	0.1142	0.2828	0.1687	0.1528	0.06	0	0	0	0.0054
2.0072	1.9943	21.7195	21.0815	21.6938	22.8511	22.8613	22.8925	0	0.004	0	0
0.0067	0	0	0.0061	0.0474	0	0.0077	0.0022	0.0011	0	0.0204	0
0.2655	0.2526	0.167	0.1486	0.1378	0.1368	0.1536	0.1517	0	0.001	0	0.068
9.6876	9.1625	8.9424	8.3057	8.7408	10.1218	9.5557	10.0425	0.0145	0.0187	0.0109	0.0177
0.0041	0	0.0288	0.0115	0.0066	0.0279	0.0272	0.0041	0.0133	0	0	0.0124
94.2684	93.2408	93.4384	91.8301	93.4252	96.1128	97.0132	96.2087	97.9179	97.3306	97.5401	1.4274
6.3932	6.4086	5.6936	5.7992	5.6518	5.6122	5.6276	5.599	0.9994	0.9996	0.9998	0.3861
0.1606	0.1254	0.1474	0.1386	0.1364	0.1298	0.1364	0.1364	0.0002	0	0	0.0057
5.082	5.1348	3.1394	3.0514	3.1768	3.08	3.1372	3.1086	0	0	0	0.1214
0	0	0	0	0	0	0	0	0	0	0	0
0.0176	0.0176	0.2156	0.264	0.2464	0.2464	0.2464	0.2442	0.0002	0.0006	0	0
0	0	0.0022	0.0132	0.033	0.0198	0.0176	0.0066	0	0	0	0.0017
0.3982	0.3982	4.5606	4.4924	4.565	4.7146	4.6486	4.7124	0	0	0	0
0	0	0	0	0.0066	0	0.0022	0	0	0	0.0002	0
0.0682	0.066	0.0462	0.0418	0.0374	0.0374	0.0396	0.0396	0	0	0	0.0495
1.6434	1.5642	1.606	1.5136	1.573	1.7864	1.6632	1.7688	0.0002	0.0002	0.0002	0.0084
0	0	0.0022	0.0022	0	0.0022	0.0022	0	0.0002	0	0	0.0034
13.7654	13.7148	15.4132	15.3186	15.4286	15.631	15.5232	15.6178	1.0004	1.0004	1.0004	0.5763

ritch53001

BH53 Image 1

-points g1-g6
-points 36-45

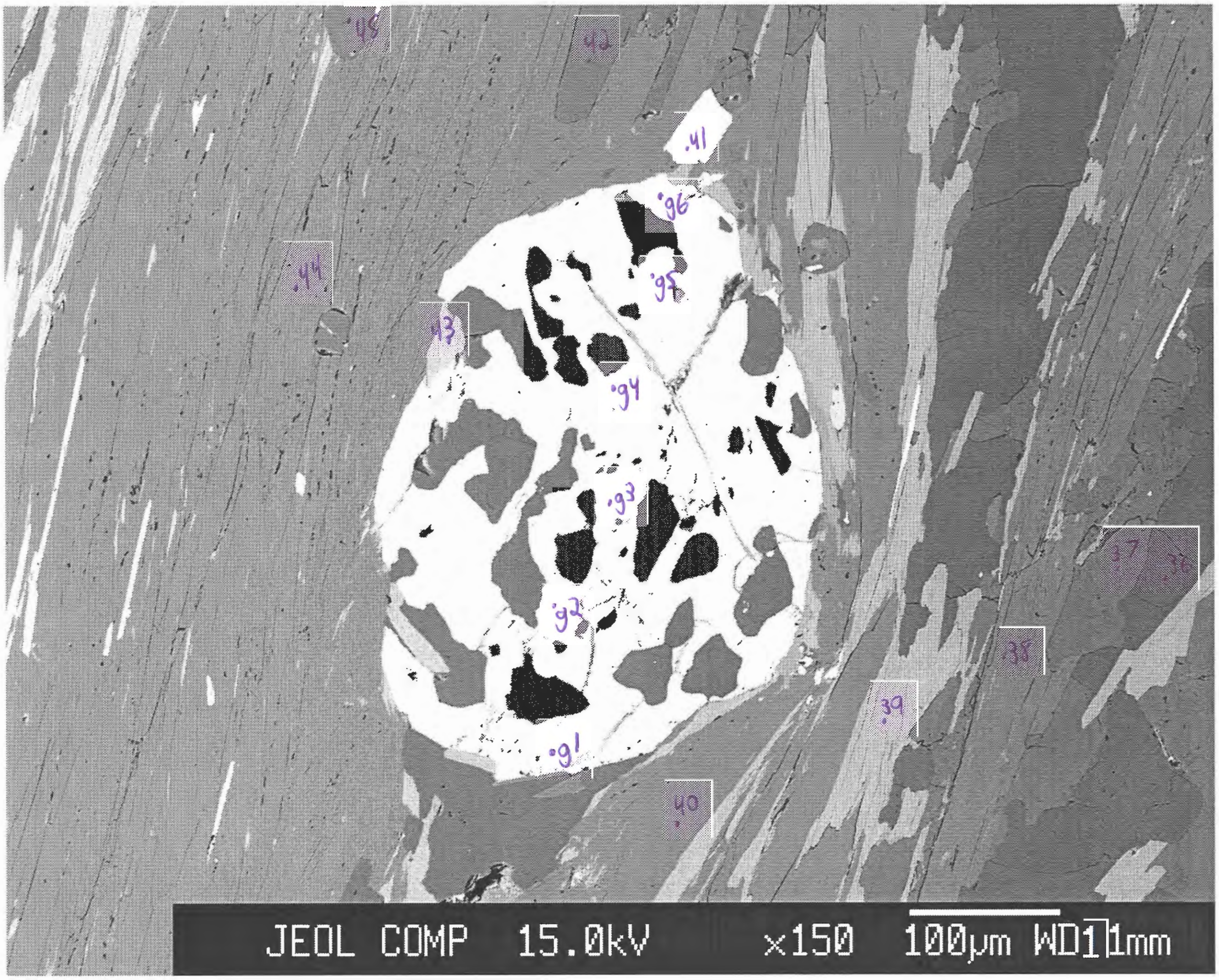

ritch53002

BH53 Image 2

-points 13-23
-points g7-g13

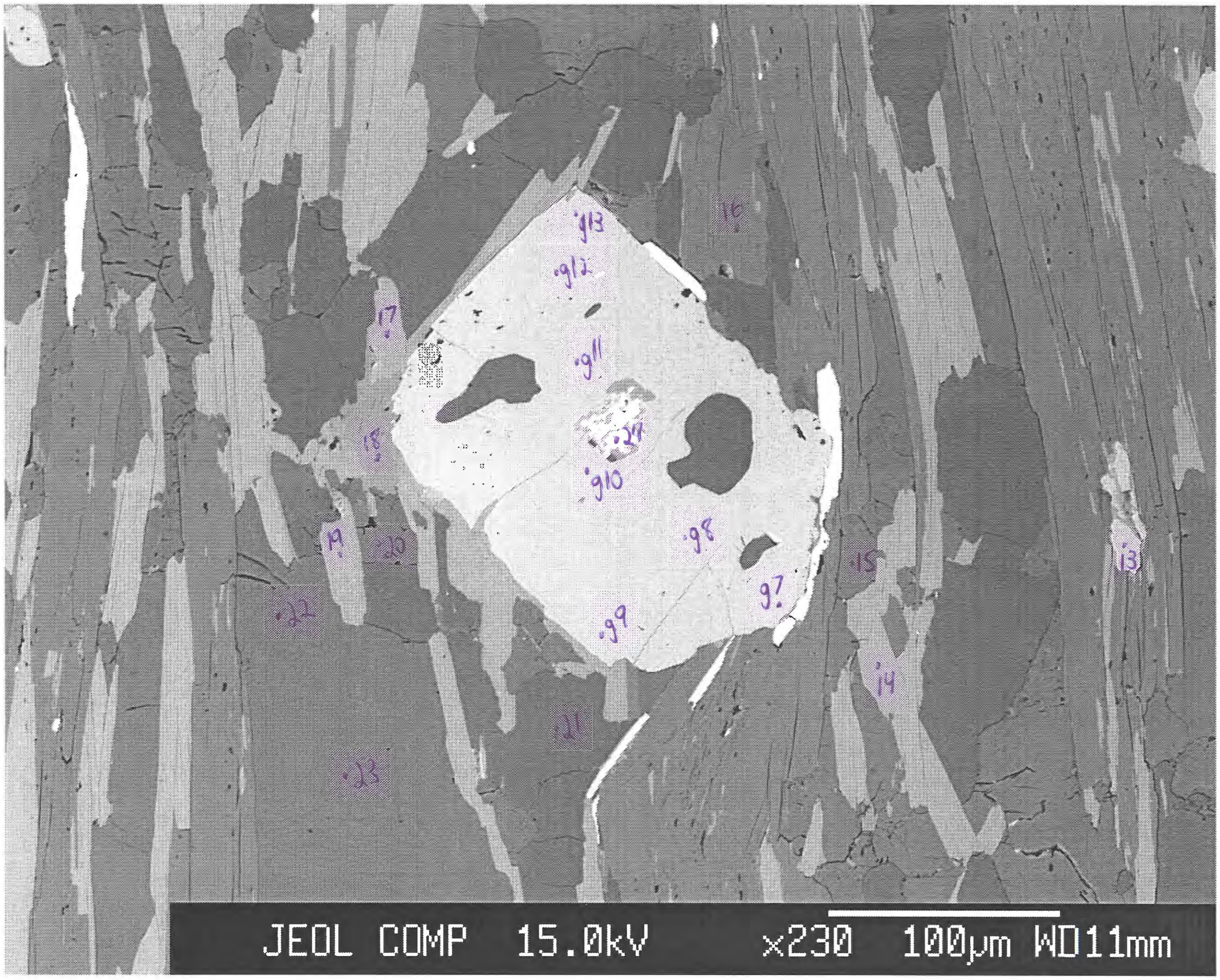

ritch53003

BH53 Image 3

-points g14-g19

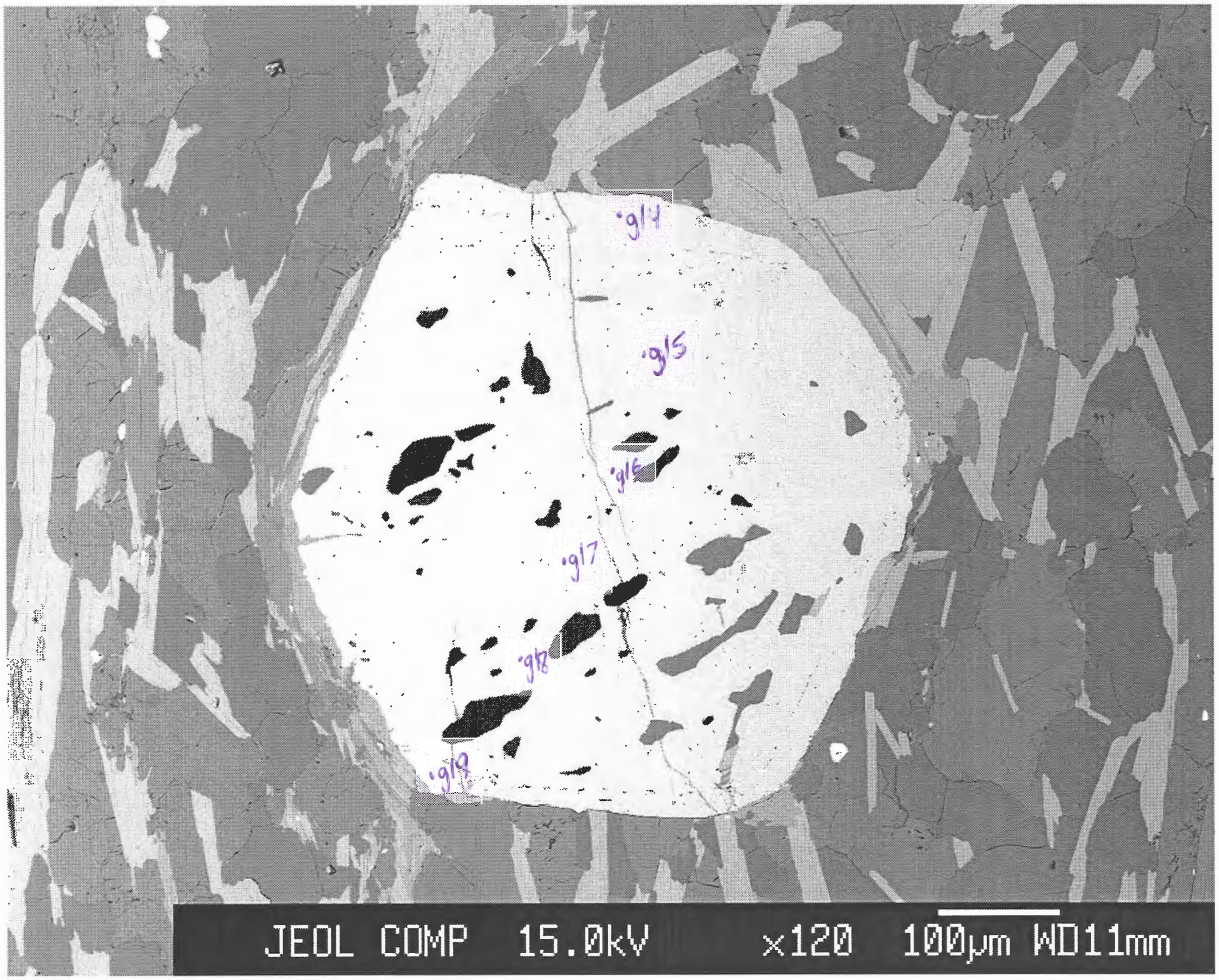

ritch53004

BH53 Image 4

-points 1-12

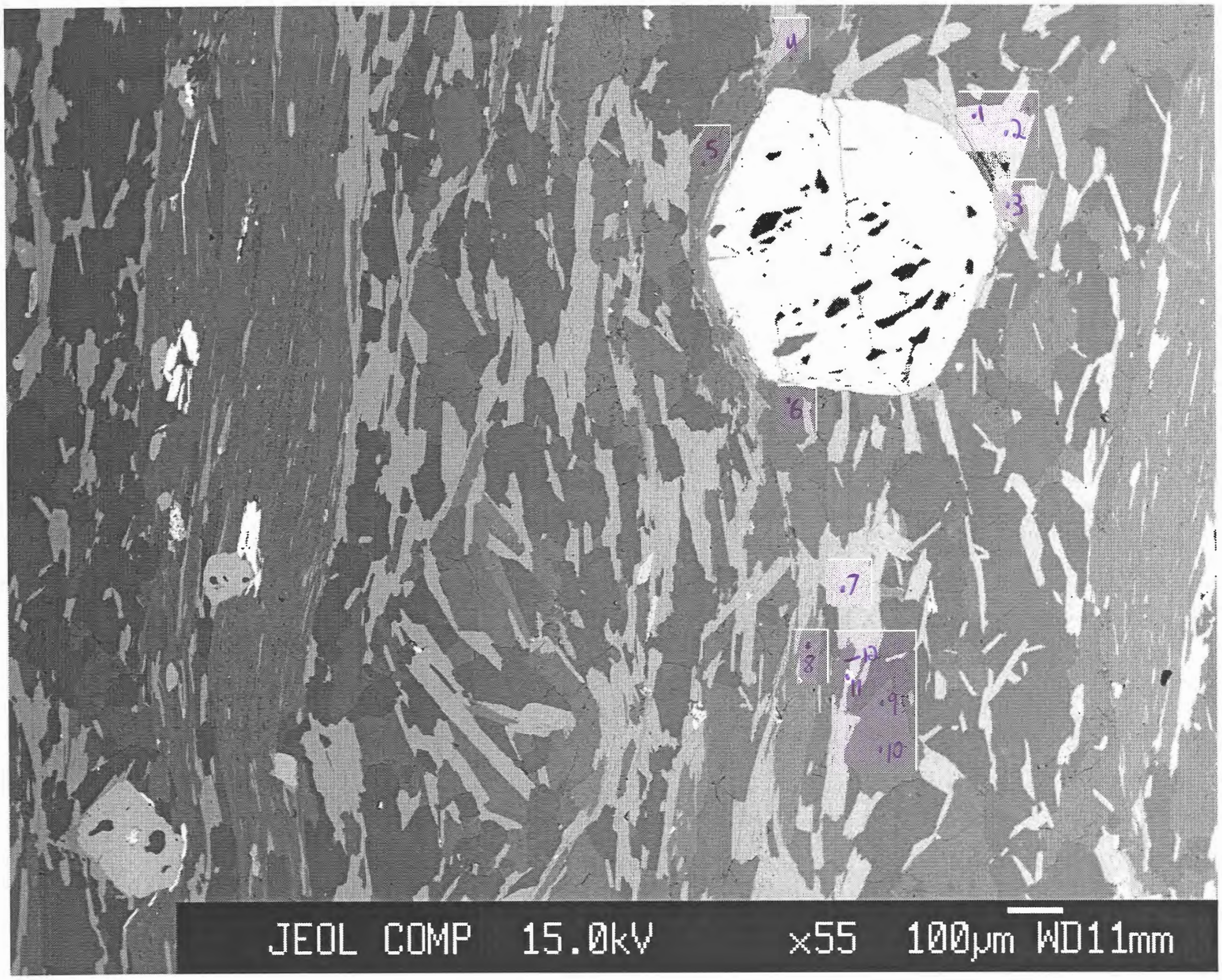

ritch53005

BH53 Image 5

-points 25-35

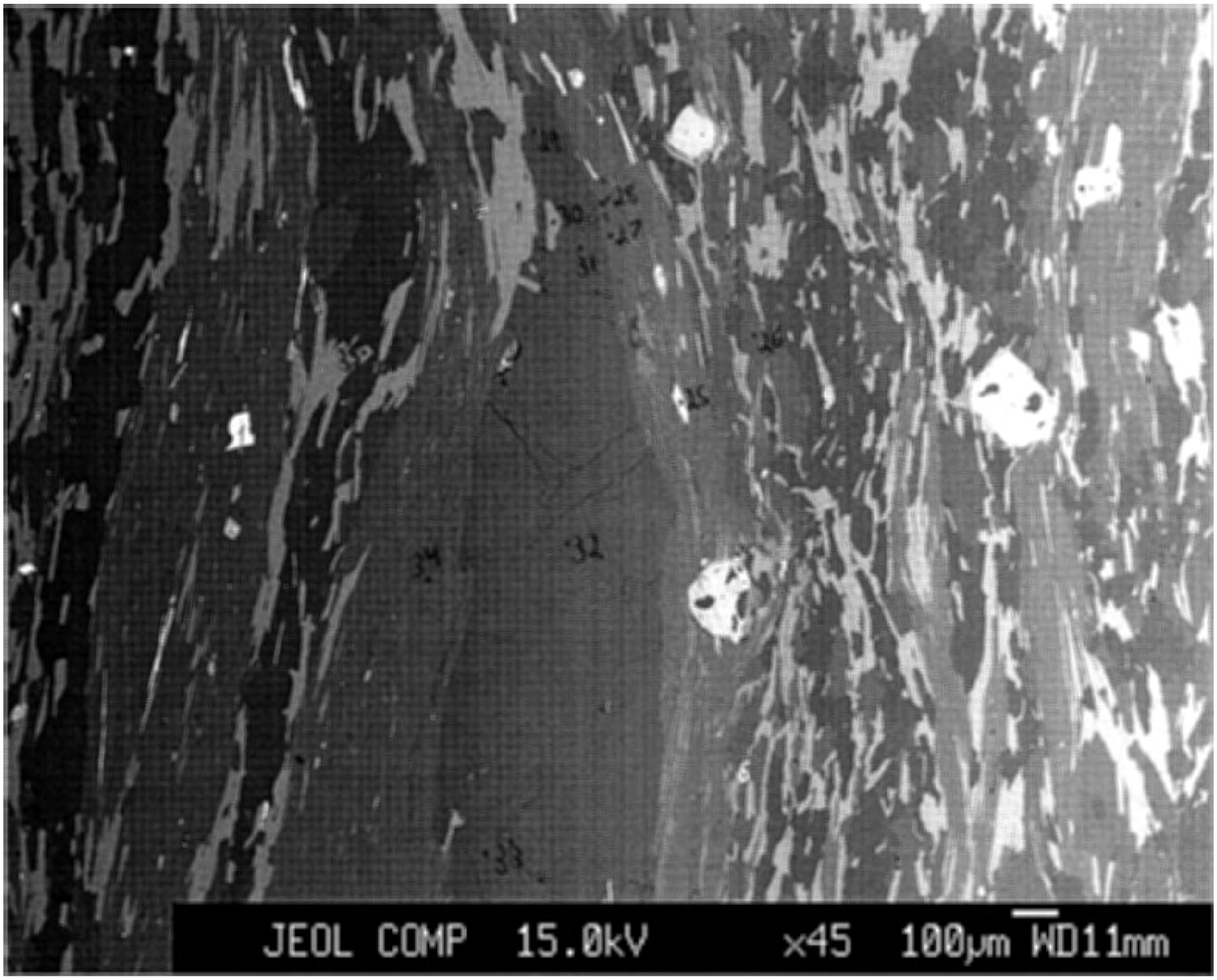

SAMPLE BH53

No.	616	617	606	607	612	619	622	624	635	640	648
Comment	bh53-11	bh53-12	bh53-1	bh53-2	bh53-7	bh53-14	bh53-17	bh53-19	bh53-30	bh53-35	bh53-43
Mineral	?	?	biotite	biotite	biotite	biotite	biotite	biotite	biotite	biotite	biotite
Weight % oxide:											
SiO2	35.9154	36.0242	37.1927	37.0292	36.7164	36.3478	36.489	36.6995	37.497	36.4825	37.1537
TiO2	0.1561	0.1363	1.774	1.8026	1.9613	1.5093	1.7459	1.3473	2.003	1.9794	1.809
Al2O3	24.8497	25.2068	18.8594	18.5981	19.0119	19.0044	18.8784	18.2736	18.7111	19.0345	18.5124
Cr2O3	0	0	0	0	0	0	0	0	0	0	0
FeO	7.249	7.0111	19.1593	18.5781	19.3319	19.6864	20.3281	20.6026	19.7082	19.2968	19.1348
MnO	0.2481	0.3077	0.1431	0.2016	0.1589	0.175	0.2328	0.1957	0.2066	0.0901	0.3653
MgO	0.2724	0.2583	10.6702	10.8216	10.3136	10.1098	10.123	10.9954	10.451	10.2516	9.8264
CaO	19.8057	20.0905	0	0	0	0.0631	0.0317	0.0797	0	0	0.0757
Na2O	0.0236	0.0249	0.138	0.1498	0.1383	0.0849	0.108	0.0983	0.1378	0.1216	0.1545
K2O	0.052	0.0618	9.4061	9.4842	9.5144	9.0461	9.0341	8.2984	9.1524	9.3955	9.6681
ZnO	0.3204	0.2695	0.1417	0.1119	0.0834	0.2153	0.2004	0.2639	0	0.0528	0.1981
Total	88.8925	89.3912	97.4845	96.7772	97.2301	96.2422	97.1715	96.8545	97.8671	96.7049	96.898
Number of cations per formula unit:											
Si	0.2491	0.2482	5.5022	5.5132	5.4604	5.4648	5.4494	5.4846	5.5264	5.4516	5.5506
Ti	0.0008	0.0007	0.198	0.2024	0.22	0.1716	0.1958	0.1518	0.2222	0.2222	0.2024
Al	0.2031	0.2047	3.289	3.2626	3.333	3.3682	3.322	3.2186	3.2494	3.3528	3.2604
Cr	0	0	0	0	0	0	0	0	0	0	0
Fe	0.042	0.0404	2.3716	2.3122	2.4046	2.475	2.5388	2.5762	2.4288	2.4112	2.3914
Mn	0.0015	0.0018	0.0176	0.0264	0.0198	0.022	0.0286	0.0242	0.0264	0.011	0.0462
Mg	0.0028	0.0027	2.354	2.4024	2.2858	2.266	2.2528	2.4508	2.2968	2.2836	2.189
Ca	0.1472	0.1483	0	0	0	0.011	0.0044	0.0132	0	0	0.0132
Na	0.0003	0.0003	0.0396	0.044	0.0396	0.0242	0.0308	0.0286	0.0396	0.0352	0.044
K	0.0005	0.0005	1.7754	1.8018	1.8062	1.7358	1.7204	1.5818	1.7204	1.7908	1.8436
Zn	0.0016	0.0014	0.0154	0.0132	0.0088	0.0242	0.022	0.0286	0	0.0066	0.022
Total	0.649	0.649	15.5628	15.5782	15.5782	15.565	15.565	15.5584	15.51	15.5672	15.5628

608	623	566	567	568	569	570	571	572	573	574	575
bh53-3	bh53-18	bh53-g1	bh53-g2	bh53-g3	bh53-g4	bh53-g5	bh53-g6	bh53-g7	bh53-g8	bh53-g9	bh53-g10
chlorite	chlorite	garnet	garnet	garnet	garnet	garnet	garnet	garnet	garnet	garnet	garnet
25.0299	25.5478	37.0959	36.9911	36.9315	37.083	36.9474	37.1826	36.8692	36.8995	37.1298	37.0087
0.112	0.0573	0.0657	0.1036	0.1696	0.1647	0.1595	0.1373	0.1133	0.1501	0.0893	0.0924
22.3686	22.5101	21.3191	21.2603	21.0759	21.1135	21.3144	21.292	21.3187	21.2503	21.3584	21.0224
0	0	0	0	0	0	0	0	0	0	0	0
22.6107	25.6331	29.9555	28.0821	27.1352	26.6222	28.229	29.8107	28.2652	29.0754	29.4021	29.0383
0.1843	0.4879	2.6993	4.4139	4.8626	6.09	3.8597	1.8986	4.8968	4.4415	2.27	3.5626
15.7361	15.1921	2.0215	1.7688	1.7402	1.552	1.8188	2.1702	1.7588	1.6773	1.9419	1.8307
0	0.047	7.5177	8.3707	8.814	8.3629	8.2656	7.5432	7.0367	7.9432	7.9562	7.4053
0	0	0.0228	0.015	0.0159	0.0159	0.0127	0.0232	0.0242	0.0229	0.0318	0.0269
0	0.0222	0	0	0	0	0	0	0	0	0	0
0.0521	0.1458	0	0.0383	0.0008	0.0099	0	0	0	0	0.0153	0
86.0938	89.6433	100.6974	101.0437	100.7457	101.0141	100.607	100.0577	100.2828	101.4602	100.1947	99.9874
5.2948	5.2724	5.919	5.895	5.8993	5.915	5.9007	5.9454	5.9159	5.8762	5.9356	5.9484
0.0168	0.0084	0.0079	0.0124	0.0204	0.0198	0.0192	0.0165	0.0137	0.018	0.0107	0.0112
5.5776	5.4768	4.0095	3.9935	3.9682	3.9695	4.0123	4.0129	4.032	3.9888	4.0245	3.9828
0	0	0	0	0	0	0	0	0	0	0	0
4.0012	4.424	3.9974	3.7427	3.625	3.5514	3.7704	3.9865	3.793	3.8723	3.9309	3.9034
0.0336	0.084	0.3648	0.5958	0.6579	0.8228	0.5221	0.2572	0.6656	0.5991	0.3074	0.485
4.9644	4.6732	0.4808	0.4202	0.4144	0.369	0.433	0.5173	0.4207	0.3982	0.4627	0.4386
0	0.0112	1.2853	1.4294	1.5086	1.4293	1.4144	1.2924	1.2098	1.3554	1.3628	1.2754
0	0	0.0071	0.0046	0.0049	0.0049	0.0039	0.0072	0.0075	0.0071	0.0099	0.0084
0	0.0056	0	0	0	0	0	0	0	0	0	0
0.0084	0.0224	0	0.0045	0.0001	0.0012	0	0	0	0	0.0018	0
19.8968	19.9808	16.0718	16.0981	16.0988	16.083	16.076	16.0354	16.0583	16.1152	16.0463	16.0532

576	577	578	579	580	581	582	583	584	618	630	646
bh53-g11	bh53-g12	bh53-g13	bh53-g14	bh53-g15	bh53-g16	bh53-g17	bh53-g18	bh53-g19	bh53-13	bh53-25	bh53-41
garnet	garnet	garnet	garnet	garnet	garnet	garnet	garnet	garnet	garnet	ilmenite	ilmenite
36.8927	36.7642	36.8049	36.999	36.8054	36.724	36.9398	36.9154	37.114	38.4403	0	0
0.0379	0.0212	0.0413	0.0112	0.1035	0.1488	0.1548	0.0812	0.0223	0.1679	54.1066	54.0346
21.122	21.1832	20.9461	21.2047	20.9602	20.9266	20.914	21.1807	21.1892	21.923	0	0
0	0	0	0	0	0	0	0	0	0	0	0
28.6231	28.3958	27.708	28.2629	27.2241	26.1123	25.0888	26.2381	28.8612	29.2494	45.0473	44.9487
3.0768	2.6705	2.8934	2.6173	5.3458	7.1182	6.8351	6.1214	2.6528	3.556	2.7314	2.8989
1.9426	2.2045	2.1396	2.0611	1.4626	1.2656	1.2693	1.4321	2.1396	1.9987	0.0603	0
7.7609	7.714	7.7761	8.3296	8.0843	7.9853	8.4249	7.9716	7.8788	7.7699	0.087	0.0837
0.0345	0.0403	0.0257	0.019	0.031	0.0324	0.0145	0.0195	0.0286	0	0	0.0123
0	0	0	0	0	0	0	0	0	0.1059	0.1163	0.0585
0.0268	0.0253	0.0092	0.0092	0.0375	0.0145	0.0452	0.0253	0.0514	0.2239	0.5392	0.4879
99.5174	99.0191	98.3444	99.5141	100.0544	100.3277	99.6865	99.9854	99.938	103.435	102.688	102.5246
5.9426	5.9364	5.9731	5.9443	5.9275	5.9143	5.9569	5.9364	5.9459	5.9568	0	0
0.0046	0.0026	0.005	0.0014	0.0125	0.018	0.0188	0.0098	0.0027	0.0192	2.001	2.0016
4.0103	4.0317	4.0068	4.0156	3.9789	3.9724	3.9753	4.0147	4.0013	4.0032	0	0
0	0	0	0	0	0	0	0	0	0	0	0
3.8559	3.8347	3.7607	3.7975	3.6668	3.517	3.3836	3.5288	3.867	3.7896	1.8522	1.8516
0.4198	0.3653	0.3978	0.3562	0.7293	0.971	0.9336	0.8338	0.36	0.4656	0.114	0.1212
0.4665	0.5306	0.5176	0.4936	0.3511	0.3038	0.3051	0.3433	0.511	0.4608	0.0042	0
1.3395	1.3347	1.3522	1.4339	1.3951	1.378	1.4557	1.3736	1.3525	1.2888	0.0048	0.0042
0.0108	0.0126	0.0081	0.0059	0.0097	0.0101	0.0045	0.0061	0.0089	0	0	0.0012
0	0	0	0	0	0	0	0	0	0.0216	0.0072	0.0036
0.0032	0.003	0.0011	0.0011	0.0045	0.0017	0.0054	0.003	0.0061	0.0264	0.0198	0.018
16.0533	16.0516	16.0224	16.0496	16.0754	16.0863	16.0389	16.0495	16.0555	16.032	4.0038	4.0014

609	613	621	632	639	643	645	649	610	611	614	615
bh53-4	bh53-8	bh53-16	bh53-27	bh53-34	bh53-38	bh53-40	bh53-44	bh53-5	bh53-6	bh53-9	bh53-10
muscovite	muscovite	muscovite	muscovite	muscovite	muscovite	muscovite	muscovite	plagioclase	plagioclase	plagioclase	plagioclase
48.13	48.6845	48.7731	48.2896	48.3126	48.3881	47.6863	48.8477	63.3805	63.247	63.1405	64.4552
0.6392	0.6226	0.5362	0.4882	0.4043	0.5434	0.7628	0.7225	0.0082	0	0.0012	0.0152
33.7157	33.9642	34.1771	34.3591	34.6968	33.3766	33.1601	32.8289	23.732	23.7679	23.8345	23.691
0	0	0	0	0	0	0	0	0	0	0	0
1.6204	1.5561	1.6894	1.4975	1.3916	1.4182	2.1391	1.7938	0.1548	0.1707	0	0.0907
0	0	0.054	0.0216	0	0	0	0.0108	0	0	0	0
1.1569	1.1118	1.0568	1.032	1.0041	1.2506	1.4785	1.354	0	0	0	0
0	0	0	0.0119	0	0	0	0	4.3766	4.4708	4.5537	5.1495
0.7805	0.6976	0.6603	0.7324	0.7254	0.6976	0.6363	0.6292	8.7466	8.6842	8.6163	8.7609
10.1748	10.1821	9.9246	9.9307	10.096	10.0795	9.4847	10.3087	0	0	0	0.1255
0	0	0.0093	0.0591	0	0	0.0148	0.0109	0	0	0	0.0313
96.2175	96.819	96.8809	96.4221	96.6309	95.7541	95.3626	96.5065	100.3987	100.3406	100.1461	102.3193
6.3338	6.358	6.358	6.325	6.3118	6.3844	6.3272	6.413	11.1424	11.1296	11.1232	11.1488
0.0638	0.0616	0.0528	0.0484	0.0396	0.055	0.077	0.0704	0	0	0	0.0032
5.2294	5.2272	5.2514	5.3042	5.3438	5.1898	5.1854	5.082	4.9184	4.928	4.9504	4.8288
0	0	0	0	0	0	0	0	0	0	0	0
0.1782	0.1694	0.1848	0.165	0.1518	0.1562	0.2376	0.198	0.0224	0.0256	0	0.0128
0	0	0.0066	0.0022	0	0	0	0.0022	0	0	0	0
0.2266	0.2156	0.2046	0.2024	0.1958	0.2464	0.2926	0.264	0	0	0	0
0	0	0	0.0022	0	0	0	0	0.8256	0.8416	0.8608	0.9536
0.2002	0.176	0.1672	0.187	0.1848	0.1782	0.1628	0.1606	2.9824	2.9632	2.944	2.9376
1.7094	1.6962	1.65	1.6588	1.683	1.6962	1.606	1.727	0	0	0	0.0288
0	0	0	0.0066	0	0	0.0022	0	0	0	0	0.0032
13.9436	13.9062	13.8776	13.9018	13.9128	13.9062	13.893	13.9194	19.8912	19.8912	19.8816	19.9168

620	625	627	628	631	634	636	637	638	642	647	626
bh53-15	bh53-20	bh53-22	bh53-23	bh53-26	bh53-29	bh53-31	bh53-32	bh53-33	bh53-37	bh53-42	bh53-21
plagioclase	plagioclase	plagioclase	plagioclase	plagioclase	plagioclase	plagioclase	plagioclase	plagioclase	plagioclase	plagioclase	quartz
63.2177	62.9547	63.006	62.1874	62.8925	62.728	62.7202	62.1075	62.8787	63.1695	63.316	98.992
0.0316	0	0.0129	0	0.0175	0.0129	0	0	0	0	0.007	0.0023
23.546	23.8307	23.5724	23.9527	23.8712	23.7574	24.0708	24.2916	23.7199	23.5866	23.1456	0
0	0	0	0	0	0	0	0	0	0	0	0
0.2081	0.2667	0.2187	0.24	0.1813	0.2294	0	0	0	0.0747	0	0.2041
0.0217	0.0379	0.1083	0.0271	0.0108	0	0	0	0	0	0.0054	0.0164
0	0.0071	0	0	0	0.0007	0	0.0028	0	0	0	0.0053
5.0494	5.4744	5.2257	5.6999	5.087	5.3882	5.4133	5.6826	5.2701	5.0883	4.9087	0
8.9314	8.4301	8.6119	8.2952	8.6545	8.4412	8.3516	8.2685	8.4669	8.5522	8.6986	0
0.1159	0.0807	0.1219	0.1187	0.097	0.1188	0	0	0	0	0.0693	0.0026
0	0	0	0.0524	0.0438	0	0	0	0	0	0	0.0244
101.1217	101.0823	100.8777	100.5733	100.8556	100.6766	100.5558	100.3529	100.3355	100.4712	100.1505	99.2472
11.088	11.0432	11.0784	10.9824	11.0496	11.0464	11.0336	10.9632	11.0816	11.1168	11.1744	0.999
0.0032	0	0.0032	0	0.0032	0.0032	0	0	0	0	0	0
4.8672	4.928	4.8864	4.9856	4.944	4.9312	4.992	5.056	4.928	4.8928	4.816	0
0	0	0	0	0	0	0	0	0	0	0	0
0.032	0.0384	0.032	0.0352	0.0256	0.0352	0	0	0	0.0096	0	0.0018
0.0032	0.0064	0.016	0.0032	0.0032	0	0	0	0	0	0	0.0002
0	0.0032	0	0	0	0	0	0	0	0	0	0
0.9504	1.0304	0.9856	1.0784	0.9568	1.0176	1.0208	1.0752	0.9952	0.96	0.928	0
3.0368	2.8672	2.9344	2.8416	2.9472	2.8832	2.848	2.8288	2.8928	2.9184	2.976	0
0.0256	0.0192	0.0288	0.0256	0.0224	0.0256	0	0	0	0	0.016	0
0	0	0	0.0064	0.0064	0	0	0	0	0	0	0.0002
20.0064	19.936	19.9648	19.9616	19.9616	19.9456	19.8944	19.9232	19.8976	19.8976	19.9136	1.0014

633	641	629	644	650
bh53-28	bh53-36	bh53-24	bh53-39	bh53-45
quartz	quartz	sheet silicate		
99.195	99.0486	31.3903	30.7085	36.4712
0	0	0.1885	1.1543	1.0278
0.0632	0	18.9301	16.0007	30.8391
0	0	0	0	0
0.1773	0.0376	10.9454	10.9611	8.4474
0	0	0.6788	0.048	0
0.024	0.0166	0.4099	9.1215	6.6082
0.0022	0	15.486	0	0.882
0	0	0.0381	0.12	2.1696
0.0265	0	0.045	6.7838	0.0057
0.0189	0	0.4381	0	0.0333
99.5071	99.1029	78.5503	74.898	86.4844
0.9984	0.9998	0.2534	0.2587	0.2448
0	0	0.0011	0.0073	0.0052
0.0008	0	0.1802	0.1589	0.244
0	0	0	0	0
0.0014	0.0004	0.0739	0.0772	0.0474
0	0	0.0046	0.0003	0
0.0004	0.0002	0.0049	0.1146	0.0661
0	0	0.134	0	0.0063
0	0	0.0006	0.002	0.0282
0.0004	0	0.0005	0.0729	0
0.0002	0	0.0026	0	0.0002
1.0016	1.0006	0.6558	0.6919	0.6422

DGB294B001

BH294 Image 1

-points 49-89

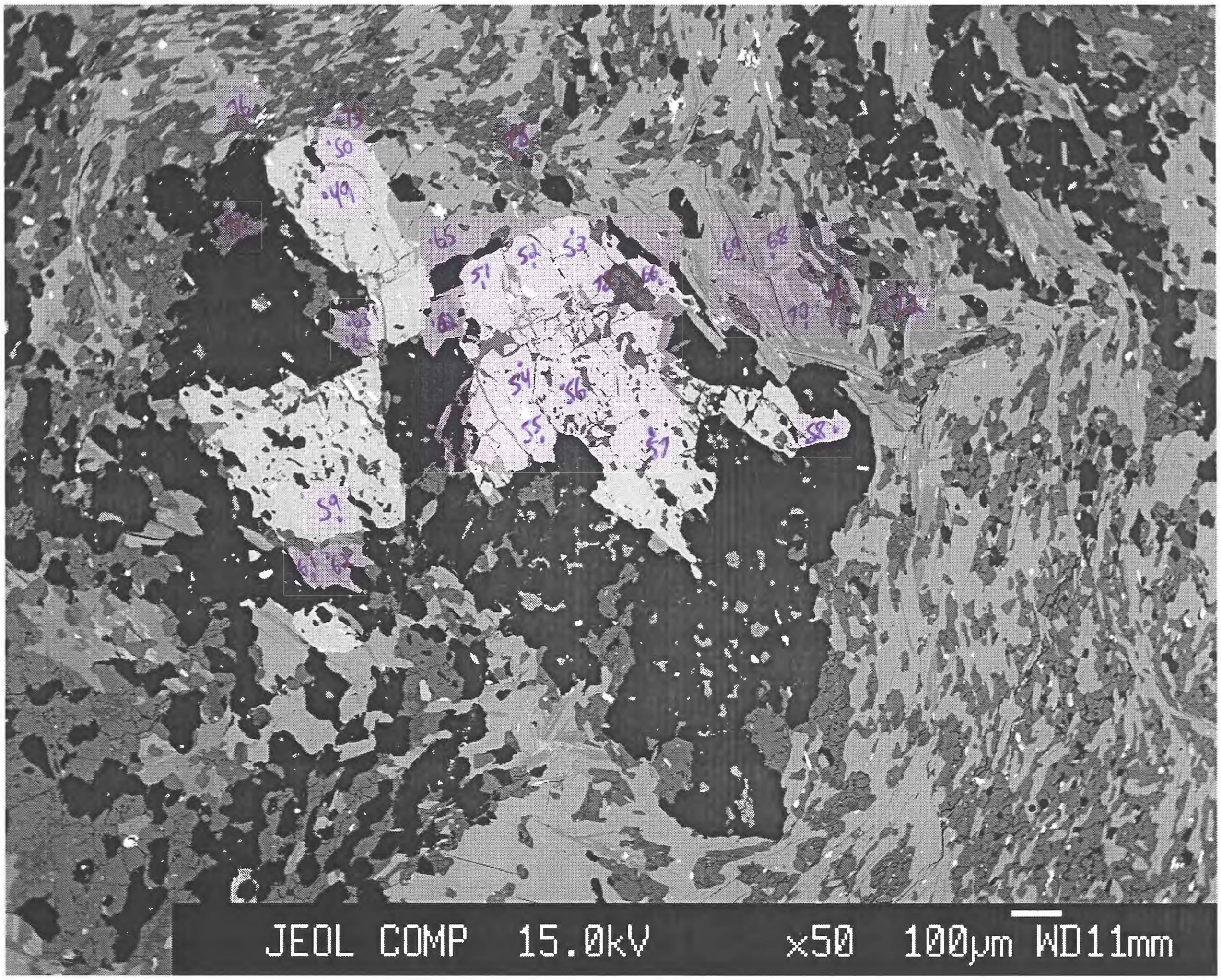

B294a001

BH294 Image 2

-points 7-13

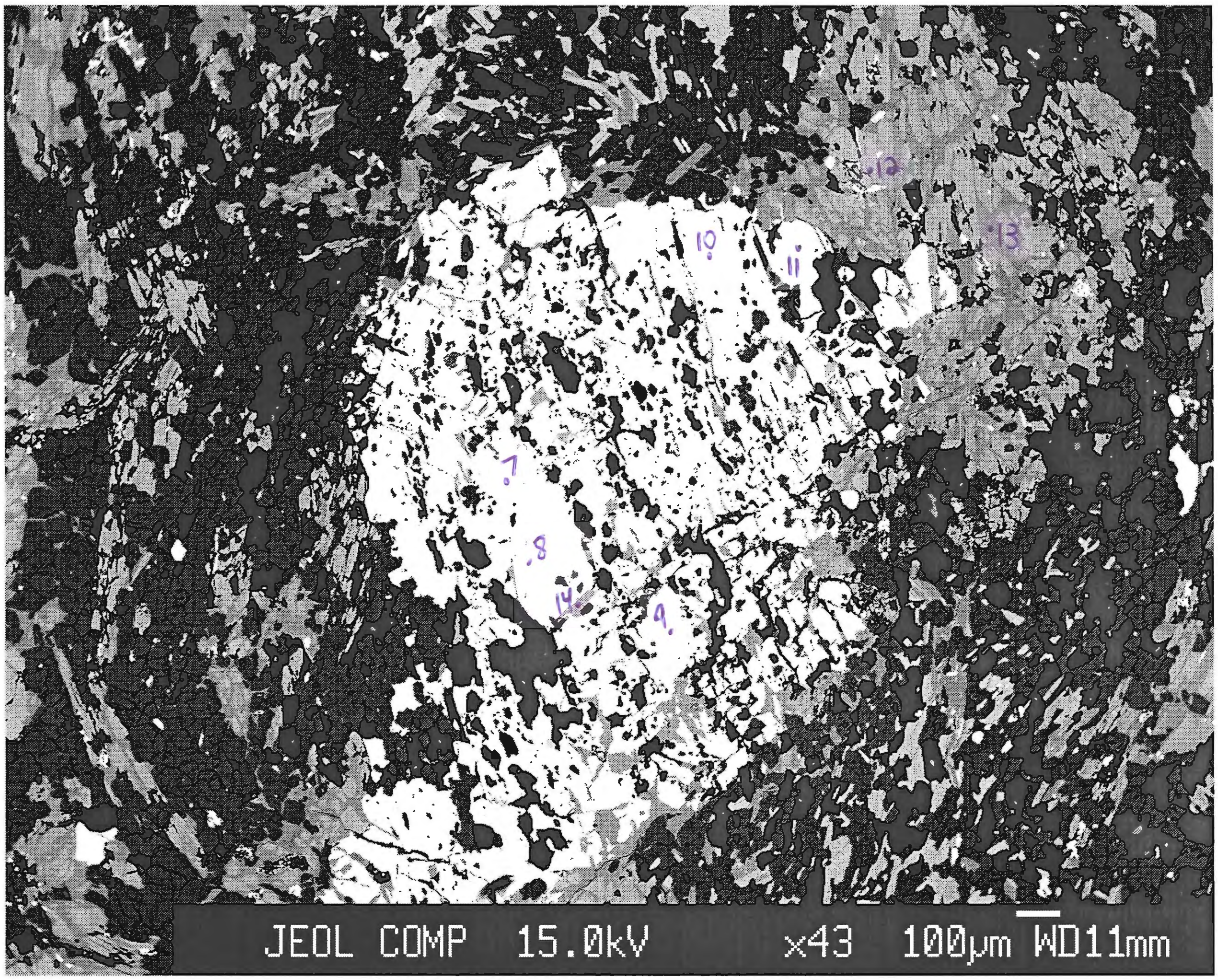

DGB294B002

BH294 Image 3

-points 80-90

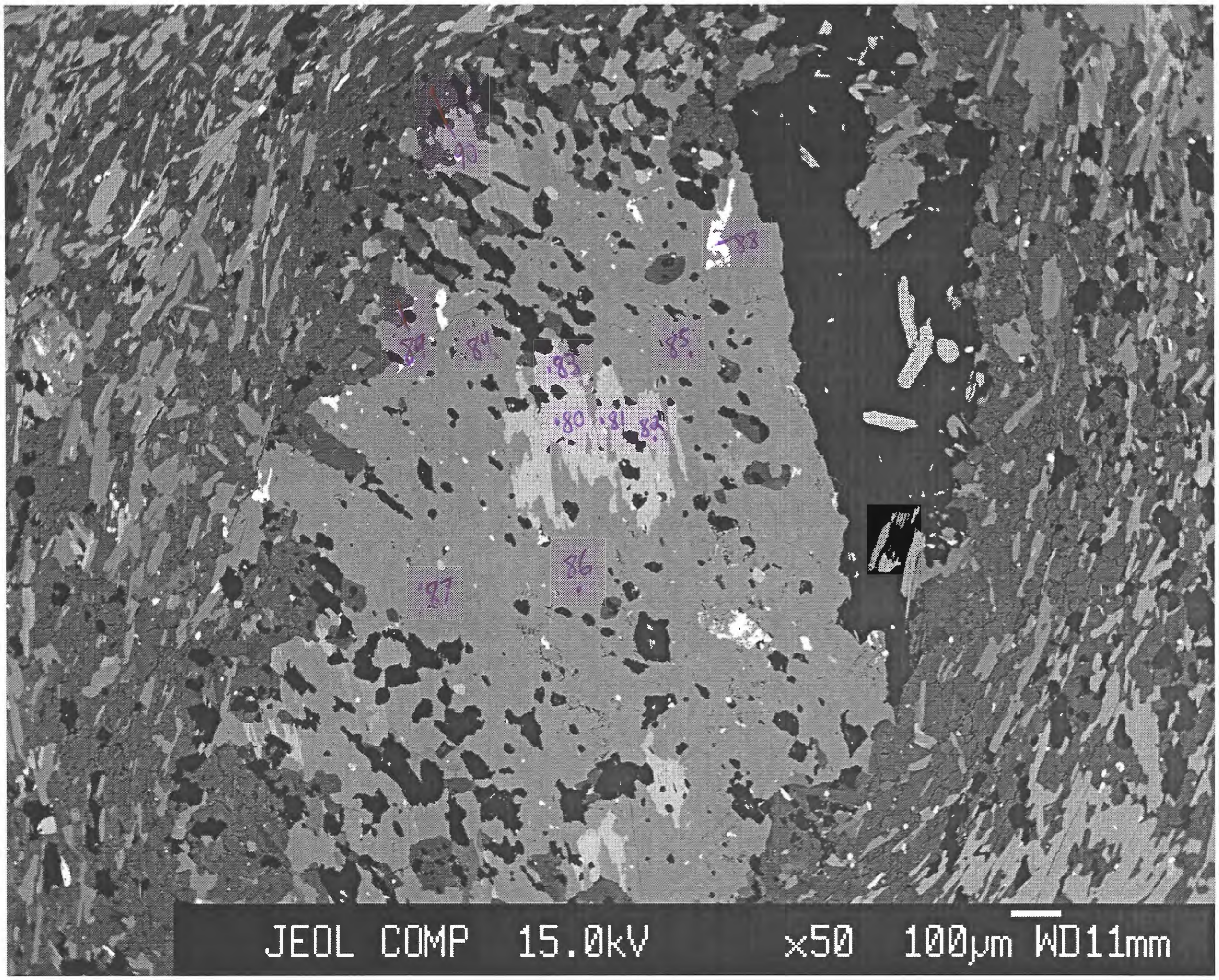

DGBCH001

BH294 Image 4

-points 34-49

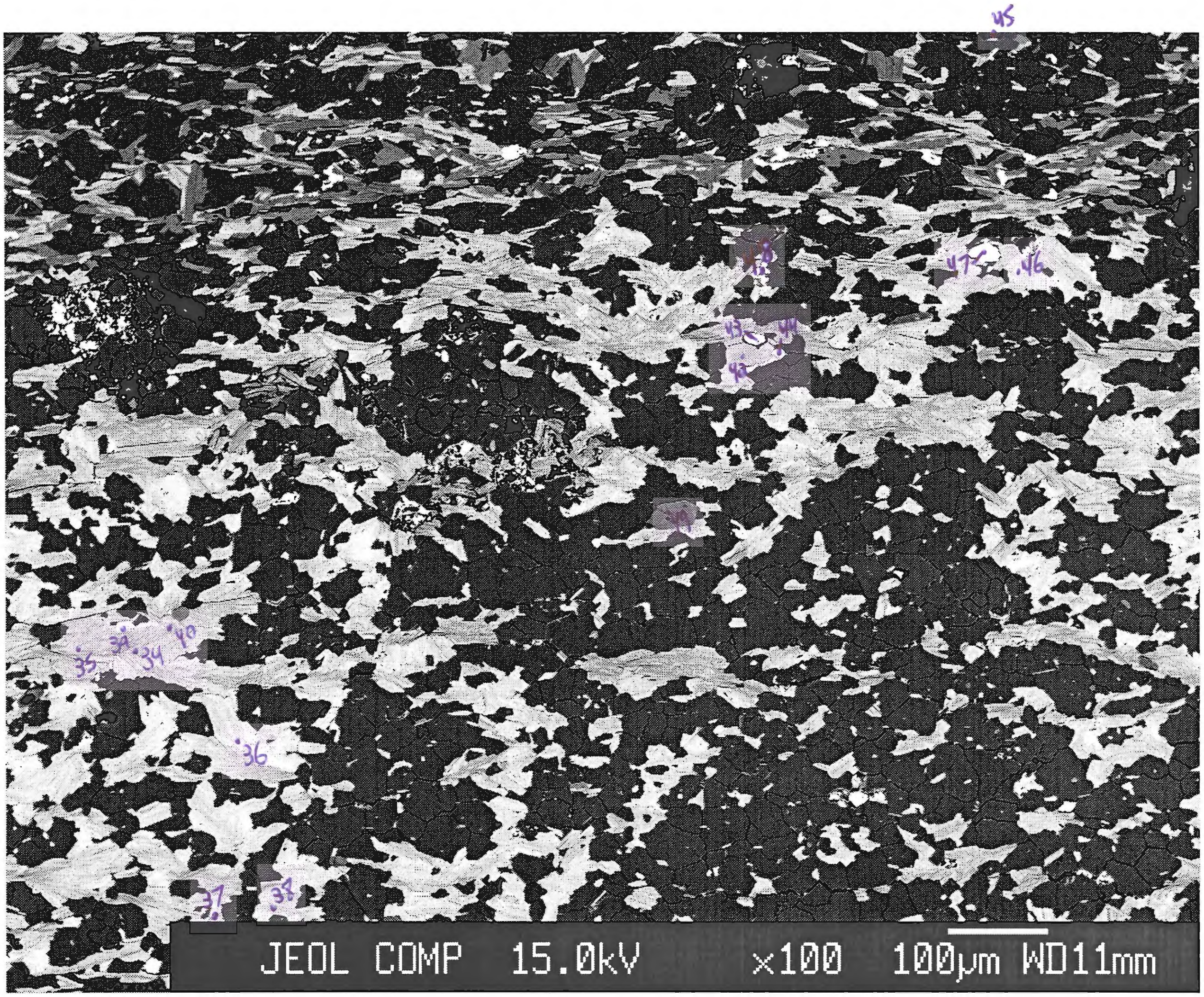

DGBCH002

BH294 Image 5

-points 24-33

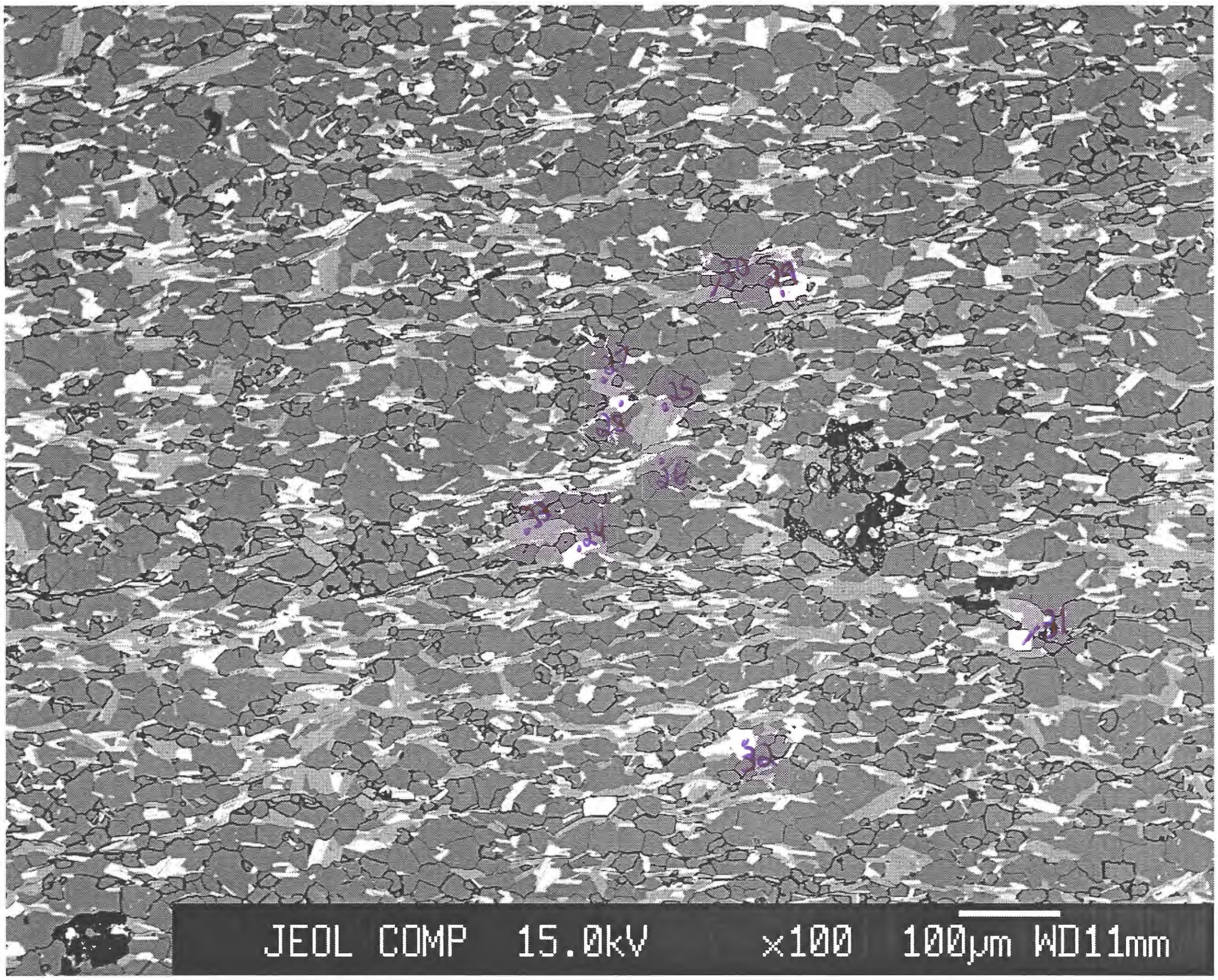

No.	31	43	45	47	21	34	36	37	39	41	42
Comment	BCH matrix	BCH matrix	BCH matrix	BCH matrix	B294A-14	BCH matrix	BCH matrix	BCH matrix	BCH matrix	BCH matrix	BCH matrix
Mineral	apatite	apatite	apatite	apatite	biotite	biotite	biotite	biotite	biotite	biotite	biotite
Weight % oxide:											
SiO2	0.094	0.078	0.0972	0.0933	35.6123	36.4933	35.5944	35.8752	35.6368	36.6456	37.3763
TiO2	0	0	0	0	2.8817	1.8186	1.9168	1.7937	1.8304	1.9664	1.9
Al2O3	0	0	0	0	15.1282	18.2019	16.6575	17.6124	17.1872	16.9951	17.3295
Cr2O3	0.0101	0.0252	0.0036	0.0195	0.0879	0	0	0	0.0218	0.004	0.024
FeO	0.322	0.4903	0.5664	0.5176	21.4052	19.9124	20.9951	21.1918	22.5798	20.5664	18.7825
MnO	0.0167	0.0666	0.0999	0.0444	0.1863	0.1727	0.0916	0.0754	0.0861	0.0754	0
MgO	0.0269	0.0233	0.0133	0.0266	10.3645	7.7853	8.1992	7.9854	8.4281	8.1299	8.1759
CaO	53.5206	53.9558	52.8847	53.4177	0.1171	0.0368	0.0123	0.057	0.0224	0.0745	0.1206
Na2O	0.0076	0.0151	0.0379	0.0395	0.0789	0.0228	0.0421	0.0172	0.0254	0.0134	0.0178
K2O	0	0	0	0	9.1528	6.8776	7.716	7.5601	8.4869	7.0759	7.0899
NiO	0.0354	0.02	0.0169	0.0467	0.1001	0	0.0282	0.0051	0.0358	0.02	0
CuO	0.0211	0.0204	0.0313	0.023	0	0	0	0	0.0032	0	0
ZnO	0.9828	1.0254	1.0581	0.9135	0	0.3546	0.4167	0.3678	0.2069	0.4144	0.3242
P2O5	37.808	37.176	37.5647	37.7372	0	0.0179	0	0.0223	0	0.0201	0
Total	92.8453	92.8961	92.3741	92.8791	95.1151	91.6939	91.67	92.5634	94.5508	92.0012	91.1408
Cations per formula unit:											
Si	0.0182	0.0156	0.0182	0.0182	5.5154	5.6914	5.6474	5.6166	5.5374	5.731	5.8278
Ti	0	0	0	0	0.3366	0.2134	0.2288	0.2112	0.2134	0.231	0.2222
Al	0	0	0	0	2.761	3.3462	3.1152	3.2516	3.1482	3.1328	3.1856
Cr	0.0026	0.0026	0	0.0026	0.011	0	0	0	0.0022	0	0.0022
Fe	0.0494	0.078	0.0884	0.0806	2.772	2.5982	2.7852	2.7742	2.9348	2.6906	2.4486
Mn	0.0026	0.0104	0.0156	0.0078	0.0242	0.022	0.0132	0.011	0.011	0.011	0
Mg	0.0078	0.0078	0.0026	0.0078	2.3936	1.8106	1.9382	1.8634	1.9514	1.8964	1.9008
Ca	10.751	10.894	10.6912	10.738	0.0198	0.0066	0.0022	0.0088	0.0044	0.0132	0.0198
Na	0.0026	0.0052	0.013	0.0156	0.0242	0.0066	0.0132	0.0044	0.0066	0.0044	0.0044
K	0	0	0	0	1.8084	1.3684	1.562	1.5092	1.683	1.4124	1.4102
Ni	0.0052	0.0026	0.0026	0.0078	0.0132	0	0.0044	0	0.0044	0.0022	0
Cu	0.0026	0.0026	0.0052	0.0026	0	0	0	0	0	0	0
Zn	0.1352	0.143	0.1482	0.1274	0	0.0418	0.0484	0.0418	0.0242	0.0484	0.0374
P	6.0008	5.9306	6.0008	5.993	0	0.0022	0	0.0022	0	0.0022	0
Total	16.9806	17.0924	16.9858	17.0014	15.6794	15.1096	15.3582	15.2966	15.521	15.1778	15.059

44	46	60	61	62	63	65	68	75	13	14	17
BCH matrix	BCH matrix	B294bMica	B294bMica	B294bMica	B294bMica	B294bMica	B294bMica	B294bFsp	B294A-7	B294A-8	B294A-10
biotite	biotite	biotite	biotite	biotite	biotite	biotite	biotite	biotite	chlorite	chlorite	chlorite
35.9864	36.8523	35.6556	35.555	35.5694	35.2287	35.5977	35.9037	35.3986	25.6243	25.5787	25.0287
1.8084	1.9005	2.0071	1.9098	2.0655	1.9344	2.3639	2.1631	2.5807	0	0.0831	0.057
17.8088	16.0034	17.5104	16.6799	16.5997	16.832	16.9168	16.5729	17.6489	19.4427	20.0514	20.5298
0.0119	0.0013	0.012	0	0.0221	0.0127	0.0127	0	0.0827	0.0006	0	0.0202
22.0201	21.2003	19.2858	19.6238	19.6092	19.9884	19.9656	19.9972	20.4507	28.0077	29.8809	28.2535
0.0592	0.0215	0.2485	0.2916	0.2646	0.2321	0.2322	0.1674	0.2589	0.6142	0.6312	0.5767
8.0163	8.6008	9.0628	9.6735	9.7394	9.3556	9.4321	9.9364	8.6508	13.7236	12.2667	13.5467
0.0565	0.032	0	0.0005	0	0	0	0.0086	0.5785	0.0363	0.0387	0.0961
0.0271	0.0587	0.1029	0.066	0.0702	0.0637	0.0708	0.1034	0.267	0.0105	0.0151	0
8.5957	8.0528	9.1844	9.1736	9.3604	9.1929	9.1509	8.9703	8.085	0	0	0.0439
0.0266	0.022	0	0.0103	0	0.0097	0	0	0.0251	0	0	0.0601
0	0	0	0	0	0	0	0	0.0146	0	0	0
0.2093	0.3002	0.0886	0	0	0	0	0	0	0	0	0
0.0133	0	0	0	0	0	0	0	0	0	0	0
94.6397	93.0459	93.1581	92.9841	93.3006	92.8503	93.7427	93.8231	94.0416	87.46	88.5458	88.2127
5.5594	5.7552	5.5572	5.5682	5.5572	5.5374	5.533	5.5682	5.4736	5.516	5.4852	5.3508
0.2112	0.2222	0.2354	0.2244	0.242	0.2288	0.2772	0.253	0.2992	0	0.014	0.0084
3.2428	2.9458	3.2164	3.08	3.058	3.1196	3.0998	3.0294	3.2164	4.9336	5.068	5.1744
0.0022	0	0.0022	0	0.0022	0.0022	0.0022	0	0.011	0	0	0.0028
2.8446	2.7676	2.5124	2.5696	2.563	2.629	2.596	2.5938	2.6444	5.0428	5.3564	5.0512
0.0088	0.0022	0.033	0.0396	0.0352	0.0308	0.0308	0.022	0.033	0.112	0.1148	0.1036
1.8458	2.002	2.1054	2.2594	2.2682	2.1934	2.1846	2.2968	1.9932	4.4044	3.92	4.3176
0.0088	0.0044	0	0	0	0	0	0.0022	0.0968	0.0084	0.0084	0.0224
0.0088	0.0176	0.0308	0.0198	0.022	0.0198	0.022	0.0308	0.0792	0.0056	0.0056	0
1.694	1.6038	1.826	1.8326	1.8656	1.8436	1.815	1.7754	1.595	0	0	0.0112
0.0044	0.0022	0	0.0022	0	0.0022	0	0	0.0022	0	0	0.0112
0	0	0	0	0	0	0	0	0.0022	0	0	0
0.0242	0.0352	0.011	0	0	0	0	0	0	0	0	0
0.0022	0	0	0	0	0	0	0	0	0	0	0
15.4594	15.3604	15.532	15.5958	15.6156	15.609	15.5628	15.5716	15.4484	20.0228	19.9724	20.0564

18	20	24	29	32	64	69	70	84	85	86	87
B294A-11 chlorite	B294A-13 chlorite	BCH matrix chlorite	BCH matrix chlorite	BCH matrix chlorite	B294bMica chlorite	B294bMica chlorite	B294bMica chlorite	94bbigmica chlorite	94bbigmica chlorite	94bbigmica chlorite	94bbigmica chlorite
25.4763	25.2886	22.9889	24.788	23.5805	25.6382	26.6066	25.1338	24.6803	24.5881	24.7331	24.7045
0.1568	0.1321	0.2026	0.0631	0.057	0.0705	0.2849	0.0561	0.002	0.0105	0	0
20.0745	20.2397	22.7926	19.8455	21.6974	20.6016	20.2092	20.7166	20.274	20.5476	20.3342	20.6233
0.0363	0.0326	0.0263	0.0158	0.0119	0.0019	0	0.0057	0.0032	0.0019	0	0
26.3345	26.4078	31.6528	28.9794	30.3041	26.8678	26.5408	25.9059	27.4	27.6309	25.8429	26.9489
0.4623	0.5405	0.3082	0.2986	0.2076	0.4915	0.3104	0.4815	0.3256	0.3574	0.3047	0.2669
13.677	14.0431	10.8549	12.3325	11.1447	12.1494	13.1379	13.2275	13.3719	13.6181	13.6272	13.602
0.0855	0.0686	0.0021	0.0062	0	0.0333	0.2536	0	0.0583	0.0036	0	0
0	0	0	0	0.0004	0.0169	0.0126	0.0031	0.0451	0.0158	0.0232	0.0226
0.289	0.0324	0	0	0	0	0	0	0	0	0	0
0.0462	0.0461	0.0387	0.0118	0.0133	0	0	0	0	0.0036	0	0
0	0	0	0	0	0	0	0	0	0	0	0
0	0	0.3029	0.2111	0.2849	0	0	0.0489	0	0	0	0
0	0	0.0022	0.0045	0	0	0	0	0	0	0	0
86.6385	86.8316	89.1722	86.5566	87.3018	85.8712	87.3561	85.5791	86.1604	86.7776	84.8654	86.1683
5.4936	5.4376	4.9588	5.4292	5.1604	5.572	5.656	5.4628	5.3788	5.3256	5.4264	5.3648
0.0252	0.0224	0.0336	0.0112	0.0084	0.0112	0.0448	0.0084	0	0.0028	0	0
5.1016	5.1296	5.796	5.124	5.5944	5.2752	5.0652	5.3088	5.208	5.2472	5.2584	5.278
0.0056	0.0056	0.0056	0.0028	0.0028	0	0	0	0	0	0	0
4.7488	4.7488	5.712	5.3088	5.544	4.8832	4.718	4.7096	4.9952	5.0064	4.7404	4.8944
0.084	0.098	0.056	0.056	0.0392	0.0896	0.056	0.0896	0.0588	0.0644	0.056	0.0504
4.396	4.5024	3.4916	4.0264	3.6344	3.9368	4.1636	4.2868	4.3456	4.3988	4.4576	4.4044
0.0196	0.0168	0	0.0028	0	0.0084	0.0588	0	0.014	0	0	0
0	0	0	0	0	0.0084	0.0056	0	0.0196	0.0056	0.0112	0.0084
0.0784	0.0084	0	0	0	0	0	0	0	0	0	0
0.0084	0.0084	0.0056	0.0028	0.0028	0	0	0	0	0	0	0
0	0	0	0	0	0	0	0	0	0	0	0
0	0	0.0476	0.0336	0.0448	0	0	0.0084	0	0	0	0
0	0	0	0	0	0	0	0	0	0	0	0
19.9612	19.978	20.1068	20.0004	20.034	19.7848	19.768	19.8772	20.0228	20.0536	19.9528	20.0004

48	7	8	9	10	11	19	49	50	51	52	53
H inclusion	B294A-1	B294A-2	B294A-3	B294A-4	B294A-5	B294A-12	94bGarnet2	94bGarnet2	94bGarnet3	94bGarnet4	94bGarnet5
Zn sulphide?	garnet	garnet	garnet	garnet	garnet	garnet	garnet	garnet	garnet	garnet	garnet
0.2952	37.5549	37.6807	37.7744	37.6981	37.6779	37.0409	37.4196	37.1314	37.5739	37.5145	37.5679
0	0.0643	0.1714	0.1399	0.1891	0.054	0.1784	0.1256	0.0447	0.1268	0.1271	0.0528
0.0076	20.6174	20.4452	20.4677	20.5416	20.7586	20.6611	20.4914	20.8513	20.7304	20.6549	20.8069
0	0.0152	0.0341	0.012	0.0039	0.0121	0.0605	0.002	0.0282	0.0066	0.0191	0.0092
2.599	25.5111	25.8159	25.0985	24.0226	26.0438	23.8935	26.2451	24.6183	25.2341	23.4699	23.9383
0	4.5001	4.4317	4.2578	4.6241	4.6365	4.2989	5.5814	6.3084	5.7577	6.3269	6.3228
0	1.5198	1.5479	1.5398	1.3679	1.4214	1.528	2.1747	1.8812	2.0681	1.8699	1.6886
0	9.1828	8.896	9.5233	11.5685	9.5599	11.205	7.3922	8.9219	8.9471	9.4921	8.8762
5.6519	0.0084	0.008	0.0134	0.0214	0.0147	0.0101	0.0099	0.0145	0.0145	0.0167	0.0273
0	0	0	0	0	0	0.0389	0	0	0	0	0
0.071	0	0	0	0.0063	0	0.0757	0	0	0	0.0026	0.024
83.7483	0	0	0	0	0	0	0.0386	0.0114	0.0317	0.0235	0
44.6126	0	0	0	0	0	0	0	0	0.0881	0	0
0.0137	0	0	0	0	0	0	0	0	0.0022	0	0
136.9993	98.9741	99.0309	98.8268	100.0434	100.1788	98.9911	99.4805	99.8114	100.5811	99.5173	99.314
0.0028	6.0528	6.0696	6.0816	6.012	6.0192	5.9688	6.0216	5.9592	5.9808	6.012	6.0336
0	0.0072	0.0216	0.0168	0.0216	0.0072	0.0216	0.0144	0.0048	0.0144	0.0144	0.0072
0.0001	3.9168	3.8808	3.8832	3.8616	3.9096	3.924	3.888	3.9432	3.8904	3.9024	3.9384
0	0.0024	0.0048	0.0024	0	0.0024	0.0072	0	0.0024	0	0.0024	0
0.0208	3.4392	3.4776	3.3792	3.204	3.48	3.2208	3.5328	3.3048	3.36	3.1464	3.2136
0	0.6144	0.6048	0.5808	0.624	0.6264	0.5856	0.7608	0.8568	0.7776	0.8592	0.8592
0	0.3648	0.372	0.3696	0.3264	0.3384	0.3672	0.5208	0.4512	0.4896	0.4464	0.4032
0	1.5864	1.536	1.644	1.9776	1.6368	1.9344	1.2744	1.5336	1.5264	1.6296	1.5264
0.1048	0.0024	0.0024	0.0048	0.0072	0.0048	0.0024	0.0024	0.0048	0.0048	0.0048	0.0096
0	0	0	0	0	0	0.0072	0	0	0	0	0
0.0005	0	0	0	0	0	0.0096	0	0	0	0	0.0024
0.6051	0	0	0	0	0	0	0.0048	0.0024	0.0048	0.0024	0
0.3151	0	0	0	0	0	0	0	0	0.0096	0	0
0.0001	0	0	0	0	0	0	0	0	0	0	0
1.0494	15.9888	15.972	15.9624	16.0368	16.0248	16.0512	16.0224	16.0656	16.0584	16.02	15.9936

54	55	56	57	58	59	79	28	88	25	27	30
94bGarnet6	94bGarnet7	94bGarnet8	94bGarnet9	4bGarnet10	4bGarnet11	B294bFsp	BCH matrix	94bbigmica	BCH matrix	BCH matrix	BCH matrix
garnet	garnet	garnet	garnet	garnet	garnet	garnet	ilmenite	ilmenite	muscovite	muscovite	muscovite
37.5164	37.0499	37.2259	36.7988	37.5369	37.2838	37.0739	0.1296	0	46.1977	47.1149	49.1081
0.1301	0.2014	0.1334	0.1724	0.0645	0.1028	0.0872	49.9929	46.6005	0.4853	0.2599	0.3835
20.5664	20.3595	20.3304	20.4236	20.6356	20.6494	20.2787	0.0119	0	28.3651	30.9809	29.0515
0.0085	0.026	0.0424	0.0215	0.0249	0	0.0091	0.0533	0.0326	0	0	0
26.0298	25.84	25.5694	25.8314	24.3159	24.5325	24.758	43.2326	40.1888	3.8449	4.2856	4.056
6.3875	7.2436	6.6332	6.9333	6.8652	6.255	5.7569	2.4436	5.9912	0	0.0055	0
2.0057	1.8529	1.9487	1.8794	1.8755	2.2196	2.1289	0.0372	0.0213	1.6836	1.9487	1.9228
7.0402	6.6238	7.1475	7.1422	7.6128	8.8343	7.3154	0.0438	0.0267	0.0378	0	0
0.0241	0.0175	0.0206	0.0191	0.0204	0.0047	0.0153	0.0036	0.0107	0.2347	0.1285	0.2516
0	0	0	0	0	0	0	0	0	8.516	7.3606	9.4724
0.024	0.0097	0.0163	0.0026	0.0358	0	0.0133	0.1228	0.1241	0	0	0
0	0	0	0.0133	0	0.0013	0	0.2042	0.185	0	0	0
0	0.0278	0	0.0324	0	0.1669	0	0.4894	0	0.3101	0.6794	0.4189
0	0	0	0	0	0	0	0.0289	0.0038	0.0115	0.0069	0
99.7327	99.2522	99.0678	99.2701	98.9875	100.0502	97.4367	96.7939	93.1848	89.6868	92.771	94.6648
6.0288	6.0048	6.0264	5.9688	6.0528	5.9664	6.0624	0.0066	0	6.5582	6.4284	6.6286
0.0168	0.024	0.0168	0.0216	0.0072	0.012	0.0096	1.9692	1.9266	0.0528	0.0264	0.0396
3.8952	3.8904	3.8784	3.9048	3.9216	3.8952	3.9096	0.0006	0	4.7476	4.983	4.6222
0	0.0024	0.0048	0.0024	0.0024	0	0	0.0024	0.0012	0	0	0
3.4992	3.5016	3.4608	3.504	3.2784	3.2832	3.3864	1.8936	1.848	0.4576	0.4884	0.4576
0.8688	0.9936	0.9096	0.9528	0.9384	0.8472	0.7968	0.1086	0.279	0	0	0
0.48	0.4488	0.4704	0.4536	0.4512	0.5304	0.5184	0.003	0.0018	0.3564	0.396	0.3872
1.212	1.1496	1.2408	1.2408	1.3152	1.5144	1.2816	0.0024	0.0018	0.0066	0	0
0.0072	0.0048	0.0072	0.0048	0.0072	0.0024	0.0048	0.0006	0.0012	0.0638	0.033	0.066
0	0	0	0	0	0	0	0	0	1.5422	1.2804	1.6302
0.0024	0.0024	0.0024	0	0.0048	0	0.0024	0.0054	0.0054	0	0	0
0	0	0	0.0024	0	0	0	0.0078	0.0078	0	0	0
0	0.0024	0	0.0048	0	0.0192	0	0.0192	0	0.033	0.0682	0.0418
0	0	0	0	0	0	0	0.0012	0	0.0022	0	0
16.0104	16.0272	16.02	16.0608	15.9792	16.0728	15.9744	4.0212	4.0728	13.8226	13.7038	13.8754

33	15	16	71	72	73	74	76	77	78	89	90
BCH matrix muscovite	B294A-8 plagioclase	B294A-9 plagioclase	B294bFsp plagioclase	B294bFsp plagioclase	B294bFsp plagioclase	B294bFsp plagioclase	B294bFsp plagioclase	B294bFsp plagioclase	B294bFsp plagioclase	94bbigmica plagioclase	94bbigmica plagioclase
46.2487	43.7732	43.5734	44.3531	53.4169	45.7089	43.5337	43.6834	42.673	58.2562	58.2404	57.9632
0.4743	0.0529	0.0046	0	0	0	0	0	0	0	0.1475	0
32.7646	33.8422	33.7999	32.5616	23.4558	31.7324	32.387	31.7163	24.7286	23.2889	23.3544	23.7979
0	0	0.009	0	0	0	0	0	0	0	0	0
2.6846	0.328	0.1514	0.1148	0.0492	0.082	0.1039	0	0.1532	0.071	0.4643	0
0	0	0	0	0	0	0	0	0	0	0	0
0.7292	0.0017	0.0087	0	0	0.0457	0	0	0.01	0	0.0253	0
0	19.238	19.2902	19.1982	8.4483	17.0733	19.7429	19.5739	22.1613	7.6441	7.4201	7.7371
0.3496	0.7085	0.7282	1.0173	5.0524	1.6332	0.7574	0.8829	0.7309	7.4219	7.4773	7.2406
9.2972	0.0035	0.0193	0	0.9321	0	0	0	0	0	0	0
0	0	0.0005	0	0	0	0	0	0	0	0	0
0	0	0	0	0	0	0	0	0	0	0	0
0.3481	0	0	0	0.2046	0	0	0.0119	0	0.081	0.0048	0.1142
0.0023	0	0	0	0	0	0	0	0	0	0	0
92.8987	97.9481	97.5853	97.2451	91.5593	96.2756	96.525	95.8684	90.4571	96.7631	97.1341	96.8531
6.3206	8.288	8.2784	8.4512	10.4832	8.7296	8.3776	8.4576	8.8864	10.7648	10.7328	10.6976
0.0484	0.0064	0	0	0	0	0	0	0	0	0.0192	0
5.2778	7.552	7.568	7.312	5.4272	7.1456	7.344	7.2384	6.0704	5.072	5.072	5.1776
0	0	0	0	0	0	0	0	0	0	0	0
0.3058	0.0512	0.0256	0.0192	0.0096	0.0128	0.016	0	0.0256	0.0096	0.0704	0
0	0	0	0	0	0	0	0	0	0	0	0
0.1496	0	0.0032	0	0	0.0128	0	0	0.0032	0	0.0064	0
0	3.9008	3.9264	3.92	1.776	3.4944	4.0704	4.0608	4.944	1.5136	1.4656	1.5296
0.0924	0.2592	0.2688	0.3744	1.9232	0.6048	0.2816	0.3328	0.2944	2.6592	2.672	2.592
1.6214	0	0.0032	0	0.2336	0	0	0	0	0	0	0
0	0	0	0	0	0	0	0	0	0	0	0
0	0	0	0	0	0	0	0	0	0	0	0
0.0352	0	0	0	0.0288	0	0	0.0032	0	0.0096	0	0.016
0	0	0	0	0	0	0	0	0	0	0	0
13.8512	20.0608	20.0768	20.0768	19.8816	20.0032	20.0896	20.096	20.224	20.0288	20.0384	20.016

67	80	81	82	83	40	66	12	26	35
B294bMica	94bbigmica	94bbigmica	94bbigmica	94bbigmica	BCH matrix	B294bMica	B294A-6	BCH matrix	BCH matrix
quartz	titanite	titanite	titanite	titanite	xxxxxxx	xxxxxxx	?	?	?
96.1075	30.2843	30.7257	30.2761	30.3932	35.7224	36.7082	45.7948	35.6159	32.8677
0	29.574	27.9431	27.5219	26.1474	0.0888	0	0.3288	0.072	1.4098
0	2.8387	3.5839	3.8888	4.8357	31.5406	22.1694	9.5286	31.456	15.7456
0	0	0	0	0	0.0845	0	0	0.013	0
0.1041	0.3527	0.4017	0.1303	0.3966	9.5868	13.3836	19.5404	8.6468	14.0806
0	0	0.0609	0	0	0	0.223	0.4595	0	0.0596
0.0403	0.1408	0.0684	0.0118	0.0701	4.9774	6.2098	9.5248	5.5774	7.5083
0	29.9181	30.1932	30.5849	30.5911	0.0139	6.1101	12.1278	0.0054	0.1002
0.007	0.0191	0.0183	0.012	0.027	1.9641	2.1652	0.6493	2.2696	0.04
0	0	0	0	0	0	0	0.2955	0	5.7669
0	0.002	0	0	0	0	0	0	0	0
0	0	0	0	0	0	0	0	0	0
1.8395	0.1578	0.1184	0.2253	0	0.0307	0.2093	0	0.1231	0.3442
0	0.0322	0.0182	0.1593	0	0.0116	0	0	0	0
98.0985	93.3197	93.1319	92.8105	92.4612	84.0209	87.1786	98.2496	83.7793	77.923
0.9922	0.212	0.2152	0.2129	0.2142	0.2466	0.2584	0.298	0.2459	0.2677
0	0.1557	0.1472	0.1455	0.1386	0.0005	0	0.0016	0.0004	0.0086
0	0.0234	0.0296	0.0322	0.0402	0.2567	0.184	0.0731	0.256	0.1511
0	0	0	0	0	0.0005	0	0	0.0001	0
0.0008	0.0021	0.0024	0.0008	0.0023	0.0554	0.0788	0.1063	0.0499	0.0959
0	0	0.0004	0	0	0	0.0013	0.0025	0	0.0004
0.0006	0.0015	0.0007	0.0001	0.0007	0.0512	0.0652	0.0924	0.0574	0.0912
0	0.2244	0.2266	0.2304	0.231	0.0001	0.0461	0.0846	0	0.0009
0.0002	0.0003	0.0002	0.0002	0.0004	0.0263	0.0296	0.0082	0.0304	0.0006
0	0	0	0	0	0	0	0.0025	0	0.0599
0	0	0	0	0	0	0	0	0	0
0	0	0	0	0	0	0	0	0	0
0.014	0.0008	0.0006	0.0012	0	0.0002	0.0011	0	0.0006	0.0021
0	0.0002	0.0001	0.0009	0	0.0001	0	0	0	0
1.0078	0.6204	0.623	0.6242	0.6274	0.6377	0.6646	0.6692	0.6407	0.6784

APPENDIX III – AX and THERMOCALC DATA

BH 332

THERMOCALC 3.21 running at 18.13 on Tue 16 Mar,2004 with thermodynamic dataset

an independent set of reactions has been calculated

Activities and their uncertainties

	phl	ann	east	py	alm	mu	cel
a	0.0480	0.0430	0.0460	0.00340	0.460	0.690	0.0180
sd(a)/a	0.36589	0.37985	0.37023	0.64968	0.15000	0.15000	0.55556

	mst	fst	q	H2O
a	0.000890	0.470	1.00	1.00
sd(a)/a	0.82127	0.20000	0	

Independent set of reactions
1) 3east + 6q = phl + py + 2mu
2) phl + east + 6q = py + 2cel
3) 18phl + 13mu + 2mst = 31east + 46q + 4H2O
4) ann + 3east + 6q = 2phl + alm + 2mu
5) 62phl + 39mu + 6fst = 8ann + 93east + 138q + 12H2O

Calculations for the independent set of reactions
(for x(H2O) = 1.0)

	P(T)	sd(P)	a	sd(a)	b	c	ln_K	sd(ln_K)
1	7.1	3.32	15.51	1.24	0.01110	-3.534	-0.225	1.371
2	7.7	2.91	60.30	1.09	0.03499	-4.079	-7.603	1.388
3	10.5	3.72	375.67	12.08	-0.50202	30.943	-21.922	13.476
4	9.7	3.19	-28.67	1.55	0.02430	-3.827	4.792	1.423
5	10.5	3.85	1586.10	36.34	-1.63273	92.886	-104.262	41.774

Average PT (for x(H2O) = 1.0)

Single end-member diagnostic information

avP, avT, sd's, cor, fit are result of doubling the uncertainty on ln a :
a ln a suspect if any are v different from lsq values.
e* are ln a residuals normalised to ln a uncertainties :
large absolute values, say >2.5, point to suspect info.
hat are the diagonal elements of the hat matrix :
large values, say >0.45, point to influential data.
For 95% confidence, fit (= sd(fit)) < 1.61
however a larger value may be OK - look at the diagnostics!

	avP	sd	avT	sd	cor	fit
lsq	8.9	1.9	661	61	-0.201	0.83

	P	sd(P)	T	sd(T)	cor	fit	e*	hat
phl	8.99	1.89	652	81	-0.249	0.82	-0.11	0.36
ann	9.08	2.03	661	61	-0.161	0.82	0.16	0.17
east	9.22	2.28	656	66	-0.370	0.82	0.18	0.40
py	9.20	1.88	685	65	-0.139	0.57	-1.02	0.19
alm	8.84	1.97	658	64	-0.085	0.82	0.11	0.11
mu	9.10	1.95	666	64	-0.095	0.81	-0.18	0.10
cel	8.55	2.18	667	64	-0.314	0.80	0.33	0.36
mst	8.68	1.89	637	66	-0.124	0.63	0.84	0.20
fst	8.89	1.88	655	64	-0.158	0.81	-0.17	0.05
q	8.94	1.87	661	61	-0.201	0.83	0	0
H2O	8.94	1.87	661	61	-0.201	0.83	0	0

T = 661°C, sd = 61,
P = 8.9 kbars, sd = 1.9, cor = -0.201, sigfit = 0.83

BH 332

Calculations for P = 8.9 kbar and T = 661∞C

-----

bi bh332-51
  Al-M1 ordered, site-mixing model + macroscopic RS gammas: (ann, phl, east, obi)
  Ferric from: Tet + Oct cation sum = 6.9 for 11 oxygens. Max Ratio = 0.15
  SF model parameters: Wpa=9, Wpe=10, Wpo=3, Wao=6, Wae=-1, Woe=10 (kJ)

oxide	wt %	cations		activity	±sd	±%
SiO2	37.12	2.719	phl	0.048	0.0117	24
TiO2	1.87	0.103	ann	0.043	0.0109	25
Al2O3	20.51	1.771	east	0.046	0.0114	25
Cr2O3	0.00	0.000				
Fe2O3	0.00	0.000				
FeO	19.26	1.180				
MnO	0.10	0.006				
MgO	10.10	1.103				
CaO	0.02	0.001				
Na2O	0.22	0.031				
K2O	8.38	0.783				
totals	97.59	7.699				

-----

g bh332-50
  2-site mixing + Regular solution gammas
  Ferric from: Cation Sum = 8 for 12 oxygens
  W: py.alm=2.5, gr.py=33, py.andr=73, alm.andr=60, spss.andr=60 kJ

oxide	wt %	cations	activity	±sd	±%

SiO2	37.00	2.989		py	0.0034	0.00148	43
TiO2	0.08	0.005		gr	0.00036	0.000188	52
Al2O3	21.30	2.028		alm	0.46	0.069	15
Cr2O3	0.00	0.000		spss	0.0000072	0.0000042	58
Fe2O3	0.00	0.000		andr	-	-	-
FeO	34.63	2.340					
MnO	0.87	0.059					
MgO	3.20	0.385					
CaO	2.11	0.183					
Na2O	0.02	0.003					
K2O	0.00	0.000					
totals	99.20	7.993					

-----

mu bh332-57
HP98 model + nonideal mu-cel-fcel-pa interactions
Ferric from: Tet + Oct cation sum = 6.05 for 11 oxygens. Max Ratio = 0.7

oxide	wt %	cations			activity	±sd	±%
SiO2	47.89	3.134		mu	0.69	0.069	10
TiO2	0.40	0.020		pa	0.535	0.0535	10
Al2O3	35.47	2.737		cel	0.018	0.0054	30
Cr2O3	0.00	0.000		ma	-	-	-
Fe2O3	0.00	0.000					
FeO	1.50	0.082					
MnO	0.00	0.000					
MgO	0.71	0.069					
CaO	0.00	0.000					
Na2O	0.65	0.082					
K2O	9.42	0.788					
totals	96.05	6.912					

AM332

-----

st bh332-32
4-site ideal Fe-Mg mixing
Ferric from: all ferrous

oxide	wt %	cations		activity	±sd	±%
SiO2	28.19	7.707	mst	0.00089	0.00049	55
TiO2	0.61	0.125	fst	0.47	0.094	20
Al2O3	54.45	17.549				
Cr2O3	0.00	0.000				
Fe2O3	0.00	0.000				
FeO	14.49	3.312				
MnO	0.00	0.000				
MgO	1.70	0.691				
CaO	0.02	0.005				
Na2O	0.01	0.007				
K2O	0.00	0.000				
totals	99.47	29.397				

BH294

THERMOCALC 3.21 running at 20.16 on Mon 15 Mar,2004 with thermodynamic dataset

an independent set of reactions has been calculated
Activities and their uncertainties

	an	ab	mu	pa	cel	py	gr
a	0.880	0.270	0.470	0.0677	0.0310	0.00113	0.0200
sd(a)/a	0.05000	0.15987	0.10000	0.26076	0.32258	0.72228	0.47772

	alm	phl	ann	east	q	H2O
a	0.150	0.0430	0.0660	0.0310	1.00	1.00
sd(a)/a	0.19769	0.37985	0.33131	0.42337	0	

Independent set of reactions
1) 2pa + gr + 3q = 3an + 2ab + 2H2O
2) 2east + 6q = mu + cel + py
3) 3east + 6q = 2mu + py + phl
4) 3an + ann = mu + gr + alm
5) 3an + phl = mu + py + gr

Calculations for the independent set of reactions
(for x(H2O) = 1.0)

	P(T)	sd(P)	a	sd(a)	b	c	ln_K	sd(ln_K)
1	9.1	0.81	143.21	0.70	-0.26635	8.340	6.295	0.791
2	7.1	2.53	35.35	1.12	0.02653	-3.931	-4.067	1.163
3	5.3	3.57	12.84	1.24	0.01459	-3.645	-1.021	1.523
4	8.5	0.76	-33.35	1.16	0.12258	-7.346	-3.463	0.640
5	7.8	1.17	10.89	0.71	0.10932	-7.052	-7.923	0.963

Average PT (for x(H2O) = 1.0)

Single end-member diagnostic information

avP, avT, sd's, cor, fit are result of doubling the uncertainty on ln a :
a ln a suspect if any are v different from lsq values.
e* are ln a residuals normalised to ln a uncertainties :
large absolute values, say >2.5, point to suspect info.
hat are the diagonal elements of the hat matrix :
large values, say >0.38, point to influential data.
For 95% confidence, fit (= sd(fit)) < 1.61
however a larger value may be OK - look at the diagnostics!

	avP	sd	avT	sd	cor	fit
lsq	8.2	1.0	715	50	0.795	0.99

	P	sd(P)	T	sd(T)	cor	√fit	√e*	hat
an	8.25	1.07	715	50	0.773	0.99	0.11	0.05
ab	8.28	1.09	723	59	0.798	0.98	-0.15	0.19
mu	8.33	1.07	720	50	0.801	0.94	-0.33	0.02
pa	8.38	1.15	733	69	0.811	0.97	0.24	0.51
cel	7.84	1.08	701	51	0.806	0.67	1.29	0.08
py	8.51	1.14	729	54	0.828	0.91	-0.63	0.19
gr	8.56	1.25	715	50	0.663	0.95	-0.35	0.54
alm	8.12	1.12	712	52	0.811	0.99	0.12	0.07
phl	8.01	1.09	705	53	0.815	0.93	-0.48	0.08
ann	8.03	1.21	709	54	0.825	0.98	-0.21	0.20
east	8.26	1.05	716	50	0.794	0.95	0.50	0.02
q	8.21	1.04	715	50	0.795	0.99	0	0
H2O	8.21	1.04	715	50	0.795	0.99	0	0

T = 715°C, sd = 50,
P = 8.2 kbars, sd = 1.0, cor = 0.795, sigfit = 0.99

Calculations for P = 8.1 kbar and T = 715°C

---

fsp 73
Holland & Powell 1992 model 1
Ferric from: all ferric
plag is I1 structure

oxide	wt %	cations		activity	±sd	±%
SiO2	45.71	2.182	an	0.88	0.0438	5
TiO2	0.00	0.000	ab	0.27	0.0289	11
Al2O3	31.73	1.786				
Cr2O3	0.00	0.000				
Fe2O3	0.00	0.000				
FeO	0.08	0.003				
MnO	0.00	0.000				
MgO	0.05	0.003				
CaO	17.07	0.873				
Na2O	1.63	0.151				
K2O	0.00	0.000				
totals	96.28	5.000				

---

mu 27
HP98 model + nonideal mu-cel-fcel-pa interactions
Ferric from: Tet + Oct cation sum = 6.05 for 11 oxygens. Max Ratio = 0.7

oxide	wt %	cations		activity	±sd	±%
SiO2	47.11	3.200	mu	0.47	0.047	10
TiO2	0.26	0.013	pa	0.0677	0.0148	22
Al2O3	30.98	2.480	cel	0.031	0.0084	27
Cr2O3	0.00	0.000	ma	-	-	-
Fe2O3	3.33	0.170				
FeO	1.29	0.073				
MnO	0.01	0.000				
MgO	1.95	0.197				
CaO	0.00	0.000				
Na2O	0.13	0.017				
K2O	7.36	0.638				
totals	92.43	6.789				

g 50
2-site mixing + Regular solution gammas
Ferric from: Cation Sum = 8 for 12 oxygens
W: py.alm=2.5, gr.py=33, py.andr=73, alm.andr=60, spss.andr=60 kJ

oxide	wt %	cations		activity	±sd	±%
SiO2	37.13	2.980	py	0.00113	0.000545	48
TiO2	0.04	0.003	gr	0.020	0.0064	32
Al2O3	20.85	1.973	alm	0.15	0.0230	15
Cr2O3	0.03	0.002	spss	0.0026	0.00117	45
Fe2O3	0.00	0.000	andr	-	-	-
FeO	24.62	1.652				
MnO	6.31	0.429				
MgO	1.88	0.225				
CaO	8.92	0.767				
Na2O	0.01	0.002				
K2O	0.00	0.000				
totals	99.80	8.032				

---

bi 65
Al-M1 ordered, site-mixing model + macroscopic RS gammas: (ann, phl, east, obi)
Ferric from: Tet + Oct cation sum = 6.9 for 11 oxygens. Max Ratio = 0.15
SF model parameters: Wpa=9, Wpe=10, Wpo=3, Wao=6, Wae=-1, Woe=10 (kJ)

oxide	wt %	cations		activity	±sd	±%
SiO2	35.60	2.766	phl	0.043	0.0109	25
TiO2	2.36	0.138	ann	0.066	0.0141	21
Al2O3	16.92	1.550	east	0.031	0.0088	28
Cr2O3	0.01	0.001				
Fe2O3	0.00	0.000				
FeO	19.97	1.298				
MnO	0.23	0.015				
MgO	9.43	1.092				
CaO	0.00	0.000				
Na2O	0.07	0.011				
K2O	9.15	0.908				
totals	93.75	7.779				

BH146

THERMOCALC 3.21 running at 19.58 on Tue 16 Mar,2004 with thermodynamic dataset

an independent set of reactions has been calculated

Activities and their uncertainties

	mu	pa	cel	phl	ann	east	py
a	0.670	0.850	0.0140	0.0400	0.0550	0.0410	0.00210
sd(a)/a	0.10000	0.09976	0.71429	0.38400	0.34563	0.38162	0.68425

	gr	alm	mst	fst	an	ab	q
a	4.20e-5	0.530	0.000920	0.470	0.180	0.880	1.00
sd(a)/a	0.83852	0.15094	0.81842	0.20000	0.20172	0.05011	0

	H2O
a	1.00
sd(a)/a	

Independent set of reactions
1) 23gr + 6fst + 48q = 8alm + 69an + 12H2O
2) mu + 2phl + 6q = 3cel + py
3) 31cel + 2mst = 18mu + 13phl + 46q + 4H2O
4) 2east + 6q = mu + cel + py
5) phl + 3an = mu + py + gr
6) ann + 3an = mu + gr + alm
7) 14mu + 4pa + 11phl + 40q = 25cel + 2mst + 4ab

Calculations for the independent set of reactions
(for x(H2O) = 1.0)

	P(T)	sd(P)	a	sd(a)	b	c	ln_K	sd(ln_K)
1	9.5	1.42	1458.57	14.31	-3.69651	143.580	112.920	23.845
2	6.4	4.50	80.38	1.14	0.05042	-4.504	-12.134	2.379
3	9.7	4.73	-295.97	10.65	-0.90809	41.104	97.258	22.829
4	6.3	2.73	35.35	1.12	0.02653	-3.931	-4.447	1.253
5	7.4	1.57	10.89	0.71	0.10932	-7.052	-8.281	1.302
6	9.0	1.29	-33.35	1.16	0.12258	-7.346	-3.068	1.105
7	9.2	5.33	443.42	8.85	0.49319	-29.519	-79.547	18.481

Average PT (for x(H2O) = 1.0)

Single end-member diagnostic information

avP, avT, sd's, cor, fit are result of doubling the uncertainty on ln a :
a ln a suspect if any are v different from lsq values.
e* are ln a residuals normalised to ln a uncertainties :
large absolute values, say >2.5, point to suspect info.
hat are the diagonal elements of the hat matrix :
large values, say >0.47, point to influential data.
For 95% confidence, fit (= sd(fit)) < 1.49
however a larger value may be OK - look at the diagnostics!

	avP	sd	avT	sd	cor	fit
lsq	8.2	1.2	654	26	0.778	0.95

	P	sd(P)	T	sd(T)	cor	fit	e*	hat
mu	8.18	1.22	655	28	0.801	0.95	-0.04	0.05
pa	8.15	1.16	659	33	0.625	0.94	0.18	0.60
cel	8.12	1.18	654	26	0.781	0.95	0.16	0.05
phl	8.09	1.19	652	28	0.791	0.94	-0.22	0.08
ann	8.27	1.24	657	28	0.808	0.94	0.24	0.15
east	8.16	1.20	654	27	0.786	0.95	0.01	0.08
py	8.55	1.20	663	27	0.794	0.77	-1.30	0.09
gr	8.39	1.33	657	27	0.786	0.94	-0.30	0.28
alm	7.96	1.25	651	27	0.796	0.93	0.30	0.08
mst	7.58	1.21	639	28	0.802	0.66	1.45	0.13
fst	8.01	1.18	653	26	0.774	0.91	-0.40	0.03
an	8.32	1.28	656	27	0.783	0.94	0.22	0.15
ab	8.16	1.16	656	28	0.721	0.95	-0.09	0.15
q	8.16	1.16	654	26	0.778	0.95	0	0
H2O	8.16	1.16	654	26	0.778	0.95	0	0

T = 654°C, sd = 26,
P = 8.2 kbars, sd = 1.2, cor = 0.778, sigfit = 0.95

BH 146

Calculations for P = 8.2 kbar and T = 654°C

---

mu bh146-100

HP98 model + nonideal mu-cel-fcel-pa interactions

Ferric from: Tet + Oct cation sum = 6.05 for 11 oxygens. Max Ratio = 0.7

oxide	wt %	cations		activity	±sd	±%
SiO2	47.63	3.117	mu	0.67	0.067	10
TiO2	0.56	0.027	pa	0.85	0.0848	10
Al2O3	35.94	2.772	cel	0.014	0.0043	31
Cr2O3	0.00	0.000	ma	-	-	-
Fe2O3	0.00	0.000				
FeO	1.11	0.061				
MnO	0.00	0.000				
MgO	0.59	0.058				
CaO	0.00	0.000				
Na2O	1.40	0.178				
K2O	8.27	0.691				
totals	95.52	6.904				

---

bi bh146-99

Al-M1 ordered, site-mixing model + macroscopic RS gammas: (ann, phl, east, obi)

Ferric from: Tet + Oct cation sum = 6.9 for 11 oxygens. Max Ratio = 0.15

SF model parameters: Wpa=9, Wpe=10, Wpo=3, Wao=6, Wae=-1, Woe=10 (kJ)

oxide	wt %	cations		activity	±sd	±%
SiO2	35.40	2.682	phl	0.040	0.0104	26
TiO2	1.93	0.110	ann	0.055	0.0127	23
Al2O3	19.72	1.762	east	0.041	0.0106	26
Cr2O3	0.00	0.000				
Fe2O3	0.00	0.000				
FeO	20.14	1.276				
MnO	0.10	0.006				
MgO	9.31	1.052				
CaO	0.00	0.000				
Na2O	0.38	0.057				
K2O	8.47	0.820				
totals	95.47	7.765				

RH146-4

g bh146-89
2-site mixing + Regular solution gammas
Ferric from: Cation Sum = 8 for 12 oxygens
W: py.alm=2.5, gr.py=33, py.andr=73, alm.andr=60, spss.andr=60 kJ

oxide	wt %	cations		activity	±sd	±%
SiO2	36.44	2.960	py	0.0021	0.00097	46
TiO2	0.04	0.002	gr	0.000042	0.0000236	56
Al2O3	21.33	2.043	alm	0.53	0.080	15
Cr2O3	0.00	0.000	spss	0.00010	0.000054	55
Fe2O3	0.00	0.000	andr	-	-	-
FeO	35.83	2.434				
MnO	2.05	0.141				
MgO	2.86	0.346				
CaO	1.03	0.090				
Na2O	0.01	0.001				
K2O	0.00	0.000				
totals	99.58	8.017				

---

st bh146-66
4-site ideal Fe-Mg mixing
Ferric from: all ferrous

oxide	wt %	cations		activity	±sd	±%
SiO2	27.24	7.564	mst	0.00092	0.00050	55
TiO2	0.66	0.138	fst	0.47	0.093	20
Al2O3	54.13	17.724				
Cr2O3	0.00	0.000				
Fe2O3	0.00	0.000				
FeO	14.26	3.312				
MnO	0.07	0.016				
MgO	1.65	0.682				
CaO	0.00	0.000				
Na2O	0.00	0.000				
K2O	0.00	0.000				
totals	98.01	29.436				

---

fsp bh146-121
Holland & Powell 1992 model 1
Ferric from: all ferric
plag is C1 structure

oxide	wt %	cations		activity	±sd	±%
SiO2	64.32	2.877	an	0.18	0.0244	13
TiO2	0.06	0.002	ab	0.88	0.0441	5
Al2O3	21.26	1.121				
Cr2O3	0.00	0.000				
Fe2O3	0.00	0.000				
FeO	0.11	0.004				
MnO	0.00	0.000				
MgO	0.00	0.000				
CaO	2.47	0.118				
Na2O	10.09	0.875				
K2O	0.00	0.000				
totals	98.33	4.998				

BH129

THERMOCALC 3.21 running at 20.14 on Mon 15 Mar,2004 with thermodynamic dataset

an independent set of reactions has been calculated
Activities and their uncertainties

	mu	cel	phl	ann	east	mst	fst
a	0.700	0.0150	0.0390	0.0720	0.0350	0.000280	0.570
sd(a)/a	0.10000	0.66667	0.38642	0.32121	0.40751	1.19523	0.20175

	py	alm	q	H2O
a	0.00180	0.660	1.00	1.00
sd(a)/a	0.75657	0.15000	0	

Independent set of reactions
1) mu + 2phl + 6q = 3cel + py
2) 31cel + 2mst = 18mu + 13phl + 46q + 4H2O
3) 2east + 6q = mu + cel + py
4) mu + phl + ann + 6q = 3cel + alm
5) 93cel + 6fst = 54mu + 31phl + 8ann + 138q + 12H2O

Calculations for the independent set of reactions
(for x(H2O) = 1.0)

	P(T)	sd(P)	a	sd(a)	b	c	ln_K	sd(ln_K)
1	6.5	4.31	80.38	1.14	0.05042	-4.504	-12.074	2.276
2	9.6	4.45	-295.97	10.65	-0.90809	41.104	97.958	21.478
3	6.9	2.83	35.35	1.12	0.02653	-3.931	-4.172	1.300
4	9.1	3.68	36.14	1.47	0.06367	-4.798	-6.783	2.070
5	9.7	4.38	-428.72	32.09	-2.85110	123.374	253.066	63.441

Average PT (for x(H2O) = 1.0)

Single end-member diagnostic information

avP, avT, sd's, cor, fit are result of doubling the uncertainty on ln a :
a ln a suspect if any are v different from lsq values.
e* are ln a residuals normalised to ln a uncertainties :
large absolute values, say >2.5, point to suspect info.
hat are the diagonal elements of the hat matrix :
large values, say >0.45, point to influential data.
For 95% confidence, fit (= sd(fit)) < 1.61
however a larger value may be OK - look at the diagnostics!

	avP	sd	avT	sd	cor	fit
lsq	8.5	1.9	627	63	-0.274	0.65

	P	sd(P)	T	sd(T)	cor	fit	e*	hat
mu	8.54	1.96	628	65	-0.206	0.65	-0.05	0.06
cel	8.37	2.14	630	66	-0.365	0.64	0.14	0.29
phl	8.52	1.97	626	82	-0.367	0.65	-0.02	0.32
ann	8.47	2.16	627	64	-0.173	0.65	-0.03	0.26
east	8.75	2.32	621	70	-0.451	0.64	0.16	0.40
mst	8.40	1.91	610	68	-0.229	0.50	0.71	0.17
fst	8.47	1.91	624	66	-0.238	0.64	-0.11	0.04
py	8.67	1.91	650	69	-0.208	0.43	-0.81	0.23
alm	8.35	2.05	623	67	-0.126	0.64	0.13	0.16
q	8.50	1.90	627	63	-0.274	0.65	0	0
H2O	8.50	1.90	627	63	-0.274	0.65	0	0

T = 627°C, sd = 63,
P = 8.5 kbars, sd = 1.9, cor = -0.274, sigfit = 0.65

BH129

Calculations for P = 8.5 kbar and T = 630°C

---

mu bh129-6

HP98 model + nonideal mu-cel-fcel-pa interactions

Ferric from: Tet + Oct cation sum = 6.05 for 11 oxygens. Max Ratio = 0.7

oxide	wt %	cations		activity	±sd	±%
SiO2	48.45	3.162	mu	0.70	0.070	10
TiO2	0.40	0.019	pa	0.712	0.0712	10
Al2O3	35.32	2.719	cel	0.015	0.0046	31
Cr2O3	0.00	0.000	ma	-	-	-
Fe2O3	0.00	0.000				
FeO	1.13	0.062				
MnO	0.02	0.001				
MgO	0.56	0.054				
CaO	0.01	0.001				
Na2O	0.88	0.111				
K2O	9.23	0.769				
totals	96.01	6.899				

---

bi bh129-2

Al-M1 ordered, site-mixing model + macroscopic RS gammas: (ann, phl, east, obi)

Ferric from: Tet + Oct cation sum = 6.9 for 11 oxygens. Max Ratio = 0.15

SF model parameters: Wpa=9, Wpe=10, Wpo=3, Wao=6, Wae=-1, Woe=10 (kJ)

oxide	wt %	cations		activity	±sd	±%
SiO2	35.44	2.738	phl	0.039	0.01028	26
TiO2	1.09	0.063	ann	0.072	0.0147	21
Al2O3	19.33	1.760	east	0.035	0.0095	27
Cr2O3	0.00	0.000				
Fe2O3	0.00	0.000				
FeO	20.62	1.332				
MnO	0.10	0.006				
MgO	8.28	0.953				
CaO	0.04	0.004				
Na2O	0.13	0.019				
K2O	9.18	0.905				
totals	94.23	7.781				

st bh129-63
4-site ideal Fe-Mg mixing
Ferric from: all ferrous

oxide	wt %	cations		activity	±sd	±%
SiO2	27.37	7.606	mst	0.00028	0.000171	61
TiO2	0.50	0.104	fst	0.57	0.115	20
Al2O3	54.19	17.755				
Cr2O3	0.00	0.000				
Fe2O3	0.00	0.000				
FeO	14.76	3.431				
MnO	0.00	0.000				
MgO	1.23	0.511				
CaO	0.00	0.000				
Na2O	0.02	0.009				
K2O	0.00	0.000				
totals	98.07	29.416				

g bh129_g10
2-site mixing + Regular solution gammas
Ferric from: Cation Sum = 8 for 12 oxygens
W: py.alm=2.5, gr.py=33, py.andr=73, alm.andr=60, spss.andr=60 kJ

oxide	wt %	cations		activity	±sd	±%
SiO2	36.46	2.984	py	0.0018	0.00085	46
TiO2	0.02	0.001	gr	-	-	-
Al2O3	21.03	2.029	alm	0.66	0.098	15
Cr2O3	0.00	0.000	spss	-	-	-
Fe2O3	0.00	0.000	andr	-	-	-
FeO	38.10	2.608				
MnO	0.39	0.027				
MgO	2.73	0.333				
CaO	0.21	0.019				
Na2O	0.01	0.002				
K2O	0.00	0.000				
totals	98.96	8.002				

+ H_2O a=1

BH 122

THERMOCALC 3.21 running at 20.15 on Mon 15 Mar,2004 with thermodynamic dataset

an independent set of reactions has been calculated
Activities and their uncertainties

	py	gr	alm	an	ab	mu	pa
a	0.00110	3.70e-5	0.470	0.270	0.830	0.710	0.568
sd(a)/a	0.72378	0.90030	0.15106	0.15987	0.05000	0.10000	0.10000
	cel	phl	ann	east	q	H2O	sill
a	0.0140	0.0252	0.0890	0.0270	1.00	1.00	1.00
sd(a)/a	0.71429	0.42463	0.29541	0.44100	0		0

Independent set of reactions
1) gr + q + 2sill = 3an
2) gr + 2pa + 3q = 3an + 2ab + 2H2O
3) mu + 2phl + 6q = py + 3cel
4) 2east + 6q = py + mu + cel
5) 3east + 7q + 2sill = 2py + 3mu
6) ann + q + 2sill = alm + mu

Calculations for the independent set of reactions
(for x(H2O) = 1.0)

	P(T)	sd(P)	a	sd(a)	b	c	ln_K	sd(ln_K)
1	7.0	1.65	25.98	0.59	-0.11368	5.274	6.277	1.020
2	8.3	1.07	143.21	0.70	-0.26635	8.340	7.035	1.044
3	6.8	4.57	80.38	1.14	0.05042	-4.504	-11.914	2.418
4	6.8	2.93	35.35	1.12	0.02653	-3.931	-4.200	1.350
5	5.1	3.12	49.71	1.47	0.01023	-5.423	-3.817	1.984
6	6.3	1.50	-7.36	1.01	0.00890	-2.072	1.322	0.347

Average PT (for x(H2O) = 1.0)
Single end-member diagnostic information

avP, avT, sd's, cor, fit are result of doubling the uncertainty on ln a :
a ln a suspect if any are v different from lsq values.
e* are ln a residuals normalised to ln a uncertainties :
large absolute values, say >2.5, point to suspect info.
hat are the diagonal elements of the hat matrix :
large values, say >0.43, point to influential data. For 95% confidence, fit (= sd(fit)) < 1.54 however a larger value may be OK - look at the diagnostics!

	avP	sd	avT	sd	cor	fit
lsq	5.6	1.1	643	29	0.911	0.60

	P	sd(P)	T	sd(T)	cor	fit	e*	hat
py	5.75	1.22	648	30	0.922	0.57	-0.40	0.15
gr	5.49	1.30	642	31	0.926	0.60	0.11	0.26
alm	5.63	1.22	645	30	0.919	0.60	-0.09	0.07
an	5.53	1.22	642	30	0.919	0.60	-0.06	0.07
ab	5.57	1.14	643	30	0.875	0.60	0.01	0.19
mu	5.67	1.20	646	30	0.918	0.59	-0.17	0.05
pa	5.57	1.15	643	35	0.806	0.60	-0.01	0.75
cel	5.38	1.16	639	29	0.914	0.44	0.93	0.05
phl	5.65	1.16	645	29	0.913	0.57	0.35	0.02
ann	5.71	1.32	646	32	0.929	0.59	0.18	0.25
east	5.48	1.16	641	29	0.913	0.56	-0.46	0.03
q	5.57	1.14	643	29	0.911	0.60	0	0
H2O	5.57	1.14	643	29	0.911	0.60	0	0
sill	5.57	1.14	643	29	0.911	0.60	0	0

T = 643°C, sd = 29,
P = 5.6 kbars, sd = 1.1, cor = 0.911, sigfit = 0.60

BH122

Calculations for P = 5.5 kbar and T = 640°C

---

g bh122_g7
2-site mixing + Regular solution gammas
Ferric from: Cation Sum = 8 for 12 oxygens
W: py.alm=2.5, gr.py=33, py.andr=73, alm.andr=60, spss.andr=60 kJ

oxide	wt %	cations		activity	±sd	±%
SiO2	36.35	2.978	py	0.00110	0.000531	48
TiO2	0.03	0.002	gr	0.000037	0.0000209	56
Al2O3	20.89	2.018	alm	0.47	0.071	15
Cr2O3	0.00	0.000	spss	0.0010	0.000488	49
Fe2O3	0.00	0.000	andr	-	-	-
FeO	34.20	2.343				
MnO	4.38	0.304				
MgO	2.27	0.277				
CaO	1.01	0.089				
Na2O	0.01	0.001				
K2O	0.00	0.000				
totals	99.14	8.012				

---

fsp bh122-13
Holland & Powell 1992 model 1
Ferric from: all ferric
plag is C1 structure

oxide	wt %	cations		activity	±sd	±%
SiO2	63.69	2.833	an	0.27	0.0288	11
TiO2	0.00	0.000	ab	0.83	0.0413	5
Al2O3	22.57	1.183				
Cr2O3	0.00	0.000				
Fe2O3	0.00	0.000				
FeO	0.03	0.001				
MnO	0.00	0.000				
MgO	0.00	0.000				
CaO	3.52	0.168				
Na2O	9.07	0.783				
K2O	0.00	0.000				
totals	98.88	4.967				

---

mu bh122-15
HP98 model + nonideal mu-cel-fcel-pa interactions
Ferric from: Tet + Oct cation sum = 6.05 for 11 oxygens. Max Ratio = 0.7

oxide	wt %	cations		activity	±sd	±%
SiO2	47.62	3.115	mu	0.71	0.071	10
TiO2	0.69	0.034	pa	0.568	0.0568	10
Al2O3	35.48	2.736	cel	0.014	0.0043	31
Cr2O3	0.00	0.000	ma	-	-	-
Fe2O3	0.00	0.000				
FeO	1.43	0.078				
MnO	0.00	0.000				
MgO	0.54	0.052				
CaO	0.00	0.000				
Na2O	0.86	0.109				
K2O	9.88	0.825				
totals	96.51	6.950				

---

bi bh122-12
Al-M1 ordered, site-mixing model + macroscopic RS gammas: (ann, phl, east, obi)
Ferric from: Tet + Oct cation sum = 6.9 for 11 oxygens. Max Ratio = 0.15
SF model parameters: Wpa=9, Wpe=10, Wpo=3, Wao=6, Wae=-1, Woe=10 (kJ)

oxide	wt %	cations		activity	±sd	±%
SiO2	35.23	2.671	phl	0.0252	0.00756	30
TiO2	2.33	0.133	ann	0.089	0.0164	18
Al2O3	19.08	1.705	east	0.027	0.0080	29
Cr2O3	0.00	0.000				
Fe2O3	0.00	0.000				
FeO	23.24	1.474				
MnO	0.06	0.004				
MgO	7.90	0.892				
CaO	0.00	0.000				
Na2O	0.21	0.030				
K2O	9.26	0.897				
totals	97.31	7.807				

+ H_2O a=1

+ sill a=1

BH116

THERMOCALC 3.21 running at 20.54 on Tue 16 Mar,2004 with thermodynamic dataset

an independent set of reactions has been calculated
Activities and their uncertainties

	mu	pa	cel	phl	ann	east	py
a	0.670	0.379	0.0320	0.0239	0.0720	0.0240	0.000570
sd(a)/a	0.10000	0.11569	0.31250	0.42882	0.30693	0.42850	0.75694

	gr	alm	an	ab	q	H2O
a	0.000210	0.330	0.190	0.870	1.00	1.00
sd(a)/a	0.79619	0.15152	0.19683	0.05023	0	

Independent set of reactions
1) 2pa + gr + 3q = 3an + 2ab + 2H2O
2) mu + 2phl + 6q = 3cel + py
3) 2east + 6q = mu + cel + py
4) ann + 3an = mu + gr + alm
5) phl + 3an = mu + py + gr

Calculations for the independent set of reactions
(for x(H2O) = 1.0)

	P(T)	sd(P)	a	sd(a)	b	c	ln_K	sd(ln_K)
1	10.3	1.07	144.50	0.70	-0.26603	8.144	5.148	1.023
2	10.7	2.91	82.70	1.14	0.04693	-4.352	-9.928	1.482
3	7.6	2.67	37.91	1.12	0.02304	-3.807	-3.853	1.190
4	9.8	1.24	-33.82	1.16	0.12278	-7.314	-2.364	1.053
5	8.2	1.61	10.37	0.71	0.10958	-7.021	-7.623	1.323

Average PT (for x(H2O) = 1.0)

Single end-member diagnostic information

avP, avT, sd's, cor, fit are result of doubling the uncertainty on ln a :
a ln a suspect if any are v different from lsq values.
e* are ln a residuals normalised to ln a uncertainties :
large absolute values, say >2.5, point to suspect info.
hat are the diagonal elements of the hat matrix :
large values, say >0.38, point to influential data.
For 95% confidence, fit (= sd(fit)) < 1.61
however a larger value may be OK - look at the diagnostics!

	avP	sd	avT	sd	cor	fit
lsq	9.8	1.6	702	43	0.721	1.30

	P	sd(P)	T	sd(T)	cor	fit	e*	hat
mu	9.91	1.57	708	44	0.728	1.26	-0.34	0.05
pa	9.82	1.63	705	55	0.681	1.30	0.05	0.32
cel	8.98	1.34	695	33	0.712	0.98	1.40	0.24
phl	9.70	1.61	699	44	0.735	1.28	-0.29	0.06
ann	9.25	1.76	684	51	0.805	1.23	-0.52	0.31
east	9.95	1.59	703	42	0.712	1.26	0.54	0.09
py	10.22	1.36	719	38	0.744	1.07	-1.25	0.15
gr	10.43	1.74	705	40	0.661	1.20	-0.64	0.37
alm	9.61	1.66	696	46	0.756	1.28	0.26	0.08
an	10.22	1.70	704	41	0.676	1.24	0.47	0.20
ab	9.80	1.60	703	45	0.708	1.30	-0.02	0.06
q	9.79	1.59	702	43	0.721	1.30	0	0
H2O	9.79	1.59	702	43	0.721	1.30	0	0

T = 702°C, sd = 43,
P = 9.8 kbars, sd = 1.6, cor = 0.721, sigfit = 1.30

BH116

Calculations for P = 9.8 kbar and T = 703°C

---

mu bh116-x4
  HP98 model + nonideal mu-cel-fcel-pa interactions
  Ferric from: Tet + Oct cation sum = 6.05 for 11 oxygens. Max Ratio = 0.7

oxide	wt %	cations		activity	±sd	±%
SiO2	47.00	3.167	mu	0.67	0.067	10
TiO2	1.20	0.061	pa	0.379	0.0379	10
Al2O3	32.30	2.566	cel	0.032	0.0086	27
Cr2O3	0.00	0.000	ma	-	-	-
Fe2O3	0.00	0.000				
FeO	1.78	0.100				
MnO	0.01	0.001				
MgO	1.03	0.103				
CaO	0.01	0.001				
Na2O	0.39	0.051				
K2O	10.81	0.930				
totals	94.53	6.980				

---

bi bh116-x5
  Al-M1 ordered, site-mixing model + macroscopic RS gammas: (ann, phl, east, obi)
  Ferric from: Tet + Oct cation sum = 6.9 for 11 oxygens. Max Ratio = 0.15
  SF model parameters: Wpa=9, Wpe=10, Wpo=3, Wao=6, Wae=-1, Woe=10 (kJ)

oxide	wt %	cations		activity	±sd	±%
SiO2	36.03	2.747	phl	0.0239	0.00727	30
TiO2	2.76	0.158	ann	0.072	0.0147	21
Al2O3	18.77	1.687	east	0.024	0.0074	30
Cr2O3	0.00	0.000				
Fe2O3	0.00	0.000				
FeO	20.90	1.332				
MnO	0.25	0.016				
MgO	7.27	0.826				
CaO	0.00	0.000				
Na2O	0.09	0.014				
K2O	9.81	0.955				
totals	95.89	7.735				

g bh116-g17
2-site mixing + Regular solution gammas
Ferric from: Cation Sum = 8 for 12 oxygens
W: py.alm=2.5, gr.py=33, py.andr=73, alm.andr=60, spss.andr=60 kJ

oxide	wt %	cations		activity	±sd	±%
SiO2	36.45	2.952	py	0.00057	0.000287	50
TiO2	0.00	0.000	gr	0.00021	0.000112	53
Al2O3	20.81	1.987	alm	0.33	0.050	15
Cr2O3	0.00	0.000	spss	0.0091	0.00343	38
Fe2O3	0.00	0.000	andr	-	-	-
FeO	30.81	2.087				
MnO	9.24	0.634				
MgO	1.90	0.229				
CaO	1.88	0.163				
Na2O	0.02	0.003				
K2O	0.00	0.000				
totals	101.10	8.056				

---

fsp bh116-x8
Holland & Powell 1992 model 1
Ferric from: all ferric
plag is C1 structure

oxide	wt %	cations		activity	±sd	±%
SiO2	66.03	2.888	an	0.19	0.0247	13
TiO2	0.00	0.000	ab	0.87	0.0437	5
Al2O3	21.77	1.122				
Cr2O3	0.00	0.000				
Fe2O3	0.00	0.000				
FeO	0.03	0.001				
MnO	0.00	0.000				
MgO	0.00	0.000				
CaO	2.60	0.122				
Na2O	9.84	0.836				
K2O	0.00	0.000				
totals	100.29	4.969				

BH53

THERMOCALC 3.21 running at 20.11 on Mon 15 Mar,2004 with thermodynamic dataset

an independent set of reactions has been calculated
Activities and their uncertainties

	py	gr	alm	an	ab	mu	pa
a	0.00179	0.0150	0.250	0.350	0.780	0.660	0.802
sd(a)/a	0.69472	0.51082	0.15000	0.15000	0.05026	0.10000	0.10000

	cel	phl	ann	east	q	H2O
a	0.0330	0.0590	0.0460	0.0470	1.00	1.00
sd(a)/a	0.30303	0.34392	0.37060	0.36805	0	

Independent set of reactions
1) mu + 2phl + 6q = py + 3cel
2) 2east + 6q = py + mu + cel
3) 3an + phl = py + gr + mu
4) ann + east + 6q = alm + 2cel
5) py + 2pa + 3ann + 9q = 3alm + 2ab + 3cel + 2H2O

Calculations for the independent set of reactions
(for x(H2O) = 1.0)

	P(T)	sd(P)	a	sd(a)	b	c	ln_K	sd(ln_K)
1	9.5	2.63	82.70	1.14	0.04693	-4.352	-10.483	1.339
2	7.2	2.39	37.91	1.12	0.02304	-3.807	-4.037	1.061
3	11.4	1.26	10.37	0.71	0.10958	-7.021	-4.961	1.037
4	11.0	1.62	16.12	1.43	0.04819	-4.373	-2.072	0.814
5	10.4	3.55	105.01	3.14	-0.06992	-4.109	1.115	1.673

Average PT (for x(H2O) = 1.0)
Single end-member diagnostic information

avP, avT, sd's, cor, fit are result of doubling the uncertainty on ln a :
a ln a suspect if any are v different from lsq values.
e* are ln a residuals normalised to ln a uncertainties :
large absolute values, say >2.5, point to suspect info.
hat are the diagonal elements of the hat matrix :
large values, say >0.38, point to influential data.
For 95% confidence, fit (= sd(fit)) < 1.61
however a larger value may be OK - look at the diagnostics!

	avP	sd	avT	sd	cor	fit
lsq	10.2	1.0	611	27	0.798	1.01

	P	sd(P)	T	sd(T)	cor	fit	e*	hat
py	10.53	1.09	621	30	0.832	0.92	-0.69	0.23
gr	10.10	1.18	610	27	0.720	1.00	0.14	0.38
alm	10.17	1.07	610	29	0.820	1.01	0.08	0.05
an	10.12	1.15	611	27	0.731	1.00	-0.12	0.30
ab	10.22	1.02	611	29	0.787	1.01	0.00	0.06
mu	10.31	1.03	615	28	0.809	0.98	-0.26	0.04
pa	10.22	1.04	611	33	0.768	1.01	-0.00	0.25
cel	10.09	1.05	610	27	0.792	0.98	0.45	0.13
phl	10.00	1.04	604	28	0.813	0.90	-0.66	0.08
ann	10.05	1.19	606	33	0.860	1.00	-0.21	0.32
east	10.40	1.02	611	27	0.791	0.67	1.33	0.05
q	10.22	1.02	611	27	0.798	1.01	0	0
H2O	10.22	1.02	611	27	0.798	1.01	0	0

T = 611°C, sd = 27,
P = 10.2 kbars, sd = 1.0, cor = 0.798, sigfit = 1.01

BH53

Calculations for P = 10.2 kbar and T = 610°C

---

g bh53-g19
2-site mixing + Regular solution gammas
Ferric from: Cation Sum = 8 for 12 oxygens
W: py.alm=2.5, gr.py=33, py.andr=73, alm.andr=60, spss.andr=60 kJ

oxide	wt %	cations		activity	±sd	±%
SiO2	37.11	2.974	py	0.00179	0.000830	46
TiO2	0.02	0.001	gr	0.015	0.00517	34
Al2O3	21.19	2.001	alm	0.25	0.037	15
Cr2O3	0.00	0.000	spss	0.00020	0.000104	53
Fe2O3	0.00	0.000	andr	-	-	-
FeO	28.86	1.934				
MnO	2.65	0.180				
MgO	2.14	0.255				
CaO	7.88	0.676				
Na2O	0.03	0.004				
K2O	0.00	0.000				
totals	99.89	8.027				

---

fsp bh53-6
Holland & Powell 1992 model 1
Ferric from: all ferric
plag is C1 structure

oxide	wt %	cations		activity	±sd	±%
SiO2	63.25	2.782	an	0.35	0.0296	9
TiO2	0.00	0.000	ab	0.78	0.0392	5
Al2O3	23.77	1.232				
Cr2O3	0.00	0.000				
Fe2O3	0.00	0.000				
FeO	0.17	0.006				
MnO	0.00	0.000				
MgO	0.00	0.000				
CaO	4.47	0.211				
Na2O	8.68	0.741				
K2O	0.00	0.000				
totals	100.35	4.973				

mu bh53-4
HP98 model + nonideal mu-cel-fcel-pa interactions
Ferric from: Tet + Oct cation sum = 6.05 for 11 oxygens. Max Ratio = 0.7

oxide	wt %	cations		activity	±sd	±%
SiO2	48.13	3.167	mu	0.66	0.066	10
TiO2	0.64	0.032	pa	0.802	0.0802	10
Al2O3	33.72	2.615	cel	0.033	0.0089	27
Cr2O3	0.00	0.000	ma	-	-	-
Fe2O3	0.00	0.000				
FeO	1.62	0.089				
MnO	0.00	0.000				
MgO	1.16	0.113				
CaO	0.00	0.000				
Na2O	0.78	0.100				
K2O	10.17	0.855				
totals	96.23	6.971				

bi bh53-2
Al-M1 ordered, site-mixing model + macroscopic RS gammas: (ann, phl, east, obi)
Ferric from: Tet + Oct cation sum = 6.9 for 11 oxygens. Max Ratio = 0.15
SF model parameters: Wpa=9, Wpe=10, Wpo=3, Wao=6, Wae=-1, Woe=10 (kJ)

oxide	wt %	cations		activity	±sd	±%
SiO2	37.03	2.758	phl	0.059	0.0131	22
TiO2	1.80	0.101	ann	0.046	0.0114	25
Al2O3	18.60	1.633	east	0.047	0.0115	25
Cr2O3	0.00	0.000				
Fe2O3	0.00	0.000				
FeO	18.58	1.157				
MnO	0.20	0.013				
MgO	10.82	1.201				
CaO	0.00	0.000				
Na2O	0.15	0.022				
K2O	9.48	0.902				
totals	96.67	7.787				

+ H_2O a=1

BH96-9

THERMOCALC 3.21 running at 19.07 on Tue 16 Mar,2004 with thermodynamic dataset

an independent set of reactions has been calculated

Activities and their uncertainties

	py	gr	alm	an	ab	phl	ann	
a	0.00280	0.00103	0.440	0.420	0.730	0.0570	0.0550	
sd(a)/a	0.66418	0.72740	0.15227	0.15000	0.05000	0.34770	0.35158	
	east	mu	pa	cel	mst	fst	q	H2O
a	0.0480	0.650	0.860	0.0220	0.00120	0.440	1.00	1.00
sd(a)/a	0.36589	0.10000	0.10012	0.45455	8.33333	0.20000	0	

Independent set of reactions

1) 3east + 6q = py + phl + 2mu
2) phl + east + 6q = py + 2cel
3) py + gr + mu = 3an + phl
4) 8py + 31gr + 24mu + 6mst = 93an + 24east + 12H2O
5) gr + alm + mu = 3an + ann
6) 69phl + 6fst + 186q = 46py + 8alm + 69cel + 12H2O
7) 4ab + 17phl + 2mst + 44q = 14py + 4pa + 17cel

Calculations for the independent set of reactions
(for x(H2O) = 1.0)

	P(T)	sd(P)	a	sd(a)	b	c	ln_K	sd(ln_K)
1	6.5	3.16	12.84	1.24	0.01459	-3.645	-0.495	1.344
2	7.7	2.50	57.86	1.09	0.03847	-4.218	-7.610	1.234
3	8.1	1.38	-10.89	0.71	-0.10932	7.052	7.720	1.142
4	9.8	2.12	1163.44	23.07	-4.66702	231.444	157.386	57.569
5	9.5	1.10	33.35	1.16	-0.12258	7.346	2.627	0.943
6	5.4	3.49	3557.68	33.13	-0.02260	-122.202	-337.725	49.956
7	5.5	5.44	681.84	8.61	0.21262	-33.538	-84.372	21.426

Average PT (for x(H2O) = 1.0)

Single end-member diagnostic information
avP, avT, sd's, cor, fit are result of doubling the uncertainty on ln a :
a ln a suspect if any are v different from lsq values. e* are ln a residuals normalised to ln a uncertainties : large absolute values, say >2.5, point to suspect info. hat are the diagonal elements of the hat matrix : large values, say >0.47, point to influential data. For 95% confidence, fit (= sd(fit)) < 1.49 however a larger value may be OK - look at the diagnostics!

	avP	sd	avT	sd	cor	fit
lsq	7.6	1.1	608	25	0.799	0.60

	P	sd(P)	T	sd(T)	cor	fit	e*	hat
py	7.87	1.13	615	27	0.826	0.54	-0.59	0.17
gr	7.69	1.26	609	27	0.803	0.60	-0.07	0.37
alm	7.66	1.09	609	26	0.803	0.60	-0.09	0.04
an	7.66	1.17	609	26	0.800	0.60	0.04	0.14
ab	7.62	1.05	607	28	0.758	0.60	0.05	0.15
phl	7.60	1.07	608	26	0.806	0.60	-0.12	0.04
ann	7.62	1.17	608	28	0.839	0.60	-0.01	0.21
east	7.67	1.07	609	25	0.799	0.59	0.22	0.05
mu	7.74	1.08	611	26	0.811	0.57	-0.26	0.03
pa	7.61	1.06	605	32	0.698	0.60	-0.10	0.59
cel	7.33	1.09	604	26	0.806	0.39	1.10	0.10
mst	7.62	1.05	608	25	0.799	0.59	0.23	0.00
fst	7.63	1.05	608	25	0.791	0.60	0.09	0.02
q	7.63	1.05	608	25	0.799	0.60	0	0
H2O	7.63	1.05	608	25	0.799	0.60	0	0

T = 608°C, sd = 25,
P = 7.6 kbars, sd = 1.1, cor = 0.799, sigfit = 0.60

BH96-9

Calculations for P = 7.6 kbar and T = 608∞C

----

g bh96-9_g6

2-site mixing + Regular solution gammas

Ferric from: Cation Sum = 8 for 12 oxygens

W: py.alm=2.5, gr.py=33, py.andr=73, alm.andr=60, spss.andr=60 kJ

oxide	wt %	cations		activity	±sd	±%
SiO2	36.73	2.961	py	0.0028	0.00122	44
TiO2	0.01	0.001	gr	0.00103	0.000498	49
Al2O3	21.02	1.998	alm	0.44	0.067	15
Cr2O3	0.00	0.000	spss	0.00012	0.000066	54
Fe2O3	0.00	0.000	andr	-	-	-
FeO	34.22	2.308				
MnO	2.22	0.152				
MgO	2.99	0.360				
CaO	2.99	0.258				
Na2O	0.03	0.005				
K2O	0.00	0.000				
totals	100.22	8.042				

----

fsp bh96-9-37

Holland & Powell 1992 model 1

Ferric from: all ferric

plag is C1 structure

oxide	wt %	cations		activity	±sd	±%
SiO2	60.43	2.700	an	0.42	0.0282	7
TiO2	0.00	0.000	ab	0.73	0.0365	5

Al2O3	24.42	1.286
Cr2O3	0.00	0.000
Fe2O3	0.00	0.000
FeO	0.14	0.005
MnO	0.01	0.000
MgO	0.00	0.000
CaO	5.98	0.286
Na2O	8.74	0.757
K2O	0.06	0.004
totals	99.78	5.038

----

bi bh96-9-38

Al-M1 ordered, site-mixing model + macroscopic RS gammas: (ann, phl, east, obi)

Ferric from: Tet + Oct cation sum = 6.9 for 11 oxygens. Max Ratio = 0.15

SF model parameters: Wpa=9, Wpe=10, Wpo=3, Wao=6, Wae=-1, Woe=10 (kJ)

oxide	wt %	cations		activity	±sd	±%
SiO2	35.56	2.708	phl	0.057	0.0129	23
TiO2	1.40	0.080	ann	0.055	0.0126	23
Al2O3	18.50	1.660	east	0.048	0.0117	24
Cr2O3	0.05	0.003				
Fe2O3	0.00	0.000				
FeO	19.66	1.252				
MnO	0.02	0.001				
MgO	10.78	1.223				
CaO	0.05	0.004				
Na2O	0.34	0.050				
K2O	8.72	0.848				
totals	95.08	7.830				

-----

mu bh96-9-56
HP98 model + nonideal mu-cel-fcel-pa interactions
Ferric from: Tet + Oct cation sum = 6.05 for 11 oxygens. Max Ratio = 0.7

oxide	wt %	cations		activity	±sd	±%
SiO2	46.98	3.147	mu	0.65	0.065	10
TiO2	0.30	0.015	pa	0.86	0.0861	10
Al2O3	33.76	2.666	cel	0.022	0.0064	29
Cr2O3	0.00	0.000	ma	-	-	-
Fe2O3	0.00	0.000				
FeO	2.15	0.120				
MnO	0.03	0.002				
MgO	0.83	0.082				
CaO	0.00	0.000				
Na2O	1.26	0.164				
K2O	9.14	0.782				
totals	94.45	6.978				

-----

st bh96-9-68
4-site ideal Fe-Mg mixing
Ferric from: all ferrous

oxide	wt %	cations		activity	±sd	±%
SiO2	27.25	7.611	mst	0.0012	0.00062	53
TiO2	0.51	0.107	fst	0.44	0.088	20
Al2O3	53.35	17.567				
Cr2O3	0.00	0.000				
Fe2O3	0.00	0.000				
FeO	14.66	3.423				
MnO	0.11	0.027				
MgO	1.80	0.750				
CaO	0.00	0.000				

Na2O	0.05	0.028
K2O	0.00	0.000
totals	97.74	29.513